STRUCTURAL DAMAGE IDENTIFICATION

FROM

MEASURED VIBRATION MODAL DATA

by

CHEN, Hua-Peng

B. Sc., M. Sc.

UNIVERSITY
of
GLASGOW

Thesis submitted to the University of Glasgow
in candidature for the degree of
Doctor of Philosophy

Department of Civil Engineering
The University of Glasgow

August 1998

To

My Family

ACKNOWLEDGEMENTS

I wish to express my deepest gratitude and sincerest thanks to Professor Nenad Bicanic, Regius Professor of civil engineering and Head of the Department, for his invaluable supervision and endless encouragement. A great deal of what has been achieved is due to his useful suggestions and clear sense of direction.

I would like to thank Dr. J. G. Herbertson, former Head of the Department, for providing me with excellent research facilities.

I would also like to thank Dr. D. Phillips, Dr. P. Bhatt, Dr. T. J. A. Agar, and Dr. C. J. Pearce for their valuable advice and help.

I am indebted to the Committee of Vice-Chancellors and Principles of the Universities of the United Kingdom for their financial support through the ORS award, and the University of Glasgow for funding this work through the University Scholarship during my stay at Glasgow.

I am grateful to my friends Dr. B. S. Zhang, Dr. B. T. Lim, Mr X. W. Gao, Mr. Y. P. Lee, Mr. A Cuthbertson, and Mr. D. Gallipoli for their friendship and support.

Thanks is also due to the computer manager of the Department Mr. K. McColl for providing ideal computing facilities.

Finally, my special thanks to my parents for their never ending support, to my wife Yanhui for her great understanding and encouragement, and to my new born daughter Helen for her giving me sufficient time to complete the work. Without their contribution, the work of this thesis could not have been finished.

SUMMARY

A novel non-linear perturbation theory based on the characteristic equations for structural dynamic systems is developed, which can provide an exact relationship between the perturbation of structural parameters and the perturbation of modal parameters. Then, depending on information about different types of the measured vibration modal data available, a system of governing equations based on the developed theory is derived, which can be utilised for general applications, such as eigendata modification, model updating, and damage identification, suitable for all types of structures, including framed structures and continua.

A number of computational procedures based on the derived non-linear governing equations are presented for structural damage identification, which can be suitable for various cases of the measured vibration modal data available, such as only natural frequencies, complete mode shapes, locally complete mode shapes, and incomplete mode shapes. The effectiveness and convergence performance for the proposed approaches are demonstrated by various numerical examples, and the sensitivities of many factors to inverse predictions of structural damage are also investigated.

The results for different types of structures, either framed structures or continua, indicate that the proposed approaches can be successful in not only predicting the location of damage but also in determining the extent of structural damage, while at the same time information about only a limited amount of the measured modal data is required. Furthermore, it is found that the proposed approaches are capable of providing information on the exact expanded damaged mode shapes, even if a very limited DOF's readings are available.

Structural modelling problems, which have to be considered in structural analysis and damage identification, are discussed. It is shown that structural damage can be identified correctly from the proposed approaches using information about different types of the measured modal data, regardless of different structural models considered and different types of elements used. Therefore, a suitable structural model can be selected in order to properly identify structural damage depending on the available information about modal data.

CONTENTS

NOMENCLATURE

A, a_{kj}, a_{kjl}	= eigenmode-stiffness sensitivity matrix and coefficients
A^+	= Moore-Penrose pseudo-inverse of matrix A
b, b_k, b_{kl}	= eigenmode-stiffness sensitivity vector and coefficients
C	= global damping matrix
C_{ik}	= mode participation factor
E	= Young's modulus
e	= residual energy
$f(t)$	= external forcing function vector
$f_m(\,)$	= non-linear generalised function
J	= cost function
K, K^*	= global stiffness matrices, original and perturbed
ΔK	= change in global stiffness matrix
K_j	= contribution of element j or Gauss point j to global stiffness matrix
$K^{(e)}$, $K^{(g)}$, $K^{(s)}$	= stiffness matrices at element, Gauss point, and subsystem level
$\Delta K^{(e)}$, $\Delta K^{(g)}$, $\Delta K^{(s)}$	= changes in stiffness matrices at element, Gauss point, and subsystem level
$K_j^{(e)}$, $K_j^{(g)}$, $K_j^{(s)}$	= sensitivities of stiffness matrices at element, Gauss point, and subsystem level
k_{st}, k_{st}^*	= coefficients of stiffness matrix, original and perturbed
δk_{st}	= modification of coefficient of stiffness matrix
M, M^*	= global mass matrices, original and perturbed
ΔM	= change in global mass matrix
$M^{(e)}$, $M^{(g)}$, $M^{(s)}$	= mass matrices at element, Gauss point, and subsystem level
$\Delta M^{(e)}$, $\Delta M^{(g)}$, $\Delta M^{(s)}$	= changes in mass matrices at element, Gauss point, and subsystem level
$M_j^{(e)}$, $M_j^{(g)}$, $M_j^{(s)}$	= sensitivities of mass matrices at element, Gauss point, and subsystem level
m_{st}, m_{st}^*	= coefficients of mass matrix, original and perturbed
δm_{st}	= modification of coefficient of mass matrix
N	= total number of DOFs

NAI, NUI	= total number of DOF's readings available and unknown for *i*th mode shape
NC	= total number of original eigenvectors considered
NE, NG, NS	= total number of elements, Gauss points, and subsystems
NEG	= total number of elements or Gauss points
NEQ	= total number of equations
NL	= total number of damaged modes available
NP	= total number of system parameters
p_j	= *j*th generic system parameter
δp_j	= modification of *j*th generic system parameter
r_i, r_i^*	= vectors of residual forces for *i*th mode, original and damaged
S_{ij}	= coefficient of eigenmode-stiffness sensitivity matrix
s_f	= acceleration factor
U, V	= orthogonal matrices for SVD method
W	= weighting matrix
$x, \dot{x}, \ddot{x}$	= displacement, velocity and acceleration vectors of DOFs
x_n	= generalised variable
y	= norm of the non-linear generalised equations
z_i	= coefficient of eigenmode-stiffness sensitivity vector

Greek

α, α_j	= structural damage parameter vector and *j*th element
β_i	= Mode Scale Factor (*MSF*) for *i*th mode
δ	= modification of quantity between perturbed and original system
Δ	= difference of quantity between perturbed and original system
ε	= convergence tolerance
Φ	= mass normalised original eigenvector matrix
ϕ_i, ϕ_i^*	= mode shapes of mode *i*, original and damaged
$\Delta\phi_i$	= change in *i*th mode shape
$\Delta\phi_i^u$	= change in *i*th mode shape restricted to the dimension for the unknown DOF's readings
ϕ_i^a, ϕ_i^u	= *i*th original eigenvector restricted to the dimension for the DOF's readings available and unknown

ϕ_i^{a*}, ϕ_i^{u*} = ith damaged eigenvector restricted to the dimension for the DOF's readings available and unknown

$\bar{\phi}_i^{a*}$ = vector containing the same dimension as ψ_i^{a*}, updated each iteration

φ_i^a = vector combining DOF's readings available and the corresponding original eigenvector for the remaining dimension

λ_i, λ_i^* = ith eigenvalues of characteristic equation, $\lambda_i = \omega_i^2$, original and damaged

$\Delta\lambda_i$ = change in ith eigenvalue

μ = vector of Lagrange multipliers

Π = Euclidian norm of structural damage parameters

π = Euclidian norm of equation errors

ρ = mass density

Σ, σ_i = singular value matrix and ith element

ω_i, ω_i^* = natural frequencies of mode i, original and damaged

$\Delta\omega_i$ = change in ith natural frequency

ψ_i^{a*} = DOF's readings available for ith damaged mode

Superscripts

$*$ = quantity of perturbed system/damaged structure

a, u = data available and unknown

e, g, s = element, Gauss point, and subsystem numbers

T = transpose

Subscripts

i, l, k = mode numbers

j, p, q, r = system parameter/damage parameter numbers

m, n = non-linear generalised equation and variable numbers

s, t = DOF numbers

CHAPTER 1

INTRODUCTION

1.1 General

Structural systems in a wide range of aeronautical, mechanical, and civil engineering applications are prone to damage during their service life. Damage in a structure may be defined as any deviation in the structure's original geometric or material properties which may cause undesirable stresses, displacements or vibrations on the structure. These deviations may develop due to a variety of factors:

* Failure of the material, i.e. corrosion, fatigue, plasticity, cracking.
* Flaws, voids, cracks and weak spots caused during manufacturing.
* Loss of structural connections, i.e. loose bolts, broken welds.
* Improper assembly or misfits during construction.

If a structure has sustained damage, and the damage remains undetected, the damage could progressively increase until the structure fails. A large number of structural failures have been reported over the past decades, causing considerable loss of life and property. Some of these accidents were originally considered as being due to a poor design, but it was gradually discovered that material deficiencies in the form of pre-existing flaws could initiate cracks and fractures, and then cause structural failures (Yao and Natke, 1994). Therefore, early detection, analysis and repair of a damaged structure, if necessary, are vital for the safe performance of the structure (Natke and Cempel, 1997).

Traditional Non-Destructive Evaluation (NDE) or Non-Destructive Testing (NDT) methods have often been employed to assess the integrity of a structure, such as radiographic inspection of welds, eddy current testing of heat exchanger tubing, ultrasonic thickness and flow measurements on piping and pressure vessels, dye penetration inspection of suspected flaws and other defects, magnetic particle inspection of fatigue crack in ferromagnetic materials, acoustic emission for continuous monitoring of cracks, as well as visual inspection for accessible areas of structures. There exist also some advanced methods for damage detection such as X-ray fluorescent spectroscopy infrared, ultraviolet and visible photography methods,

etc. Theories and techniques of all those methods can be found in books on the NDE, for instance Mix (1985). Such NDE methods give the effective deterioration state of only a local area and tend to be used only when the approximate damaged location is known.

Vibration measurements have been used for NDE in a more traditional sense with the frequency signature in the structural response functions used as a fingerprint to identify changes in the monitored system. These methods, however, do not produce quantitative damage information that can be used to design a repair or assess the safety of the damaged structure. These shortcomings can be overcome when vibration measurements are used with system identification algorithms. A mathematical model of the undamaged structure, usually correlated with test data of the undamaged structure, is used with the vibration information measured from the damaged structure. This damage detection approach is in principle similar to the verification of structural properties in specific locations (often referred to as model updating). This non-traditional use of vibration measurements shows promise in particular in the application to on-orbit, remote NDE even for large space structures.

However, these NDE methods differ greatly in their range of applicability and have certain kinds of limitation in practical application, particularly for civil engineering structures. Therefore, an effective and practicable non-destructive damage detection technique is urgently required to be developed.

1.2 Objectives

An effective and practicable structural damage detection method should require only limited information on vibration measurements which can be obtained from modal testing, and also it should have the following noteworthy aspects:

* Be capable of "detecting" the presence of damage
* Be capable of "locating" the position of damage
* Be capable of "quantifying" the extent of damage

With the above background and requirements in mind, the general aims of the research described in this thesis are:

* To establish a general theory for structural damage detection using modal parameters, which should be suitable for various types of structures such as large space structures, continua, composite structures, etc.

* To choose a suitable set of structural damage parameters which can represent both the location and the extent of structural damage for different types of structures.
* To develop procedures which require a minimum of measured modal data, which in turn may be incomplete, i.e. not all DOF's readings available, and/or inconsistent, i.e. modal data with noise.
* To develop effective computational techniques to solve the problem of system parameter identification and to obtain correctly the structural damage parameters.
* To develop a computer programme in order to demonstrate the effectiveness of the proposed approaches by the computational simulation.
* To demonstrate the practicability of the proposed methods by employing experimental measured modal data and applying them to real engineering structures, as much as possible.

1.3 Scope and Layout of the Thesis

The body of the thesis is divided into seven chapters (Chapter 2 to 8) and a brief layout is as follows.

In Chapter 2, the effects of damage in structure on the structural parameters and the modal parameters are discussed. Various methods for model updating are reviewed, and different techniques for structural damage identification are outlined. In addition, techniques for model reduction and mode shape expansion are discussed.

In Chapter 3, a system of governing equations based on the non-linear perturbation theory is developed, which can be utilised for general applications, such as eigendata modification, model updating, and damage identification, and which is suitable for all types of structures, including framed structures and continua. System parameters at different levels, such as matrix coefficient level, element level, Gauss point level, and substructure level, are also investigated.

In Chapter 4, several computational procedures based on the derived governing equations are developed. Both the location and the extent of structural damage can be determined using information about only one or two complete damaged modes. Structural damage at local area can also be estimated correctly using information about only the damaged DOFs readings measured completely near the damage

location. Furthermore, the effects of noise in modal data at certain nodes on structural damage identification are investigated.

In Chapter 5, a number of additional computational techniques based on the developed non-linear perturbation theory are proposed, where this time only natural frequencies for the damaged structure are required. The effectiveness and convergence performance of the proposed techniques are demonstrated by various numerical examples. Effects of various factors, such as the number of damaged frequencies adopted, the number of original eigenvectors available, and the noise existing in the information about damaged frequencies, are also investigated for all proposed computational techniques.

In Chapter 6, again based on the developed non-linear perturbation theory, a number of computational techniques which utilise directly the incomplete damaged modal data are presented. Several numerical examples are used to demonstrate the effectiveness and convergence performance of the proposed approaches. Furthermore, the effects of various factors on inverse predictions of structural damage are investigated.

In Chapter 7, the discretisation effects and model categories in modelling a specific structure, a cantilever beam, when considering damage identification are discussed. The same cantilever beam is considered though various structural models i.e. by utilising different types of elements, such as one-dimensional beam, two-dimensional continuum as well as three-dimensional solid. The results show that structural damage can be determined properly using the proposed approaches for each of the structural modelling frameworks.

In Chapter 8, conclusions are drawn from various numerical examples for the proposed approaches, and some suggestions for future study are also considered.

Information about the computer program developed to support the theory presented, including various element stiffness matrices and mass matrices as well as their sensitivity to system parameters, is given in Appendices.

CHAPTER 2

DAMAGE DETECTION FROM VIBRATION MEASUREMENTS

2.1 Structural and Modal Parameters at Damage

Whenever damage occurs, structural parameters such as stiffness, mass, flexibility, energy, etc., and consequently modal parameters such as natural frequency, mode shape, damping, etc., will be changed. The effects of damage in a structure on these parameters are discussed as follows.

2.1.1 Structural parameters

Stiffness

It is obvious that the introduction of a damage in a structure will cause a local change in stiffness. In the context of continuum damage mechanics, for example, it is assumed that material undergoes a change in internal structure due to damage and the material properties are subsequently degraded due to loss of integrity. With an assumption that the stiffness degrades proportionally to the damage, the damaged material stiffness for one-dimensional material can be expressed by

$$E^* = (1+\alpha)E \tag{2.1}$$

Where E and E^* are the Young's modulus for the original and the damaged structure, respectively; α is a damage parameter ranging from -1 to 0. For multi-dimensional material models, a similar relation also can be obtained (see e.g. DiPasquale *et al.*, 1990). Therefore, in most cases, the effects of structural damage on the damaged stiffness can be represented by reducing the Young's modulus.

Moreover, the stiffness of the damaged structure may be established and directly related to the location and the size of structural damage. Haisty and Springer (1988) presented the stiffness of a general beam element containing crack by using Castigliano's theory, where the strain energy is associated with stress intensity factors. Garcia and Stubbs (1995) discussed the effects of damage size and location on the stiffness of a rectangular beam using finite element analysis. Gounaris *et al.* (1996)

developed an element stiffness matrix for cracked three-dimensional beam by inverting the compliance matrix.

Mass

The change of mass for the damaged structure can often be neglected since the effect of structural damage on mass is usually very small. However, the loss or dislocation of non-structural mass, e.g. the mass of the top site on an offshore platform, will lead to change in modal parameters. In these cases, change in mass should be considered.

Flexibility

Since flexibility is the inverse of stiffness, reduction in stiffness caused by structural damage will produce an increase in the flexibility of the structure. Flexibility can be directly obtained from Castigliano's theory, which is related to the location and the size of a crack in a beam. Also, a flexibility matrix can be defined easier from measured modal data than the stiffness matrix, since the flexibility matrix mainly depends upon only a few of the lower frequency modes (Pandey and Biswas, 1995a), which makes it more practicable in structural damage detection.

Energy

Change of energy with respect to material damage is also an important property. According to the Griffith balance of energy, a crack can form in an elastic body only if such a process causes the total potential energy of the body to decrease, with the consequent reduction of the material stiffness. The total potential energy of the body can be regarded as a sum of a potential energy that would exist in an undamaged state and an additional term due to the presence of the crack. For a beam, the potential energy associated with the crack can be expressed via the stress intensity factors which are related to the location and the size of crack. Therefore, an energy approach is rather useful for the location and quantification of a crack in a beam. Moreover, DiPasquale *et al.* (1990) discovered that the parameter based on global damage indices can be related to local damage variables through averaging operations over the body volume. Based on this theoretical foundation, Tseng (1993) developed the defect energy parameter to detect structural damage.

2.1.2 Modal parameters

Natural frequency

Usually an introduction of structural damage is related to a decrease in stiffness and thereby in the natural frequencies. Natural frequency changes of structures due to

small geometric changes, such as cracks, notches, are studied by Gudmundson (1982) using a perturbation method. It was found that the natural frequencies decreased as functions of crack length. In addition, Mazurek and DeWolf (1990) tested a two-span plate girder bridge model to obtain natural frequencies as well as mode shapes due to presence of damage. Farrar *et al.* (1994) performed the dynamic characterisation and the damage detection experiments on a three span steel girder bridge (I-40 bridge) across the Rio Grande.

The main reason for the great popularity of using natural frequencies for structural damage detection is that natural frequencies are rather easy to measure with a relatively high level of accuracy. In fact, one sensor placed on a structure and connected to a frequency analyser can give estimates for several natural frequencies. Furthermore, natural frequencies are sensitive to all kind of damage, both local and global damage.

However, the feasibility of using changes in natural frequency to detect damage in structures is limited because even significant damage may induce very small changes in vibration frequencies, particularly for large scale structures, and these changes may go undetected due to measurement or processing errors (Rubin and Coppolino, 1993). In addition, only few lower natural frequencies can be measured for large scale structures, which makes it difficult to detect damage in the structures from a very limited information about natural frequencies.

Mode shape

In an effort to overcome the difficulties associated with very small changes in natural frequencies even for cases with significant damage and limited available measured information, research efforts have also focused on monitoring changes in mode shapes (Rubin and Coppolin, 1993). As it can be reasonably expected, it was concluded that the mode shapes were much more sensitive to damage than the natural frequencies.

Many parameters related to the mode shape were proposed as damage indicators, and some of these suggestions are rather promising. Sunder and Ting (1985) proposed a flexibility monitoring technique based on mode shapes to be used instead of natural frequencies in connection with the performance of damage detection on offshore platforms. Biswas *et al.* (1990) used the Modal Assurance Criteria (MAC) and Coordinate Modal Assurance Criteria (COMAC) of mode shapes to detect damage, although these parameters seem not sensitive enough. Pandey *et al.* (1991) found that the rotation and the curvature of mode shape are much more sensitive than the

displacement components of the mode shape. Bernasconi and Ewins (1989) and Yao *et al.* (1992) employed the concept of the strain mode shape which demonstrates quite good sensitivity to detect local damage.

However, to get estimates for the mode shape one has to perform a measurement at each of the points where estimates are wanted. Thus, the duration of a measurement session will increase considerably if a detailed mode shape needs to be estimated. Meanwhile the estimates of mode shape are obtained with a much lower level of accuracy compared to those of natural frequency, and these are probably the main disadvantages in using mode shapes to detect structural damage.

Damping

The introduction of damage in a structure will usually cause changes in the damping capacity of the structure. From the experiments of a beam, Rytter (1993) found that the modal damping ratios of the cantilevers were extremely sensitive to even small cracks. Similar results were reported in Hearn and Testa (1991), where wire ropes are used for experiments.

However, the changes in damping are highly dependent on several additional factors such as temperature, load history, the treatment during manufacturing, etc., which makes damping an impracticable candidate to be used to detect structural damage. Alampalli *et al.* (1992) have investigated the possibility of using modal damping ratios for damage detection in connection with the performance of vibration monitoring on bridges. Repetitive tests performed on a model of a composite bridge deck showed that the modal damping ratios are very sensitive to environmental conditions, e.g. temperature, which clearly makes it difficult to use modal damping ratios for damage detection.

2.2 Model Reduction and Mode Shape Expansion Techniques

Due to practical testing limitations, the dimension of the experimental eigenvectors is typically much less than that of the analytical eigenvectors. To compare the undamaged analytical model and the damaged test model for model updating or damage detection, both two models must have the same order of DOFs. Therefore, the order of the analytical model (system mass and stiffness matrices) often has to be reduced or the order of test results (mode shapes) has to be expanded.

2.2.1 Model reduction techniques

Model reduction techniques can be used to reduce dimension of the analytical model in order to match that of the experimental eigenvector. Most often in the past, Guyan or static reduction method has been used (Guyan, 1965). The reduced model (test-analysis model) developed in this manner will be referred to the sequel as a static reduction. An improved reduction technique called an IRS reduction (O'Callahan, 1989) can be obtained by statically approximating the dynamic terms which are neglected by the static reduction. However, both of these reduced models are approximations of the finite element dynamic model which may require a very large number of sensors to obtain a reasonable level of accuracy when the kinetic energy of vibration is spread out over a large portion of the structure, which is precisely the case for large scale structures. Even when only a small number of mode shapes are targeted for identification and correlation, approximate reduction techniques require too many sensors. Almost at the same time, a System Equivalent Reduction Expansion Process (SEREP) based on a global mapping technique was presented by O'Callahan *et al.* (1989) to provide improved accuracy in applications such as cross orthogonality checks and analytical model improvement.

Another reduction method was introduced by Kammer (1987) which uses mode shapes of the finite element model to reduce the finite element model itself. The resulting model exactly reproduces all of mode shapes and frequencies of the finite element model used in the reduction process, and has been successfully applied in test-analysis correlation for several large structures such as that presented in Kammer *et al.* (1989). Later on, a hybrid reduction approach (Kammer, 1991) was used to reduce sensitivity to the test-analysis differences due to residual dynamics. Moreover, Kim and Bartkowicz (1993) presented a method by selecting an intermediate DOFs set to satisfy both computational efficiency and sufficient detail to locate damage. Liu and Onoda (1996) proposed the partitioned model reduction method for large space structural control problem, based on the idea that the control model of the structure can be partitioned into several subdomains. Good comparison of various existing test-analysis model reduction methods can be found in the works of Freed and Flanigan (1991), and Hemez and Farhat (1994) as well.

However, the studies of He and Ewins (1991) and Lin and Lim (1996) showed that using such approaches may cause difficulties when trying to locate damage, since reducing the analytical model tends to change the location of errors existing in the model. Hence, it would appear that the alternative technique of using mode shape expansion techniques is more suitable for damage detection.

2.2.2 Mode shape expansion techniques

Mode shape expansion techniques are used to extrapolate values for the unmeasured DOFs based on both modal dynamic information and available measured DOFs. Generally, there are four broad categories for mode shape expansion.

Spatial interpolation methods

Spatial interpolation methods use geometric information to infer the data about mode shapes at unmeasured locations. Kim and Stubbs (1995a) presented a mode shape expansion method for a highway bridge by using spline functions. Park and Stubbs (1995) used Shannon's sampling theorem to reconstruct the mode shapes, which results from equidistantly spaced sampling points obtained in the field. However, spatial interpolation methods are only limited to very simple structures, thereby not suitable for most structures.

Direct methods

Direct methods use the dynamic equations of motions to obtain a closed-form solution of the expanded mode shape. This includes the Guyan (static) expansion method (Guyan, 1965) and the Kidder (dynamic) expansion method (Kidder, 1973). These methods can formally be interpreted as constrained optimisation problems.

Projection methods

Projection methods are formulated as a constrained quadratic optimisation problem to minimise the error between the set of measured and expanded mode shapes. Smith and Beattie (1990) developed the Procrustes method which is based on finding the orthogonal Procrustes transformation of the experimental eigenvectors into the space spanned by the predicted analytical eigenvectors at the measured DOFs. The method simultaneously expands and orthogonalises the mode shape vectors. Furthermore, Zimmerman and Kaouk (1992) presented an optimal least square expansion method to obtain the best "achievable" expanded mode shapes.

Error methods

Error methods formulate the expanded mode shape in terms of the uncertainty in the measurement or in the model. This includes penalty methods and the expansion techniques based on least-squares minimisation techniques with quadratic inequality constraints. In the work of Levine-West *et al.* (1996), several mode shape expansion methods were used for comparison of their mathematical and structural performances.

Note that the model reduction process would introduce errors in finite element model and the mode shape expansion process would introduce additional errors in the expanded mode shapes. The ideal situation would clearly be to measure all finite element model's DOFs, if anyhow possible.

2.3 Model Updating

The structural damage detection techniques based upon modal analysis utilise changes in modal parameters such as natural frequencies, mode shapes, modal damping, etc., which are closely related to those for structural model updating. Numerous works on model updating have been done by using various approaches. The detailed coverage of the modal testing is provided by Ewins (1984) and the review of recent literature is presented by Mottershead and Friswell (1993). Here, an outline of modal updating techniques which are often used and related to damage detection is described as follows.

2.3.1 Representation model techniques

The strategy of representation model techniques has been used to update a numerical model such that it exactly reproduces an incomplete set of measured eigendata. Four representation model approaches are considered here.

Reference basis methods

The reference basis methods were introduced by Baruch and Bar Itzhack (1978), by Berman and Nagy (1983), and later on by Caesar and Peter (1987). According to these methods, the reference basis, which must be formed by one parameter set taken from either the masses, stiffness or measured modes, is considered to be inviolate. The two remaining parameter sets are then updated separately by minimising an objective function, with constraints imposed through Lagrange multipliers (also called optimal matrix update).

Later, Kabe (1985) proposed a minimisation of the objective function subject to symmetric Lagrange multiplier constraints, where the structural connectivity is preserved. However, to find the Largrange multipliers is computationally expensive. Kammer (1988) used a projector matrix method which was computationally efficient and turns out to be equivalent to Kabe's method in most cases. Moreover, Smith and

Beattie (1991) considered quasi-Newton methods for stiffness updating which preserve the structural connectivity. Ladeveze *et al.* (1994) developed a method based on the computation of the error measure on the constitutive relation to correct both the stiffness and mass matrices, which can also be found in the work of Maia *et al.* (1994).

Eigenstructure assignment techniques

Control system designers have traditionally used eigenstructure assignment techniques to force a structure to respond in a predetermined way. The eigenstructure assignment approach for model updating was pioneered by Minas and Inman (1990). In this approach, state feedback is used to describe the right side of the dynamic equation of motion in terms of the displacement and velocity states. The problem then reduces to one of determining the terms in the feedback gain matrix such that the eigenvalues and eigenvectors of the closed loop system are identical to the measured eigendata. Later on, Zimmerman and Widengren (1990) used eigenstructure assignment combined with a generalised algebraic Riccati equation to calculate symmetric corrections to the stiffness and damping matrices directly.

Matrix mixing approach

The matrix mixing approach uses finite element methods where test data is unavailable, since the number of measured eigendata is usually significantly smaller then the order of the required model (Link *et al.*, 1987). To *et al.* (1990) used this approach to update the analytical mass and stiffness matrices by enforcing orthogonality with respect to the measured modal vectors. The method can be extended to include the eigendynamic system equation, together with the orthogonality relations, and it has the advantage of preserving the physical connectivity of the updated model.

Inverse eigenvalue techniques

Inverse eigenvalue techniques have been described in the book by Gladwell (1986). Later on, Lancaster and Maroulas (1987) solved an inverse eigenvalue problem for a second order system when the complete spectral data are given. Bucher and Braun (1993) presented an analysis of the inverse problem whereby mass and stiffness modifications are found by an eigendata assignment technique. Rather than updating a finite element model, the purpose is to determine structural modifications which can be implemented on a physical system in order to assign particular eigenmodes and natural frequencies.

2.3.2 Penalty function methods

There are two penalty function methods, for use in conjunction with measured Frequency Response Function (FRF) data and with modal data, respectively.

Using measured FRF data

The penalty function methods associated with using measured FRF data optimise a penalty function involving the FRF data directly. There are two approaches for model updating using FRF data, i.e., equation error approach minimising the error in the equation of motion, and output error approach minimising the error between the measured and estimated response. Fritzen and Zhu (1991) have discussed these approaches in more detail.

A frequency domain filter can also be used for directly minimising the output error. Simonian (1981a, b) developed a filter based on measured power spectral densities for the estimation of wind forces. Mottershead and Stanway (1986) modified the algorithm for sequential estimation of states and parameters to update the structural parameters by minimising the output error. He (1993) proposed the fundamentals of using FRF data based on the form of orthogonality in the modal domain. In the practical implementation of these methods, the Singular Value Decomposition (SVD) is used to solve the system of equations, and the solution is sought that is closest to that of the original analytical model (Foster and Mottershead, 1990).

Using modal data

The object of methods using modal data based on a penalty function is to maximise the correlation between the measured and analytical modal data. These methods allow a wide choice of parameters to update, but the requirement to optimise a non-linear penalty function implies an iterative procedure, with the possible convergence problems. The methods generally are based on the use of a truncated Taylor series of the modal data function of the unknown parameters. This series is often truncated to produce the first-order sensitivity equation (see e.g. Link, 1990a and 1990b). However, for the large change problems higher order perturbation of eigensystem should be considered.

Chen and Garba (1980) considered the case in which there are more parameters than measurements. The parameter vector closest to the original analytical parameters was sought which reproduced the required measurement change. Kim *et al.* (1983) proposed non-linear inverse perturbation method for redesign the modal

characteristics. Kuo and Wada (1987) suggested using the non-linear or second order sensitivity equations, and produced correction terms to give improved convergence properties compared to that of the linearised algorithm. To and Ewins (1991) employed non-linear sensitivity analysis to determine the revised modal parameters.

Based on the above knowledge of model updating, it is assumed that, except for special cases, a refined (i.e., the measured and analytical modal parameters are in agreement) finite element model of the structure has been developed before damage has occurred.

2.4 Damage Detection Using System's Response Information

Traditional measurements for modal analysis consist of measuring displacement, velocity and acceleration in time domain. If they are measured under unit excitations and transferred to frequency domain by Fourier or Fast Fourier Transformation (FFT), then they become compliance, mobility and inertance frequency response function respectively. Changes of these parameters due to damage can be used for damage detection.

2.4.1 Frequency Response Function (FRF) analysis

FRFs are often used to detect structural damage, such as in the works of Jerry and Yao (1987), Roitman *et al.* (1992) and Samman *et al.* (1994a, b). Moreover, Samman *et al.* (1991) applied the Freeman's code for pattern recognition and image processing to accentuate the differences in the FRF between the intact bridge and the cracked bridge signal. Significant slope and curvature differences were found whenever a crack was introduced especially near the natural frequency range. Biswas *et al.* (1990) studied several dynamic parameters for damage detection in a full scale modal testing. It was found that changes in frequency spectra are detectable but are difficult to quantify while changes in FRF are detectable and quantifiable. Recently, Biswas *et al.* (1994) modified chain code computer vision technique for interrogation of vibration signatures for structural fault detection.

Transfer function can directly be used for detecting structural damage (Fritzen *et al.* 1990). Lew (1995a, b) presented an approach for damage detection of large flexible structures by using the parameter change of the transfer function, where an interval modelling technique was introduced to distinguish the structural damage from the

environmental change. Lim *et al.* (1996) employed a real-time model parameter identification algorithm implemented in a digital-signal-processor-based data acquisition system, in order to detect damage in a laboratory truss structure.

Anti-resonance frequencies can also used for damage detection and localisation (Afolabi, 1987). The results from a cantilever model show that as the point of measurement gets closer to the location of the defect, fewer and fewer anti-resonances are shifted from their original values until one gets to the location of the defect, at which all the anti-resonances are exactly as they were in the undamaged state.

2.4.2 Random decrement method

The random decrement signature is extracted from a time series by averaging the segments of the time series. This signature is closely related to the auto-correlation function and thereby the free decay of a linear structure, when the load is represented by a white-noise. Tsai *et al.* (1985) presented a damage detection scheme based on the use of random decrement signature, where the modal frequencies, damping, and the complex amplitudes were resolved by curve fitting and then were used for damage detection. The same technique was applied to an offshore model structure to detect the presence of damage presence successfully (Yang *et al.*, 1984). Moreover, the random decrement technique in connection with estimation of natural frequencies and damping ratio is attractive for damage detection (Brinker *et al.*, 1991). The advantage of the random decrement method is that it requires only measurement of the dynamic response of the structure and not the input force.

2.4.3 Sub-/Super-harmonic peeks method

The introduction of a crack in a beam can often imply that the stiffness of the beam becomes non-linear. This non-linearity in a beam is generally included by means of a rotational spring with a piece-wise linear relationship between the bending moment and the rotation. It can be shown (see, e.g., Friswell and Pendy, 1992) that this kind of non-linearity will cause sub-harmonic and super-harmonic peaks in the auto-spectral density function for the response of the structure. The most simple and still efficient approach for damage detection was suggested by Tsyfanskii *et al.* (1985), which uses the ratio between the spectral value at load frequencies and/or natural frequencies and their sub-/super-harmonic frequencies after each periodical measurement.

2.4.4 Electrical analogy method

Damage in framed structures can be evaluated by using electrical analogy method. Two approaches, using the relative transmissibility change from the dynamic response (Akgun *et al.*, 1985), and using the relative inertance change from the transmissibility difference between the intact and the damaged system (Akgun *et al.*, 1990), were utilised to detect the presence of damage. However, the method requires that the response station has to be very close to the neighbourhood of and yet can not be at the pseudo mode point.

2.5 Damage Detection Using Modal Parameter Information

It has already been said several times that damage in structure will cause changes in structural parameter such as stiffness, mass, flexibility, energy, and that any changes in the structural parameters will cause changes in modal parameters, such as natural frequency, mode shape, modal damping, etc. Consequently, the modal parameters can be used for damage evaluation by various techniques. The majority of these techniques used to address damage detection can be broadly categorised as follows.

2.5.1 Changes in structural/modal parameter methods

Changes in structural parameters and modal parameters can directly be used for damage detection.

Changes in stiffness were introduced by Park *et al.* (1988) where they found that the comparison of absolute values of the changes in stiffness matrix (error matrix) may cause problems. A more complicated error matrix related to stiffness as damage indicator was suggested by He and Ewins (1986). In addition, Agbabian *et al.* (1988) proposed the ratios of changes in stiffness for estimating the location of damage in a structure. Peterson *et al.* (1993) developed a procedure for damage detection which uses results from the eigensystem realisation algorithm and the common basis structural identification algorithm in order to synthesise mass and stiffness matrices for the structure.

Changes in flexibility were utilised by Raghavendrachar and Aktan (1992), and Pandey and Biswas (1995a) for damage detection based on the estimation of the flexibility matrix, which was demonstrated by experimental results (Pandey and

Biswas, 1995b). Also, the flexibility ratios were used to locate damage in a cantilever by Tsai *et al.* (1985) and in space trusses by Smith and Hendricks (1987). A useful damage indicator which results from estimated flexibility matrix multiplied by the original analytical stiffness matrix was suggested by Lin (1990).

Energy approach is often used to detect damage in a beam since the additional energy due to a crack can be calculated from the stress intensity factors, such as in the works of Kam and Lee (1994a, b) and Sundermeyer and Weaver (1995). In addition, Lim (1991) and Kashangaki *et al.* (1992) suggested fractional modal strain energy as a damage indicator for damage detection in substructures. Osegueda and DSouza (1992) proposed internal modal energy distribution among the elements to evaluate damage in offshore structures. Kim and Stubbs (1995a) employed the ratio of the fraction of modal energy to obtain a damage indicator (ratio of Young's modulus) for detecting damage in plate girders. This method was also used for detection of damage in offshore jacket structures (Kim and Stubbs, 1995b), and in a highway bridge (Kim and Stubbs, 1995c) which has been tested by Farrar and Cone (1995), but impracticable in a prestressed concrete beam (Abraham *et al.*, 1995).

Most structural damage detection approaches using measured modal data are based on changes in natural frequencies and mode shapes (discussed later in detail). Among these approaches, the ratios of change in natural frequencies were often used for damage detection, such as in the works of Coppolino and Rubin (1980) and Liang *et al.* (1992).

Also, changes in mode shapes can directly be used for locating damage. Rubin and Coppolino (1983), Sunder and Ting (1985), and Shahrivar and Bouwkamp (1986) utilised changes in the deflection shapes to detect potential damage in offshore jacket platforms. Yuen (1985) proposed the change of eigenparameters, i.e., mode shape normalised by natural frequency, to locate damage in a cantilever. Fox (1992) suggested that the plots of the absolute and the relative changes in mode shapes to detect structural damage. Lim and Kashangaki (1994) presented a method for damage location by minimising the Euclidean distances between the measured mode shapes and the best achievable eigenvectors. Mayes (1995) found that the static flexibility is sensitive to damage using experimental data from a full scale bridge damage test series. Other parameters related to mode shape used for damage indicators have been discussed in Section 2.1.2.

2.5.2 Sensitivity (Perturbation) methods

Sensitivity (perturbation) analysis can be used to repeat the full dynamic analysis in order to compute the changes in the modal parameters due to damage, which makes it possible to locate damage, such as in the works of Cawley and Adams (1979a), Chondros and Dimarogonas (1985), and Natke and Cempel (1991). Cawley and Adams (1979a, b) used the ratio of natural frequencies to identify damage location in a structure. To first order, this frequency ratio is dependent on the damage location but not the level of damage. Similar idea was introduced by Yin *et al.* (1992) to develop a method based on pattern recognition for diagnosing the location of local damage. It was found that the ratio of changes in natural frequencies due to a local damage is related to the curvature of the corresponding mode shape. Friswell and Penny (1994) improved their methods and suggested a statistical method to identify the damage site and mechanism using the generalised least squares theory. Different approaches were compared using simulated and experimental data. Generally, these methods can predict the location of damage but are not capable of giving the information on the extent of damage.

Stubbs *et al.* (1990, a & b) extended the concept of continuum modelling of structures to the problem of damage identification of large space structures, where the first-order dynamic sensitivity equations for structures involving structural parameters and modal parameters are developed. Sanayei and Onipede (1991) provided a first-order static sensitivity equation for damage assessment in framed structures or in plates (Sanayei and Scampoli, 1991) using static test data. Farhat and Hemez (1993) suggested a sensitivity based element-by-element updating methodology for damage location using incomplete modal data, which was also employed in their later works (Hemez and Farhat, 1993, 1995b). Topole and Stubbs (1995a, b) used sensitivity analysis for evaluating damage in a large space structure and a shear building. To solve the derived sensitivity equations, computational algorithms such as pseudo-inverse, least squares, Singular Value Decomposition (SVD) are required to obtain damage parameters. The discussion of these computational algorithms can be found in the works of Maia (1989), Ojalvo and Zhang (1993), and Hemez and Farhat (1995c).

Sensitivity methods for damage detection based on sensitivity derivatives of modal parameters with respect to physical design variables are similar to the penalty function methods using modal data for model updating (see, e.g., Adelmam and Haftka, 1986). These sensitivity coefficients are then used to calculate damage parameters that would force the analysis frequencies and modes to match those measured in a test. Various

optimisation techniques, such as conjugate gradient method, can be used to converge on near-optimal solution (see, e.g., Huang and Yan, 1996). In addition, Hajela and Soeiro (1990a) utilised the non-linear optimisation to solve for the damage detection problem. Hassiotis and Jeong (1993) introduced a method to solve for a quadratic programming problem with linear equality and inequality constraints, which is obtained from the first-order perturbation of the eigenvalue problem.

For model refinement, the first-order approximation in computing eigenvalues and eigenvectors performs properly since the changes in structural parameters from the initial model to the refined model may be small. For damage detection, this first-order approximation may be inaccurate since a large parameter change due to damage needs to be detected. For instance, the results in Mazurek and DeWolf (1990) show that released supports in a two-span bridge model will cause a new mode and a sharp increase in resonant frequency. Consequently, a novel perturbation-based approach using the exact relationship between the changes of structural parameters and the changes of modal parameters should be developed for damage identification.

Recently, a new general non-linear perturbation theory, which satisfies the above requirements and can be used for model updating or damage identification, is proposed by Chen and Bicanic (1996a). The application of the proposed theory can be found in the works of Bicanic and Chen (1997), Chen and Bicanic (1996b, 1997a, 1997b, and 1997c).

2.5.3 Modal force error approaches.

Modal force error criteria for damage location was proposed by Ojalvo and Pilon (1988). A residual force vector (damage vector) associated with structural perturbation matrices that reflect the nature of the structural damage was introduced. By inspecting the elements of the residual force vector, the degrees of freedom which have been affected by damage can be determined. The residual force vector also reveals that only a single mode of vibration needs to be measured exactly to determine exact damage locations. This is true even for multiple member damage situations. Meanwhile, a similar method for damage assessment was employed by Chen and Garba (1988). Moreover, Ricles and Kosmatka (1992) employed the residual force vector to locate potential damage regions and utilised the first-order sensitivity analysis to assess damage severity. Baruh and Ratan (1993) discussed the effects of uncertainties in structural parameters and inaccuracies in modal data on damage location using modal force error approaches. However, Gysin (1990) observed that in certain specific cases

of eigenvector errors the residual force vector may lead to incorrect conclusions concerning the location of damage.

In order to provide an alternate view of the state of damage, Zimmerman and Kaouk (1994) and Kaouk and Zimmerman (1994, 1995) developed a more reasonable indicator of damage which uses the deviation of the angle between two vectors from the 90 degree, corresponding to orthogonality. With location determined, a minimum rank update is used to determine the extent of structural damage (also see Zimmerman *et al.*, 1994). Sheinman (1994) used the residual force vector for damage detection in framed structures where multiple damage parameters are used in the local stiffness matrix of a structural member. Recently, Sheinman (1996) reconstructed the residual force vector for grouping uncoupled damage regions, which significantly reduces the order of the problem. A mode scanning procedure was employed for finding the minimum measured modes needed for completing the process. Li and Smith (1995) combined the advantages of both eigensesitivity and matrix adjustment techniques (using residual force vector) to create a hybrid approach for detection of damage in flexible structures. However, these approaches were only used to identify the changes in matrix coefficients, thus no information on structural members corresponding to damage was given.

2.5.4 Eigenstructure assignment techniques

As indicated earlier, the eigenstructure assignment techniques have been used often for modal updating (see Section 2.3.1). For damage location, the desired eigenstructure, i.e., eigenvalues and eigenvectors, is the one that is measured in the test for the damaged structure. Zimmerman and Kaouk (1992) applied this eigenstructure model refinement algorithm to structural damage detection. A major difficulty associated with their approach is that the method identifies matrix coefficients changes and thus requires an additional step to identify structural members corresponding to the changes.

To avoid this difficulty, Lim (1995) developed the constrained eigenstructure assignment approach for the same purpose without enforcing the preservation of the structural connectivity. Thus, detection of both partial and complete loss of stiffness is possible, and the additional step of correlating matrix coefficient changes to structural parameter changes is avoided. However, this technique may not be suitable for detection of multiple damage since it may not provide a clear indication of the damaged members.

2.5.5 Optimisation methods

Several optimal matrix update algorithms have been used for modal updating by minimising the selected matrix norm (see an earlier Section 2.3.1, Reference basis methods). However, its applicability for damage detection is questionable since damage typically results in localised changes in the property matrices, whereas the matrix norm minimisation would tend to "smear" the changes through the entire stiffness matrix.

Alternative optimisation methods directly use a non-linear optimisation method to find an estimate for the damage parameters. The objective function to be minimised expresses a scalar measure for the differences between the measured modal parameters and calculated modal parameters given certain damage parameters. Shen and Taylor (1991) suggested a method for diagnosing a cracked beam by minimising the means square difference. Hajela and Soeiro (1990b) presented a method for structural damage detection by minimising the difference between the measured and predicted response based on both static and modal analysis, and then similar method was used for detection of damage in composite material (Soeiro and Hajela, 1993). In addition, the damage identification problem can be formulated as an optimisation program in which either the error norm of the eigenequation (Liu, 1995) or the deviation between measured and analytical modal frequencies and partial mode shapes (Cobb *et al.*, 1996) is minimised.

2.5.6 Neural networks and genetic algorithms

During the last decade, the field of neural networks has been subject to intense studies from many different disciplines, including structural damage detection. The basic strategy for developing a neural network-based approach to be used in connection with structural damage detection is to train a neural network to recognise different damage scenarios from the measured response of the structure such as static displacements (Szewczyk and Hajela, 1994), strain (Kudva *et al.*, 1992 and Worden *et al.*, 1993), and modal parameters (Wu *et al.*, 1992), etc. For instance, a neural network might be trained with natural frequencies as input and the corresponding damage state as output. Thus optimally, when a neural network, trained with such data, is given a set of natural frequencies as input it should be able to recognise the corresponding damage state.

Genetic algorithms are stochastic algorithms which imitate the natural processes of selection and mating to finally evolve into a high performance set of individuals. It was found that genetic algorithms are efficient optimisation algorithms compared to other exhaustive search techniques. Lately, genetic algorithms have been applied to a variety of structural dynamics problems such as model updating (Larson and Zimmerman, 1993). The application of genetic algorithms to the problem of locating and identifying structural damage can also be found in the works of Arkadan *et al.* (1994) and Hemez and Farhat (1995a).

2.6 Conclusions

Structural damage may be developed due to a variety of reasons. For proper maintenance and avoidance of catastrophic failures, timely and rapid damage diagnosis of structures is critical.

When damage occurs, the structural parameters and the modal parameters will be changed. Thus, both structural and modal parameters can be used as damage indicators in structural damage detection.

Structural damage detection techniques using measured modal data are closely related to those for model updating. Some of model updating approaches can directly be used for damage detection. However, most of model updating approaches only identify the changes in physical matrix coefficients, and some approaches may be inadequate for damage detection, e.g. first-order approximation in sensitivity methods.

Structural damage can be detected and located by various techniques using system's response information. However, it is found that to quantify the extent of structural damage using these techniques is very difficult.

Structural damage detection techniques using modal parameter information are most promising. Only limited information on measured modal parameters, such as natural frequencies and mode shapes, is required to identify structural damage, and even quantify the extent of structural damage.

Mode reduction techniques or mode shape expansion techniques can be used to overcome the difficulty caused by the limited sensor locations in test. Note that either

mode reduction techniques or mode shape expansion techniques introduce additional error, rendering them difficult to properly detect structural damage.

Consequently, it is desirable that an effective and practicable technique for structural damage detection using a minimum of measured vibration modal data should be developed.

CHAPTER 3

NON-LINEAR PERTURBATION THEORY

In order to update model or assess damage accurately, an exact relationship between the perturbation of structural parameters, such as mass and stiffness, and the perturbation of dynamic modal parameters, such as eigenvalues and eigenvectors or natural frequencies and mode shapes, has to be established. Here, a system of general nonlinear perturbation theory is developed, which can be utilised for eigendata modification, model updating, and damage identification.

3.1 Characteristic Equations

The governing equation for the structural dynamic system in finite element representation can be written as

$$M\ddot{x} + C\dot{x} + Kx = f(t) \tag{3.1}$$

where the matrices M, C, and K represent the discretised mass or inertia, damping, and stiffness distribution; $\ddot{x}$, $\dot{x}$, and x are the acceleration, velocity, and displacement vectors of the degrees of freedom (DOFs) being modelled, and $f(t)$ is the external forcing function vector. The homogeneous solutions to equation (3.1) are the eigenvalues and the eigenvectors. For simplicity, the damping terms will be ignored at the present time, thus

$$M\ddot{x} + Kx = 0 \tag{3.2}$$

Let

$$x = \phi_i \sin\omega_i t \tag{3.3}$$

where ω_i is the ith natural frequency, and ϕ_i is the corresponding mode shape. Upon substitution into equation (3.2), the relationship between the structural parameters M and K and the dynamic modal parameters ω_i and ϕ_i can be established as

$$K\phi_i - \omega_i^2 M\phi_i = 0 \tag{3.4}$$

It is clear that values of ω_i and ϕ_i are functions of the mass $\boldsymbol{M}$ and the stiffness $\boldsymbol{K}$ of the system. In other words, any changes in $\boldsymbol{M}$ and $\boldsymbol{K}$ due to the loss of mass or loss of stiffness of certain parts of the structural system will be reflected in its natural frequency and mode shape measurements. A discovery of a deviation of the measured natural frequency and mode shape with respect to those previously measured when the system was in an original condition indicates the occurrence of modification.

Rearranging equation (3.4), the characteristic equation for the original (undamaged) structural system can expressed as

$$(K - \lambda_i M)\phi_i = 0 \tag{3.5}$$

where λ_i and ϕ_i indicate the *i*th eigenvalue and the corresponding eigenvector of the characteristic equations, respectively, and λ_i is defined as

$$\lambda_i = \omega_i^2 \tag{3.6}$$

For the modified (damaged) structural system, the characteristic equation can be expressed as

$$(K^* - \lambda_i^* M^*)\phi_i^* = 0 \tag{3.7}$$

where quantities with a superscript * indicate those associated with the modified structural system.

3.2 Perturbation Theory

Suppose that the modifications of stiffness matrix and mass matrix are defined as $\Delta\boldsymbol{K}$ and $\Delta\boldsymbol{M}$, respectively. The stiffness and mass matrices for the modified structural system, therefore, can be expressed as

$$K^* = K + \Delta K \tag{3.8a}$$

$$M^* = M + \Delta M \tag{3.8b}$$

Meanwhile, the modifications of *i*th eigenvalue and the corresponding eigenvector, which are caused by the modifications of stiffness matrix and mass matrix, are defined as $\Delta\lambda_i$ and $\Delta\phi_i$, respectively. The eigenvalue and the corresponding eigenvector for the modified structural system, therefore, can be expressed as

$$\lambda_i^* = \lambda_i + \Delta\lambda_i \tag{3.9a}$$

$$\phi_i^* = \phi_i + \Delta\phi_i \tag{3.9b}$$

Upon substitution of equations (3.8a, b) and (3.9a, b), the characteristic equation for the modified structural system, equation (3.7), can be rewritten as

$$[\Delta K - (\lambda_i + \Delta\lambda_i)\Delta M]\{\phi_i + \Delta\phi_i\} + [K - (\lambda_i + \Delta\lambda_i)M]\{\phi_i + \Delta\phi_i\} = 0 \tag{3.10}$$

Premultiplying equation (3.10) by ϕ_k^T, and using the transpose of equation (3.5), yields

$$\phi_k^T[\Delta K - (\lambda_i + \Delta\lambda_i)\Delta M]\{\phi_i + \Delta\phi_i\} - ((\lambda_i + \Delta\lambda_i) - \lambda_k)\phi_k^T M\{\phi_i + \Delta\phi_i\} = 0 \tag{3.11}$$

where k ranges from 1 to N, and N is the total number of DOFs for the original structural system.

It is assumed that the mode shapes of the original structural system are mass normalised in the form

$$\phi_k^T M\phi_k = 1 \tag{3.12}$$

Premultiplying equation (3.11) by ϕ_k, then summing up these equations from 1 to N, and using equation (3.12), leads to

$$\sum_{k=1}^{N} \frac{\phi_k^T[\Delta K - (\lambda_i + \Delta\lambda_i)\Delta M]\{\phi_i + \Delta\phi_i\}}{(\lambda_i + \Delta\lambda_i) - \lambda_k}\phi_k - \{\phi_i + \Delta\phi_i\} = 0 \tag{3.13}$$

Here, only eigenvalues that differ between the original structural system and the modified structural system are considered in order to avoid the denominator of equation (3.13) vanishing.

Assuming that the mode shapes of the modified structural system are also mass normalised in a form

$$\phi_k^T M \phi_k^* = 1 \tag{3.14}$$

Using equations (3.9b) and (3.12), equation (3.14) can be rewritten as

$$\phi_k^T M \Delta\phi_k = 0 \tag{3.15}$$

Premultiplying equation (3.10) by ϕ_i^T, and using equation (3.15), yields

$$\phi_i^T [\Delta K - (\lambda_i + \Delta\lambda_i)\Delta M]\{\phi_i + \Delta\phi_i\} - \Delta\lambda_i = 0 \tag{3.16}$$

Upon substitution of equation (3.16), equation (3.13) can be rewritten as

$$\sum_{k=1,k\neq i}^{N} \frac{\phi_k^T [\Delta K - (\lambda_i + \Delta\lambda_i)\Delta M]\{\phi_i + \Delta\phi_i\}}{(\lambda_i + \Delta\lambda_i) - \lambda_k} \phi_k - \Delta\phi_i = 0 \tag{3.17}$$

It is found from equation (3.17) that the modification of an eigenvector of a structural system can be expressed as the linear combination of the original eigenvectors except the corresponding original one. Hence, the equation (3.17) can be rewritten as

$$\Delta\phi_i = \sum_{k=1,k\neq i}^{N} C_{ik}\phi_k \tag{3.18}$$

where the mode participation factor C_{ik} is defined as

$$C_{ik} = \frac{\phi_k^T [\Delta K - (\lambda_i + \Delta\lambda_i)\Delta M]\{\phi_i + \Delta\phi_i\}}{(\lambda_i + \Delta\lambda_i) - \lambda_k} \tag{3.19}$$

The above general nonlinear perturbation theory which represents the exact relationship between the perturbations of structural parameters and modal parameters can be further developed for various applications.

3.3 General Applications

Depending on the information about available parameters of the modified structural system, the general perturbation theory developed above can be utilised for various

applications, such as eigendata modification, model updating, and damage identification.

3.3.1 Eigendata modification

When the modifications of structural parameters, ΔK and ΔM, are known, the modifications of modal parameters (eigendata), $\Delta\lambda_i$ and $\Delta\phi_i$, can be computed using equations (3.16) and (3.17). These two equations can be rewritten as

$$\Delta\lambda_i = \phi_i^T[\Delta K - (\lambda_i + \Delta\lambda_i)\Delta M]\{\phi_i + \Delta\phi_i\} \tag{3.20a}$$

$$\Delta\phi_i = \sum_{k=1,k\neq i}^{N} \frac{\phi_k^T[\Delta K - (\lambda_i + \Delta\lambda_i)\Delta M]\{\phi_i + \Delta\phi_i\}}{(\lambda_i + \Delta\lambda_i) - \lambda_k}\phi_k \tag{3.20b}$$

In order to obtain the exact modifications of modal parameters, an iterative procedure has to be employed. When the modifications of structural parameters are small enough, only first-order approximation may be sufficient to obtain the modifications of modal parameters. The set of nonlinear equations (3.20a, b), then, can be simplified to linear relationship in the form

$$\Delta\lambda_i = \phi_i^T[\Delta K - \lambda_i\Delta M]\phi_i \tag{3.21a}$$

$$\Delta\phi_i = \sum_{k=1,k\neq i}^{N} \frac{\phi_k^T[\Delta K - \lambda_i\Delta M]\phi_i}{\lambda_i - \lambda_k}\phi_k \tag{3.21b}$$

The above linear relationship is very commonly utilised for sensitivity analysis of modal parameters, such as in the works of Beliveau *et al.* (1996) and Chondros and Dimarogonas (1989).

3.3.2 Model updating

When the modifications of modal parameters, $\Delta\lambda_i$ and/or $\Delta\phi_i$, are known, the modifications of structural parameters, ΔK and ΔM, can be determined using the above general perturbation theory. Different procedures are utilised for model updating depending on information about modal data available.

Information on complete λ_i^* and ϕ_i^* available

Rewriting the characteristic equation for the modified structural system, equation (3.10), yields

$$[\Delta K - \lambda_i^* \Delta M]\phi_i^* + [K - \lambda_i^* M]\phi_i^* = 0 \tag{3.22}$$

The modifications of structural parameters, ΔK and ΔM, can directly be determined using above linear equation, as sufficient information about modal data is available.

Information on only λ_i^* available

A set of non-linear equations has to be utilised to solve for the modifications of structural parameters since the eigenvectors for the modified structural system are not available.

Rewriting equation (3.16), leads to

$$\phi_i^T [\Delta K - \lambda_i^* \Delta M]\{\phi_i + \Delta\phi_i\} = \Delta\lambda_i \tag{3.23}$$

while the modification of eigenvectors can be calculated using equation (3.17), which is rewritten as

$$\Delta\phi_i = \sum_{k=1, k\neq i}^{N} \frac{\phi_k^T [\Delta K - \lambda_i^* \Delta M]\{\phi_i + \Delta\phi_i\}}{\lambda_i^* - \lambda_k} \phi_k \tag{3.24}$$

The first-order approximation can be obtained by neglecting the higher order terms in equation (3.23), which leads to the linear relationship in the form

$$\phi_i^T [\Delta K - \lambda_i^* \Delta M]\phi_i = \Delta\lambda_i \tag{3.25}$$

This linear equation is widely used for model updating, such as in the works of Lallement (1988), Link (1990b), Natke and Cempel (1997). It should be noted that the linear equation may be insufficient, if a large modification of structural parameters has to be updated.

Information on λ_i^* and incomplete ϕ_i^* available

When some DOF's readings of the modified structural system are not measured, the eigenvector of the modified structural system becomes incomplete, which is assumed in the form

$$\phi_i^* = \varphi_i^a + \Delta\phi_i^u \tag{3.26}$$

where φ_i^a is a vector combining the available DOF's readings $\phi_i^{a^*}$ and the corresponding original eigenvector for the remaining dimension ϕ_i^u, and $\Delta\phi_i^u$ is a vector containing the modification of the unknown DOF's readings. The detailed information about these vectors and their relationship can be found in Section 6.1.

Rewriting equation (3.13), and using equation (3.26), yields the following set of equations constructed by only the equations in which the DOF's readings are available, i.e.,

$$\sum_{k=1}^{N} \frac{\phi_k^T[\Delta K - \lambda_i^* \Delta M]\{\varphi_i^a + \Delta\phi_i^u\}}{\lambda_i^* - \lambda_k} \phi_k^a - \phi_i^{a^*} = 0 \tag{3.27}$$

where ϕ_k^a is the original eigenvector restricted to the same dimension as $\phi_i^{a^*}$, and $\Delta\phi_i^u$ can be calculated using equation (3.17), which is rewritten as

$$\Delta\phi_i^u = \sum_{k=1,k\neq i}^{N} \frac{\phi_k^T[\Delta K - \lambda_i^* \Delta M]\{\varphi_i^a + \Delta\phi_i^u\}}{\lambda_i^* - \lambda_k} \phi_k^u \tag{3.28}$$

where ϕ_k^u is the original eigenvector restricted to the dimension for the unknown DOF's readings.

A set of nonlinear equations (3.27) and (3.28) can be utilised to solve for the modifications of structural parameters, ΔK and ΔM.

The first-order approximation for equation (3.27) can be obtained by neglecting the modification of unknown DOF's readings, which leads to the linear relationship in the form

$$\sum_{k=1}^{N} \frac{\phi_k^T[\Delta K - \lambda_i^* \Delta M]\varphi_i^a}{\lambda_i^* - \lambda_k} \phi_k^a - \phi_i^{a^*} = 0 \tag{3.29}$$

and, an estimate of the modifications of structural parameters can be obtained using the above linear equation.

The application of general perturbation theory to damage identification will be discussed in Section 3.5.

3.4 System Parameters

System parameters, such as coefficients of stiffness or mass matrix, and parameters for material properties and geometric properties, are employed to represent the modifications of structural parameters, e.g., stiffness matrix and/or mass matrix.

3.4.1 Matrix coefficient level

The coefficients of the modification of stiffness matrix δk_{st} and mass matrix δm_{st} can be computed using equations (3.8a) and (3.8b)

$$\delta k_{st} = k_{st}^{*} - k_{st} \tag{3.30}$$

$$\delta m_{st} = m_{st}^{*} - m_{st} \tag{3.31}$$

where k_{st}^{*}, m_{st}^{*} and k_{st}, m_{st} indicate the coefficients of stiffness matrix and mass matrix for the modified structural system and for the original structural system, respectively, and s and t are DOF numbers. Here, each coefficient of the modification of stiffness matrix and mass matrix represents an independent system parameter, which will be updated using information on the measured modal data.

Note that, in general, the proposed method that utilises coefficients of stiffness and/or mass matrix as system parameters is only suitable for model updating. It may not be applicable to damage identification since no information on specific damage for structural members or elements can be provided. In addition, the physical connectivity of the original model in the updated stiffness and mass matrices may not be preserved using some methods for model updating.

3.4.2 Element level

It is assumed that the modification of stiffness matrix and mass matrix can be expressed as

$$\Delta K = \sum_{e=1}^{NE} \Delta K^{(e)} \tag{3.32}$$

$$\Delta M = \sum_{e=1}^{NE} \Delta M^{(e)} \tag{3.33}$$

where NE denotes the total number of elements considered, and $\Delta K^{(e)}$ and $\Delta M^{(e)}$ are defined as

$$\Delta K^{(e)} = K^{(e)}(p_j + \delta p_j) - K^{(e)}(p_j) \tag{3.34}$$

$$\Delta M^{(e)} = M^{(e)}(p_j + \delta p_j) - M^{(e)}(p_j) \tag{3.35}$$

where p_j indicates a generic system parameter related to structural element stiffness and/or mass matrix such as Young's modulus, shear modulus, mass density, cross-sectional area, thickness, or moment of inertia, j ranges from 1 to NP where NP indicates the total number of system parameters characterising a given element level stiffness and/or mass matrix, and δp_j represents the perturbation of system parameter p_j.

Using a first-order Taylor series expansion, and neglecting the higher order terms, equations (3.34) and (3.35) can be rewritten as

$$\Delta K^{(e)} = \sum_{j=1}^{NP} \frac{\partial K^{(e)}}{\partial p_j} \delta p_j = \sum_{j=1}^{NP} K_j^{(e)} \delta p_j \tag{3.36}$$

$$\Delta M^{(e)} = \sum_{j=1}^{NP} \frac{\partial M^{(e)}}{\partial p_j} \delta p_j = \sum_{j=1}^{NP} M_j^{(e)} \delta p_j \tag{3.37}$$

where each matrix $K_j^{(e)}$ and $M_j^{(e)}$ describes the sensitivity of the element level stiffness matrix and mass matrix to a variation in parameter p_j, respectively.

Note that system parameters characterising an element level are often applied to framed structures such as trusses and frames, where a structural member can naturally be considered as a structural element.

3.4.3 Gauss point level

When a structural element stiffness matrix is computed from numerical integrations, the modification of structural element stiffness matrix and mass matrix in equations (3.32) and (3.33), $\Delta K^{(e)}$ and $\Delta M^{(e)}$, can be expressed as

$$\Delta K^{(e)} = \sum_{g=1}^{NG} \Delta K^{(g)} \tag{3.38}$$

$$\Delta M^{(e)} = \sum_{g=1}^{NG} \Delta M^{(g)} \tag{3.39}$$

where NG denotes the total number of integrating points for Gauss integrations (Gauss points) in a structural element, and $\Delta K^{(g)}$ and $\Delta M^{(g)}$ are defined as

$$\Delta K^{(g)} = K^{(g)}(p_j + \delta p_j) - K^{(g)}(p_j) \tag{3.40}$$

$$\Delta M^{(g)} = M^{(g)}(p_j + \delta p_j) - M^{(g)}(p_j) \tag{3.41}$$

where p_j indicates a generic system parameter related to the contribution of a Gauss point in a structural element to the element stiffness and/or mass matrix.

Using a first-order Taylor series expansion, and neglecting the higher order terms, equations (3.40) and (3.41) can be rewritten as

$$\Delta K^{(g)} = \sum_{j=1}^{NP} \frac{\partial K^{(g)}}{\partial p_j} \delta p_j = \sum_{j=1}^{NP} K_j^{(g)} \delta p_j \tag{3.42}$$

$$\Delta M^{(g)} = \sum_{j=1}^{NP} \frac{\partial M^{(g)}}{\partial p_j} \delta p_j = \sum_{j=1}^{NP} M_j^{(g)} \delta p_j \tag{3.43}$$

where NP indicates the total number of system parameters characterising a given contribution of a Gauss point in a structural element to the element stiffness and/or mass matrix, and each matrix $K_j^{(g)}$ and $M_j^{(g)}$ describes the sensitivity of the contribution of a Gauss point to the element stiffness matrix and mass matrix to a variation in parameter p_j, respectively.

Note that system parameters characterising a Gauss point level are generally applied to continuum problems such as plane stress/strain problems, plate bending problems, and 3-D solid problems, where various types of finite element mesh may be produced to model these structures. It should be noted that the method discussed here can also be applicable to framed structures, when structural element stiffness and/or mass matrix are computed using the Gauss integration.

3.4.4 Subsystem level

The modifications of system parameters associated with subsystems of the total system are introduced to reduce computational expenditure and related numerical problems.

The modification of stiffness matrix and mass matrix are assumed as

$$\Delta K = \sum_{s=1}^{NS} \Delta K^{(s)} \tag{3.44}$$

$$\Delta M = \sum_{s=1}^{NS} \Delta M^{(s)} \tag{3.45}$$

where NS denotes the total number of subsystems considered, and $\Delta K^{(s)}$ and $\Delta M^{(s)}$ are defined as

$$\Delta K^{(s)} = K^{(s)}(p_j + \delta p_j) - K^{(s)}(p_j) \tag{3.46}$$

$$\Delta M^{(s)} = M^{(s)}(p_j + \delta p_j) - M^{(s)}(p_j) \tag{3.47}$$

where p_j indicates a generic system parameter related to stiffness and/or mass matrix for a subsystem.

Using a first-order Taylor series expansion, and neglecting the higher order terms, equations (3.46) and (3.47) can be rewritten as

$$\Delta K^{(s)} = \sum_{j=1}^{NP} \frac{\partial K^{(s)}}{\partial p_j} \delta p_j = \sum_{j=1}^{NP} K_j^{(s)} \delta p_j \tag{3.48}$$

$$\Delta M^{(s)} = \sum_{j=1}^{NP} \frac{\partial M^{(s)}}{\partial p_j} \delta p_j = \sum_{j=1}^{NP} M_j^{(s)} \delta p_j \tag{3.49}$$

where NP indicates the total number of system parameters characterising a given subsystem level stiffness and/or mass matrix, and each matrix $K_j^{(s)}$ and $M_j^{(s)}$ describes the sensitivity of stiffness matrix and mass matrix at subsystem level to a variation in parameter p_j, respectively.

Note that system parameters characterising a subsystem level are usually applied to very large scale systems, where the whole system can be divided into a number of

subsystems. In general, the subsystems represent a single element or a group of elements of the structure having the same assumed geometry, material properties, boundary conditions, and modelling assumptions. A significant reduction of system parameters can be achieved by judiciously grouping the structural elements with the same characteristics. Moreover, modifications of structural parameters at a local area may directly be obtained, when the chosen system parameters characterise the local area in a subsystem where local modifications possibly occur. However, it may not be applicable for further model updating or damage identification within a subsystem, after system parameters at subsystem level are determined.

It should be pointed out that wherever $K^{(e)}$, $M^{(e)}$, $K^{(g)}$, $M^{(g)}$, $K^{(s)}$, or $M^{(s)}$ is a linear function of a parameter p_j, the expansion (3.36), (3.37), (3.42), (3.43), (3.48), or (3.49) can handle arbitrarily large parameter perturbation δp_j. However, when $K^{(e)}$, $M^{(e)}$, $K^{(g)}$, $M^{(g)}$, $K^{(s)}$, or $M^{(s)}$ is a higher order or transcendental function of p_j, only small perturbation δp_j should be considered in principle. Example of sensitivity matrices $K_{,p}^{(e)}$ and $M_{,p}^{(e)}$ is given in Appendix A.3.

3.5 Application to Damage Identification

It is assumed that a sound finite element model of the structure has been developed before structural damage has occurred.

3.5.1 Damage parameter

Since the effects of damage in a structure on stiffness can be represented by reducing its Young's modulus in most cases, without a loss of generality, a scalar damage model is assumed using the theory of system parameter discussed early, i.e., the change of structural stiffness matrix can be expressed in the form

$$\Delta K = \sum_{j=1}^{NEG} \alpha_j K_j \tag{3.50}$$

where *NEG* is the total number of structural elements if damage parameters characterise an element level or the total number of Gauss points if damage parameters characterise a Gauss point level, K_j is the contribution of element j or the contribution of Gauss point j to the global stiffness matrix, α_j is the damage parameter for the jth element or the jth Gauss point and ranges from 0 to -1.

It should be pointed out that the damage parameter α_j is capable of providing information about not only the location of damage but also the extent of damage in a structure. For example, for damage detection, structural damage exists in a structure if any damage parameter α_j does not equal zero; for damage location, the jth element or the jth Gauss point is considered as the damaged one if the damage parameter α_j is not equal to zero; for damage quantification, the extent of structural damage at jth element or jth Gauss point is determined if the magnitude of the damage parameter α_j is calculated. Consequently, damage in a structure can be detected, located, and quantified when the damage parameter α_j is determined.

It will be postulated that the mass distribution of the system remains either unchanged or is changed by only a known quantity. This is a reasonable assumption because most structural damage for engineering structures will result in stiffness losses instead of complete separation or breakage with a loss of mass. Also, for certain engineering structures such as the satellite, the machine, the offshore platform, and the large span bridge, the major contribution to the mass matrix comes from nonload-carrying components such as equipments, fuel tanks, and pavements. These weights can be often estimated with high level of accuracy.

Here, it is assumed that the structural mass matrix remains unchanged, i. e.,

$$\Delta M = 0 \tag{3.51}$$

3.5.2 Governing equations

In order to determine damage parameter α_j, different governing equations can be developed depending on the available information about different types of modal data.

Information on complete λ_i^* and ϕ_i^* available

Using equations (3.50) and (3.51), the characteristic equation for the damaged structure, equation (3.10), can be rewritten as

$$\sum_{j=1}^{NEG} K_j \phi_i^* \alpha_j + [K - \lambda_i^* M]\phi_i^* = 0 \tag{3.52}$$

This linear governing equation can directly be utilised to solve for damage parameter.

Information on only λ_i^* available

A set of governing equations associated with the damage parameter α_j and the mode participation factor C_{ik} have to be developed since the eigenvectors for the damaged structure are not available.

Using equations (3.18), (3.50) and (3.51), equation (3.16) can be rewritten as

$$\sum_{j=1}^{NEG} \phi_i^T K_j \phi_i \alpha_j + \sum_{j=1}^{NEG} \sum_{l=1, l\neq i}^{N} \phi_i^T K_j \phi_l C_{il} \alpha_j - \Delta\lambda_i = 0 \qquad (3.53)$$

and equation (3.19) as

$$\sum_{j=1}^{NEG} \phi_k^T K_j \phi_i \alpha_j + \sum_{j=1}^{NEG} \sum_{l=1, l\neq i}^{N} \phi_k^T K_j \phi_l C_{il} \alpha_j - (\lambda_i^* - \lambda_k) C_{ik} = 0 \qquad (3.54)$$

which, after rewriting, yields a recursive relationship

$$C_{ik} = \frac{\sum_{j=1}^{NEG} \phi_k^T K_j \phi_i \alpha_j + \sum_{j=1}^{NEG} \sum_{l=1, l\neq i,k}^{N} \phi_k^T K_j \phi_l \alpha_j C_{il}}{\lambda_i^* - \lambda_k - \sum_{j=1}^{NEG} \phi_k^T K_j \phi_k \alpha_j} \qquad (3.55)$$

The first-order approximation can be obtained by neglecting the higher order terms in equation (3.53), which leads to the linear relationship in the form

$$\sum_{j=1}^{NEG} \phi_i^T K_j \phi_i \alpha_j - \Delta\lambda_i = 0 \qquad (3.56)$$

The above linear equation is often utilised for damage detection, such as in the works of Cawley and Adams (1979), Hassiotis and Jeong (1993), Hearn and Testa (1991), Natke and Cempel (1991). It should be pointed out that this linear equation may be insufficient for damage identification, in particular for the location and the quantification of damage in a structure.

Information on λ_i^* and incomplete ϕ_i^* available

Using equations (3.26), (3.50) and (3.51), equation (3.13) leads to the following set of equations constructed by only the equations for which the DOF's readings for the damaged mode shapes are available, i.e.,

$$\sum_{j=1}^{NEG}\sum_{k=1}^{N}\frac{\phi_k{}^T K_j\{\varphi_i{}^a+\Delta\phi_i{}^u\}}{\lambda_i^{\bullet}-\lambda_k}\phi_k{}^a\alpha_j-\phi_i{}^{a^{\bullet}}=0 \tag{3.57}$$

where $\Delta\phi_i{}^u$ can be calculated using equation (3.18), which is rewritten as

$$\Delta\phi_i{}^u=\sum_{k=1,k\neq i}^{N}C_{ik}\phi_k{}^u \tag{3.58}$$

where the mode participation factor C_{ik} can be obtained from equation (3.55) using an iterative solution procedure.

The first-order approximation for equation (3.57) can be obtained by neglecting the change of unknown DOF's readings, which leads to a linear relationship of the form

$$\sum_{j=1}^{NEG}\sum_{k=1}^{N}\frac{\phi_k{}^T K_j\varphi_i{}^a}{\lambda_i^{\bullet}-\lambda_k}\phi_k{}^a\alpha_j-\phi_i{}^{a^{\bullet}}=0 \tag{3.59}$$

The above linear equation can directly be used for estimating damage parameters.

Depending on the available information about modal data, different governing equations developed here for damage identification will be applied in further chapters to solve for the damage parameters using various computational techniques.

3.6 Conclusions

A novel general non-linear perturbation theory is developed, which can provide an exact relationship between the perturbations of structural parameters and the associated modal parameters. Different sets of system parameters characterising structural parameters at different levels are discussed, which can be utilised for different types of structures and for different purposes such as model updating or damage identification. Depending on the available information about parameters of the modified structural system, various general governing equations are developed, which can be used for general applications, such as eigendata modification, model updating, and damage identification.

CHAPTER 4

DAMAGE IDENTIFICATION FROM COMPLETE MODAL DATA

A set of governing equations based on the characteristic equations for the damaged structures are developed when information about the complete modal data for the damaged structure (damaged mode), e.g., the damaged natural frequency and the corresponding mode shape, are available. Several computational procedures based on the derived governing equations are presented to solve for the damage parameters. The effectiveness of these techniques to both locate and quantify structural damage is studied for the case when a limited amount of measured data exists, in particular for the frequently encountered case when the information about only a single arbitrary complete damaged mode is available. It is also argued that the information on locally complete modal data can be utilised to estimate local structural damage. In addition, the effects of the noise in modal data to the identification of structural damage are investigated using inconsistent mode shapes. Finally, numerical examples for statically determinate trusses and statically indeterminate trusses are included to demonstrate the effectiveness of the proposed methods.

4.1 Governing Equations

When information about complete damaged mode is available, the linear equation derived from the characteristic equation for the damaged structure, equation (3.52), can be rewritten as

$$A^{(i)}\alpha + b^{(i)} = 0 \tag{4.1}$$

where i represents the ith damaged mode used, α is the vector of damage parameters, $A^{(i)}$ and $b^{(i)}$ can be interpreted as the eigenmode-stiffness sensitivity matrix and vector associated with ith damaged mode, respectively. The coefficients for $A^{(i)}$ and $b^{(i)}$ are defined as

$$a_{kj}^{(i)} = \sum_{l=1}^{N} K_{(kl)j}\phi_{(l)i}^{*} \tag{4.2a}$$

$$b_k^{(i)} = [K - \lambda_i^* M]\phi_i^* \tag{4.2b}$$

where k and l indicate the numbers of DOFs.

It is assumed that a total NL number of damaged modes are available. Therefore, equation (4.1) can be rewritten as

$$A\alpha + b = 0 \tag{4.3}$$

where A and b are the eigenmode-stiffness sensitivity matrix and vector associated with the total NL damaged modes, respectively, defined as

$$A = \sum_{i=1}^{NL} A^{(i)} \tag{4.4a}$$

$$b = \sum_{i=1}^{NL} b^{(i)} \tag{4.4b}$$

Note that there are NEG number of unknowns (damage parameters) and a total number of equations $NEQ=NL\times N$ in (4.3). In principle, a solution to equation (4.3) might not exist, since the number of unknowns NEG and the total number of equations NEQ may not be equal. Three different cases arise depending on NEG and NEQ.

Case 1, $NEG>NEQ$

If the number of unknowns is greater than the number of equations, equation (4.3) yields an infinite number of solutions. An optimal solution can be obtained by minimising the Euclidian norm of damage parameters subject to equation (4.3).

The procedure can be formulated as

$$\Pi = \tfrac{1}{2}\alpha^T\alpha + \mu^T(A\alpha + b) \tag{4.5}$$

where μ is a vector of Lagrange multipliers. The minimisation procedure will provide

$$\partial\Pi/\partial\alpha = 0 \tag{4.6a}$$

$$\partial\Pi/\partial\mu = 0 \tag{4.6b}$$

which yields

$$\alpha = -A^{+}b \tag{4.7}$$

where A^{+} is the Moore-Penrose pseudo-inverse of matrix A, defined as

$$A^{+} = A^{T}[AA^{T}]^{-1} \tag{4.8}$$

Case 2, *NEG<NEQ*

If the number of equations is greater than the number of unknowns, in general, no exact solution to equation (4.3) exists, and any approximate solution to the equation will lead to residual errors of the equation. On the other hand, when information on the measured complete modes for the damaged structure is employed, the left side of equation (4.3) will often give the equation errors instead of the null vector due to errors existing in measurements. Therefore, the equation errors, which can be interpreted as residual forces, are defined as

$$\pi = A\alpha + b \tag{4.9}$$

An approximate solution can be obtained by minimising the Euclidian norm of the errors. In order to choose a relative emphasis of the components of the vector norm being minimised, a weighted norm is employed and defined as

$$\left\|\pi^{2}\right\| = \pi^{T}W\pi \tag{4.10}$$

where W is the weighting matrix which should be positive definite.

The minimisation procedure will provide

$$\partial\left\|\pi^{2}\right\|/\partial\alpha = 0 \tag{4.11}$$

which leads to

$$\alpha = -(A^{T}WA)^{-1}A^{T}Wb \tag{4.12}$$

Case 3, *NEG=NEQ*

when the number of unknowns is equal to the number of equations, an exact solution to equation (4.3) can be obtained, i.e.,

$$\alpha = -A^{-1}b \tag{4.13}$$

Consequently, structural damage parameters can be determined from the above governing equations for different cases depending on the amount of available information about modal data.

4.2 Weighting Matrices

In order to define weighting matrix W introduced in equation (4.10), two cases associated with the minimisation of residual force and residual energy are discussed.

4.2.1 Minimisation of residual force

If the weighting matrix W is assumed to be a unit matrix, i.e.,

$$W = I \tag{4.14}$$

where I is a unit matrix, then the computational procedure for case 2 discussed above can be interpreted as the minimisation of Euclidian norm of residual forces when equations (4.9) and (4.10) are considered.

Consequently, the governing equation for case 2, equation (4.12), can be rewritten as

$$\alpha = -(A^T A)^{-1} A^T b \tag{4.15}$$

The procedure, which is used for estimating structural damage parameters in the sense of Minimisation of Residual Force, is therefore referred to as the Procedure **MRF**.

4.2.2 Minimisation of residual energy

Here, the weighting matrix W is chosen as

$$W = M^{-1} = \Phi\Phi^T \tag{4.16}$$

where Φ is the mass normalised eigenvector matrix of the original structure. Using equation (4.9), the residual energy can be defined as

$$e = \Phi^T \pi \tag{4.17}$$

then, considering equations (4.17) and (4.10) the computational procedure for case 2 can be interpreted as the minimisation of Euclidian norm of residual energy.

Consequently, equation (4.12) can be rewritten as

$$\alpha = -[(\Phi^T A)^T (\Phi^T A)]^{-1} (\Phi^T A)^T \Phi^T b \tag{4.18a}$$

or

$$\alpha = -[A^T M^{-1} A]^{-1} A^T M^{-1} b \tag{4.18b}$$

The procedure used for estimating structural damage parameters in the sense of Minimisation of Residual Energy is consequently referred to as the Procedure **MRE**.

4.3 Local Damage Identification

When information about locally complete damaged mode is available, i.e., the DOF's readings for the damaged structure at a given local area are completely measured, structural damage in this local area can be estimated using the following procedure.

In order to ensure that the locally complete damaged DOF's readings $\psi_i^{a^*}$ have a scale close to the corresponding dimension of the original eigenvector ϕ_i^a, a scaled vector containing the locally complete damaged DOF's readings available, $\phi_i^{a^*}$, can be computed from

$$\phi_i^{a^*} = \beta_i \psi_i^{a^*} \tag{4.19}$$

where β_i is the Mode Scale Factor (*MSF*) for *i*th locally complete mode shape of the damaged structure, defined as

$$\beta_i = \frac{\phi_i^{a^T} \psi_i^{a^*}}{\psi_i^{a^{*T}} \psi_i^{a^*}} \tag{4.20}$$

Therefore, the mode shape of the damaged structure can approximately be computed by combining the scaled locally complete damaged DOF's readings available and the corresponding original eigenvector for the remaining DOFs up to the full dimension, i.e.,

$$\phi_i^* \approx \begin{Bmatrix} \phi_i^{a^*} \\ \phi_i^u \end{Bmatrix} \tag{4.21}$$

where ϕ_i^u is the *i*th original eigenvector restricted to the remaining dimension.

Consequently, structural damage in a local area can be estimated if the above approximate damaged mode shape is applied to the governing equations developed previously. Note that only the procedure for minimisation of residual force, Procedure **MRF**, is considered in order to keep the sparse and banded features of the eigenmode-stiffness sensitivity matrix.

4.4 Solution Algorithms

Structural damage identification techniques using modal data can often lead to indeterminate or non-unique solutions to ill-conditioned algebraic equations, which are in general rather sensitive to computational accuracy. In order to obtain a stable and accurate solution, solution algorithms, such as the Singular Value Decomposition (SVD) method (e.g. in the work of Maia (1989)), should be applied to solve for the ill-conditioned equations.

4.4.1 SVD method

The SVD of an $M \times N$ real matrix A with $M \geq N$ is expressed by

$$A_{M\times N} = U_{M\times M} \Sigma_{M\times N} V_{N\times N}^T \tag{4.22}$$

where U and V are orthogonal matrices, i.e.,

$$U^T U = U U^T = I \tag{4.23a}$$

$$V^T V = V V^T = I \tag{4.23b}$$

and Σ is a real matrix with elements

$$\begin{cases} \sigma_{ij} = \sigma_i , & for \ \ i = j \\ \sigma_{ij} = 0 , & for \ \ i \neq j \end{cases} \tag{4.24}$$

The values σ_i are called the singular values of matrix A.

4.4.2 Application to pseudo-inverse

Using equations (4.22) and (4.23a, b), the Moore-Penrose pseudo-inverse of matrix A, defined in equation (4.8), can be expressed as

$$A^+_{N\times M} = V_{N\times N} \Sigma^+_{N\times M} U^T_{M\times M} \tag{4.25}$$

where Σ^+ is an $N\times M$ real diagonal matrix comprising the inverse values of the non-zero singular values σ_i.

Each element of A^+ can be computed from

$$a_{ij}^+ = \sum_{\sigma_k \neq 0} \frac{1}{\sigma_k} v_{ik} u_{jk} \tag{4.26}$$

where v_{ik} and u_{jk} are the corresponding elements of matrix V and matrix U^T. Note that, in practical terms, only the singular values that are larger than a critical value are considered.

After the Moore-Penrose pseudo-inverse of matrix A is obtained, structural damage parameters can be determined using equation (4.7).

4.4.3 Application to ill-conditioned system

For an inverse problem such as a structural damage identification, in general, the eigenmode-stiffmess sensitivity matrix A in equations (4.13) and the weighted matrix $A^T W A$ in equation (4.12) are ill-conditioned.

Using equation (4.22), the inverse of matrix A can be computed from

$$A^{-1} = V\Sigma^{-1}U^T \tag{4.27}$$

Upon substitution of equation (4.27), equation (4.13) can be rewritten as

$$\alpha = -\sum_{\sigma_k > \tau} \frac{1}{\sigma_k}(u_k^T b)v_k \tag{4.28}$$

where u_k and v_k are the corresponding column vectors of matrix U and matrix V. Again, only the singular values that are larger than the critical value τ are considered.

Structural damage parameters can directly be obtained from equation (4.28) if the SVD of matrix A is available. Moreover, the above procedure can be applied to equations (4.15) and (4.18a, b) in order to determine the structural damage parameters for the case of *NEG<NEQ* as discussed earlier in Section 4.2.

4.5 Numerical Examples

Two examples, a plane statically indeterminate truss and a plane statically determinate truss, are treated to demonstrate the effectiveness of the proposed procedures using information about damaged modal readings for all DOF's or locally complete DOF's.

4.5.1 Plane statically indeterminate truss

Figure 4.1 illustrates the statically indeterminate plane truss with 18 nodes, 33 DOFs and 41 structural members. All members have an identical elasticity modulus E=2.1×10^{11}N/m^2, and density ρ=7860kg/m^3. The geometry of the structure and the element numbering are also shown in Figure 4.1. The cross sections of all members are assumed to have the same area with 0.006m^2.

Hypothetical damage scenario in the structure is induced in several elements by reducing the Young's modulus as shown in Figure 4.1. A finite element analysis was performed for both the original and the damaged cases, and eigenfrequencies and the corresponding mode shapes have been calculated. In the following, the computed damaged modes are used in place of the modal information about the damaged structure, which would normally be furnished from experiments.

A series of inverse damage identification analyses are now initiated, aimed at reconstructing the damage parameters α_j for the given hypothetical damage scenario. It is assumed that only one or two modes of the damaged structure are available to determine the location and the extent of structural damage. A comparison is made for the estimates obtained from the two procedures, Procedure **MRF** and Procedure **MRE**. Moreover, predictions of the damage scenario from a single damaged mode are compared with the exact solution, which is achieved when the information about two damaged modes is available. The results of the damage prediction are depicted in Figures 4.2(a) and (b), and Figures 4.3(a) and (b) for different damaged mode information and different procedures, indicating that satisfactory results can be obtained using any of the single damaged mode and any of the two procedures.

It can be seen from the results that the proposed procedures are capable of successfully predicting both the location and the extent of structural damage. Although the truss considered here is statically indeterminate, using the information about a single damaged mode only, the location and the extent of the structural damage can be approximated quite well. On closer inspection, it can be seen that the location of damage in element 31 (shown in Figure 4.2(a)) can not be identified using the damaged mode 2, and the extent of damage around element 7 (shown in Figure 4.2(b)) can not be quantified well when using damaged mode 3 as a single mode. The reason for these discrepancies is probably that the modal strain energy distributions contained in these structural elements for the adopted mode are very small. However, the location and the extent of structural damage of the statically indeterminate structures can be predicted exactly using the information on a pair of damaged modes (shown in Figure 4.3(a) and (b)) irrespective of whether the Procedure **MRF** or the Procedure **MRE** used.

Parameters of the Problem	
Total DOFs	33
Structural members	41
Damage parameters	41

Hypothetical Damage Scenario

Element No	Damage Amount
7, 9, 11	-30%
31, 34, 35	-10%

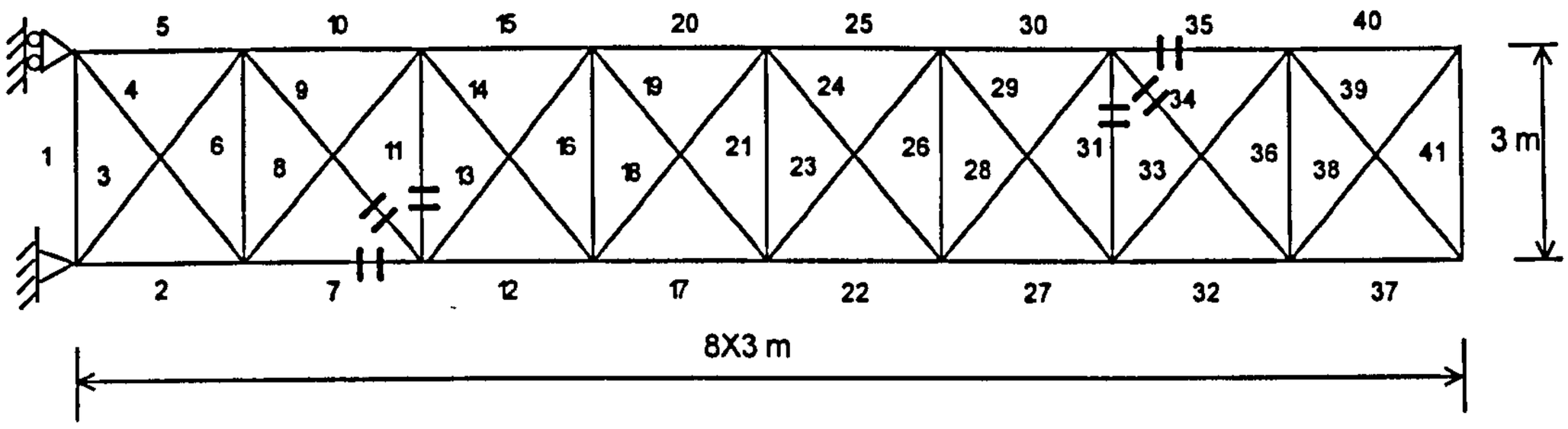

Figure 4.1 Statically indeterminate model plane truss problem

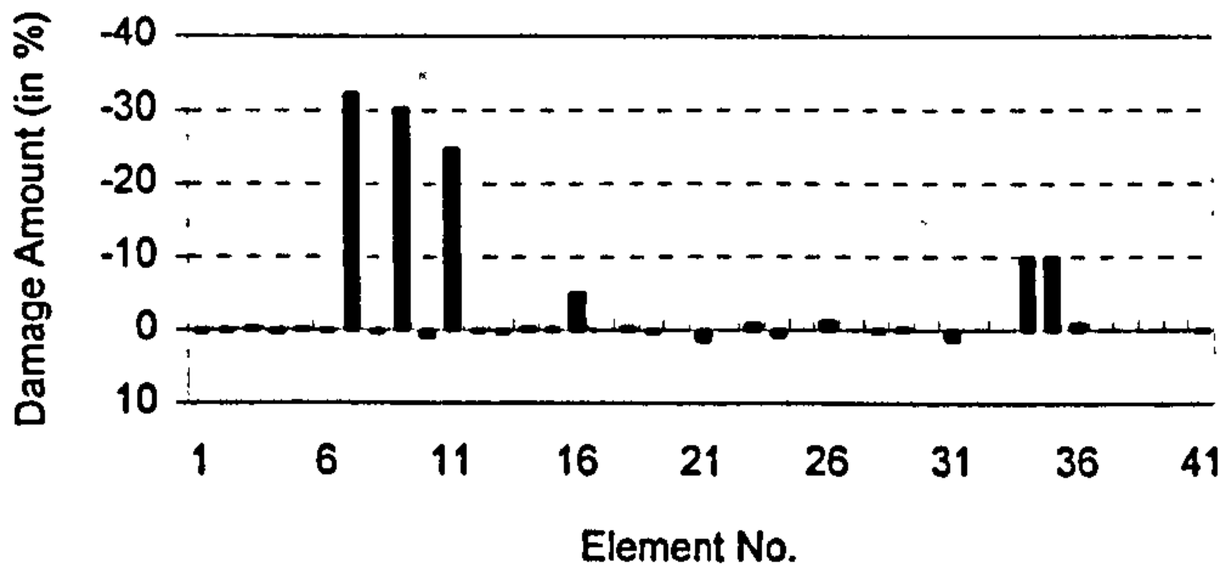

Figure 4.2(a) Information on a single damaged mode 2 used

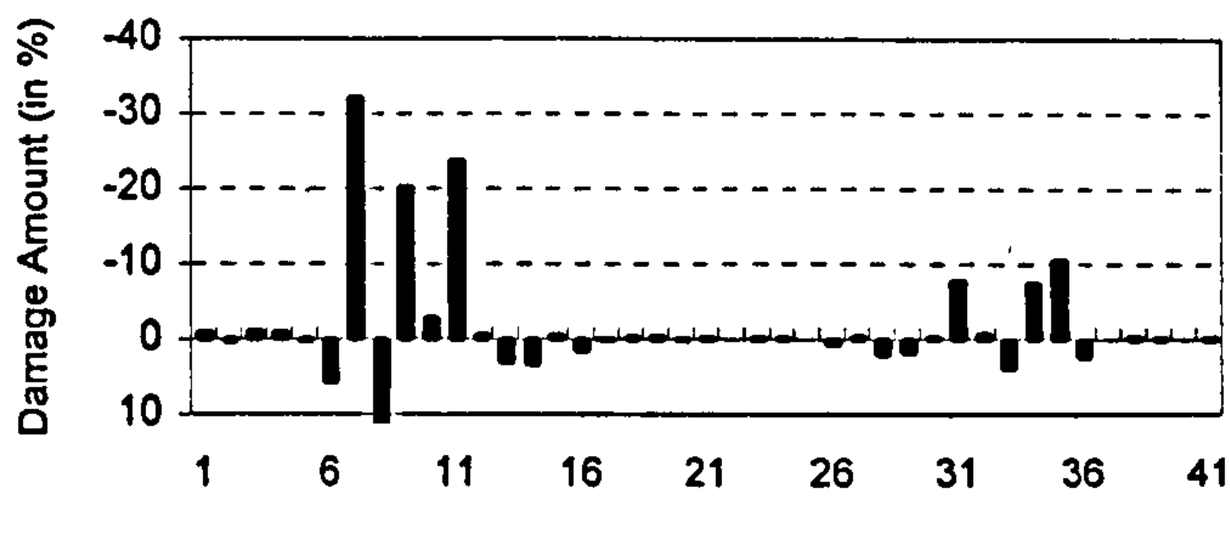

Figure 4.2(b) Information on a single damaged mode 3 used

Figure 4.2 Inverse predictions for the given damage scenario, Procedure **MRF** used

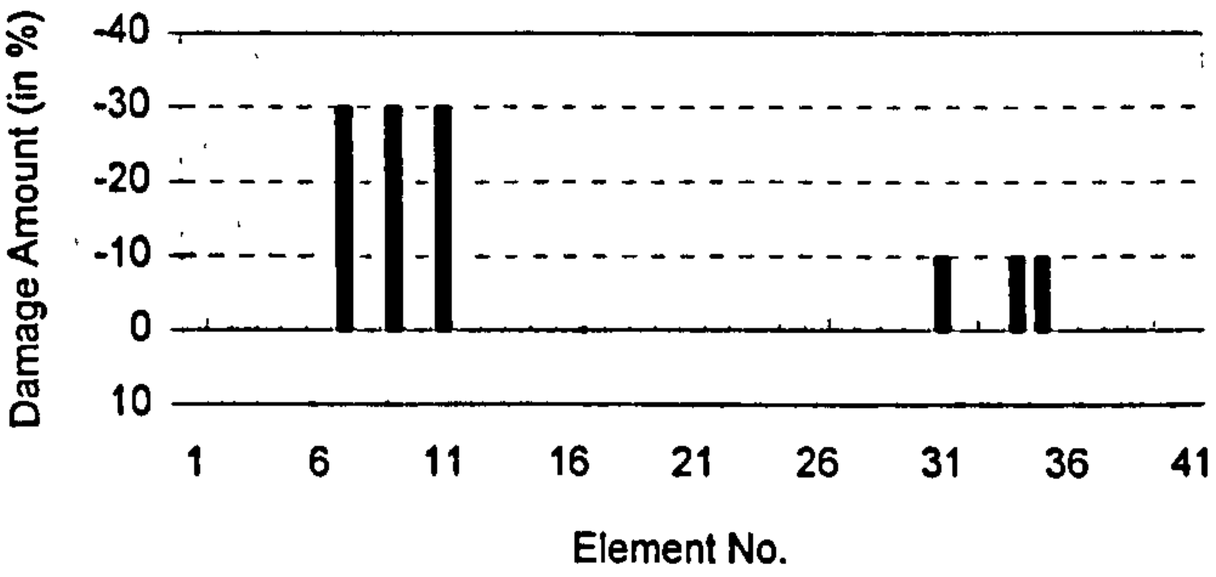

Figure 4.3(a) Procedure **MRF** based inverse predictions of damage

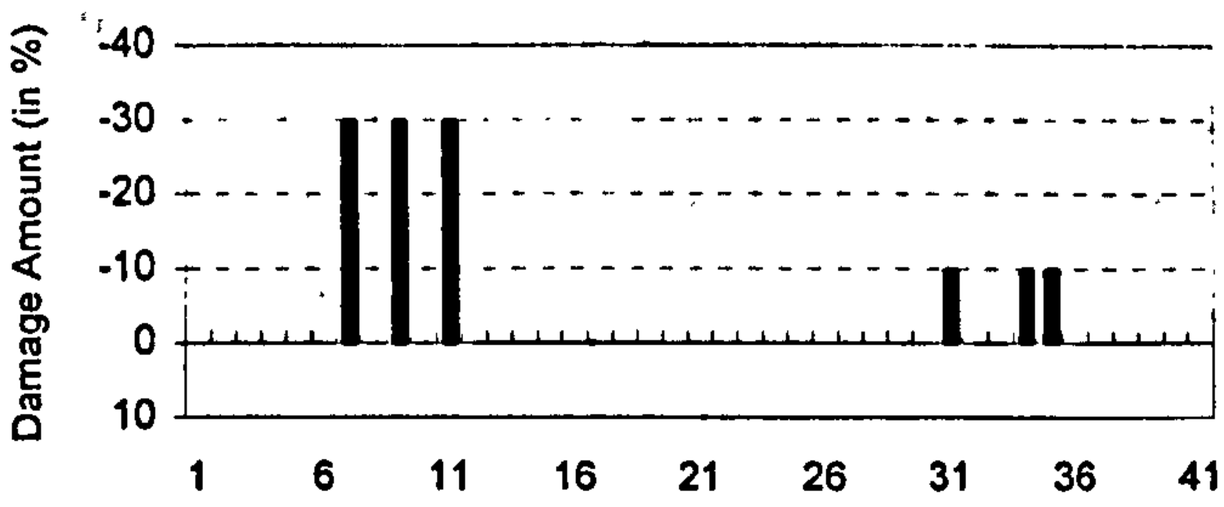

Figure 4.3(b) Procedure **MRE** based inverse predictions of damage

Figure 4.3 Comparison between the Procedures **MRF** and **MRE**, information on both damaged modes 3 and 2 used

4.5.2 Plane statically determinate truss

A plane statically determinate truss structure is modelled with 18 nodes, 33 members with a total of 33 DOFs. The material properties and the geometry of the structure are the same as those for the example in Section 4.5.1. A hypothetical damage in the structure is considered with the damage induced at different locations with different magnitudes, as shown in Figure 4.4.

It can be seen from the results in Figures 4.5(a) and 4.5(b) that both the location and the extent of the structural damage can be predicted exactly irrespective of the procedure used. As the model structure represents a statically determinate plane truss, a single damaged mode is sufficient to properly identify the structural damage. Moreover, the location and the extent of structural damage can be identified exactly from the information about an arbitrary single damaged mode.

Furthermore, structural damage at a local area can be estimated using information on locally complete DOF's readings for the damaged structure. From the results shown in Figures 4.6(a) and (b), it can be seen that predictions of a local structural damage in elements where local DOF's readings for their joining nodes are measured completely, such as elements 1-12 (joining nodes 1-8) in Figure 4.6(a) and elements 22-33 (joining nodes 11-18) in Figure 4.6(b), are quite good. This provides a very practical approach to estimate the structural damage at a local area by only using information on damaged DOF's readings completely measured at the local area, which represents a useful approach especially for large scale structures.

Parameters of the Problem	
Total DOFs	33
Structural members	33
Damage parameters	33

Hypothetical Damage Scenario

Element No	Damage Amount
6, 7, 9	-30%
25, 27, 28	-10%

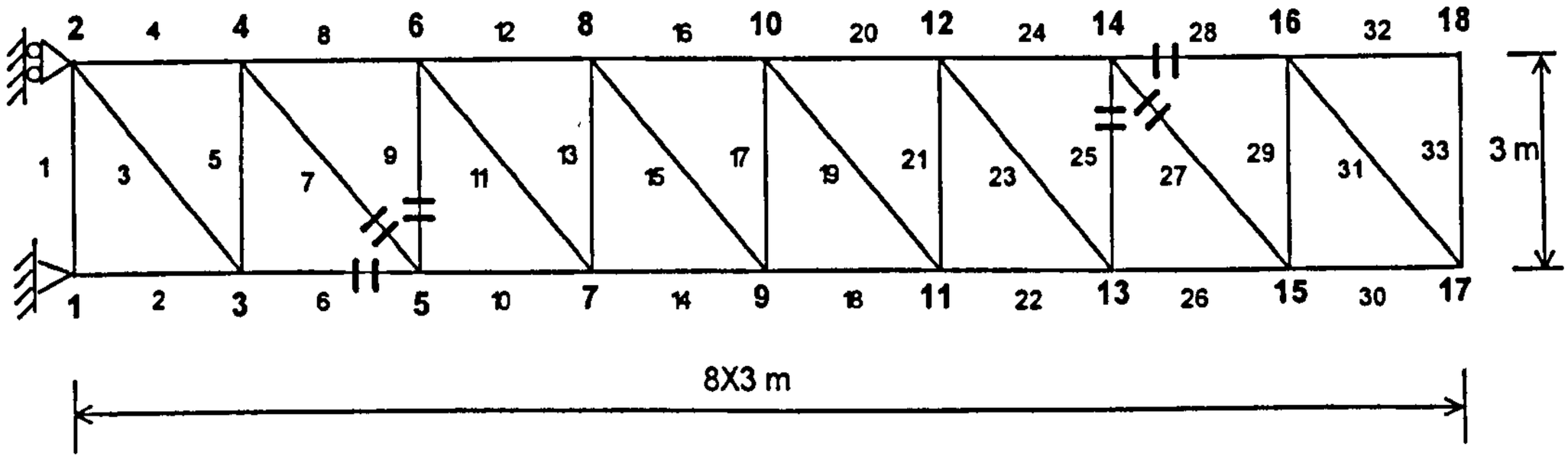

Figure 4.4 Statically determinate model plane truss problem

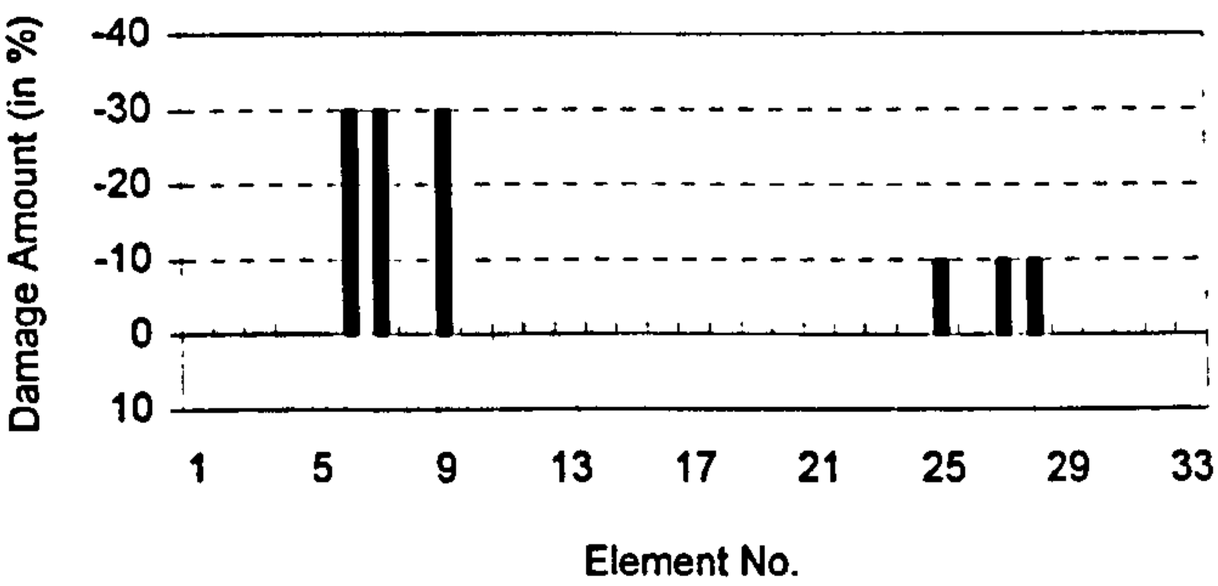

Figure 4.5(a) Procedure **MRF** based inverse predictions of damage

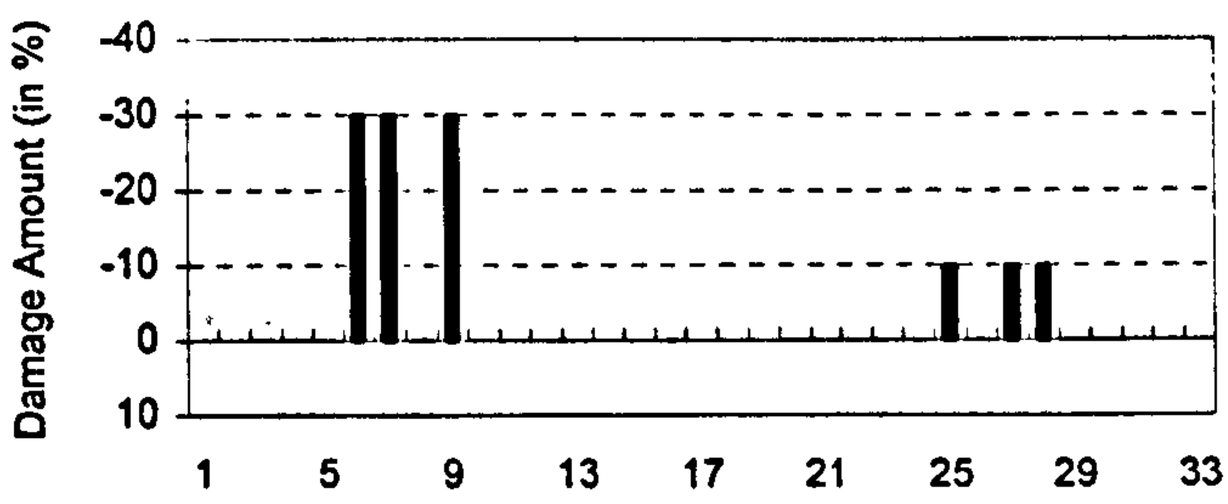

Figure 4.5(b) Procedure **MRE** based inverse predictions of damage

Figure 4.5 Comparison between the Procedures **MRF** and **MRE**, information on only the damaged mode 3 used

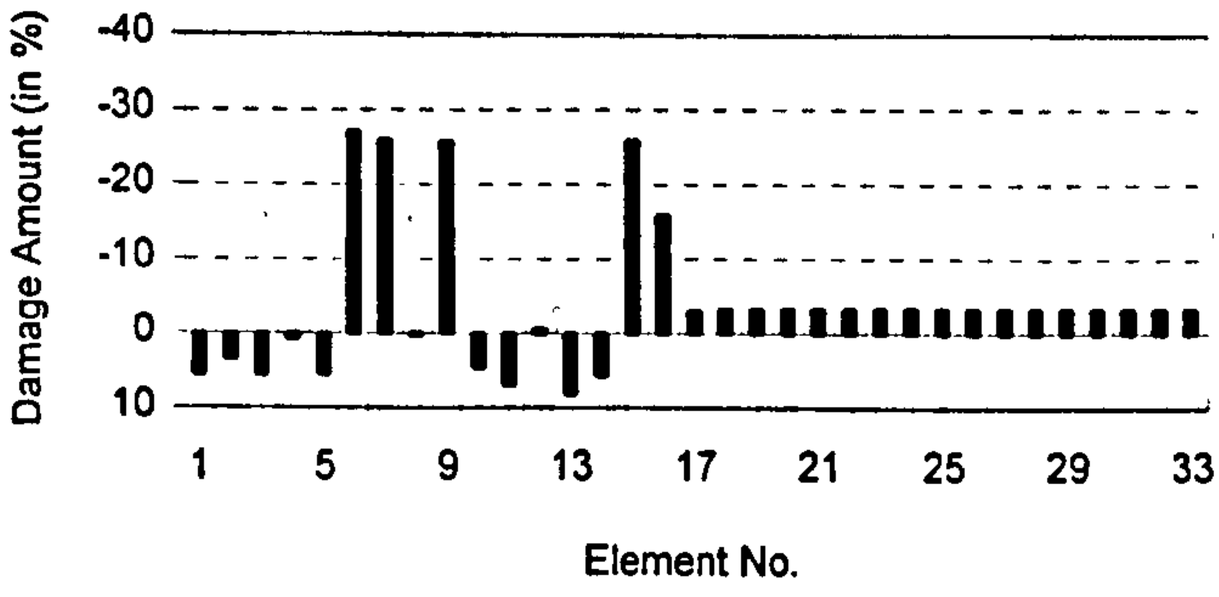

Figure 4.6(a) Only DOF's readings for the local nodes 1-8 completely measured

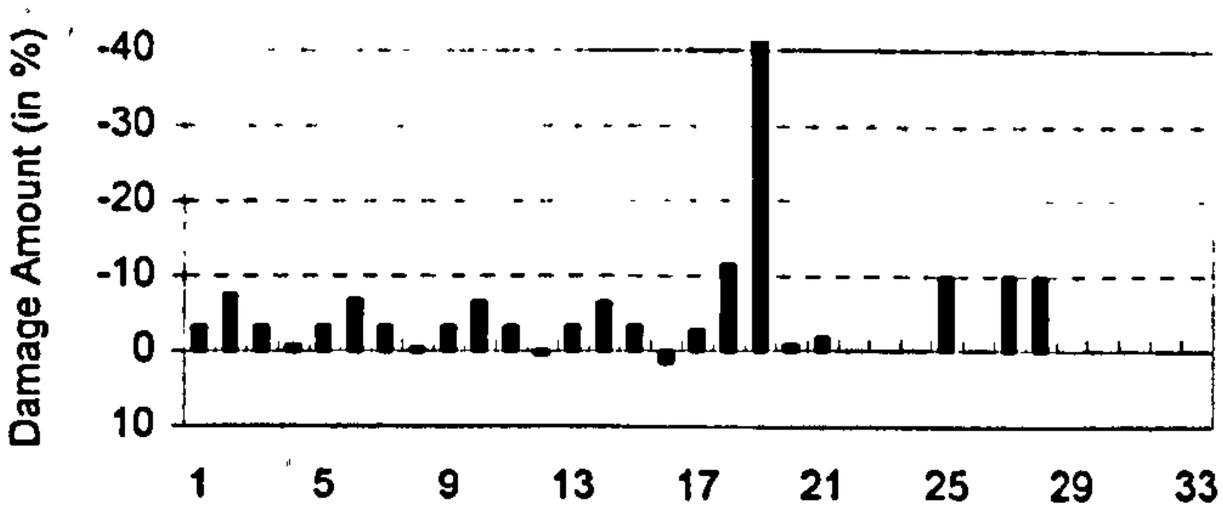

Figure 4.6(b) Only DOF's readings for the local nodes 11-18 completely measured

Figure 4.6 Inverse predictions for local damage, information on approximate mode 3 used

4.6 Effects of Noise

Effects of the noise in modal data on damage identification are investigated, where the identification of structural damage is performed using "imperfect" mode shapes. These imperfections are simulated by corrupting the exact analytical damaged mode shapes (have utilised in place of the measured data) with some noise, while natural frequencies are assumed to be noise free. The exact eigenvector terms corresponding to specific DOF's data for damaged mode shapes are scaled by the factor $1+\varepsilon$ where ε indicates a level of random noise. In the examples to follow, the hypothetical damage for the plane statically determinate truss structure as shown in Figure 4.4 is considered.

4.6.1 Effects of noise levels

It is assumed that each of the DOF's readings for the damaged mode shape is corrupted by a certain random noise level in order to investigate the effects of noise level present in the corrupted damaged mode shape on the identification of structural damage.

In the results of Figures 4.7(a)–(d), only a single corrupted damaged mode 3 is considered, and the Procedure **MRF** is utilised for evaluating the structural damage. The results show that predictions of structural damage are highly sensitive to the levels of noise in modal data. When modal data with 1.0% random noise level are considered, predictions of damage in the structure are unsatisfactory, although predictions in some local areas may not be badly affected, as shown in Figure 4.7(d). However, when the damaged mode shape is imperfect with 0.1% random noise level, predictions of structural damage are quite good, as shown in Figure 4.7(a). As expected, predictions of structural damage improve with a reduction of random noise level existing in the damaged mode shape.

The results shown in Figures 4.8(a) and (b) are utilised to compare the predictions of structural damage using different procedures, the Procedure **MRF** and the Procedure **MRE**, where information on the corrupted damaged modes 3 and 2 with 0.2% random noise level is considered. The results indicate that there are no significant differences between the two procedures and that no obvious improvements is achieved even if two corrupted damaged modes are used. The reason for these is probably that the

weighting matrix considered in this example for the Procedure **MRE**, M^{-1}, contains coefficients closely associated with the corresponding components of equation errors.

It should be noted that the effects of noise in modal data on predictions of structural damage are significant, which is caused by the fact that the governing equations for structural damage identification are in general ill-conditioned systems

4.6.2 Effects of local noise

Effects of the noise in modal data at certain local area related to the predictions of structural damage are investigated. The hypothetical damage for the plane statically determinate truss structure as shown in Figure 4.4 is estimated using the damaged mode 2 corrupted by 5% level of random noise at certain DOFs. Only the Procedure **MRF** is employed for predicting the structural damage.

Four series of illustrative examples concern the localised "imperfections". In two examples, the imperfections are applied to the positions far removed from the zone of damaged elements, i.e., at nodes 8, 9, 10 and 11 shown in Figure 4.9(a) and at nodes 9, 10, 17 and 18 shown in Figure 4.9(b), whereas for the other two the imperfections are applied to the positions located at the nodes joining the damaged elements, i.e., at nodes 3, 4, 5 and 6 shown in Figure 4.9(c) and at nodes 13, 14 15 and 16 shown in Figure 4.9(d). From the results shown in Figure 4.9(a)–(d), it can be seen that predictions of structural damage in elements which are not joined to nodes with corrupted mode shape data are good, whereas the quality of predictions is significantly affected in the vicinity of the corrupted zone.

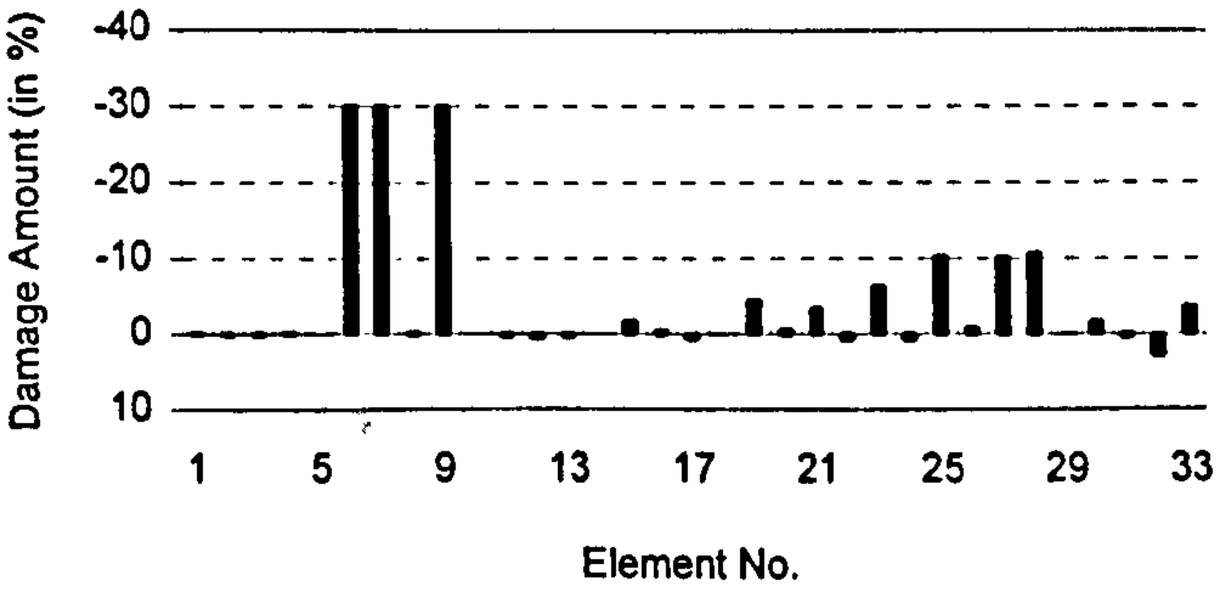

Figure 4.7(a) With 0.1% random noise level

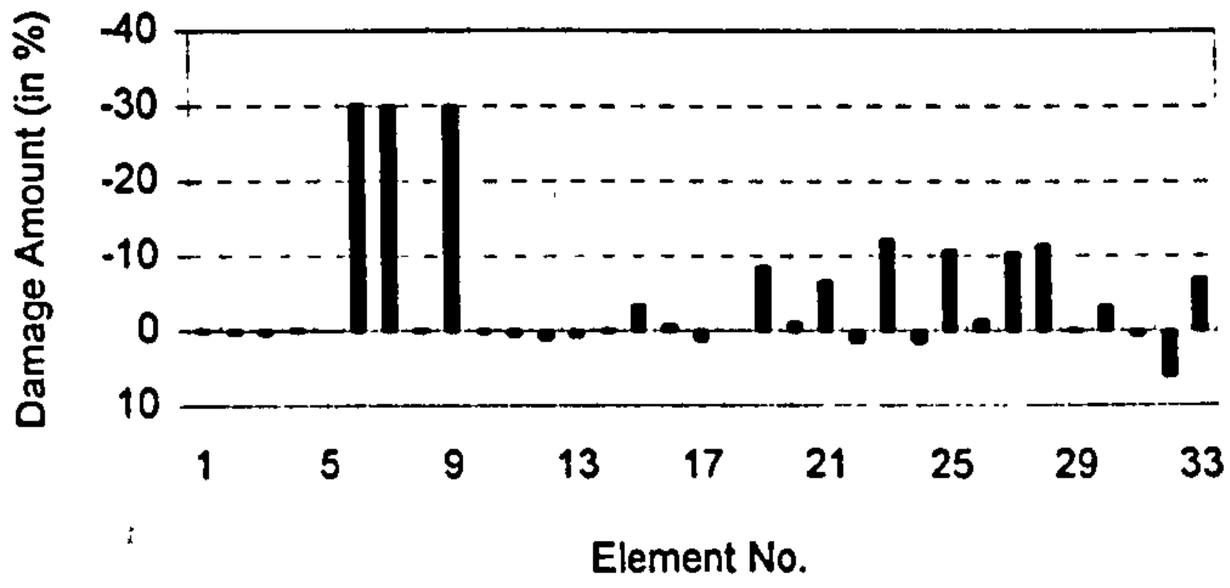

Figure 4.7(b) With 0.2% random noise level

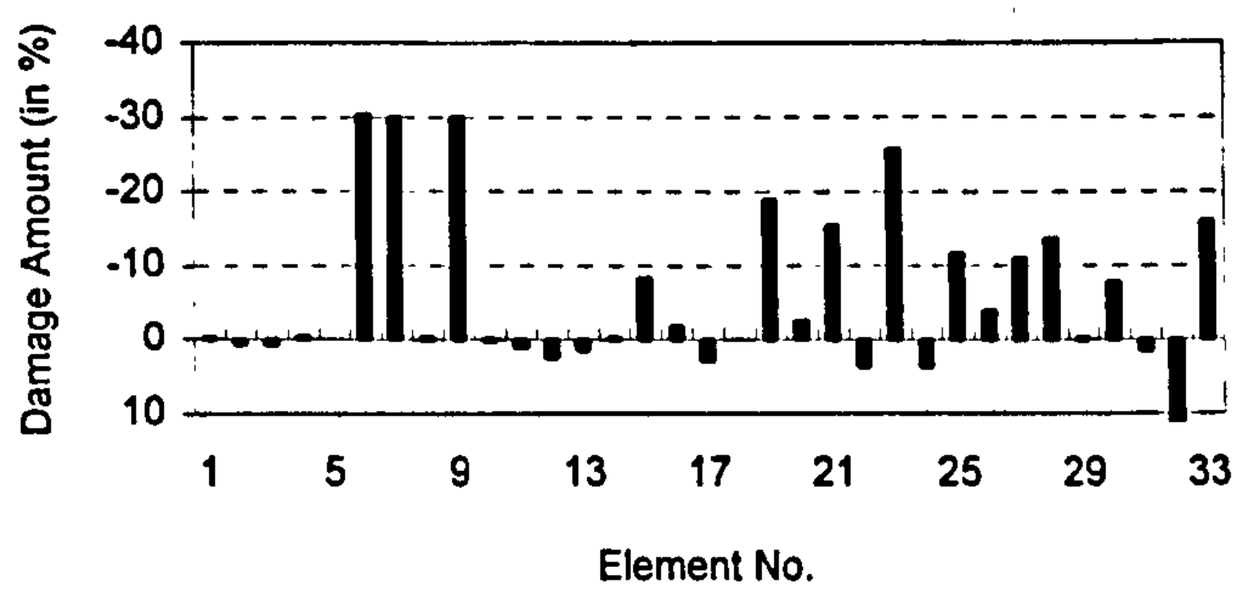

Figure 4.7(c) With 0.5% random noise level

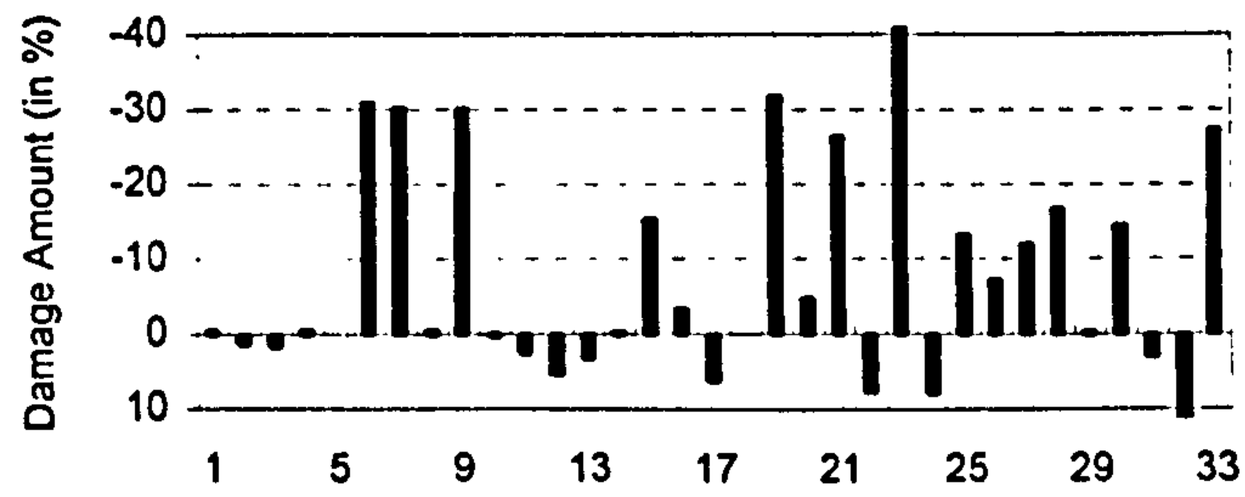

Figure 4.7(d) With 1.0% random noise level

Figure 4.7 Procedure **MRF** based inverse predictions of damage, information on the damaged mode 3 with various levels of random noise used

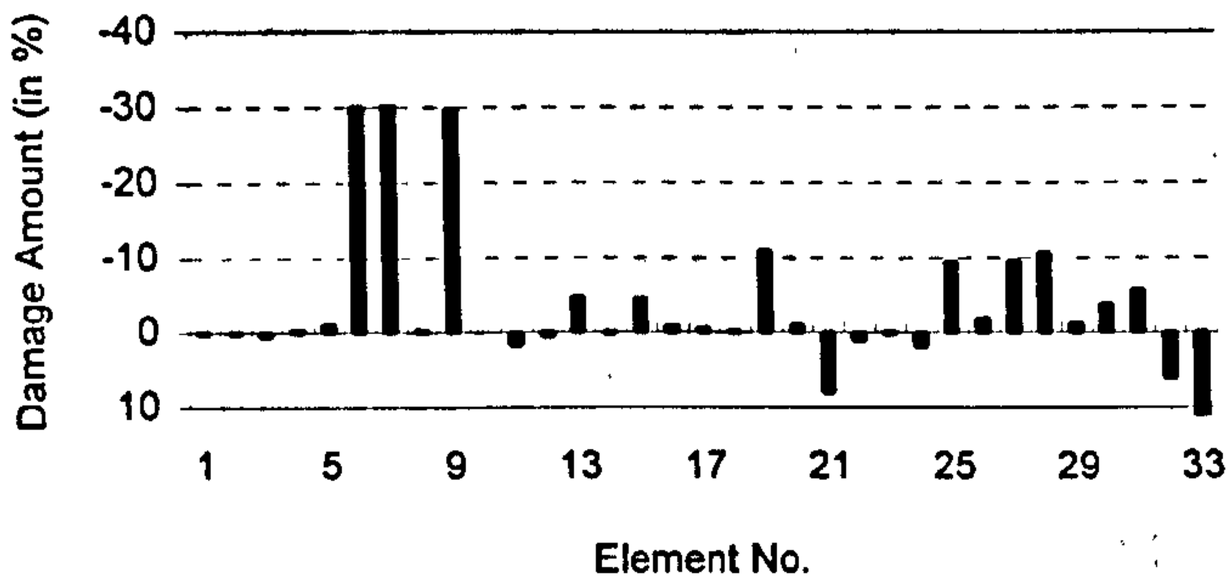

Figure 4.8(a) Procedure **MRF** based inverse predictions of damage

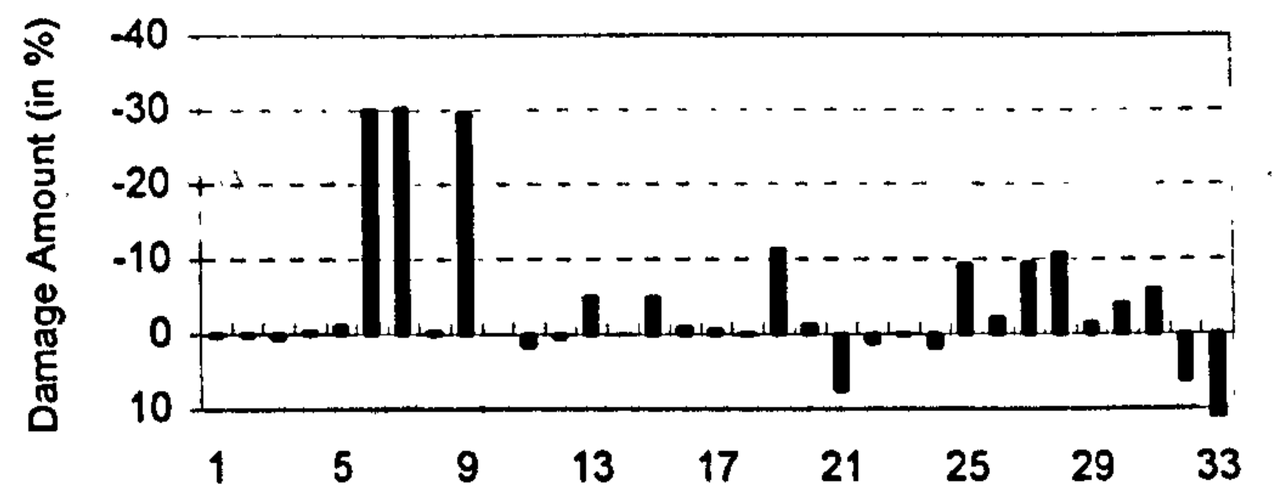

Figure 4.8(b) Procedure **MRE** based inverse predictions of damage

Figure 4.8 Comparison between the Procedures **MRF** and **MRE**, information on damaged modes 3 and 2 with 0.2% random noise level used

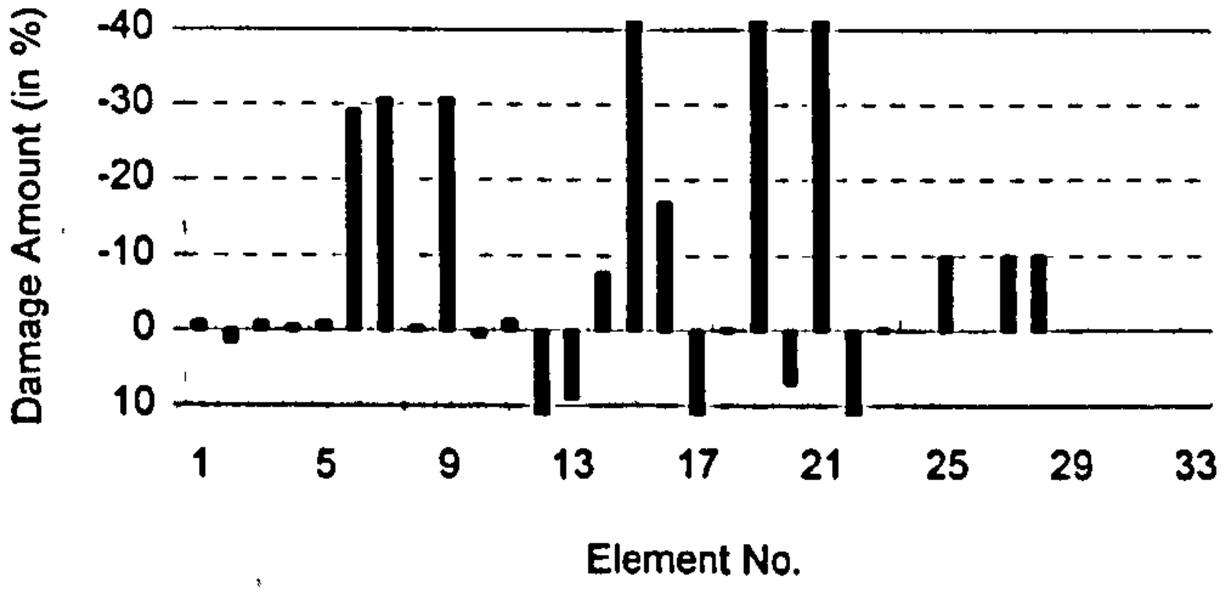

Figure 4.9(a) Noise in the DOFs for nodes 8, 9, 10 and 11

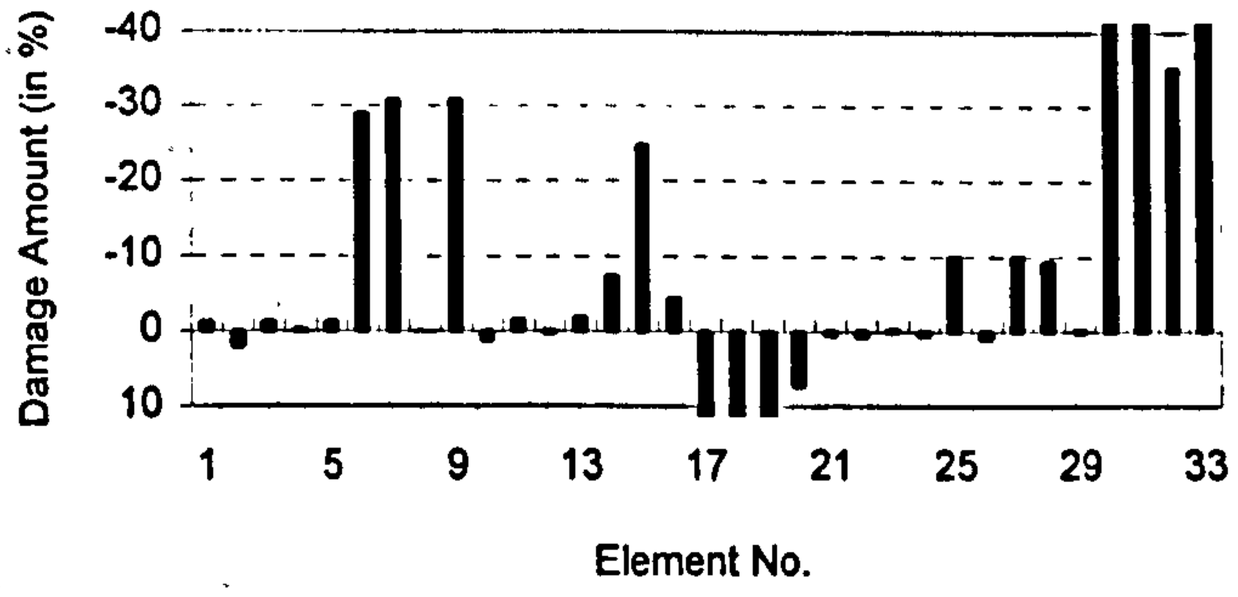

Figure 4.9(b) Noise in the DOFs for nodes 9, 10, 17 and 18

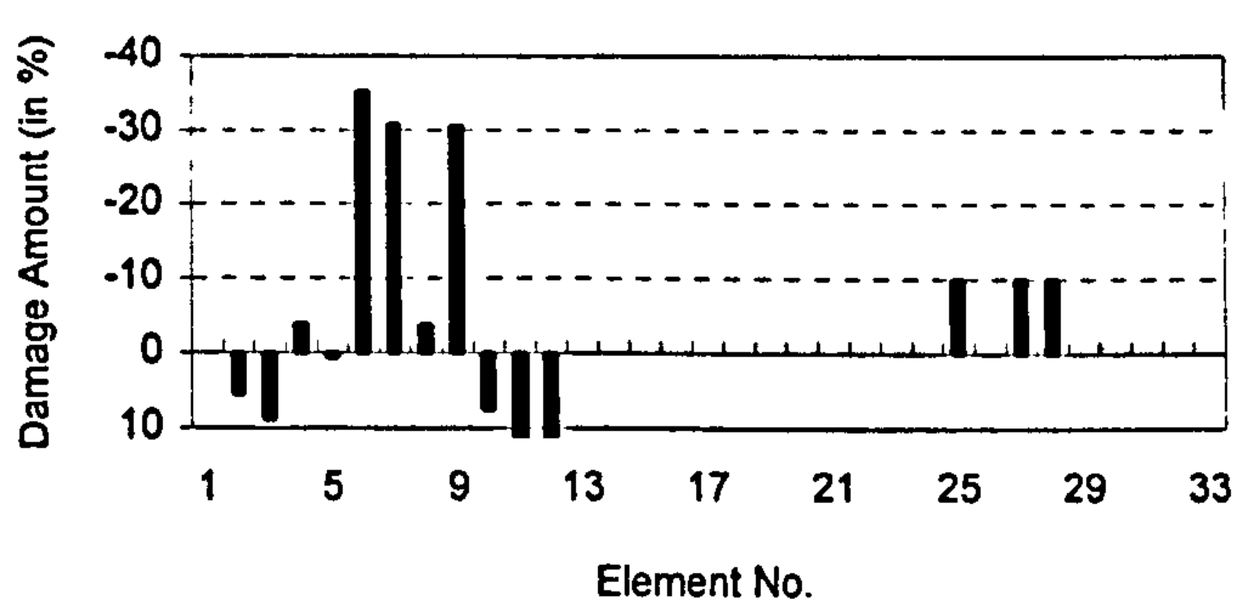

Figure 4.9(c) Noise in the DOFs for nodes 3, 4, 5 and 6

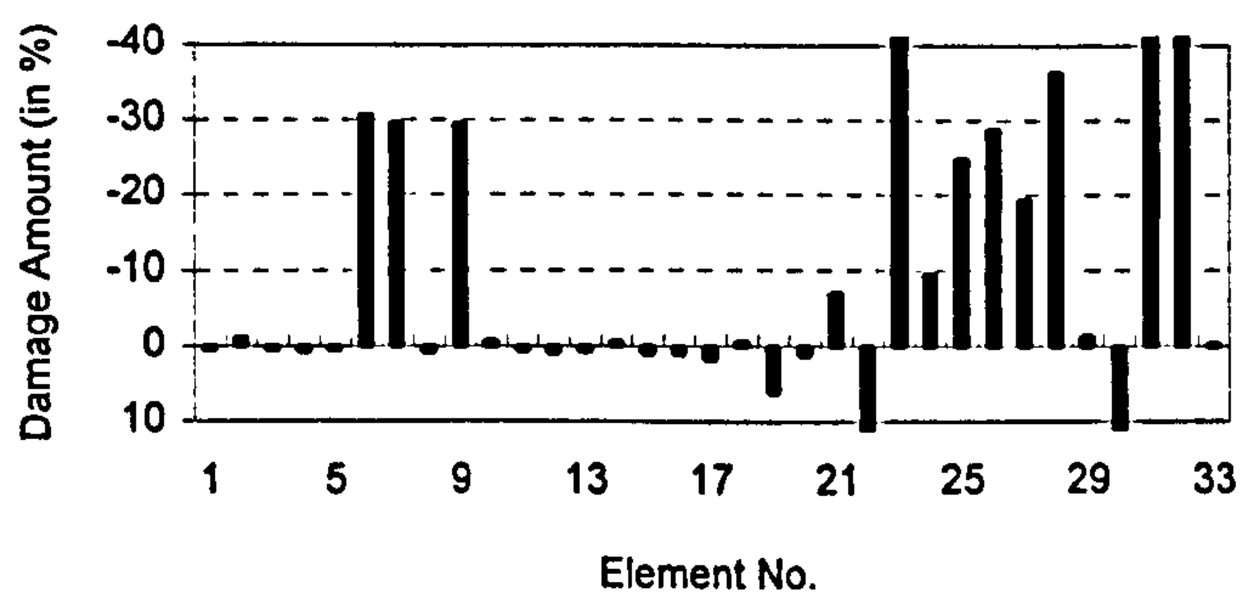

Figure 4.9(d) Noise in the DOFs for nodes 13, 14, 15 and 16

Figure 4.9 Procedure **MRF** based inverse predictions of damage, information on the damaged mode 3 with 5% random noise level in certain DOFs used

4.7 Conclusions

The procedures based on the characteristic equations for the damaged structure have been considered and their effectiveness investigated with respect to a specific case, when the information about only one of the damaged modes is available. It has been shown that the proposed procedures lead to an exact solution for damage parameters for statically determinate trusses irrespective of which of the single damaged modes is utilised. In the case of statically indeterminate trusses, the availability of a single arbitrary damaged mode leads to very good estimates for damage parameters, whereas the availability of two damaged modes is generally sufficient to solve for the exact location and the extent of damage. Furthermore, structural damage at a local area can correctly be estimated when information about only the damaged DOF's readings is completely measured at the local area, which offers a very practical approach for large scale structures. Finally, it is shown that the proposed procedures are quite sensitive to the quality of mode shape data available for structural damage assessment. However, it was found that the noise of modal data at certain nodes only affects elements connected to these nodes, whereas away from the noise region the level of structural damage is predicted quite well.

CHAPTER 5

DAMAGE IDENTIFICATION FROM ONLY NATURAL FREQUENCIES

Structural damage detection techniques based on the measurements of natural frequencies are potentially attractive. The main reason is that natural frequencies are rather easy to measure with a relatively high level of accuracy. As it has already been suggested, these properties can be measured at one point of a structure and are to a large extent independent of the position chosen. Moreover, natural frequencies are sensitive to all kinds of damage, both of a local and global nature.

In a previous chapter, a novel non-linear perturbation theory has been developed in order to avoid the insufficiency of the first-order sensitivity analysis, since a large change of structural parameters due to damage might need to be detected. Several computational techniques based on the developed non-linear perturbation theory, such as the Direct Iteration (**DI**), the Gauss-Newton Least Squares (**GNLS**), the Two Stage Iteration (**TSI**), the Approximate Equation (**AE**), the Non-Linear Optimisation (**NLO**), and the Optimisation and Iteration (**OI**) techniques, will be proposed to identify structural damage. Finally, the results from different numerical examples show that both the location and the extent of structural damage can correctly be identified from a limited number of natural frequencies.

5.1 Governing Equations

When information about damaged frequencies only, i.e., natural frequencies for the damaged structure, is available, the governing equations associated with the damage parameter α_j and the mode participation factor C_{ik}, equations (3.53) and (3.54), can be rewritten as

$$\sum_{j=1}^{NEG} a_{iji}\alpha_j + \sum_{j=1}^{NEG}\sum_{l=1,l\neq i}^{NC} a_{ijl}C_{il}\alpha_j - \Delta\lambda_i = 0 \qquad (5.1)$$

and

$$\sum_{j=1}^{NEG} a_{kji}\alpha_j + \sum_{j=1}^{NEG}\sum_{l=1,l\neq i}^{NC} a_{kjl}C_{il}\alpha_j - (\lambda_i^* - \lambda_k)C_{ik} = 0 \tag{5.2}$$

where a_{iji}, a_{ijl}, a_{kji}, and a_{kjl} are the eigenmode-stiffness sensitivity coefficients, which can be defined in a general form as

$$a_{kjl} = \phi_k^T K_j \phi_l \tag{5.3}$$

In addition, the non-linear governing equation (5.2) can be rewritten in a recursive relationship for computing the mode participation factor C_{ik}, i.e.,

$$C_{ik} = \frac{\sum_{j=1}^{NEG} a_{kji}\alpha_j + \sum_{j=1}^{NEG}\sum_{l=1,l\neq i}^{NC} a_{kjl}\alpha_j C_{il}}{\lambda_i^* - \lambda_k} \tag{5.4}$$

Rewriting equation (5.4), leads to

$$C_{ik} = \frac{\sum_{j=1}^{NEG} a_{kji}\alpha_j + \sum_{j=1}^{NEG}\sum_{l=1,l\neq i,k}^{NC} a_{kjl}\alpha_j C_{il}}{\lambda_i^* - \lambda_k - \sum_{j=1}^{NEG} a_{kjk}\alpha_j} \tag{5.5}$$

From equation (5.4), it can be seen that when k is large enough the terms with subscripts greater than k can be neglected. Therefore, N can be suitably replaced by NC, denoting the number of the original eigenvectors available.

To solve for the damage parameter α_j and the mode participation factor C_{ik}, various computational techniques will be developed using the above non-linear governing equations.

Once the mode participation factor C_{ik} is found, using equations (3.9b) and (3.18) the eigenvectors for the damaged structure can be calculated as

$$\phi_i^* = \phi_i + \sum_{k=1,k\neq i}^{NC} C_{ik}\phi_k \tag{5.6}$$

The pairing of the eigenvalues for the original structure and the damaged structure can be checked using the *MAC* factors (Modal Assurance Criterion), defined as

$$MAC(k,i) = \frac{\left|\phi_k{}^T \phi_i{}^*\right|^2}{\left|\phi_k{}^T \phi_k\right| \left|\phi_i{}^{*T} \phi_i{}^*\right|} \tag{5.7}$$

where the highest $MAC(k,i)$ factors indicate the most possible pairings of the original mode k and the damaged mode i.

5.2 Direct Iteration (DI) Technique

The basic equations and computational procedure for the **DI** technique will be outlined as follows.

5.2.1 Basic equations

Rewriting equation (5.1), yields

$$\sum_{j=1}^{NEG} S_{ij}\alpha_j = z_i \tag{5.8}$$

where S_{ij} and z_i are the eigenmode-stiffness sensitivity matrix and vector, respectively, which are defined as

$$S_{ij} = a_{iji} + \sum_{l=1,l\neq i}^{NC} C_{il} a_{ijl} \tag{5.9a}$$

$$z_i = \Delta\lambda_i \tag{5.9b}$$

Similarly, equation (5.5) is rewritten as

$$b_{ki} + \sum_{l=1,l\neq i,k}^{NC} C_{il} b_{kl}$$

$$C_{ik} = \frac{}{\lambda_i^* - \lambda_k - b_{kk}} \tag{5.10}$$

where b_{kk}, b_{ki}, and b_{kl} can be defined in a general form as

$$b_{kl} = \sum_{j=1}^{NEG} a_{kjl}\alpha_j \tag{5.11}$$

The above formulation will be applied to develop an iterative solution procedure.

5.2.2 Computational procedure

The procedure is initiated by supposing that the initial mode participation factors C_{ik} are zero. Physically, this implies that the initial damage parameters are obtained from the assumption that the damaged eigenvectors are identical to the original ones. A first approximation for damage parameters α_j is then obtained from equation (5.8). Depending on the number of damaged natural frequencies available *NL* (number of equations), and the number of structural damage parameters present *NEG* (number of unknowns), the eigenmode-stiffness sensitivity matrix may not be square.

In order to find a solution for what is in general an ill-conditioned system, the filtered Singular Value Decomposition (SVD) technique as discussed in Section 4.4 is employed.

After the initial damage parameters α_j are obtained, the next approximation for the mode participation factors C_{ik} can be calculated from equation (5.10). Therefore, equations (5.8) and (5.10) are used recursively to compute further approximation for α_j and C_{ik}, and the above recursive process is repeated until convergence for damage parameters α_j is achieved.

In order to clarify the above description, the adopted computational procedure is elaborated in Box 5.1.

5.3 Gauss-Newton Least Squares (GNLS) Technique

The basic equations and computational procedure for the **GNLS** technique will be developed as follows.

5.3.1 Basic equations

Combining the two sets of equations (5.1) and (5.2), an enlarged set of a total of *NEQ=NL*NC* equations related to variables α_j and C_{ik} is written as a system of nonlinear equations to determine the damage parameter α_j as well as the mode participation factor C_{ik}, i.e.,

Box 5.1 Computational procedure for the Direct Iteration (**DI**) technique

Step 1 Assume the initial mode participation factors C_{ik}^0 *to be zero, i.e., no changes in eigenvectors. Establish the initial values for* α_j^1 *and* C_{ik}^1 *from*

$$\sum_{j=1}^{NEG} S_{ij}^1 \alpha_j^1 = z_i \quad , \quad where \quad S_{ij}^1 = a_{iji}$$

$$C_{ik}^1 = \frac{b_{ki}^1}{\lambda_i^* - \lambda_k - b_{kk}^1} \quad , \quad where \quad b_{ki}^1 = \sum_{j=1}^{NEG} a_{kji} \alpha_j^1$$

Step 2 Evaluate current estimate for α_j^n *from*

$$\sum_{j=1}^{NEG} S_{ij}^n \alpha_j^n = z_i \quad , \quad where \quad S_{ij}^n = a_{iji} + \sum_{l=1, l\neq i}^{NC} C_{il}^{n-1} a_{ijl}$$

Step 3 Evaluate new modal participation factors C_{ik}^n *from*

$$C_{ik}^n = \frac{b_{ki}^n + \sum_{l=1, l\neq i,k}^{NC} C_{il}^{n-1} b_{kl}^n}{\lambda_i^* - \lambda_k - b_{kk}^n} \quad , \quad where \quad b_{ki}^n = \sum_{j=1}^{NEG} a_{kji} \alpha_j^n$$

and return to step 2 if solution has not converged.

$$f_m(\alpha_j, C_{ik}) = 0 \tag{5.12}$$

The above set of *NEQ* equations (5.12) comprises two parts, which are obtained by combining the set of *NL* equations (5.1) and the set of (*NEQ-NL*) equations (5.2). Consequently, the range of index m=1, *NL* covers the set of equations (5.1), while the range m=*NL*+1, *NEQ* represents the set of equations (5.2).

The nonlinear solution algorithm developed later will require the first derivative of function $f_m(\alpha_j, C_{ik})$ with respect to α_j and C_{ik}.

For the first part, i.e., for the range m=1, *NL*, the derivatives with respect to damage parameter α_r are as follows

$$\frac{\partial f_m}{\partial \alpha_r} = a_{iri} + \sum_{l=1, l\neq i}^{NC} a_{irl} C_{il} \tag{5.13a}$$

where r=1, NEG and m=i. The corresponding derivatives with respect to mode participation factor C_{st} are

$$\frac{\partial f_m}{\partial C_{st}} = \begin{cases} \sum_{j=1}^{NEG} a_{ijt}\alpha_j , & s = i \\ 0 , & s \neq i \end{cases} \tag{5.13b}$$

where the ranges for s and t are s=1, NL and t=1, NC ($s\neq t$), and again m=i.

Per analogiam, the derivatives for the second part, i.e., m=NL+1, NEQ, follow from

$$\frac{\partial f_m}{\partial \alpha_r} = a_{kri} + \sum_{l=1, l\neq i}^{NC} a_{krl} C_{il} \tag{5.14a}$$

where r=1, NEG, and m=(i-1)*NC+k ($i\neq k$), and from

$$\frac{\partial f_m}{\partial C_{st}} = \begin{cases} \sum_{j=1}^{NEG} a_{kjt}\alpha_j , & s = i,\ t \neq k \\ \sum_{j=1}^{NEG} a_{kjk}\alpha_j - (\lambda_i^* - \lambda_k) , & s = i,\ t = k \\ 0 , & s \neq i \end{cases} \tag{5.14b}$$

where the range of indices s and t is s=1, NL and t=1, NC ($s\neq t$), and m=(i-1)*NC+k ($i\neq k$).

The set of basic equations (5.12) represents a set of nonlinear equations to be solved by an iterative algorithm. The filtered Singular Value Decomposition (SVD) technique as discussed in Section 4.4 is utilised to solve the set of linearised equations at every iteration.

The computational procedure using the combination of the Gauss-Newton iteration method and the least squares techniques is developed.

5.3.2 Computational procedure

Rewriting the basic set of nonlinear equations (5.12) as

$$f_m(x_n) = 0 \tag{5.15}$$

The set of generalised unknowns x_n is defined as

$$x_n = \{\alpha_j,\ C_{ik}\}^T \tag{5.16}$$

where m=1, *NEQ*, n=1, *NV*. As *NL* may not be equal to *NEG*, the number of available equations *NEQ* may not equal the total number of variables in equation (5.12) *NV*=*NEG*+*NL**(*NC*-1).

The generalised variables x_n can be seen to be partitioned into two parts – for the first part n=1, *NEG*, the generalised variables are $x_n=\alpha_j$ where j=1, *NEG*, i.e., $n=j$; and for the second part n=*NEG*+1, *NV*, the generalised variables are $x_n=C_{ik}$ where i=1, *NL* and k=1, *NC* ($i\neq k$), i.e., $n=(i-1)*NC+k$ ($i\neq k$).

The norm y of the equation (5.15) is defined as

$$y = y(x_n) = \sum_{m=1}^{NEQ} f_m^{\,2}(x_n) \tag{5.17}$$

If $|y| = |y(\bar{x}_n)| \prec \varepsilon$ where ε is convergence tolerance, then $\bar{x}_n$ will be considered as the solution to the equation (5.15) in a least square sense.

Moreover, the first derivative of a function $f_m(x_n)$ with respect to x_n is expressed as

$$f_{m,n} = \frac{\partial f_m}{\partial x_n} \tag{5.18}$$

The iterative procedure employed here is detailed in Box 5.2.

Box 5.2 Computational procedure for the Gauss-Newton Least Squares (**GNLS**) technique

Step 1 Assume initial value for variables, $x_n^{(0)}$

Step 2 Find the increment of variables, $\Delta x_n^{(0)}$

$$\Delta x_n^{(0)} = -(D_{mn}^{(0)})^{-1} f_m(x_n^{(0)})$$

where $(D_{mn}^{(0)})^{-1}$ *is the generalised inverse of* $(D_{mn}^{(0)})$ *obtained from SVD technique, and the algorithmic tangent is defined as*

$$D_{mn}^{(0)} = f_{m,n}\Big|_{x_n = x_n^{(0)}}$$

Step 3 Search acceleration factor $s_f^{(0)}$*, which satisfies*

$$y = y(x_n^{(0)} + s_f^{(0)} \Delta x_n^{(0)}) = Minimum$$

Step 4 Evaluate new approximation for variables, $x_n^{(1)}$

$$x_n^{(1)} = x_n^{(0)} + s_f^{(0)} \Delta x_n^{(0)}$$

If $|y| \prec \varepsilon$ or $\left|s_f^{(0)} \Delta x_n^{(0)}\right| \prec \varepsilon$*, than* $x_n^{(1)}$ *is considered as the solution of equation (5.15), otherwise go to Step 2 until the condition of convergence is satisfied.*

5.4 Two Stage Iteration (TSI) Technique

As indicated earlier, structural damage parameters can be identified using computational techniques, such as the Direct Iteration and the Gauss-Newton Least Squares techniques. However, since the number of natural frequencies available (*NL*) is often much less than the number of structural damage parameters (*NEG*), it is rather difficult to identify exactly both the location and the extent of structural damage. To overcome the difficulty, a computational procedure, Two Stage Iteration (**TSI**) technique, is developed as follows.

5.4.1 Basic equations

The basic equations used here are identical to those for the **DI** and the **GNLS** techniques.

5.4.2 Computational procedure

The computational procedure for this technique can be divided into two stages.

Stage 1

At first stage, computational technique, either the **DI** technique or the **GNLS** technique, is employed to calculate the approximate values for structural damage parameter α_j. A good estimate of structural damage parameters can be obtained after reasonable convergence is achieved.

Stage 2

At second stage, the current estimate of damage parameter α_j is then checked. If a value of structural damage parameter is less than a threshold, the corresponding structural damage parameter is subsequently removed from the system of equations in order to reduce the number of unknowns, and the corresponding value will be fixed to zero. Then, the remaining structural damage parameters are computed using the procedure described in Stage 1. The above recursive process is repeated until solution converges.

The Two Stage Iteration procedure discussed here is elaborated in Box 5.3.

5.5 Approximate Equation (AE) Technique

Structural damage parameter α_j can directly be estimated from the following procedure, where the approximate mode participation factor C_{ik} is applied to the governing equation (5.1) associated with different levels of approximation.

5.5.1 Basic equations

First-order approximation (AE1)

Considering non-linear governing equation (5.1), the first-order approximation of the equation can be obtained from the assumption for the mode participation factor

Box 5.3 Computational procedure for the Two Stage Iteration (**TSI**) technique

Stage 1

An estimate of structural damage parameter α_j can be obtained using a computational technique, either the **DI** *technique or the* **GNLS** *technique, i.e.*

the **DI** *technique*	*or*	*the* **GNLS** *technique*
See		*See*
Box 5.1		*Box 5.2*
Computational procedure		*Computational procedure*
for		*for*
the **DI** *technique*		*the* **GNLS** *technique*

Stage 2

Step 2.1 Start with from α_j obtained in stage 1.

Step 2.2 If α_j is less than a threshold, then let α_j be fixed to zero. Subsequently, update the system of basic equations to reduce the number of unknowns.

Step 2.3 Go to stage 1 until solution converges.

$$C_{il}^{(l)} = 0 \tag{5.19}$$

which implies that no change of eigenvectors between the damaged structure and the original structure exists.

Therefore, non-linear governing equation (5.1) reduces to a linear relationship that is widely used for damage identification, i.e.

$$\sum_{p=1}^{NEG} a_{ipi}^{(l)} \alpha_p - \Delta\lambda_i = 0 \tag{5.20}$$

where $a_{ipi}^{(l)}$ stands for the eigenmode-stiffness sensitivity coefficients, defined as

$$a_{ipi}^{(l)} = \phi_i^T K_p \phi_i \tag{5.21}$$

Second-order approximation (AE2)

Considering the governing equation (5.4), the mode participation factor C_{ik} can approximately be computed from

$$C_{il}^{(2)} = \sum_{q=1}^{NEG} \frac{a_{lqi}}{\lambda_i^{\bullet} - \lambda_l} \alpha_q \tag{5.22}$$

Upon substitution of (5.22), the second-order approximation for the non-linear governing equation (5.1) can be obtained, i.e.,

$$\sum_{p=1}^{NEG} a_{ipi}^{(1)} \alpha_p + \sum_{p=1}^{NEG} \sum_{q=1}^{NEG} a_{ipqi}^{(2)} \alpha_p \alpha_q - \Delta\lambda_i = 0 \tag{5.23}$$

where the eigenmode-stiffness sensitivity coefficients $a_{ipqi}^{(2)}$ are defined as

$$a_{ipqi}^{(2)} = \sum_{l=1, l\neq i}^{NC} \frac{a_{ipl} a_{lqi}}{\lambda_i^{\bullet} - \lambda_l} \tag{5.24}$$

Third-order approximation (AE3)

The higher order approximation for the mode participation factor C_{ik} can be calculated from equation (5.4) in the form

$$C_{il}^{(3)} = C_{il}^{(2)} + \sum_{q=1}^{NEG} \sum_{r=1}^{NEG} \left(\sum_{k=1, k\neq i}^{NC} \frac{a_{lqk} a_{kri}}{(\lambda_i^{\bullet} - \lambda_l)(\lambda_i^{\bullet} - \lambda_k)} \right) \alpha_q \alpha_r \tag{5.25}$$

Upon substitution of (5.25), the third-order approximation of equation (5.1) can be expressed by

$$\sum_{p=1}^{NEG} a_{ipi}^{(1)} \alpha_p + \sum_{p=1}^{NEG} \sum_{q=1}^{NEG} a_{ipqi}^{(2)} \alpha_p \alpha_q + \sum_{p=1}^{NEG} \sum_{q=1}^{NEG} \sum_{r=1}^{NEG} a_{ipqri}^{(3)} \alpha_p \alpha_q \alpha_r - \Delta\lambda_i = 0 \tag{5.26}$$

where coefficients $a_{ipqri}^{(3)}$ are defined as

$$a_{ipqri}^{(3)} = \sum_{l=1, l\neq i}^{NC} \sum_{k=1, k\neq i}^{NC} \frac{a_{ipl} a_{lqk} a_{kri}}{(\lambda_i^{\bullet} - \lambda_l)(\lambda_i^{\bullet} - \lambda_k)} \tag{5.27}$$

The above basic approximate equations, i.e., equations (5.20), (5.23), and (5.26), comprise a total of *NL* equations.

5.5.2 Computational procedure

In order to solve the proposed approximate equations, i.e. the basic equations for the **AE1, AE2** and **AE3** techniques, the **GNLS** technique developed in Section 5.3.2 is now employed.

With reference to the **GNLS** technique, these basic approximate equations (5.20), (5.23), and (5.26) can be expressed in a generalised form as given in equation (5.15), i.e.,

$$f_m(\alpha_j) = 0 \tag{5.28}$$

where m ranges from 1 to NL.

Since the **GNLS** technique requires the first derivative of function $f_m(\alpha_j)$ with respect to α_j, the derivatives for the basic approximate equations will be developed.

The derivative for the first-order approximate equation (5.20) is expressed as

$$\frac{\partial f_m}{\partial \alpha_j} = a_{iji}^{(1)} \tag{5.29}$$

for second-order approximate equation (5.23) as

$$\frac{\partial f_m}{\partial \alpha_j} = a_{iji}^{(1)} + \sum_{p=1}^{NEG}\left(a_{ipji}^{(2)} + a_{ijpi}^{(2)}\right)\alpha_p \tag{5.30}$$

and for the third-order approximate equation (5.26) as

$$\frac{\partial f_m}{\partial \alpha_j} = a_{iji}^{(1)} + \sum_{p=1}^{NEG}\left(a_{ipji}^{(2)} + a_{ijpi}^{(2)}\right)\alpha_p + \sum_{p=1}^{NEG}\sum_{q=1}^{NEG}\left(a_{ipqji}^{(3)} + a_{ipjqi}^{(3)} + a_{ijpqi}^{(3)}\right)\alpha_p\alpha_q \tag{5.31}$$

The detail of the computational procedure for the **GNLS** technique has been discussed in Section 5.3.2. The computational procedure for the three **AE** techniques is outlined in Box 5.4.

Box 5.4 Computational procedure for the Approximate Equation (**AE**) technique

Step 1 Choose one of the following basic approximate equations as governing equation, i.e.

$$\textit{for the } \mathbf{AE1}, \quad \sum_{p=1}^{NEG} a_{ipi}^{(1)} \alpha_p - \Delta\lambda_i = 0$$

$$\textit{for the } \mathbf{AE2}, \quad \sum_{p=1}^{NEG} a_{ipi}^{(1)} \alpha_p + \sum_{p=1}^{NEG}\sum_{q=1}^{NEG} a_{ipqi}^{(2)} \alpha_p \alpha_q - \Delta\lambda_i = 0$$

$$\textit{for the } \mathbf{AE3}, \quad \sum_{p=1}^{NEG} a_{ipi}^{(1)} \alpha_p + \sum_{p=1}^{NEG}\sum_{q=1}^{NEG} a_{ipqi}^{(2)} \alpha_p \alpha_q + \sum_{p=1}^{NEG}\sum_{q=1}^{NEG}\sum_{r=1}^{NEG} a_{ipqri}^{(3)} \alpha_p \alpha_q \alpha_r - \Delta\lambda_i = 0$$

Step 2 Compute the eigenmode-stiffness sensitivity coefficients for the chosen governing equation, i.e.

$$\textit{for the } \mathbf{AE1}, \quad a_{ipi}^{(1)} = \phi_i^T K_p \phi_i$$

$$\textit{for the } \mathbf{AE2}, \quad a_{ipqi}^{(2)} = \sum_{l=1, l\neq i}^{NC} \frac{a_{ipl} a_{lqi}}{\lambda_i^* - \lambda_l}$$

$$\textit{for the } \mathbf{AE3}, \quad a_{ipqri}^{(3)} = \sum_{l=1, l\neq i}^{NC}\sum_{k=1, k\neq i}^{NC} \frac{a_{ipl} a_{lqk} a_{kri}}{(\lambda_i^* - \lambda_l)(\lambda_i^* - \lambda_k)}$$

Step 3 Calculate structural damage parameter α_j using the **GNLS** *technique, i.e.*

the **GNLS** *technique*

See

Box 5.2

Computational procedure

for

the **GNLS** *technique*

5.6 Non-Linear Optimisation (NLO) Technique

The optimisation techniques are employed to solve the problem of structural damage identification in order to reduce the requirements of the measurements of natural frequencies, since only the first few natural frequencies are typically available.

5.6.1 Basic equations

Considering the characteristic equation for the damaged structure, i.e., equation (3.52), a vector of residuals for the *i*th original mode, $\boldsymbol{r}_i$, can be defined as

$$r_i = \sum_{j=1}^{NEG} K_j \phi_i \alpha_j + [K - \lambda_i^* M]\phi_i \tag{5.32}$$

where the mode shape for the damaged structure is replaced by the corresponding one for the original structure.

Using the characteristic equation for the original structure, i.e., equation (3.5), equation (5.32) can be rewritten as

$$r_i = \sum_{j=1}^{NEG} K_j \phi_i \alpha_j - \Delta\lambda_i M \phi_i \tag{5.33}$$

The weighted Euclidan norm of the vectors of residuals for a total of *NL* modes is expressed by

$$J = \sum_{i=1}^{NL} \left\| r_i^2 \right\| = \sum_{i=1}^{NL} \left\| r_i^T W_i r_i \right\| \tag{5.34}$$

where W_i is the weighting matrix for the *i*th mode. The weighting matrix should be symmetric and positive definite, and its definition has been discussed in Section 4.2. Two procedures associated with weighting matrices have been presented there, i.e., the Procedure **MRF** (Minimisation of Residual Force) and the Procedure **MRE** (Minimisation of Residual Energy).

Upon substitution of equation (5.32), equation (5.34) can be rewritten as

$$J = \sum_{p=1}^{NEG} \sum_{q=1}^{NEG} b_{pq}^{KK} \alpha_p \alpha_q + 2 \sum_{p=1}^{NEG} b_p^{KM} \alpha_p + b^{MM} \tag{5.35}$$

where coefficients b_{pq}^{KK}, b_p^{KM}, and b^{MM} are defined as

$$b_{pq}^{KK} = \sum_{i=1}^{NL} \phi_i^T K_p W_i K_q \phi_i \tag{5.36a}$$

$$b_p^{KM} = -\sum_{i=1}^{NL} \Delta\lambda_i \phi_i^T K_p W_i M \phi_i \tag{5.36b}$$

$$b^{MM} = \sum_{i=1}^{NL} \Delta\lambda_i^2 \phi_i^T M W_i M \phi_i \tag{5.36c}$$

To ensure that the change in the stiffness is always negative, since a positive change in the stiffness can never be produced by structural damage, the structural damage parameter α_j has to satisfy the inequality, i.e.,

$$\alpha_j \leq 0 \tag{5.37}$$

Based on the knowledge presented above, and using the basic approximate equations discussed in Section 5.5, the optimisation problem can now be stated as follows

Minimise the objective function

$$J = \sum_{p=1}^{NEG}\sum_{q=1}^{NEG} b_{pq}^{KK}\alpha_p\alpha_q + 2\sum_{p=1}^{NEG} b_p^{KM}\alpha_p \tag{5.38a}$$

Subject to the equality constraint

for the first-order approximation **(NLO1)**

$$\sum_{p=1}^{NEG} a_{ipi}^{(1)}\alpha_p - \Delta\lambda_i = 0 \tag{5.38b1}$$

or for the second-order approximation **(NLO2)**

$$\sum_{p=1}^{NEG} a_{ipi}^{(1)}\alpha_p + \sum_{p=1}^{NEG}\sum_{q=1}^{NEG} a_{ipqi}^{(2)}\alpha_p\alpha_q - \Delta\lambda_i = 0 \tag{5.38b2}$$

or for the third-order approximation **(NLO3)**

$$\sum_{p=1}^{NEG} a_{ipi}^{(1)}\alpha_p + \sum_{p=1}^{NEG}\sum_{q=1}^{NEG} a_{ipqi}^{(2)}\alpha_p\alpha_q + \sum_{p=1}^{NEG}\sum_{q=1}^{NEG}\sum_{r=1}^{NEG} a_{ipqri}^{(3)}\alpha_p\alpha_q\alpha_r - \Delta\lambda_i = 0 \tag{5.38b3}$$

and the inequality constraint

$$\alpha_j \leq 0 \tag{5.38c}$$

Note that the constant term in equation (5.35) has been dropped in equation (5.38a) since it does not influence a minimisation procedure.

The problem discussed above is a dual quadratic programming problem with linear or non-linear equality constraint and linear inequality constraint, depending on the different approximate equations used for the equality constraint. That is, the problem is a constrained linear optimisation problem if first-order approximate equation is utilised for equality constraint, otherwise, the problem is a constrained non-linear optimisation problem if second or third-order approximate equation is considered.

5.6.2 Computational procedure

The constrained non-linear optimisation methods, such as the Flexible Tolerance method (Himmelblau, 1972), can be employed for solving the optimisation problem discussed above. The details of the computational procedure for the Flexible Tolerance method can be found in Himmelblau's book. The adopted computational procedure for the three **NLO** techniques, i.e. the **NLO1**, **NLO2** and **NLO3**, is elaborated in Box 5.5.

5.7 Optimisation and Iteration (OI) Technique

The Optimisation and Iteration (**OI**) technique combines the optimisation technique discussed in Section 5.6 and the direct iteration technique discussed in Section 5.2.

5.7.1 Basic equations

Optimisation technique

Here, it is assumed that the mode participation factor C_{ik} has been known, then the eigenvector for the damaged structure ϕ_i^* can be computed using equation (5.6). The characteristic equation (3.52) for the damaged structure can be rewritten in the form

$$r_i^* = \sum_{j=1}^{NEG} K_j \phi_i^* \alpha_j + [K - \lambda_i^* M]\phi_i^* \tag{5.39}$$

where r_i^* is a vector of residuals of the characteristic equation for the ith damaged mode, which can be interpreted as the residual forces for the system.

Box 5.5 Computational procedure for the Non-Linear Optimisation **(NLO)** technique

Step 1 Choose one of the following basic approximate equations (given in Section 5.5) as the equality constraint of the corresponding non-linear optimisation problem, i.e.

for the **NLO1,** $$\sum_{p=1}^{NEG} a_{ipi}^{(1)} \alpha_p - \Delta\lambda_i = 0$$

for the **NLO2,** $$\sum_{p=1}^{NEG} a_{ipi}^{(1)} \alpha_p + \sum_{p=1}^{NEG}\sum_{q=1}^{NEG} a_{ipqi}^{(2)} \alpha_p \alpha_q - \Delta\lambda_i = 0$$

for the **NLO3,** $$\sum_{p=1}^{NEG} a_{ipi}^{(1)} \alpha_p + \sum_{p=1}^{NEG}\sum_{q=1}^{NEG} a_{ipqi}^{(2)} \alpha_p \alpha_q + \sum_{p=1}^{NEG}\sum_{q=1}^{NEG}\sum_{r=1}^{NEG} a_{ipqri}^{(3)} \alpha_p \alpha_q \alpha_r - \Delta\lambda_i = 0$$

Step 2 Compute the eigenmode-stiffness sensitivity coefficients for the objective function and the chosen equality constraint, using equations (5.36a,b) and equations (5.21), (5.24) and (5.27).

Step 3 Establish the corresponding optimisation problem, i.e.

Minimise the objective function

$$J = \sum_{p=1}^{NEG}\sum_{q=1}^{NEG} b_{pq}^{KK} \alpha_p \alpha_q + 2\sum_{p=1}^{NEG} b_{p.}^{KM} \alpha_p$$

Subject to the equality constraint

(Equation developed at Step 1)

and the inequality constraint

$$\alpha_j \leq 0$$

Step 4 Structural damage parameter α_j can be evaluated using the Flexible Tolerance method (See Himmelblau, 1972).

The weighted Euclidan norm of the vectors of residuals for a total of NL modes is expressed by

$$J = \sum_{i=1}^{NL} \left\| r_i^{*2} \right\| = \sum_{i=1}^{NL} \left\| r_i^{*T} W_i r_i^{*} \right\| \tag{5.40}$$

where requirements for the weighting matrix W_i and its relationship with optimisation procedures have been discussed in Section 5.6.

Upon substitution of equation (5.39), equation (5.40) can be rewritten as

$$J = \sum_{p=1}^{NEG} \sum_{q=1}^{NEG} b_{pq}^{KK^*} \alpha_p \alpha_q + 2 \sum_{p=1}^{NEG} b_p^{KM^*} \alpha_p + b^{MM^*} \tag{5.41}$$

where coefficients $b_{pq}^{KK^*}$, $b_p^{KM^*}$, and b^{MM^*} are defined as

$$b_{pq}^{KK^*} = \sum_{i=1}^{NL} \phi_i^{*T} K_p W_i K_q \phi_i^{*} \tag{5.42a}$$

$$b_p^{KM^*} = \sum_{i=1}^{NL} \phi_i^{*T} K_p W_i (K - \lambda_i^{*} M) \phi_i^{*} \tag{5.42b}$$

$$b^{MM^*} = \sum_{i=1}^{NL} \phi_i^{*T} (K - \lambda_i^{*} M) W_i (K - \lambda_i^{*} M) \phi_i^{*} \tag{5.42c}$$

Furthermore, using equations (5.3) and (5.6), the governing equation (5.1) can be rewritten as

$$\sum_{j=1}^{NEG} a_{iji}^{*} \alpha_j - \Delta\lambda_i = 0 \tag{5.43}$$

where the eigenmode-stiffness sensitivity coefficient a_{iji}^{*} is defined as

$$a_{iji}^{*} = \phi_i^{T} K_j \phi_i^{*} \tag{5.44}$$

Based on the knowledge presented above, and using equation (5.37) for inequality constraint, the optimisation problem can now be stated as follows

Minimise the objective function

$$J = \sum_{p=1}^{NEG}\sum_{q=1}^{NEG} b_{pq}^{KK^*}\alpha_p\alpha_q + 2\sum_{p=1}^{NEG} b_p^{KM^*}\alpha_p \qquad (5.45a)$$

Subject to the equality constraint

$$\sum_{j=1}^{NEG} a_{iji}^{*}\alpha_j - \Delta\lambda_i = 0 \qquad (5.45b)$$

and the inequality constraint

$$\alpha_j \leq 0 \qquad (5.45c)$$

It should be noted that the constant term in equation (5.41) has been dropped in equation (5.45a).

The problem described above is a dual quadratic programming problem with linear equality and inequality constraints.

Direct Iteration technique

Using the optimisation technique presented previously, the estimate of damage parameter α_j is then obtained. Consequently, the mode participation factor C_{ik} can be computed using basic equation (5.10) and then the estimate of eigenvector for the damaged structure ϕ_i^* can be computed using equation (5.6).

5.7.2 Computational procedure

The computational procedure for the Optimisation and Iteration technique combines the computational procedure for optimisation technique where the Flexible Tolerance method is employed to solve the constrained linear optimisation problem, and the computational procedure for direct iteration technique which has been developed in Section 5.2.

The computational procedure for the Optimisation and Iteration technique is elaborated in Box 5.6.

Box 5.6. Computational procedure for the Optimisation and Iteration (**OI**) technique

Step 1 Assume the initial mode participation factors C_{ik}^0 to be zero, i.e., no changes in eigenvectors. Establish the initial converged values for α_j^1 from the optimisation technique, i.e.

Minimise the objective function

$$J = \sum_{p=1}^{NEG}\sum_{q=1}^{NEG} {}^0b_{pq}^{KK^*}\alpha_p^1\alpha_q^1 + 2\sum_{p=1}^{NEG} {}^0b_p^{KM^*}\alpha_p^1$$

Subject to the equality constraint

$$\sum_{j=1}^{NEG} {}^0a_{iji}^*\alpha_j^1 - \Delta\lambda_i = 0$$

and the inequality constraint

$$\alpha_j^1 \le 0$$

and C_{ik}^1 from the iteration technique

$$C_{ik}^1 = \frac{b_{ki}^1}{\lambda_i^* - \lambda_k - b_{kk}^1} \quad , \quad where \quad b_{ki}^1 = \sum_{j=1}^{NEG} a_{kji}\alpha_j^1$$

Step 2 Evaluate current converged estimate for α_j^n from the optimisation technique

Minimise the objective function

$$J = \sum_{p=1}^{NEG}\sum_{q=1}^{NEG} {}^{n-1}b_{pq}^{KK^*}\alpha_p^n\alpha_q^n + 2\sum_{p=1}^{NEG} {}^{n-1}b_p^{KM^*}\alpha_p^n$$

Subject to the equality constraint

$$\sum_{j=1}^{NEG} {}^{n-1}a_{iji}^*\alpha_j^n - \Delta\lambda_i = 0$$

and the inequality constraint

$$\alpha_j^n \le 0$$

Step 3 Evaluate new modal participation factors C_{ik}^n from the iteration technique

$$C_{ik}^n = \frac{b_{ki}^n + \sum_{l=1,l\neq i,k}^{NC} C_{il}^{n-1}b_{kl}^n}{\lambda_i^* - \lambda_k - b_{kk}^n} \quad , \quad where \quad b_{ki}^n = \sum_{j=1}^{NEG} a_{kji}\alpha_j^n$$

and return to step 2 if solution has not converged.

5.8 Verification of Proposed Techniques

A simple grid structure illustrated in Figure 5.1 is employed to demonstrate the effectiveness and the convergence performance of the proposed techniques, such as the **DI**, the **GNLS**, the **TSI**, the **AE**, the **NLO**, and the **OI** techniques. The model, which is simply supported at each of the outer corner points, has 5 structural members, 4 nodes and 9 DOFs. All structural members have the same material properties with Young's modulus E=2.1×10^{11}N/m^2, Poisson's ratio υ=0.3 and density ρ=7800kg/m^3, and the same cross section area A=0.0045m^2, second moment of area I=4.25×10^{-6}m^4 and torsional constant J=8.50×10^{-6}m^4. The geometry of the structure with outer dimensions of 3m, 4m and 5m, and the element numbering are shown in Figure 5.1.

A hypothetical damage scenario is induced by reducing the Young's modulus of different elements, with different magnitudes as summarised in Figure 5.1. A finite element analysis was performed for both the original and the damaged cases to calculate natural frequencies and the corresponding mode shapes. The first 5 natural frequencies for the original and the damaged structure are listed in Table 5.1.

Table 5.1 First 5 natural frequencies (Hz) for original and damaged structure

Mode	1	2	3	4	5
Original	5.7189	14.0371	21.6589	28.3530	46.5395
Damaged	5.3127	13.4261	20.9949	26.3554	44.0490

5.8.1 Verification of DI technique

The information about five "damaged" frequencies is now used (in place of the measured modified frequencies) to determine inversely the location and the amount of structural damage. The convergence performance of structural damage parameters for the **DI** technique is shown in Figure 5.2. It can be seen that the **DI** technique achieves convergence after only a few iterations. Note that both the location and the extent of structural damage can be exactly identified using five damaged natural frequencies since the number of damaged natural frequencies adopted here equals the number of structural damage parameters.

The correlation between eigenvectors for the original structure and the damaged structure is checked using the *MAC* factors, resulting in values shown in Table 5.2. It

can be seen that the modes for the damaged structure obtained from the **DI** technique match very well the corresponding modes for the original structure.

Table 5.2 *MAC* factors of the eigenvectors for original and damaged structure

	Original eigenvector								
Damaged	1	2	3	4	5	6	7	8	9
1	0.9998	0.0236	0.0845	0.0003	0.0102	0.2053	0.1267	0.0780	0.0608
2	0.0215	0.9995	0.0152	0.1228	0.0158	0.1916	0.1473	0.0005	0.0296
3	0.0741	0.0188	0.9961	0.0001	0.0018	0.1459	0.1043	0.0709	0.0036
4	0.0003	0.1342	0.0082	0.9979	0.1235	0.0375	0.0250	0.1208	0.2565
5	0.0205	0.0049	0.0003	0.0950	0.9934	0.0210	0.0153	0.0991	0.0362

5.8.2 Verification of GNLS technique

Again, the information about five damaged frequencies is adopted to identify in an inverse manner the location and the extent of the given structural damage. The results in Figure 5.3 show the convergence performance of structural damage parameters for the **GNLS** technique. It can be seen that the convergence of the **GNLS** technique is achieved rapidly after only a few iterations. Furthermore, it is found that the modes for the damaged structure obtained from the **GNLS** technique match very well the corresponding modes for the original structure, which is similar to the results listed in Table 5.2.

5.8.3 Verification of TSI technique

Here, the information about only four damaged frequencies is utilised for inverse identification of the location and the extent of structural damage. The **DI** technique is employed for computing the values of structural damage parameters in this example.

The convergence performance of structural damage parameters for the **TSI** technique is shown in Figure 5.4. At first stage, the structural damage parameters are considered to be converged after three iterations. The estimate of structural damage parameters is checked. Since the value of the damage parameter for element 1 is less then the chosen threshold, element 1 is treated as an intact, i.e. undamaged element. Consequently, the damage parameter for element 1 is removed from the system of equations, and the corresponding value is fixed to be zero. Finally, the remaining four structural damage parameters can exactly be determined using the information on the given four damaged frequencies, as shown in Figure 5.4.

5.8.4 Verification of AE technique

In order to predict inversely the location and the extent of structural damage, the information about five damaged frequencies is now considered . Three **AE** techniques, i.e., the first-order approximate equation (**AE1**), the second-order approximate equation (**AE2**), and the third-order approximate equation (**AE3**) techniques, are utilised to compare their effectiveness as shown in Figure 5.5. It can be seen that structural damage can be predicted quite well using all three **AE** techniques. As expected, the predictions of structural damage improve clearly with an increase of the order of approximate equation.

5.8.5 Verification of NLO technique

Here, the information about only four damaged frequencies is used to identify inversely the given structural damage. Three **NLO** techniques, i.e., the first-order approximate equation for equality constraint (**NLO1**), the second-order approximate equation for equality constraint (**NLO2**), and the third-order approximate equation for equality constraint (**NLO3**) techniques, are utilised to compare their effectiveness as shown in Figure 5.6. From the results, it is found that structural damage can be predicted correctly using all three **NLO** techniques. The predictions of structural damage improve with an increase of the order of the approximate equation adopted for equality constraint, as expected.

5.8.6 Verification of OI technique

The information about only four damaged frequencies is again employed for inverse prediction of the location and the extent of structural damage. The **OI** technique is utilised to compare the effectiveness of structural damage identification with the **AE** technique and the **NLO** technique, as shown in Figure 5.7, where the first-order approximation is considered for both the **AE** and the **NLO** techniques. It can be seen that predictions of structural damage from the **NLO** technique are better than those from the **AE** technique, while predictions from the **OI** technique yield the best results from all computational techniques considered.

Parameters of the Problem	
Total DOFs	9
Structural members	5
Damage parameters	5

Hypothetical Damage Scenario					
Element No	1	2	3	4	5
Damage Amount	0%	-5%	-10%	-15%	-20%

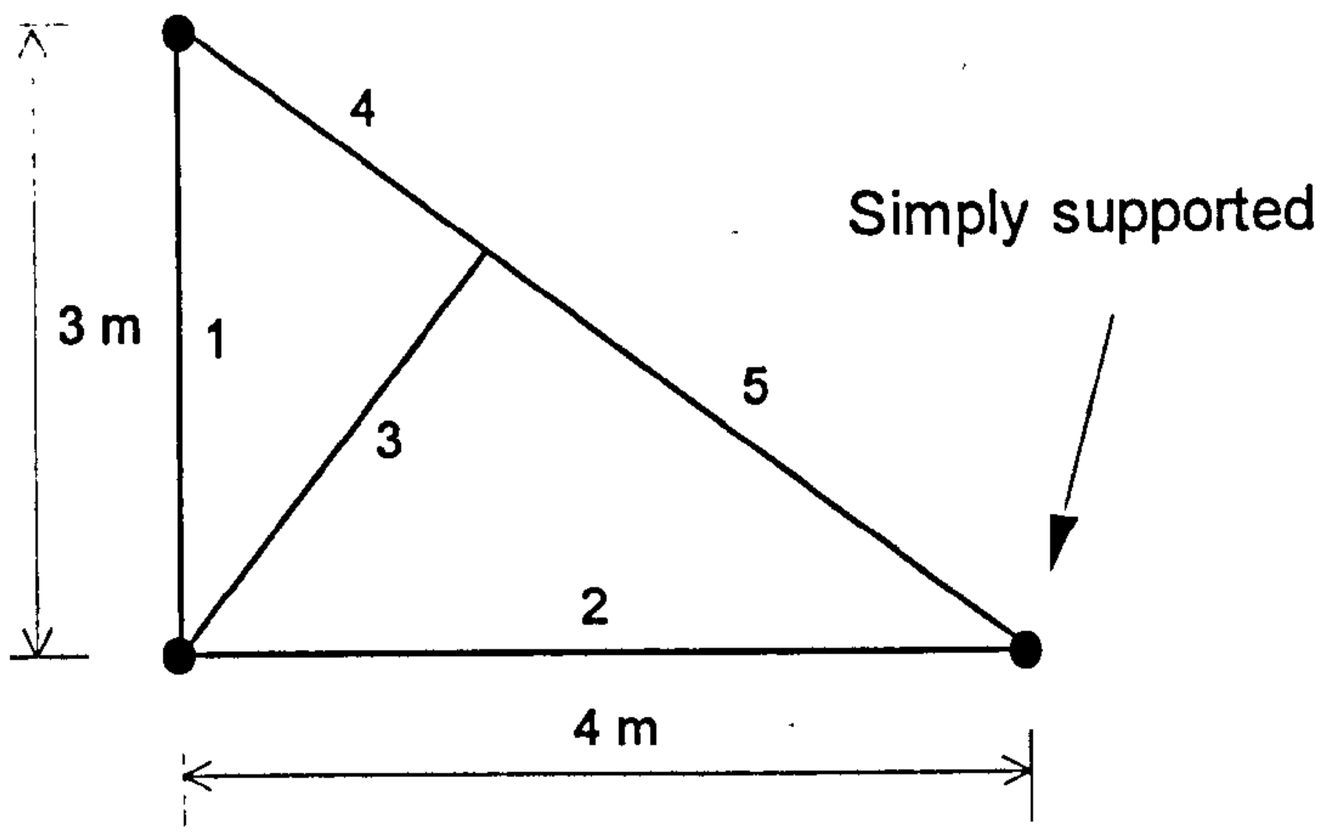

Figure 5.1 Grid model problem (plane view)

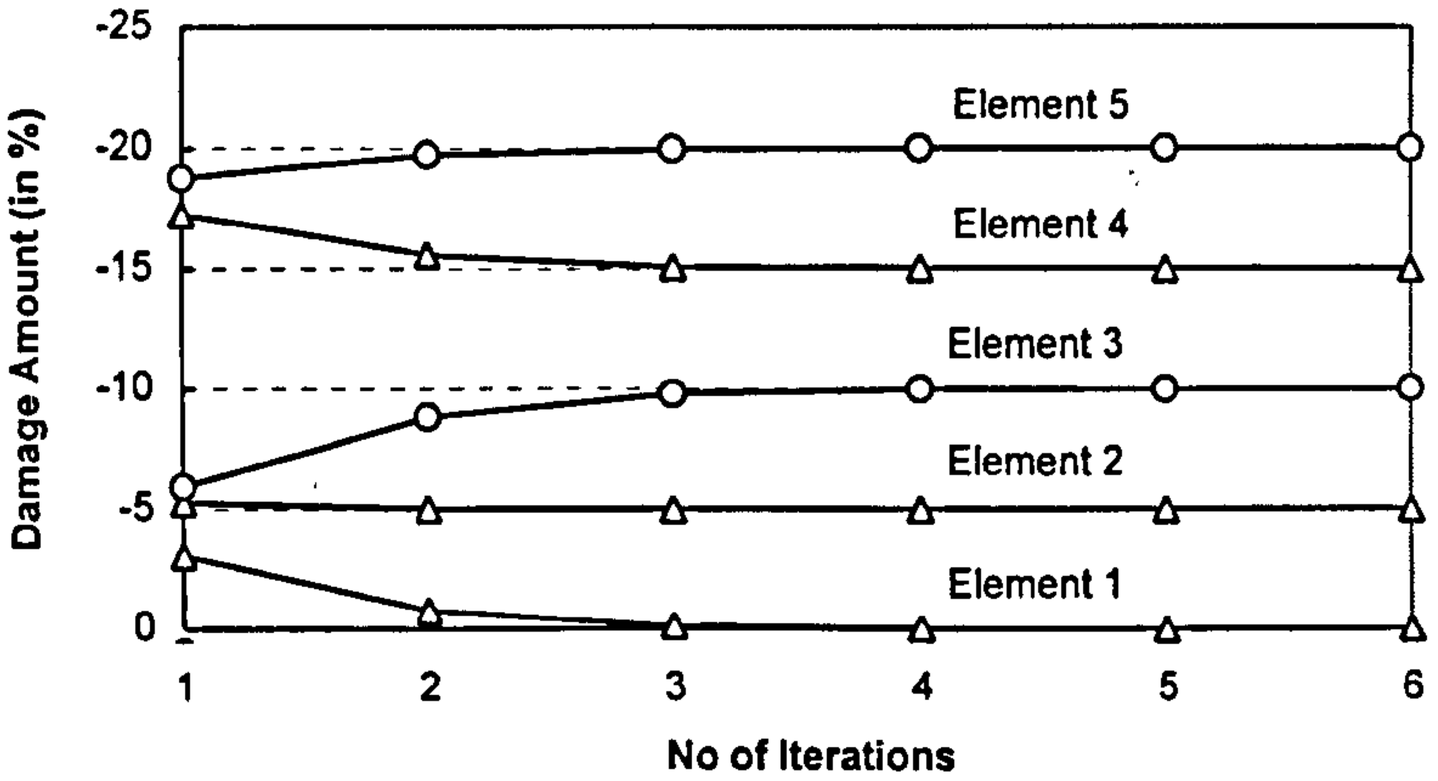

Figure 5.2 Convergence performance of the **DI** technique

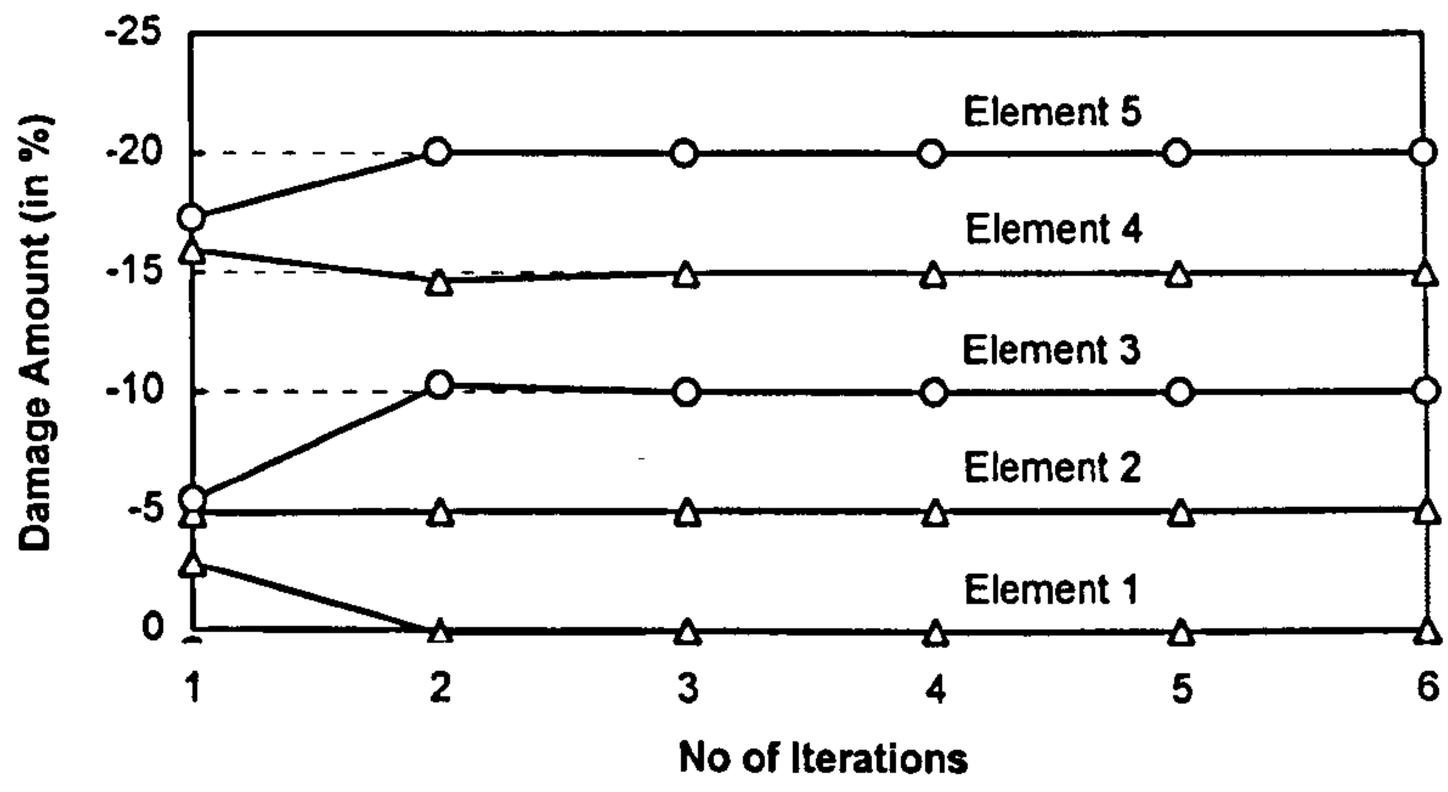

Figure 5.3 Convergence performance of the **GNLS** technique

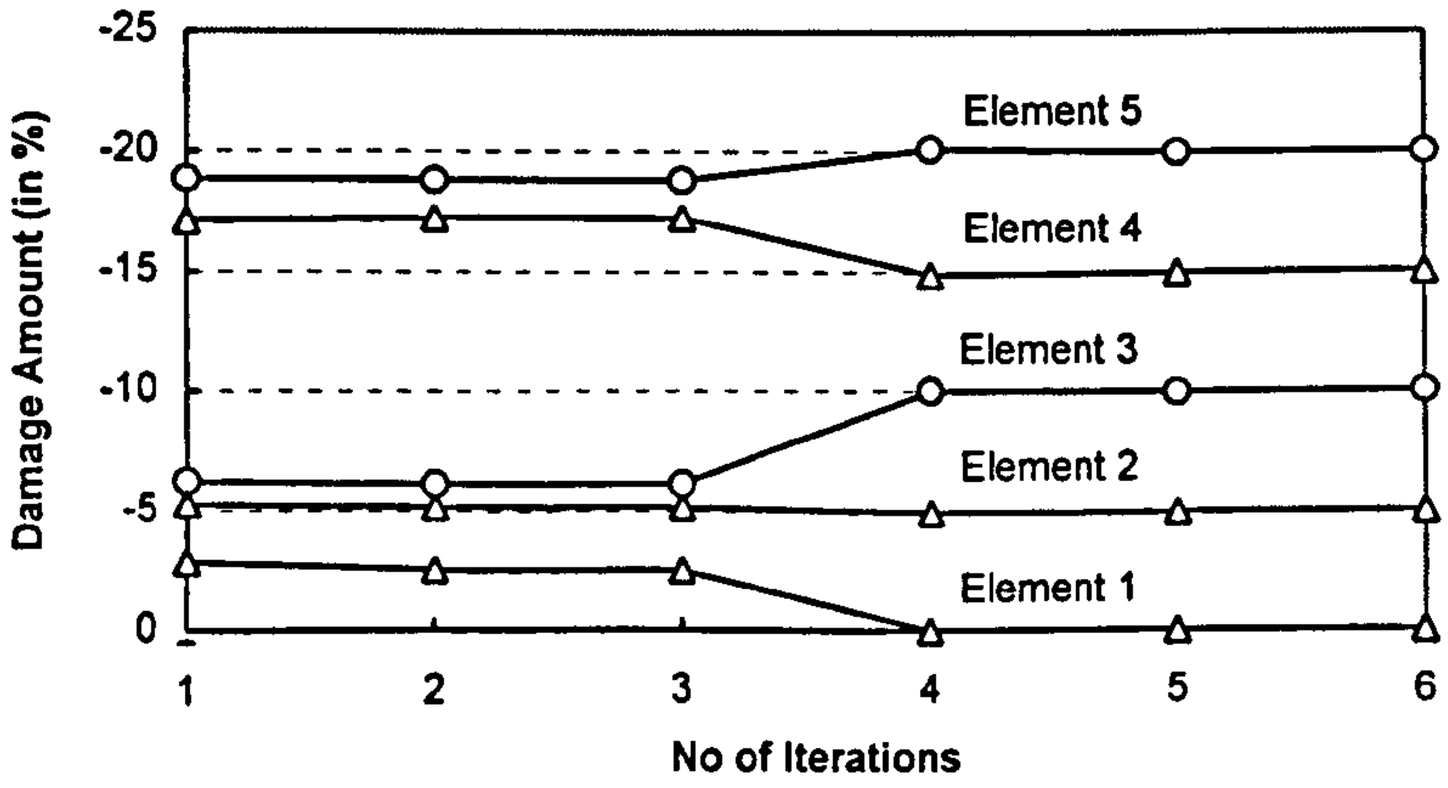

Figure 5.4 Convergence performance of the **TSI** technique

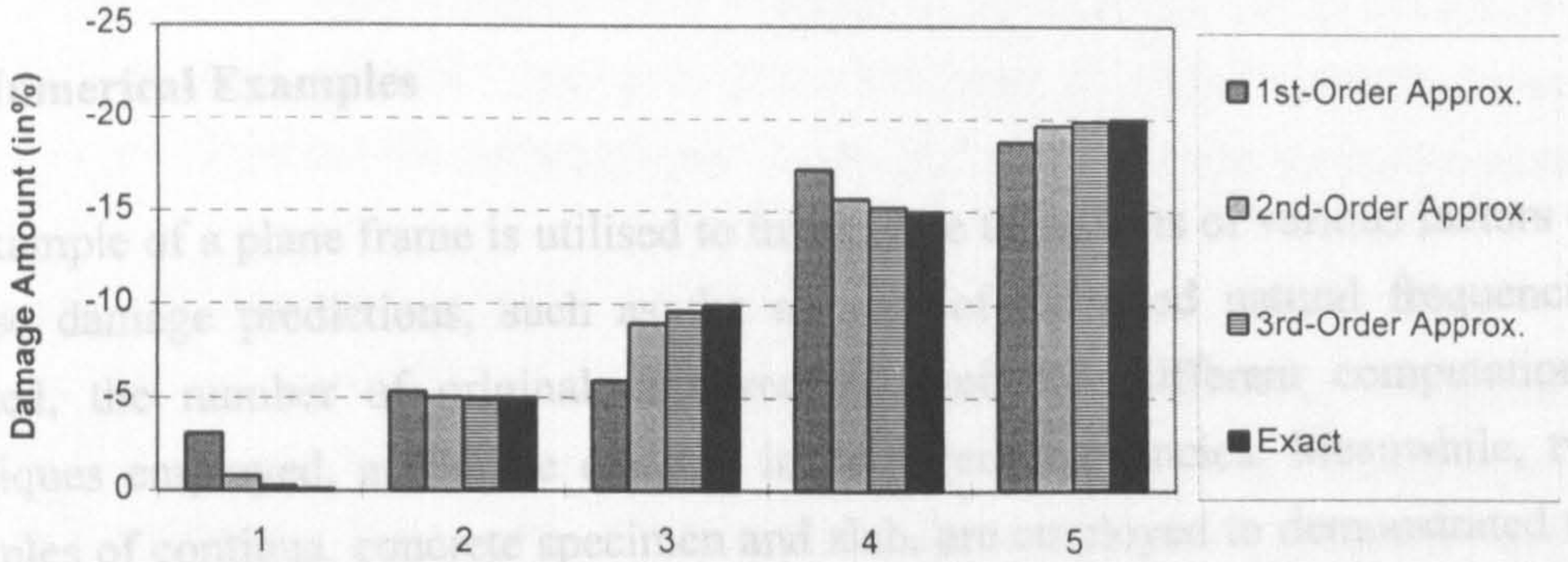

Figure 5.5 Comparison for various approximations for the **AE** technique

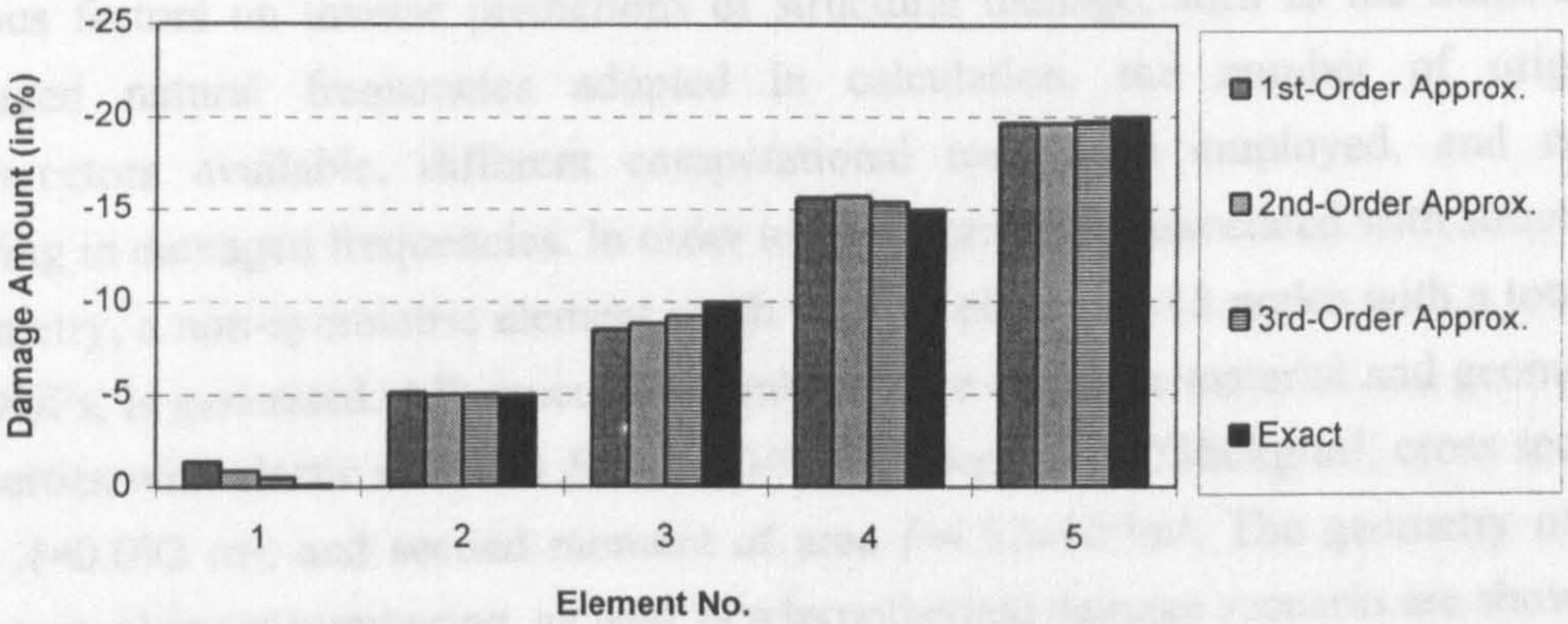

Figure 5.6 Comparison for various approximations for the **NLO** technique

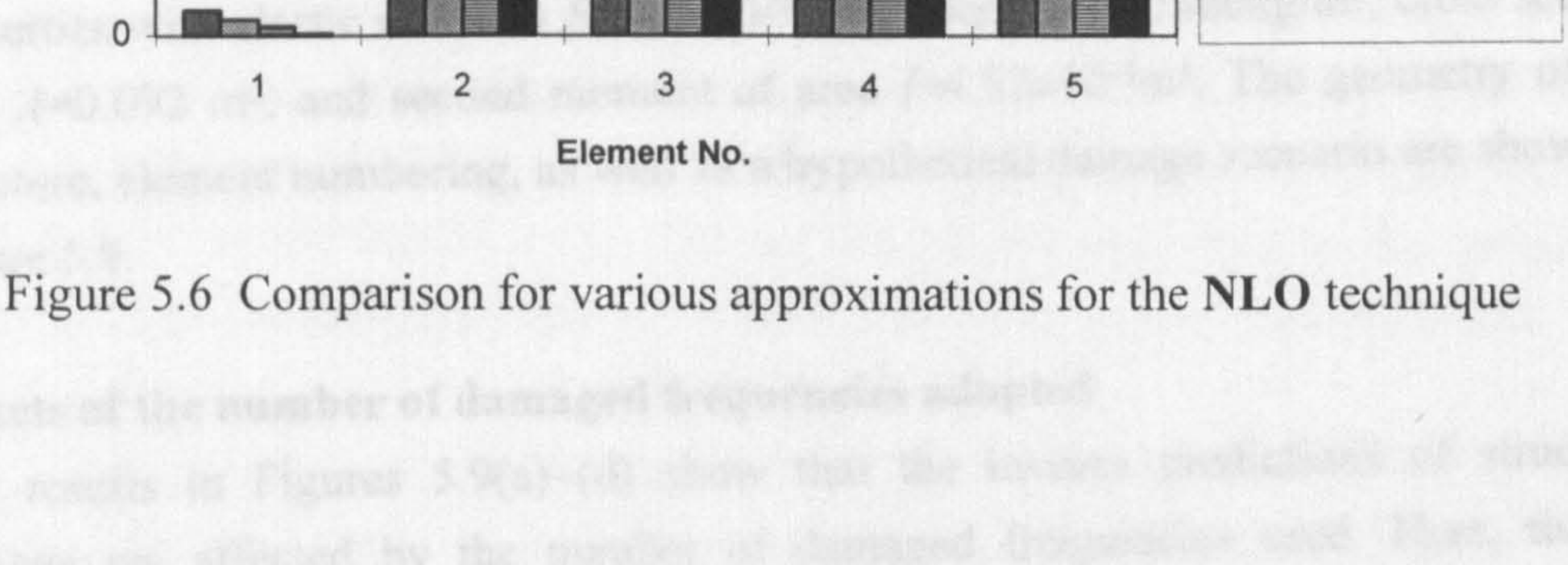

Figure 5.7 Comparison for the **OI** technique with other techniques

5.9 Numerical Examples

An example of a plane frame is utilised to investigate the effects of various factors on inverse damage predictions, such as the number of damaged natural frequencies adopted, the number of original eigenvectors available, different computational techniques employed, and noise existing in damaged frequencies. Meanwhile, two examples of continua, concrete specimen and slab, are employed to demonstrated the effectiveness of the proposed approaches using information about only the damaged natural frequencies.

5.9.1 Plane frame

A symmetric plane frame illustrated in Figure 5.8 is used to investigate the effects of various factors on inverse predictions of structural damage, such as the number of damaged natural frequencies adopted in calculation, the number of original eigenvectors available, different computational techniques employed, and noise existing in damaged frequencies. In order to avoid problems associated with structural symmetry, a non-symmetric element mesh with 18 elements, 18 nodes with a total of 48 DOFs, is generated. All structural members have the same material and geometric properties with elastic modulus E=2.1×10^{11}N/m^2, density ρ=7860kg/m^3, cross section area A=0.092 m^2, and second moment of area I=4.52×10^{-5}m^4. The geometry of the structure, element numbering, as well as a hypothetical damage scenario are shown in Figure 5.8.

Effects of the number of damaged frequencies adopted

The results in Figures 5.9(a)–(d) show that the inverse predictions of structural damage are affected by the number of damaged frequencies used. Here, the **DI** technique is employed and all original eigenvectors are considered in structural damage identification. It is found that structural damage can roughly be predicted using only 10 damaged frequencies. As expected, the predictions of structural damage improve with an increase of the number of damaged frequencies used, reaching the values very close to the exact solution when 16 damaged frequencies are used.

Effects of the number of original eigenvectors available

The effectiveness of the proposed approaches with respect to the number of original eigenvectors is investigated as shown in Figures 5.10(a)–(d), where the **DI** technique is employed and 16 damaged frequencies are used. It is found that only a limited

knowledge of the original eigenvectors is required, even 24 original eigenvectors (half the number of all original eigenvectors) are sufficient to predict correctly structural damage, which makes the proposed approaches applicable to large scale structures.

Comparison of the results from different approaches

The results in Figures 5.11(a)–(d) are obtained from different computational techniques, such as the **AE1** technique, the **NLO1** technique, the **OI** technique, and the **TSI** technique. Here, only 10 damaged frequencies are used and all original eigenvectors are considered in the calculation for each computational technique. It is found that structural damage can roughly be estimated using the **AE1** technique and the **NLO1** technique, while structural damage can correctly be determined using the **OI** technique and the **TSI** technique from only 10 damaged frequencies.

Effects of the noise existing in damaged frequencies

The effects of random noise existing in damaged frequencies at different levels ranging from 0.10% to 1.00% on predictions of structural damage are shown in Figures 5.12(a)–(d), where 16 damaged frequencies are used and all original eigenvectors are considered in inverse damage predictions from the **DI** technique. The noise in "measured" data is simulated by corrupting the corresponding exact analytical damaged natural frequency with some random noise, i.e., the exact natural frequency is scaled by the factor $1+\varepsilon$ where ε indicates a level of random noise. From the results, it can be seen that the quality of predictions for structural damage is significantly affected by the noise levels existing in damaged frequencies, even when random noise is introduced at the 0.20% level. The reason for this may be that the governing equations used for structural damage identification are in general ill-conditioned.

Parameters of the Problem	
Total DOFs	48
Structural members	18
Damage parameters	18

Hypothetical Damage Scenario

Element No	5	10	15
Damage Amount	-10%	-20%	-30%

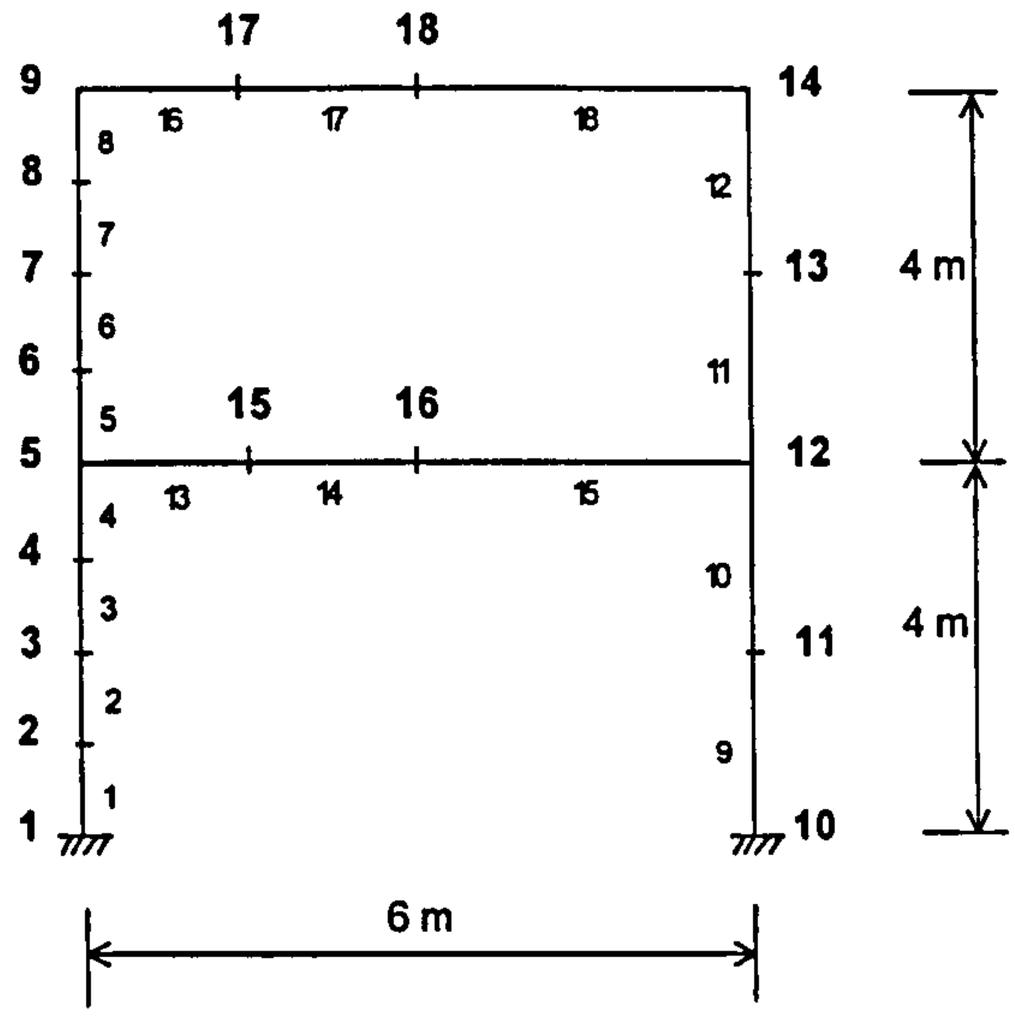

Figure 5.8 Symmetric model plane frame problem

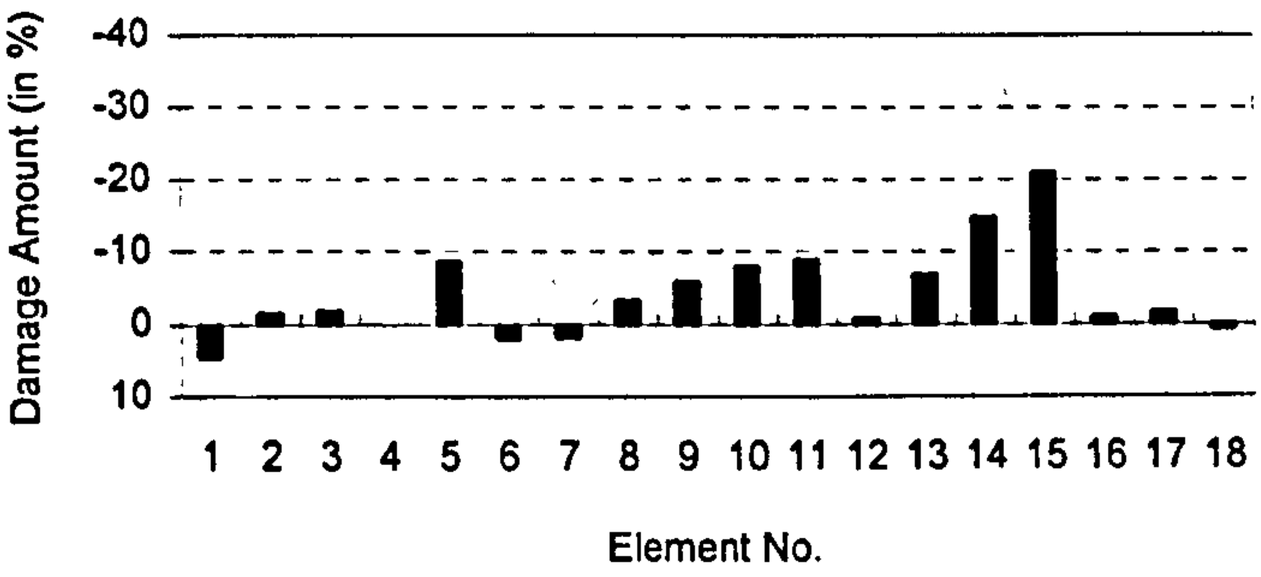

Figure 5.9(a) 8 damaged frequencies used

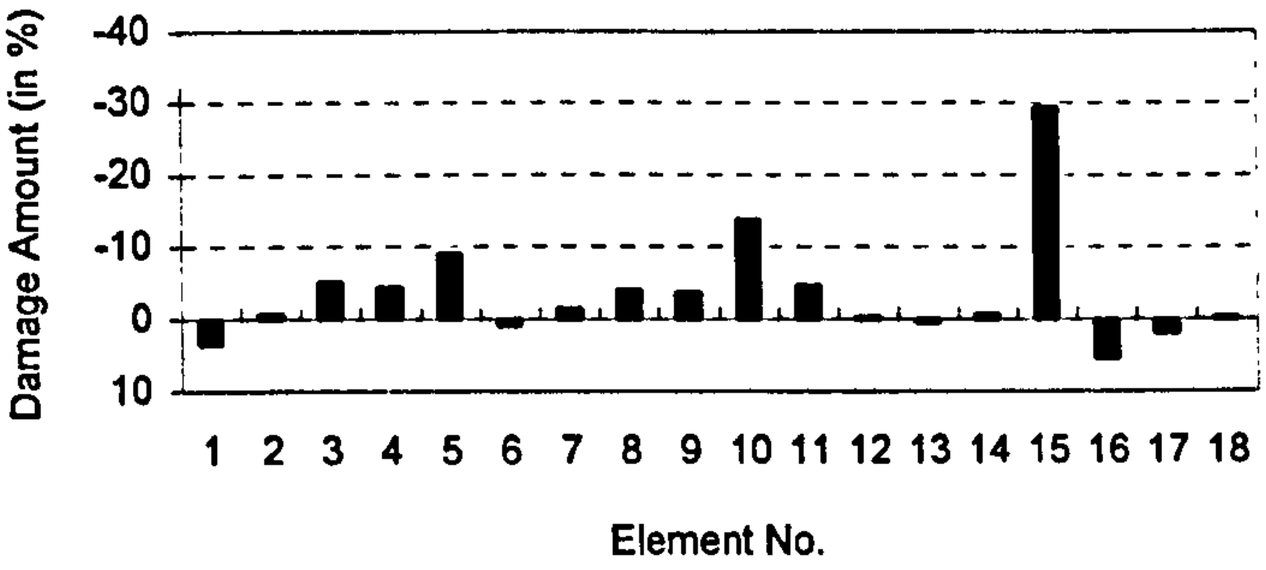

Figure 5.9(b) 10 damaged frequencies used

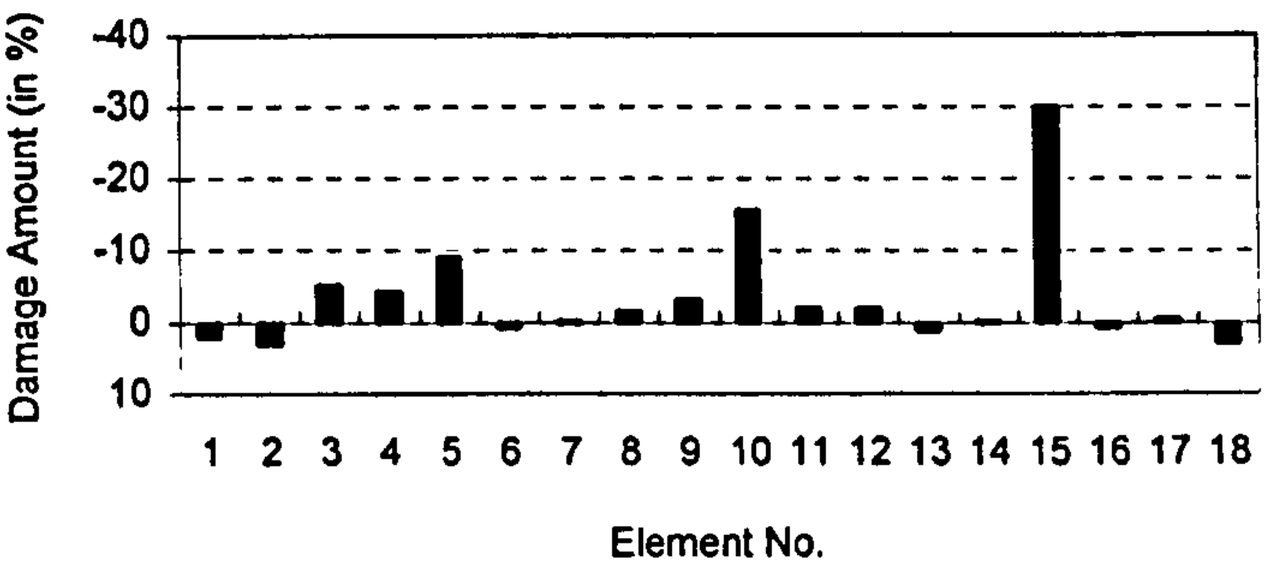

Figure 5.9(c) 12 damaged frequencies used

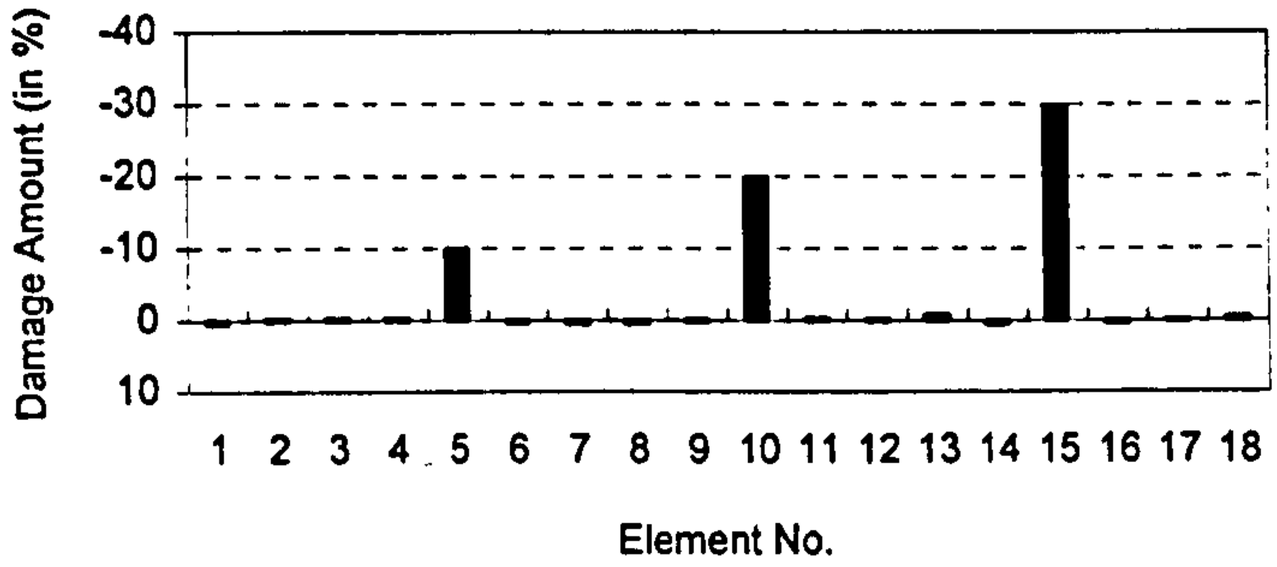

Figure 5.9(d) 16 damaged frequencies used

Figure 5.9 Inverse damage predictions affected by the number of damaged frequencies, all original eigenvectors used

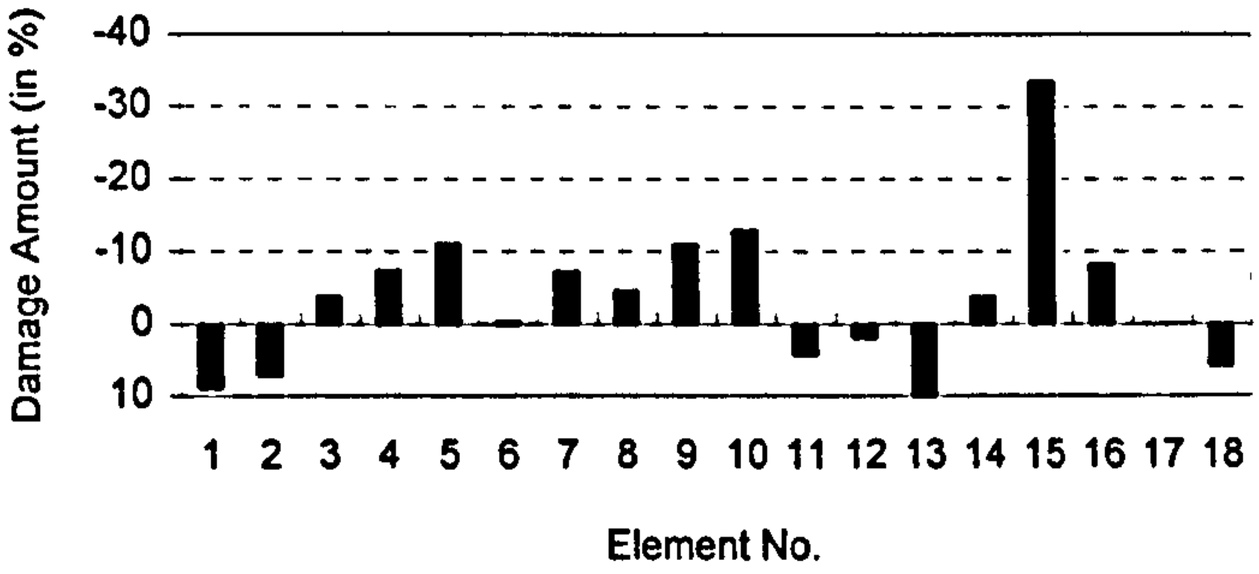

Figure 5.10(a) 16 original eigenvectors used

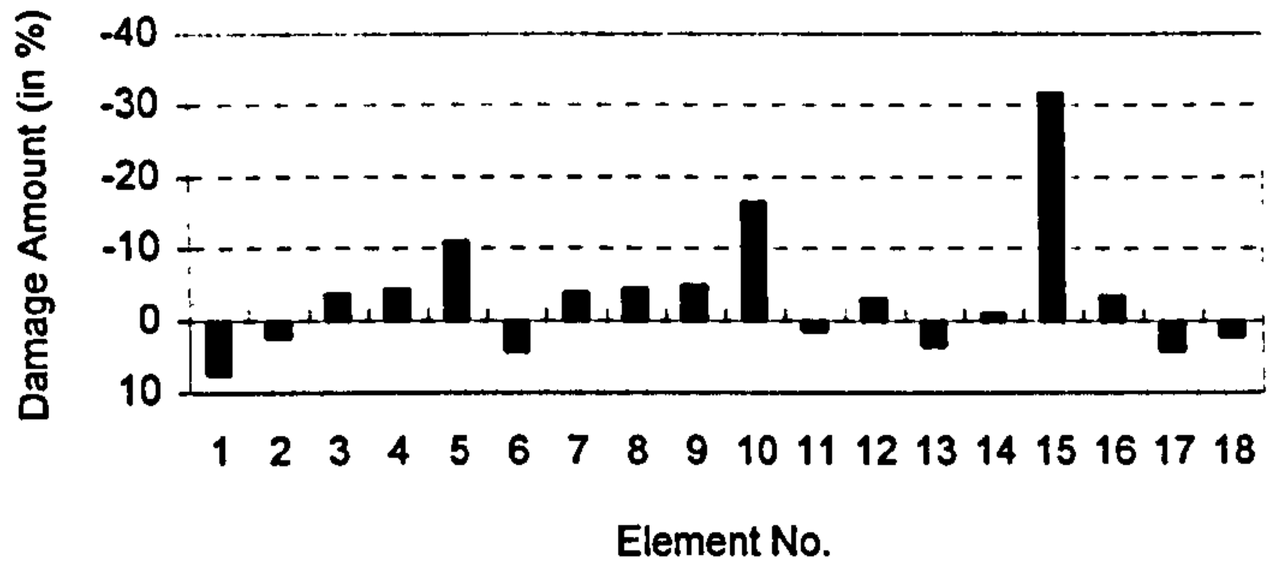

Figure 5.10(b) 18 original eigenvectors used

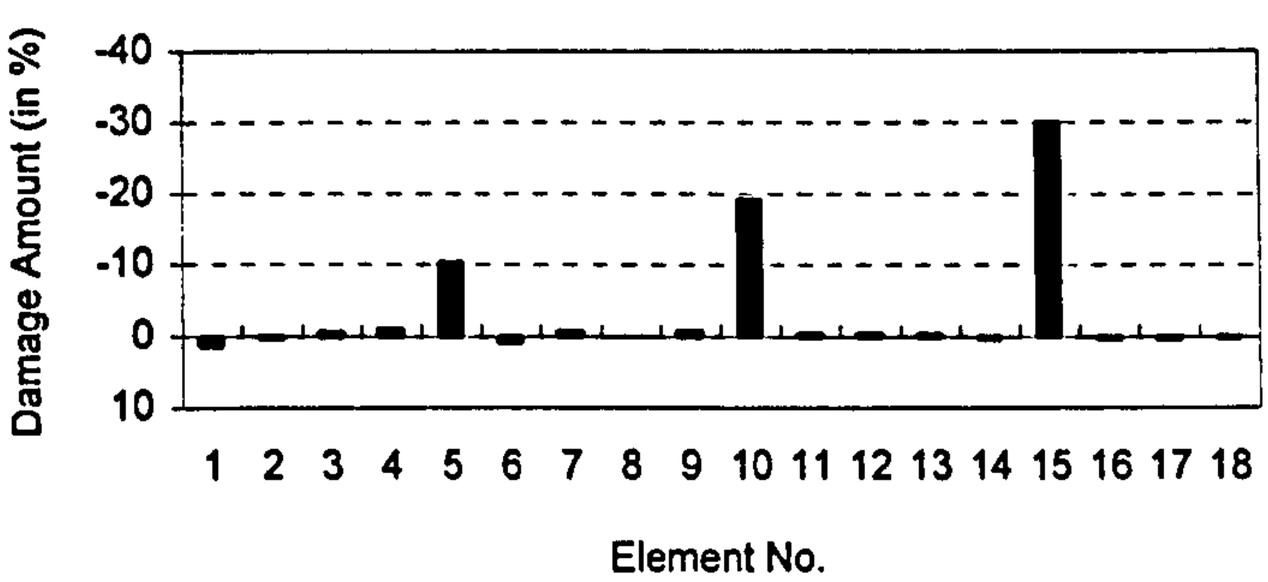

Figure 5.10(c) 24 original eigenvectors used

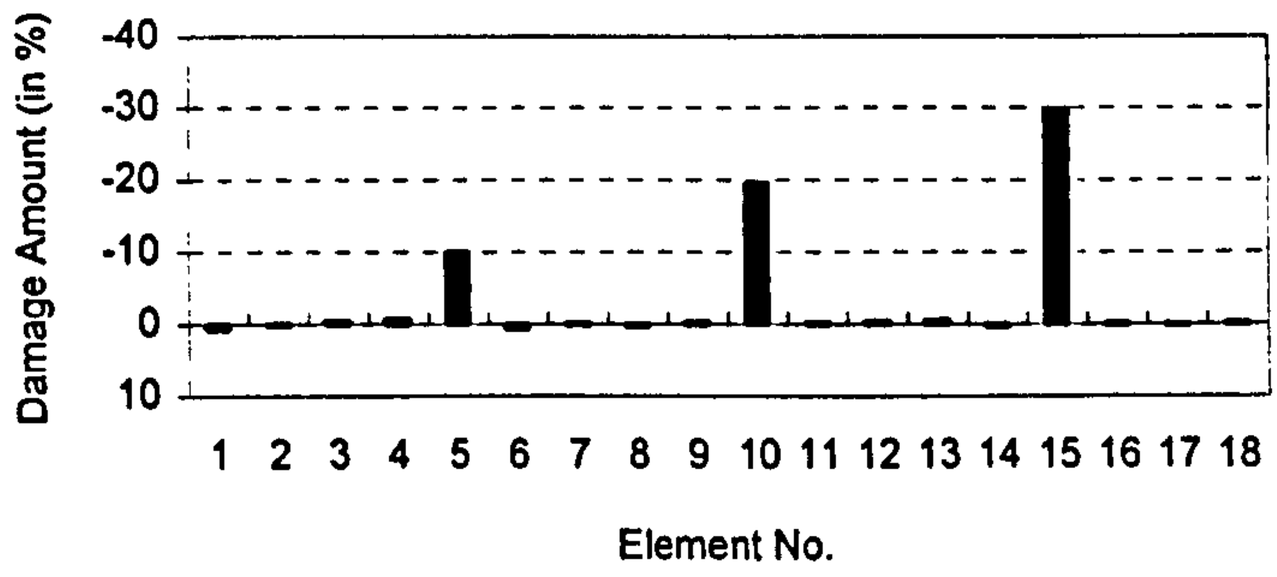

Figure 5.10(d) 36 original eigenvectors used

Figure 5.10 Inverse damage predictions affected by the number of original eigenvectors, 16 damaged frequencies used

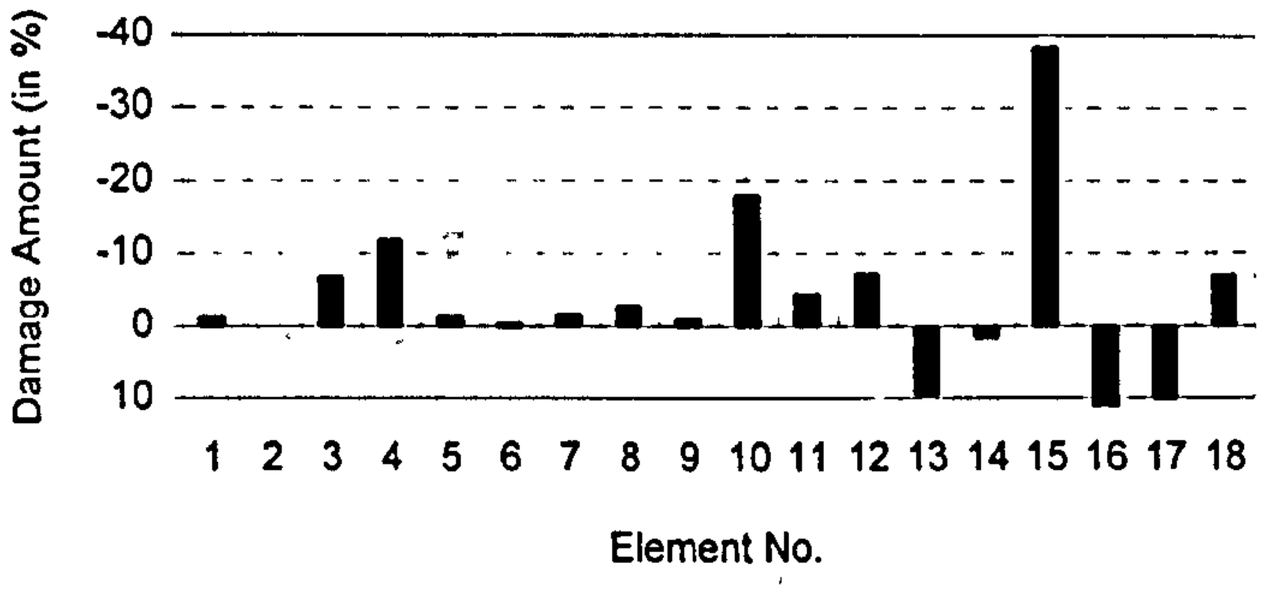

Figure 5.11(a) The **AE1** technique used

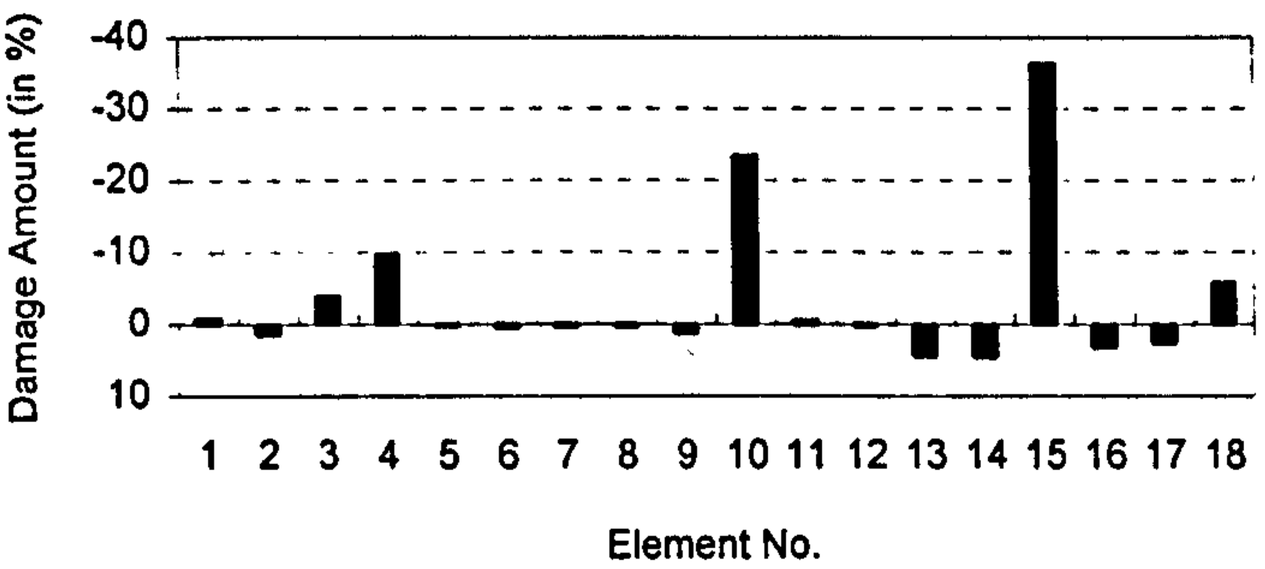

Figure 5.11(b) The **NLO1** technique used

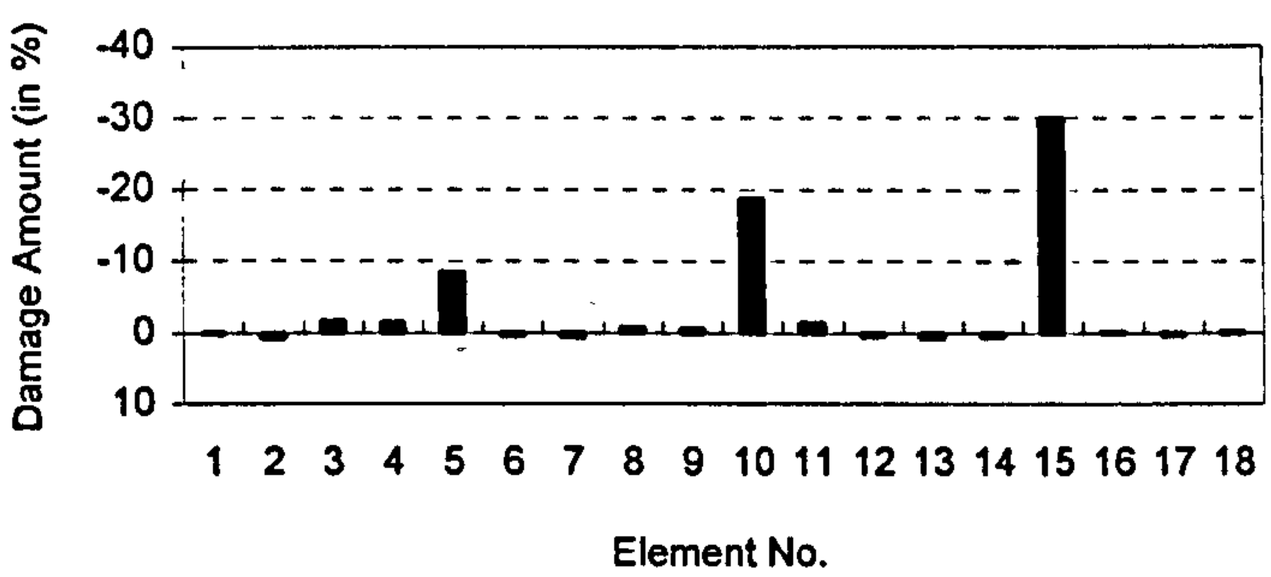

Figure 5.11(c) The **OI** technique used

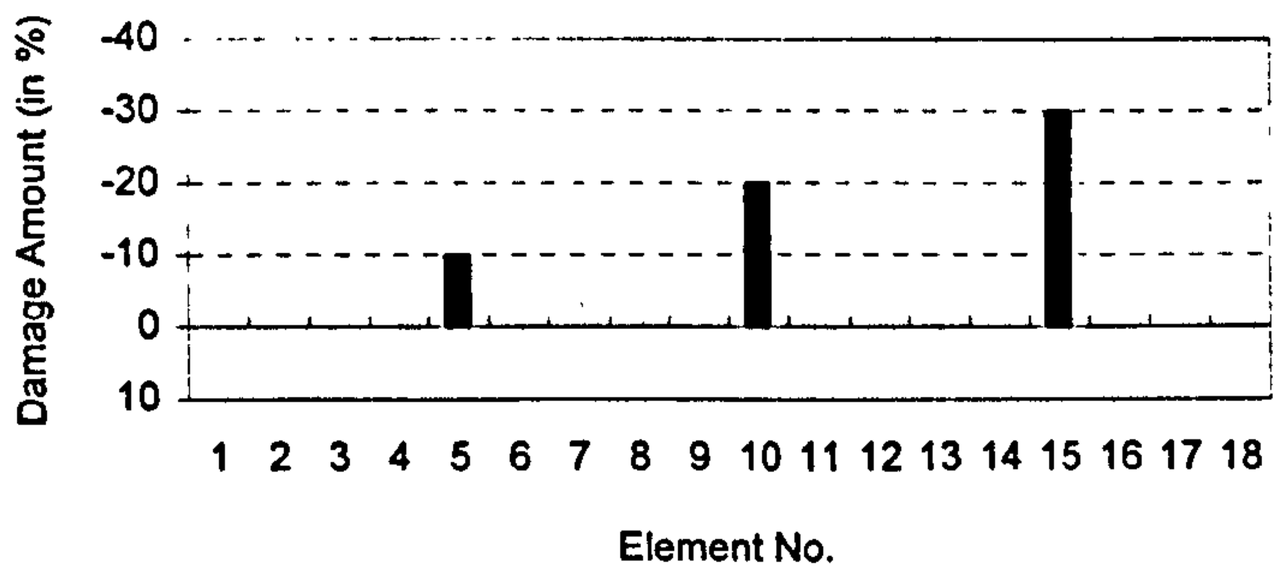

Figure 5.11(d) The **TSI** technique used

Figure 5.11 Comparison of inverse damage predictions from different computational techniques, 10 damaged frequencies and all original eigenvectors used

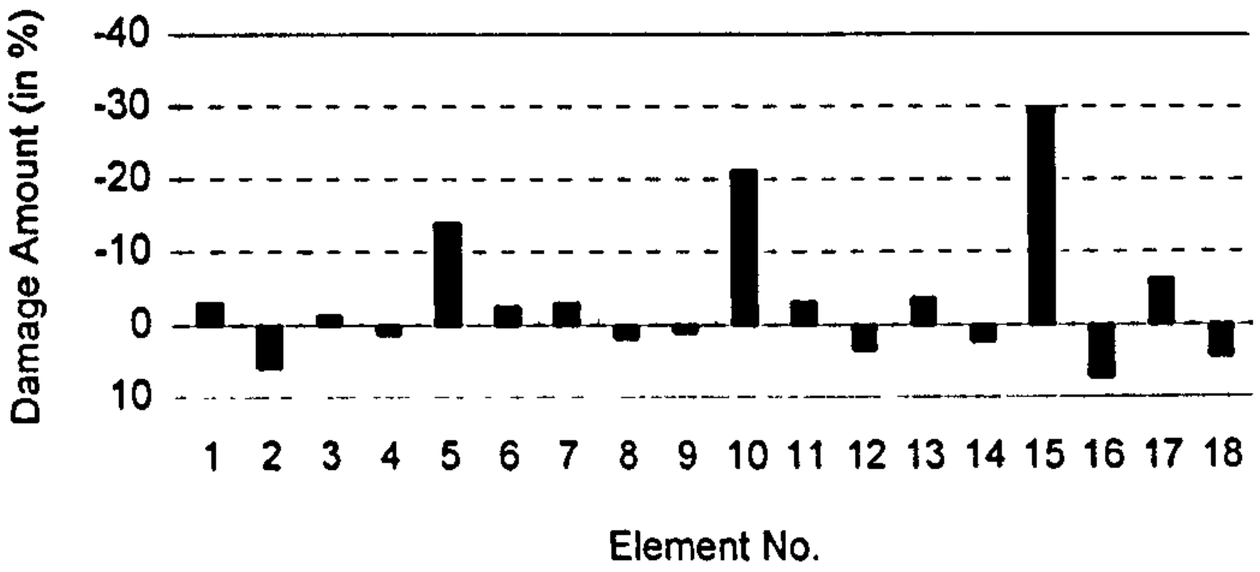

Figure 5.12(a) 0.10% random noise level introduced

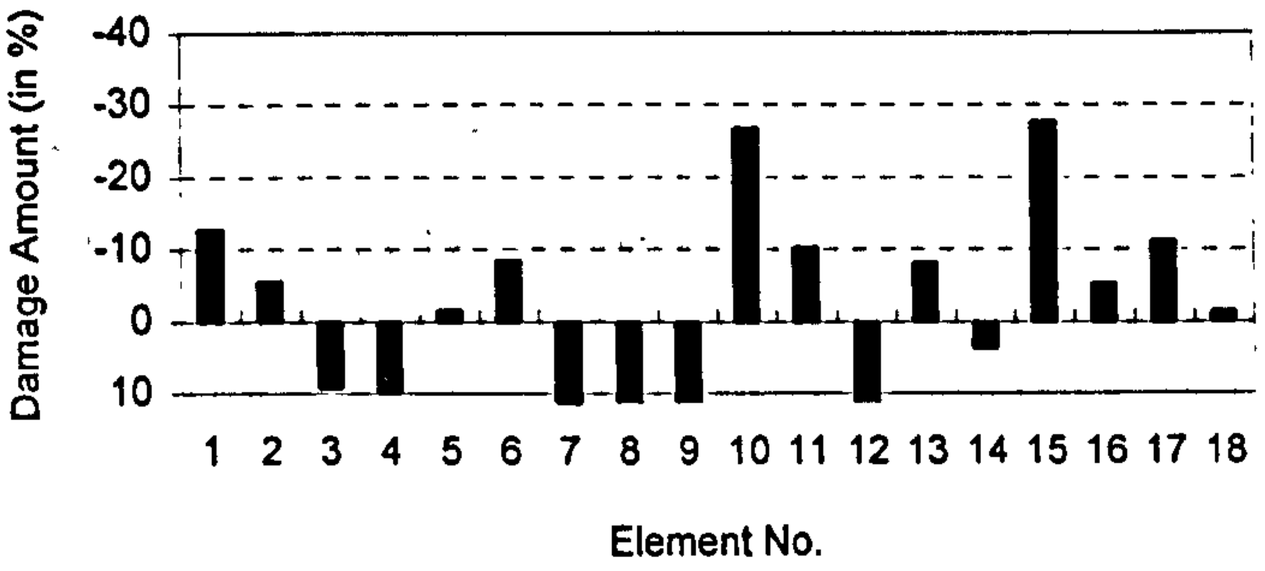

Figure 5.12(b) 0.20% random noise level introduced

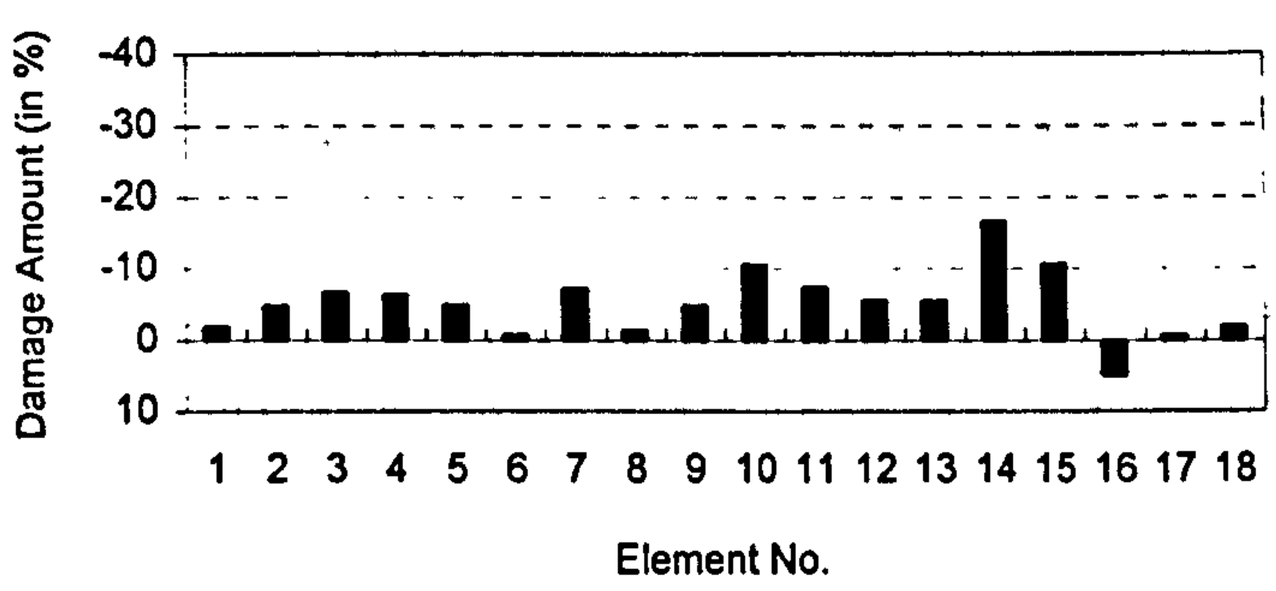

Figure 5.12(c) 0.50% random noise level introduced

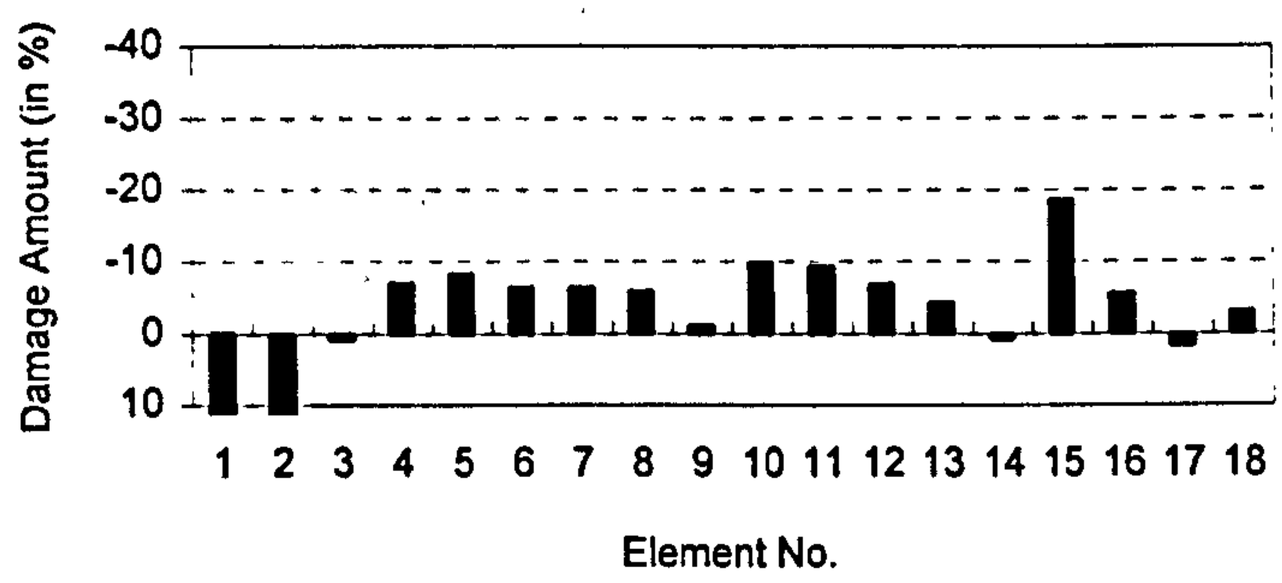

Figure 5.12(d) 1.00% random noise level introduced

Figure 5.12 Inverse damage predictions affected by various noise levels for damaged frequencies, 16 damaged frequencies and all original eigenvectors used

5.9.2 Concrete specimen

Resonance method, one of non-destructive testing techniques for evaluating the quality of concrete, is often utilised to determine the dynamic modulus of elasticity for concrete. The procedure for testing, in general, is that a concrete specimen such as a beam is clamped at its centre and subjected to vibration. Since changes in the quality of concrete are related to changes in the dynamic modulus of elasticity, which result in changes in the natural frequencies of the structure, the quality of concrete can be evaluated from changes in frequencies measured from testing.

A concrete specimen illustrated in Figure 5.13 is used to demonstrate that changes in the dynamic modulus of elasticity can be predicted using the proposed approaches from measured natural frequencies, and then the dynamic modulus of elasticity can be estimated after its changes have been obtained if the initial modulus of elasticity is assumed to be known.

The specimen, modelled as a cantilever beam 0.375m in length, 0.150m in width and height, respectively, is divided into two 20-node 3-D solid brick elements. Eight Gauss integrating points are considered for each element. Initially, all Gauss points have the same material properties with an elastic modulus of E=2.8×10^{10}N/m^2, Poisson's ratio υ=0.15 and density ρ=2400kg/m^3. The geometry of the structure, element and Gauss point numbering, as well as two different hypothetical damage scenarios simulated by reducing elastic modulus in some Gauss points are shown in Figure 5.13.

The **DI** technique is employed for structural damage identification, and different number of damaged frequencies are used in the calculation. The inverse predictions for damage scenario 1 are shown in Figures 5.14(a) and (b), where 8 and 12 damaged frequencies are used, respectively. It is found that a good estimate for damage scenario 1 can be obtained using only 8 damaged frequencies, while the estimate improves when 12 damaged frequencies are used.

The results in Figures 5.14(c) and (d) show inverse predictions for damage scenario 2, where Gauss point 5 has an increase of elastic modulus. It can be seen that the structural damage can also correctly be predicted using 12 damaged frequencies, even if elastic modulus in some Gauss points increase, which may often be the case for model updating.

Parameters of the Problem

Total DOFs	72
Structural elements	2
Gauss points	2×8=16
Damage parameters	16

Hypothetical Damage Scenarios

	Damage Scenario 1		Damage Scenario 2	
Element No	1	2	1	2
Gauss Point No	4	12	5	14
Damage Amount	-30%	-20%	+20%	-30%

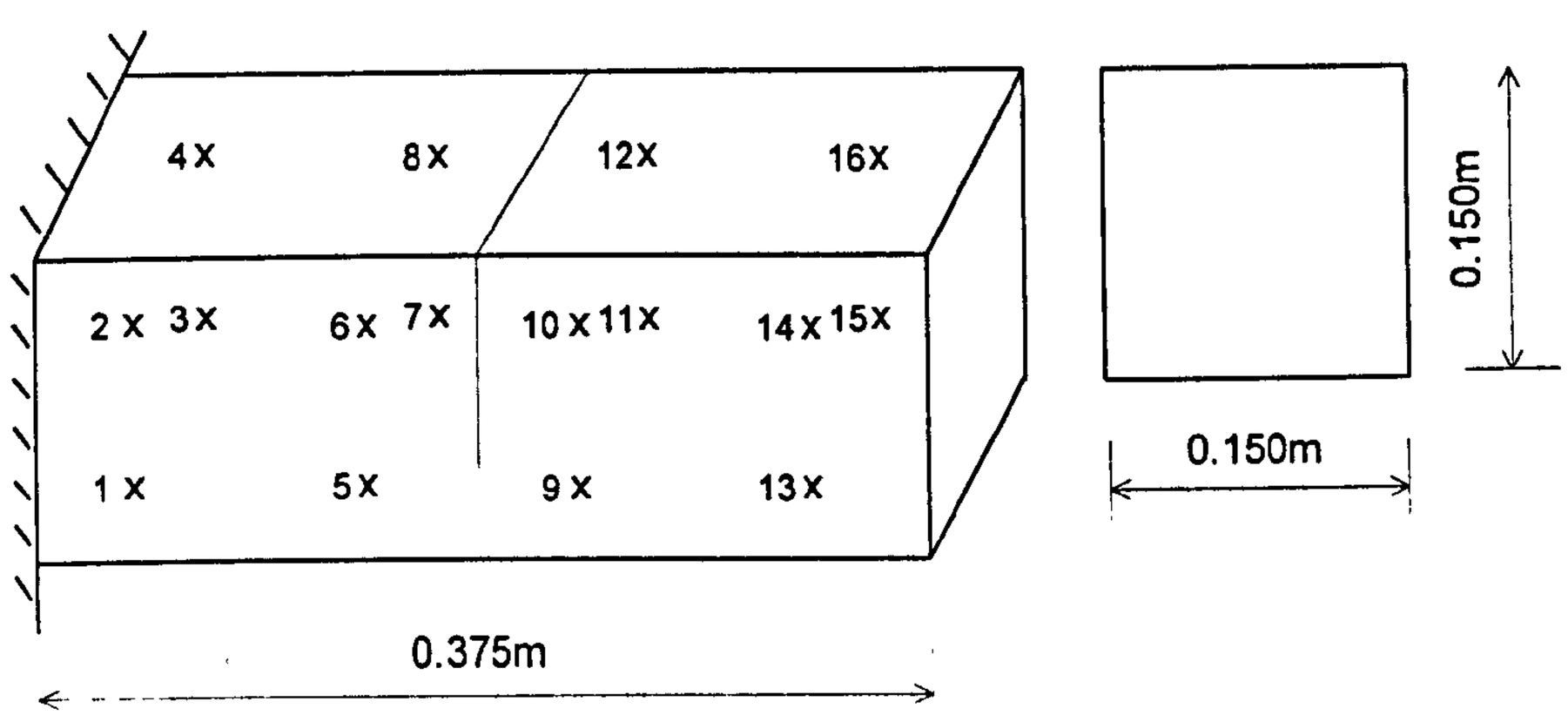

Figure 5.13 Concrete specimen model problem

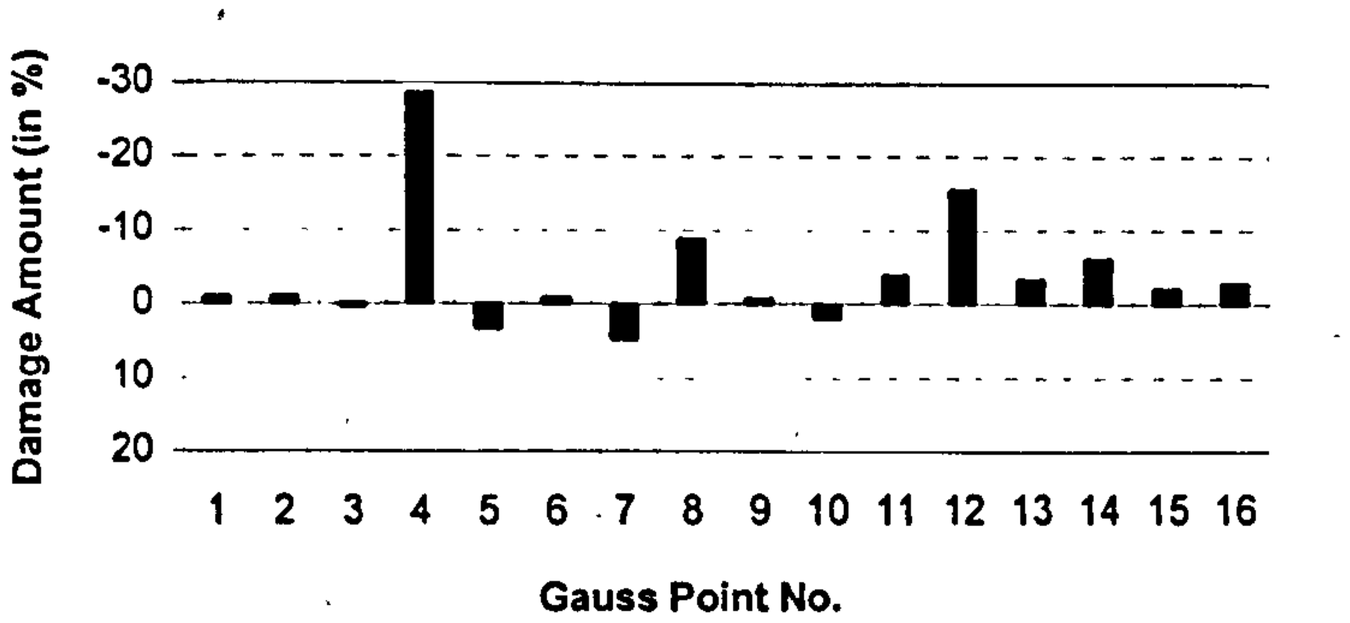

Figure 5.14(a) Predicted damage for scenario 1, 8 damaged frequencies used

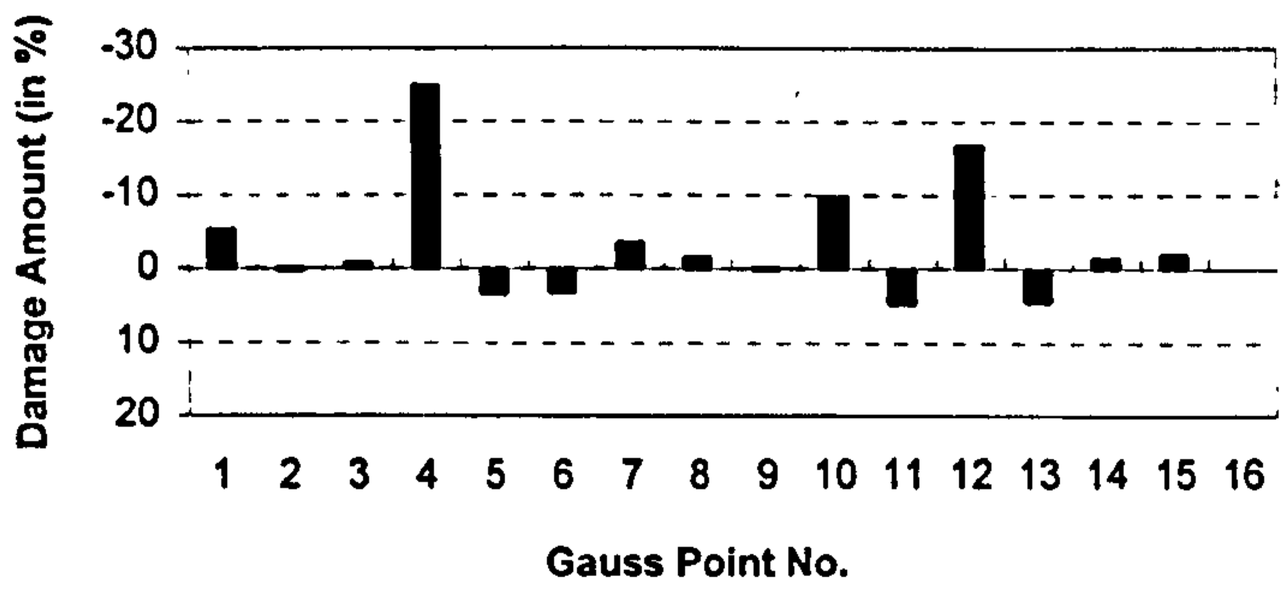

Figure 5.14(b) Predicted damage for scenario 1, 12 damaged frequencies used

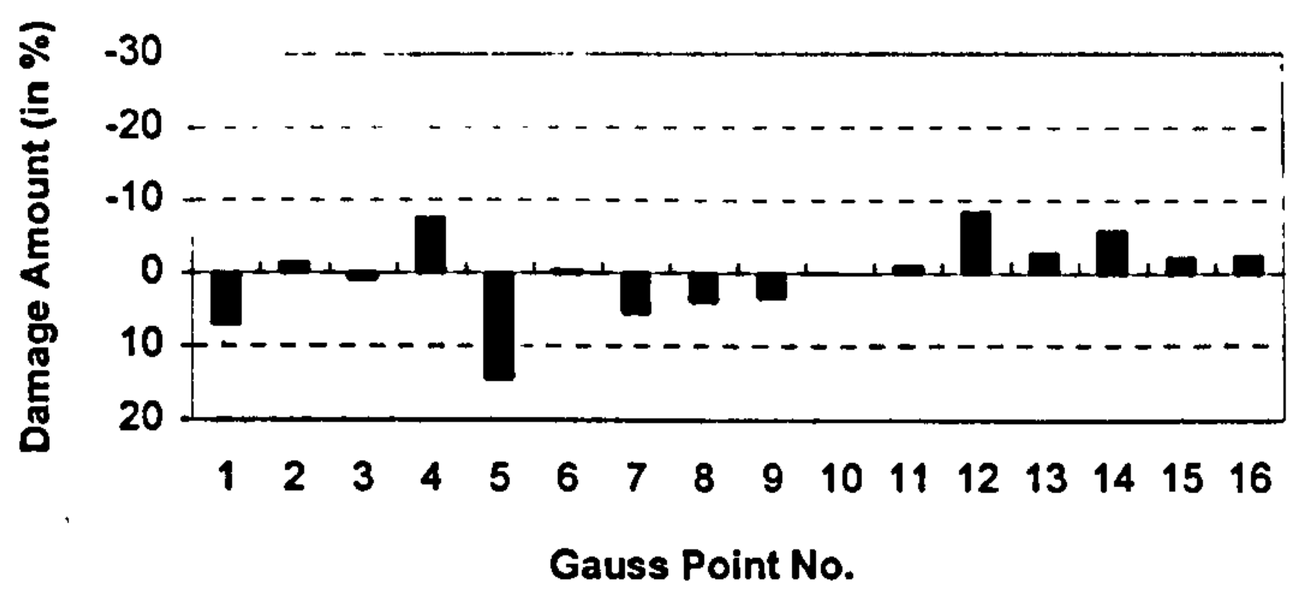

Figure 5.14(c) Predicted damage for scenario 2, 8 damaged frequencies used

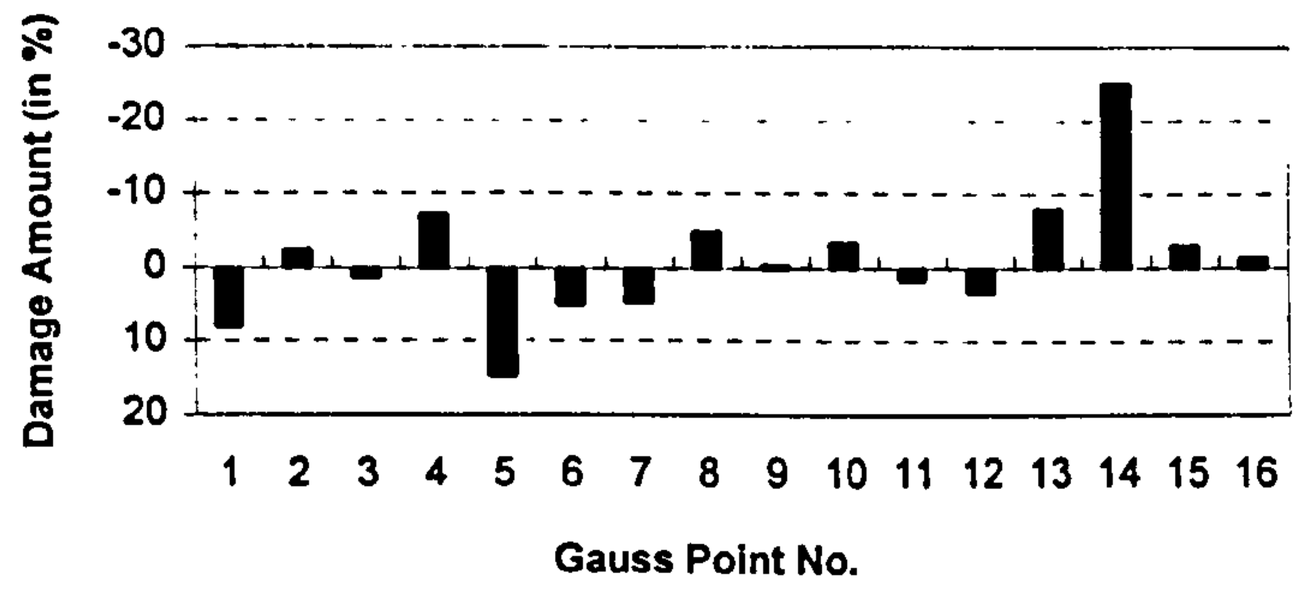

Figure 5.14(d) Predicted damage for scenario 2, 12 damaged frequencies used

Figure 5.14 Inverse damage predictions for different damage scenarios using different number of damaged frequencies, the **DI** technique used

5.9.3 Slab

A slab of 0.2m in thickness, 6.0m in length and width, respectively, shown in Figure 5.15 is used to investigated the effects of boundary conditions on structural damage identification. The slab model is divided into 16 8-node isoparametric plate bending elements. Four Gauss integrating points are considered for each element. All Gauss points have the same material properties with elastic modulus E=2.8×10^{10}N/m^2, Poisson's ratio υ=0.15 and density ρ=2400kg/m^3. It is assumed that structural damage only exists in four elements, i.e., elements 3, 7, 10, and 14, while the remaining elements are considered to be intact. The geometry of the structure, four different cases of boundary conditions, element and Gauss point numbering, as well as a hypothetical damage scenario are shown in Figure 5.15.

Four different boundary conditions are considered in order to investigated their effects on structural damage identification. Figures 5.16(a) and (b) show the cases of all four sides simply supported and only sides AB and CD simply supported, i.e. case 1 and case 2, respectively. For these two cases of boundary conditions, the structure is symmetric with respect to two axes. The **AE1** technique is employed for structural damage identification and 10 damaged frequencies are used in the calculation. It is found that structural damage can only roughly be estimated for both two cases.

The results in Figures 5.16(c) and (d) are for the cases of three sides AB, AC and CD simply supported, and only side AB clamped, i.e. case 3 and case 4, respectively. For these two cases of boundary conditions, the structure now becomes symmetric only with respect to one axis. The **DI** technique is employed and 10 damaged frequencies are used in the calculation. The predictions of structural damage improve significantly, and reach the values very close to the exact solution when the case for only side AB clamped is considered.

The results indicate that it is very important to consider boundary conditions for the structure which is used for vibration testing in order to identify correctly damage existing in the structure.

Parameters of the Problem

Total DOFs	varying with boundary conditions
Structural elements	16
Gauss points	16×4=64
Damage parameters	64

Hypothetical Damage Scenario

Element No	3	7	10	14
Gauss Point No	10, 12	25, 27	40	55
Damage Amount	-10%	-10%	-20%	-20%

Cases of Boundary Conditions

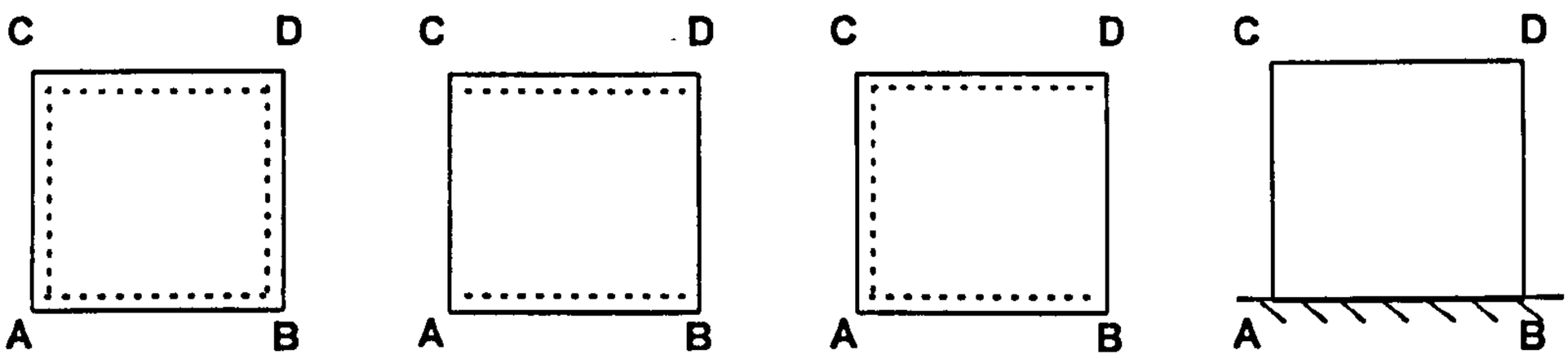

Case 1 Case 2 Case 3 Case 4

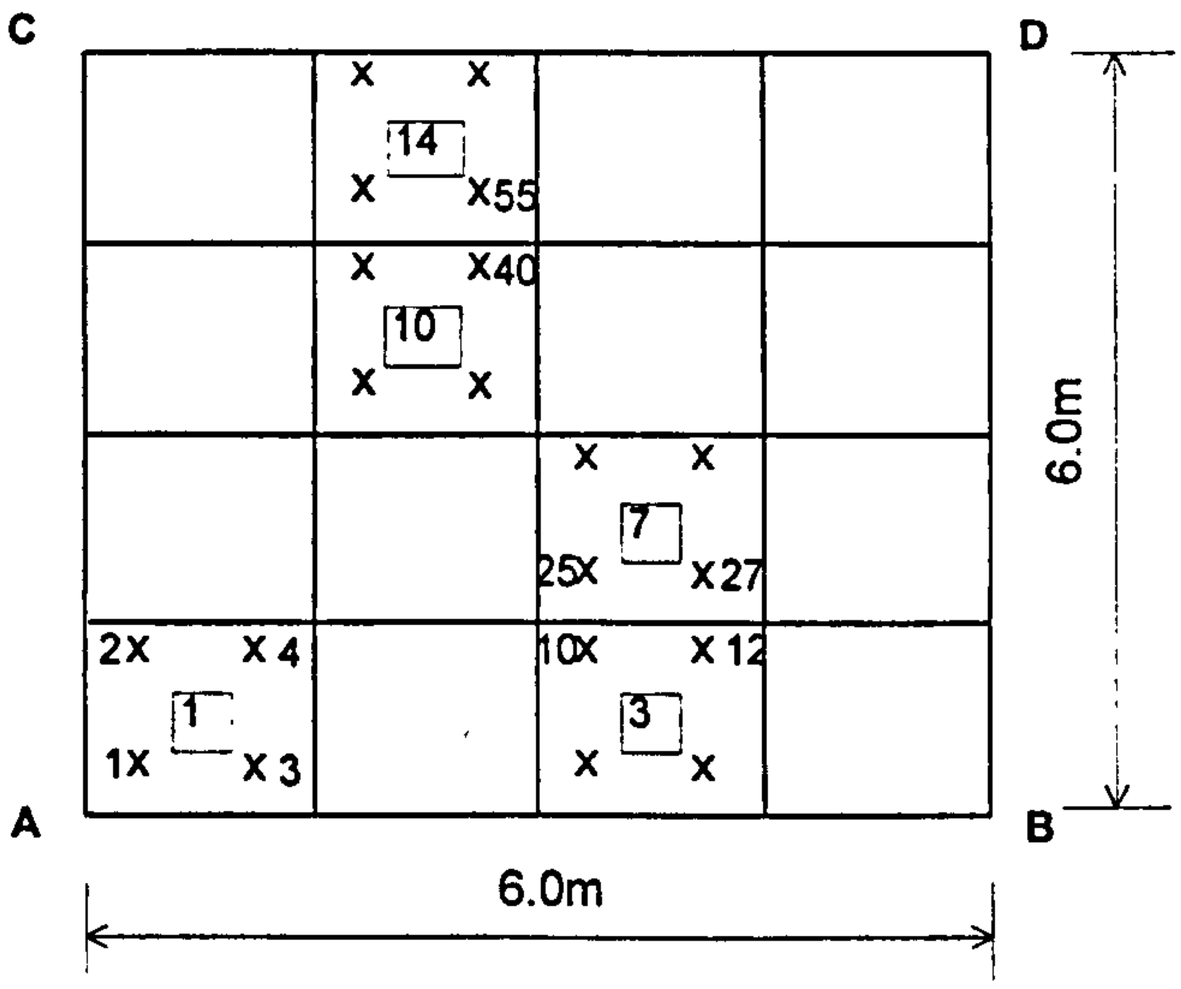

Figure 5.15 Slab model problem with different boundary conditions

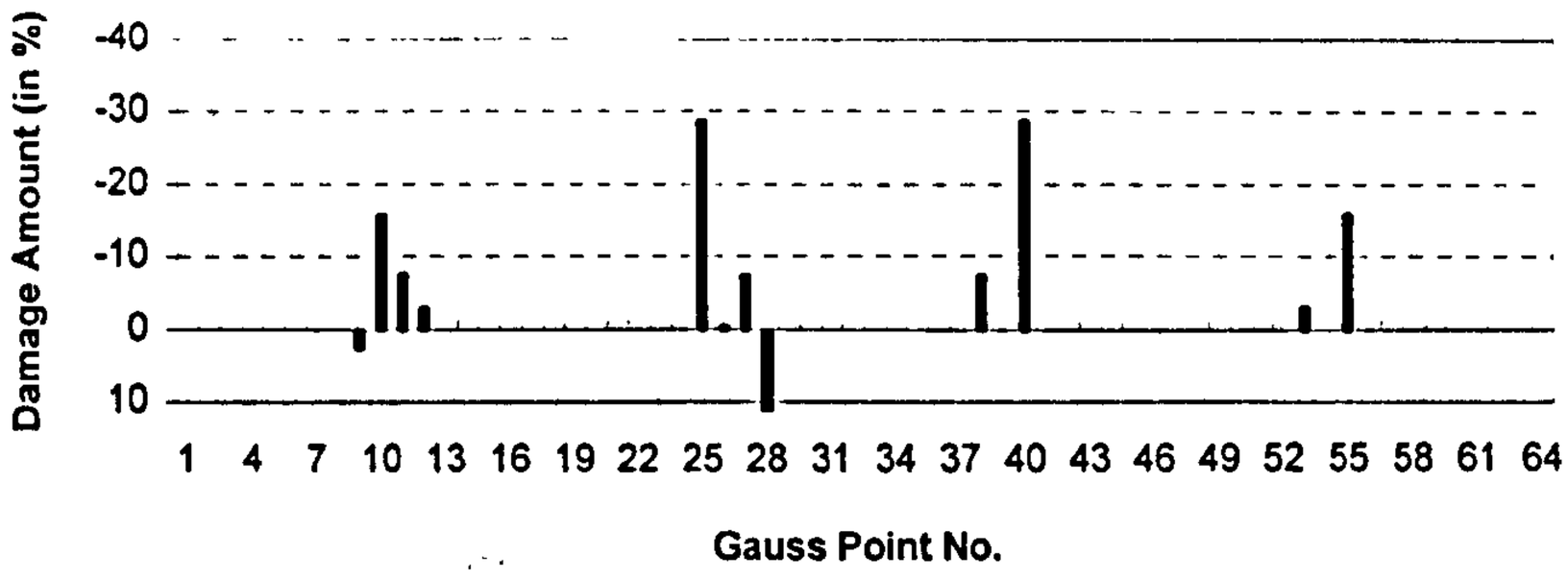

Figure 5.16(a) Damage prediction for support case 1, the **AE1** technique used

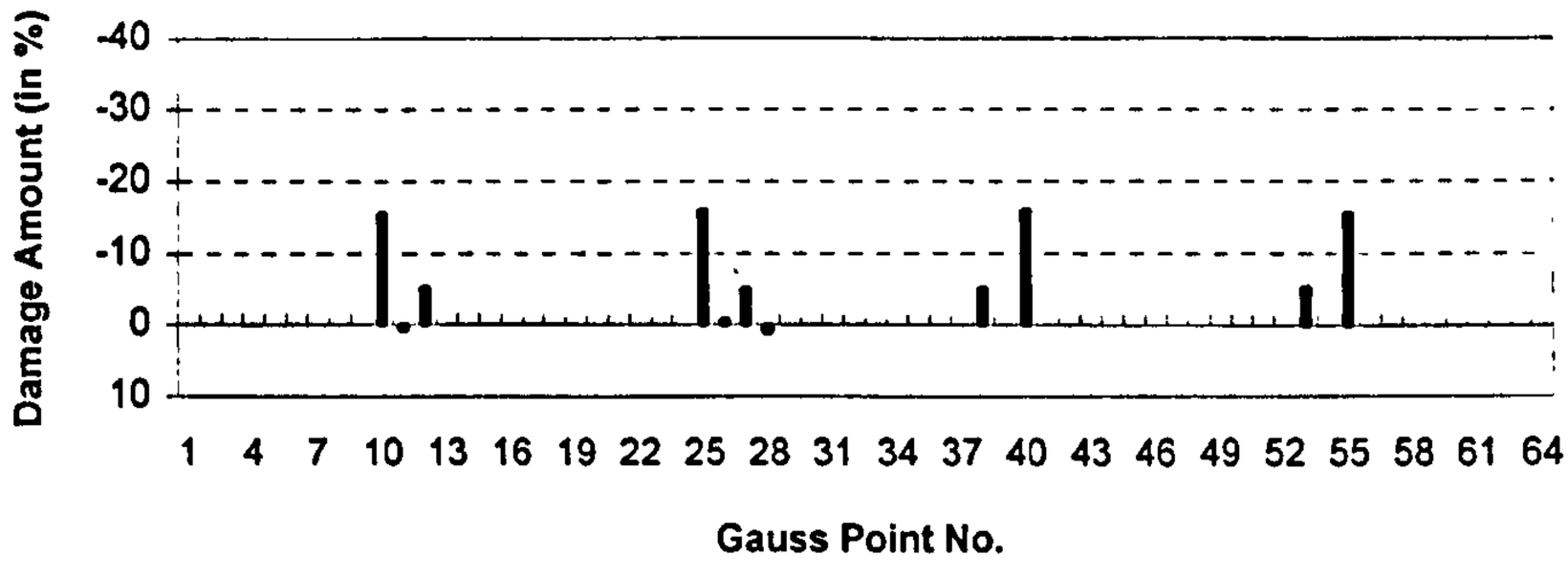

Figure 5.16(b) Damage prediction for support case 2, the **AE1** technique used

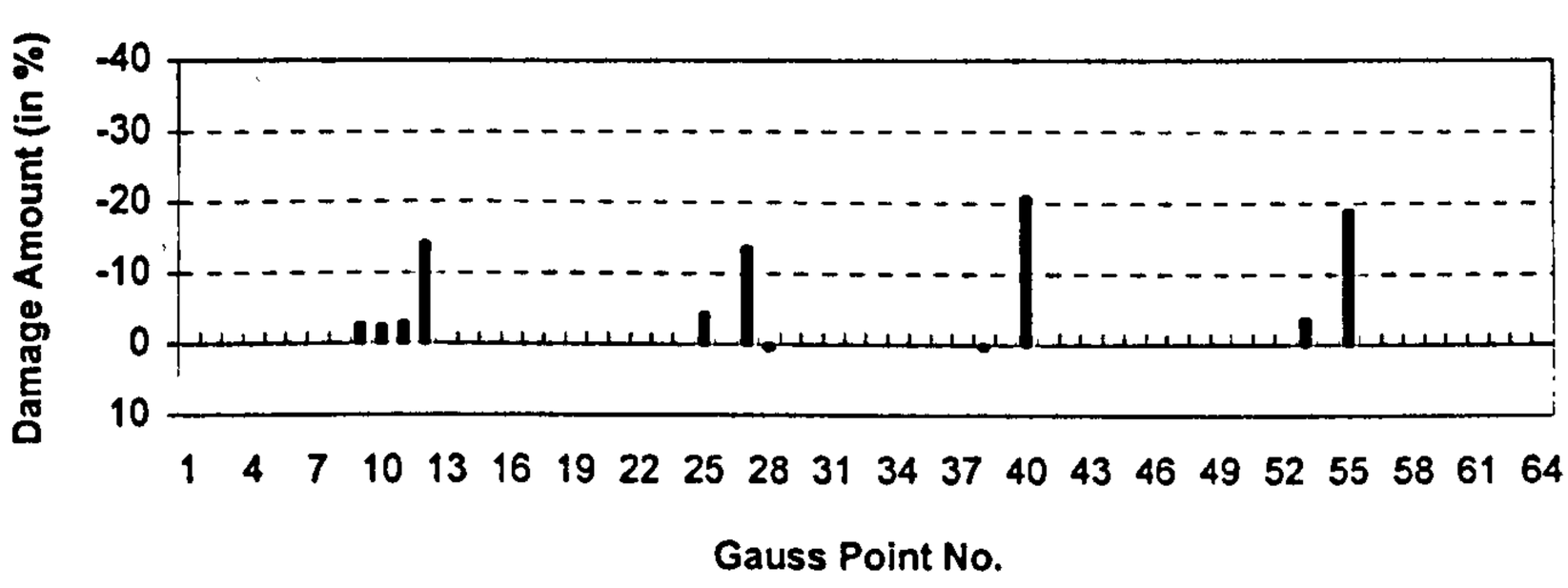

Figure 5.16(c) Damage prediction for support case 3, the **DI** technique used

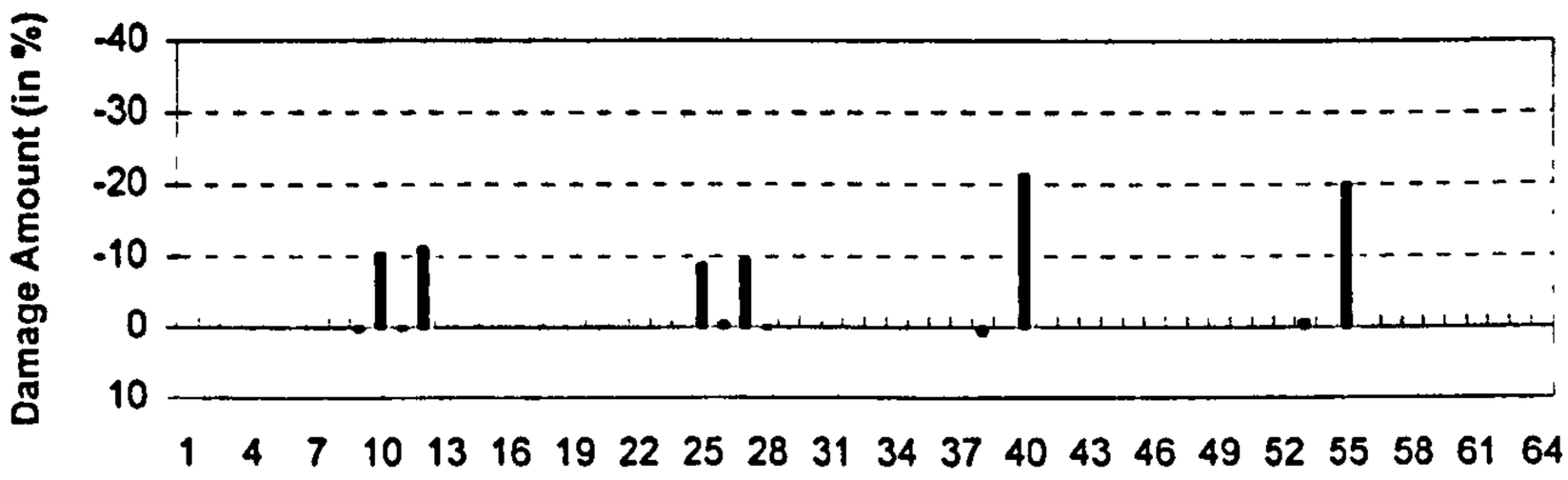

Figure 5.16(d) Damage prediction for support case 4, the **DI** technique used

Figure 5.16 Inverse damage predictions affected by boundary conditions of the structure, 10 damaged frequencies used

5.10 Conclusions

The presented results for different types of structures, either framed structures or continua, indicate that the proposed approaches can be successful in not only predicting the location of damage but also in determining the extent of structural damage. Several distinct advantages have been highlighted.

1) A set of non-linear equations is developed using the non-linear sensitivity analysis, which offers a promising approach to exactly identify structural damage regardless of slight or serious damage in structures.

2) Several computational techniques are proposed, and their effectiveness and convergence performance have been demonstrated using various numerical examples.

3) Only a limited number of damaged natural frequencies are required to predict both the location and the size of damage. The predictions of structural damage improve with an increase of the number of damaged frequencies adopted.

4) No knowledge of mode shapes for the damaged structure is required. In fact, the mode shapes for the damaged structure can be obtained as a result of the proposed approaches and they may be utilised to check the pairings of modes for the original structure and the damaged structure.

5) The proposed approaches are also suitable for symmetric structures, if some methods are employed to desymmetrise the structure, such as non-symmetric element mesh generated, suitable boundary conditions selected, and additional concentrated mass applied.

Furthermore, it is shown that the proposed approaches are quite sensitive to the quality of the measured natural frequencies for structural damage identification. The reason for this may be due to the fact the governing equations for the inverse problems are in general ill-conditioned.

CHAPTER 6

DAMAGE IDENTIFICATION FROM INCOMPLETE MODAL DATA

The incompleteness of the measured modal data represents a considerable problem in structural damage identification, since the number of DOF's readings measured from modal testing is often significantly smaller than the number of DOFs in an analytical model. In addition, not all DOF's readings of a structure can be measured or accessed, such as internal DOFs in a continuum. Although the problem can be solved using either a model reduction technique or a mode shape expansion technique to overcome the incompleteness of modal data (See Section 2.2), it has been pointed out that the model reduction process introduces errors in an analytical model and destroy the conectivity of the original model, whereas the mode shape expansion process introduces additional errors in the expanded mode shapes which directly affect the accuracy of the estimate of structural damage.

In Chapter 3, a novel non-linear perturbation theory has been developed in order to solve the problems discussed above. So far the theory was adopted to deal with complete mode shapes, locally complete mode shapes, and only natural frequencies, which will be extended to directly utilise incomplete modal data for structural damage identification. In a similar view as before, several computational techniques based on the developed non-linear perturbation theory, (Direct Iteration (**DI**), Gauss-Newton Least Squares (**GNLS**), Two Stage Iteration (**TSI**), Approximate Equation (**AE**), Non-Linear Optimisation (**NLO**), and Optimisation and Iteration (**OI**) techniques), will be proposed to identify structural damage for cases of incomplete measured modal data. Finally, the results from different numerical examples show that both the location and the extent of structural damage can correctly be identified from a minimum of measured incomplete modal data.

6.1 Governing Equations

In order to understand clearly the computational procedures which directly adopt incomplete modal data, the vectors associated with the measured DOF's readings and the unknown DOF's readings as well as their relationship are discussed in more detail.

It is assumed that information about incomplete DOF's readings for the damaged structure $\psi_i^{a^*}$ is available, i.e., only *NAI*(<*N*) DOF's readings of a total *N* DOF's readings for the *i*th measured mode. The measured incomplete mode shape for the damaged structure, $\psi_i^{a^*}$, can be paired to the mode shape for the original structure, ϕ_i, by using *MAC* factors, as defined in equation (5.7). A scaled vector, $\phi_i^{a^*}$, related to the measured incomplete modal data with a proper scale with respect to the corresponding original mode shape restricted to the same dimension, ϕ_i^a, can be computed from

$$\phi_i^{a^*} = \overline{\beta}_i \psi_i^{a^*} \tag{6.1}$$

where $\overline{\beta}_i$, similar to the definition in Section 4.3, is the *MSF* for the *i*th measured mode of the damaged structure, and will be discussed later.

Meanwhile, the remaining dimension (corresponding to unknown DOF's readings) for the damaged structure, $\phi_i^{u^*}$, is defined as

$$\phi_i^{u^*} = \phi_i^u + \Delta\phi_i^u \tag{6.2}$$

where ϕ_i^u is the part of the original eigenvector restricted to the same dimension as $\phi_i^{u^*}$, and the change of unknown DOF's readings, $\Delta\phi_i^u$, can be calculated from equation (3.58), and rewritten here as

$$\Delta\phi_i^u = \sum_{l=1, l\neq i}^{NC} C_{il}\phi_l^u \tag{6.3}$$

Furthermore, $\Delta\phi_i^u$ can be calculated from a linear combination of only a limited number of original eigenvectors in order to reduce the number of unknowns for the mode participation factor C_{ik}, i.e.,

$$\Delta\phi_i^u = \sum_{l=1}^{NUI} C_{il}\phi_l^u \tag{6.4}$$

where *NUI* is the total number of unknown DOF's readings for the *i*th damaged mode shape, i.e., *NUI=N-NAI*.

Consequently, the *i*th complete eigenvector for the damaged structure can be expressed by

$$\phi_i^* = \phi_i^{a^*} + \phi_i^{u^*} \tag{6.5}$$

which, after using equation (6.2), is rewritten in the same form as equation (3.26), i.e.,

$$\phi_i^* = \varphi_i^a + \Delta\phi_i^u \tag{6.6}$$

where φ_i^a, after using equation (6.1), is defined as

$$\varphi_i^a = \phi_i^a + \phi_i^{u^*} = \beta_i \psi_i^a + \phi_i^{u^*} \tag{6.7}$$

therefore, the definition for φ_i^a is the same as that in Section 3.3.2.

It should be pointed out that $\bar{\beta}_i$ in equations (6.1) and (6.7) has to be updated for each iteration (if an iterative procedure is required), which can be defined as

$$\bar{\beta}_i = \frac{\bar{\phi}_i^{a^{*T}} \psi_i^{a^*}}{\psi_i^{a^{*T}} \psi_i^{a^*}} \tag{6.8}$$

where $\bar{\phi}_i^{a^*}$ is a vector of the same dimension as $\psi_i^{a^*}$, updated for each iteration during the updating of the mode participation factor C_{ik}. Considering equation (6.3), the vector $\bar{\phi}_i^{a^*}$ can be expressed as

$$\bar{\phi}_i^{a^*} = \phi_i^a + \sum_{l=1, l\neq i}^{NC} C_{il} \phi_l^a \tag{6.9}$$

The reason for the arguments discussed above is that $\phi_i^{a^*}$ must be scaled in such a way as to be close to $\phi_i^{u^*}$. The vector $\phi_i^{u^*}$ has the same scale factor as $\bar{\phi}_i^{a^*}$ since both $\phi_i^{u^*}$ and $\bar{\phi}_i^{a^*}$ are the partitioned parts of the same vector. Consequently, ϕ_i^* can be simply computed from equation (6.5) since the mode scale factors (*MSF*) for $\phi_i^{a^*}$ and $\phi_i^{u^*}$ are close.

The consideration presented above will be applied to the non-linear perturbation theory, which will be developed to the governing equations for structural damage identification directly using incomplete modal data.

Using equations (6.4) and (6.6), the characteristic equation for the damaged structure, equation (3.52), can be rewritten as

$$\sum_{j=1}^{NEG}\sum_{l=1}^{NUI} a_{jl}^{Ku} C_{il}\alpha_j + \sum_{j=1}^{NEG} a_{ji}^{Ka}\alpha_j + \sum_{l=1}^{NUI} a_l^{Mu} C_{il} + a_i^{Ma} = 0 \tag{6.10}$$

where the eigenmode-stiffness sensitivity vectors a_{jl}^{Ku}, a_{ji}^{Ka}, a_l^{Mu}, and a_i^{Ma} are defined as

$$a_{jl}^{Ku} = K_j \phi_l^u \tag{6.11a}$$

$$a_{ji}^{Ka} = K_j \varphi_i^a \tag{6.11b}$$

$$a_l^{\lambda u} = [K - \lambda_i^{\bullet} M]\phi_l^u \tag{6.11c}$$

$$a_i^{Ma} = [K - \lambda_i^{\bullet} M]\varphi_i^a \tag{6.11d}$$

Meanwhile, the non-linear governing equation (3.57) can be rewritten, after using equations (6.3) and (6.6), in the form

$$\sum_{j=1}^{NEG} a_{ji}^a \alpha_j + \sum_{j=1}^{NEG}\sum_{l=1,l\neq i}^{NC} a_{jl}^u C_{il}\alpha_j - \phi_i^{a\bullet} = 0 \tag{6.12}$$

where the eigenmode-stiffness sensitivity vectors a_{ji}^a and a_{jl}^u are defined as

$$a_{ji}^a = \sum_{k=1}^{NC} \frac{\phi_k^T K_j \varphi_i^a}{\lambda_i^{\bullet} - \lambda_k}\phi_k^a \tag{6.13a}$$

$$a_{jl}^u = \sum_{k=1}^{NC} \frac{\phi_k^T K_j \phi_l^u}{\lambda_i^{\bullet} - \lambda_k}\phi_k^a \tag{6.13b}$$

and the recursive relation for computing the mode participation factor C_{ik}, defined in equation (5.4), can be rewritten as

$$C_{ik} = \frac{\sum_{j=1}^{NEG} a_{kji}^a \alpha_j + \sum_{j=1}^{NEG}\sum_{l=1,l\neq i}^{NC} a_{kjl}^u \alpha_j C_{il}}{\lambda_i^{\bullet} - \lambda_k} \tag{6.14}$$

where a_{kji}^a and a_{kjl}^u are the eigenmode-stiffness sensitivity coefficients, defined as

$$a_{kji}^a = \phi_k^T K_j \varphi_i^a \tag{6.15a}$$

$$a_{kjl}^{u} = \phi_k^T K_j \phi_l^u \tag{6.15b}$$

or alternatively in the improved form for the iterative procedure, equation (5.5), is rewritten here as

$$C_{ik} = \frac{\sum_{j=1}^{NEG} a_{kji}\alpha_j + \sum_{j=1}^{NEG}\sum_{l=1,l\neq i,k}^{NC} a_{kjl}\alpha_j C_{il}}{\lambda_i^{\bullet} - \lambda_k - \sum_{j=1}^{NEG} a_{kjk}\alpha_j} \tag{6.16}$$

It should be pointed out that the governing equations for using only natural frequencies and for directly using incomplete modal data are very different, although the forms of these governing equations appear very similar.

Various computational techniques, which have previously been employed to solve for the damage parameter α_j and the mode participation factor C_{ik} when using only natural frequencies as presented in Chapter 5, will be developed here to solve for α_j and C_{ik} when using directly incomplete modal data based on the non-linear governing equations formulated above.

6.2 Direct Iteration (DI) Technique

The basic equations and computational procedure for the **DI** technique will be outlined as follows.

6.2.1 Basic equations

Rewriting equation (6.12), yields

$$\sum_{j=1}^{NEG} S_{mj}\alpha_j = z_m \tag{6.17}$$

where m ranges from 1 to NA and NA indicates the total number of the measured DOF's readings for the total NL measured damaged modes, and S_{mj} and z_m are the eigenmode-stiffness sensitivity matrix and vector, respectively, which are defined as

$$S_{mj} = a_{ji}^{a} + \sum_{l=1,l\neq i}^{NC} C_{il} a_{jl}^{u} \tag{6.18a}$$

$$z_m = \phi_i^{a^*} \tag{6.18b}$$

The equation (6.16) can be rewritten in the same form as equation (5.10), i.e.,

$$C_{ik} = \frac{b_{ki} + \sum_{l=1, l\neq i,k}^{NC} C_{il} b_{kl}}{\lambda_i^* - \lambda_k - b_{kk}} \tag{6.19}$$

where coefficients b_{kk}, b_{ki}, and b_{kl} have been defined in equation (5.11).

The above formulation will be applied to develop an iterative solution procedure.

6.2.2 Computational procedure

Since the basic equation (6.17) is of the form similar to the basic equation (5.8) in Section 5.2, and the basic equation (6.19) has the same form as equation (5.10), the computational procedure for the **DI** technique using incomplete modal data is similar to the computational procedure discussed in Section 5.2.2, where the detailed procedure for the **DI** technique using only natural frequencies has been developed.

6.3 Gauss-Newton Least Squares (GNLS) Technique

The basic equations and computational procedure for the **GNLS** technique will be developed as follows.

6.3.1 Basic equations

Considering *NL* incomplete mode shapes available for the damaged structure, the non-linear governing equation (6.10) can be expressed as a generalised system of nonlinear equations for determining the damage parameter α_j as well as the mode participation factor C_{ik}, i.e.,

$$f_i(\alpha_j, C_{ik}) = 0 \tag{6.20}$$

where *i* ranges from 1 to *NL*.

The nonlinear solution algorithm will require the first derivative of the function $f_i(\alpha_j, C_{ik})$ with respect to α_j and C_{ik}.

Based on the governing equation (6.10), the derivatives with respect to damage parameter α_r are as follows

$$\frac{\partial f_i}{\partial \alpha_r} = a_{ri}^{Ka} + \sum_{l=1}^{NUI} a_{rl}^{Ku} C_{il} \tag{6.21a}$$

where r=1, *NEG*. The corresponding derivatives with respect to mode participation factor C_{st} are

$$\frac{\partial f_i}{\partial C_{st}} = \begin{cases} a_t^{Mu} + \sum_{j=1}^{NEG} a_{jt}^{Ku} \alpha_j, & s = i \\ 0, & s \neq i \end{cases} \tag{6.21b}$$

where the ranges for s and t are s=1, *NL* and t=1, *NUI*.

The computational procedure using the combination of the Gauss-Newton iteration method and the least squares techniques, which has been developed in Section 5.3.2, is now employed.

6.3.2 Computational procedure

Rewriting the basic set of nonlinear equations (6.20) as

$$f_i(x_n) = 0 \tag{6.22}$$

The set of generalised unknowns x_n is defined as

$$x_n = \{\alpha_j, C_{ik}\}^T \tag{6.23}$$

Note that the basic equation (6.22) comprises a total *NEQ=NL*N* equations and a total of *NV=NEG+NU* variables, i.e., *NEG* variables for α_j and a total of *NU* variables for C_{ik} that are used for constructing the incomplete mode data to be the total *NL* number of complete mode shapes for the damaged structure.

The weighted norm y of the equation (6.22) is defined as

$$y = y(x_n) = \sum_{i=1}^{NL} f_i^T(x_n) W_i f_i(x_n) \tag{6.24}$$

where W_i is the weighting matrix for the ith mode. As indicated previously, the weighting matrix should be symmetric, and positive definite, and its definition has been discussed in Section 4.2. Two procedures related to weighting matrix have been presented there, i.e., the Procedure **MRF** (Minimisation of Residual Force) and the Procedure **MRE** (Minimisation of Residual Energy).

If $|y| = |y(\bar{x}_n)| \prec \varepsilon$ where ε is convergence tolerance, then $\bar{x}_n$ will be considered as the solution to the equation (6.22) in a least square sense.

The computational procedure for the **GNLS** technique directly using incomplete modal data is formally the same as that when using only natural frequencies, which have been developed in Section 5.3.2. However, it should be noted that the basic equations presented here differ from those in Section 5.3, since the information about modal data adopted for structural damage identification is different.

6.4 Two Stage Iteration (TSI) Technique

The **TSI** technique using incomplete modal data can be applied to structural damage identification in order to reduce the requirements for modal data.

6.4.1 Basic equations

The basic equations used here are identical to those for the **DI** and the **GNLS** techniques directly using incomplete modal data, as developed previously.

6.4.2 Computational procedure

The computational procedure for the **TSI** technique using incomplete modal data is very similar to that using only natural frequencies which has been developed in Section 5.4.2 where details of computational procedure for the **TSI** technique are given.

6.5 Approximate Equation (AE) Technique

Closely following the procedures developed in Section 5.5 where the AE technique using only natural frequencies has been proposed, the AE technique directly using incomplete modal data is now outlined as follows.

6.5.1 Basic equations

First-order approximation (AE1)

The first-order approximation for non-linear governing equation (6.12) can be obtained from the assumption that no change for the unknown DOF's readings between the damaged structure and the original structure exists, i.e., the mode participation factor C_{ik} can be expressed as

$$C_{il}^{(1)} = 0 \tag{6.25}$$

Consequently, the non-linear governing equation (6.12) becomes the linear relationship in the form

$$\sum_{p=1}^{NEG} a_{pi}^{(1)} \alpha_p - \phi_i^{a^*} = 0 \tag{6.26}$$

where $a_{pi}^{(1)}$ is the eigenmode-stiffness sensitivity vector, defined as

$$a_{pi}^{(1)} = \sum_{k=1}^{NC} \frac{a_{kpi}^{a}}{\lambda_i^* - \lambda_k} \phi_k^a \tag{6.27}$$

Second-order approximation (AE2)

The mode participation factor C_{ik} can approximately be computed using the governing equation (6.14), i.e.,

$$C_{il}^{(2)} = \sum_{q=1}^{NEG} \frac{a_{lqi}^{a}}{\lambda_i^* - \lambda_l} \alpha_q \tag{6.28}$$

Therefore, the second-order approximation for the non-linear governing equation (6.12) can be written as

$$\sum_{p=1}^{NEG} a_{pi}^{(1)} \alpha_p + \sum_{p=1}^{NEG} \sum_{q=1}^{NEG} a_{pqi}^{(2)} \alpha_p \alpha_q - \phi_i^{a^*} = 0 \tag{6.29}$$

where vector $a_{pqi}^{(2)}$ is defined as

$$a_{pqi}^{(2)} = \sum_{l=1,l\neq i}^{NC} \frac{a_{pl}^{u} a_{lqi}^{a}}{\lambda_i^{*} - \lambda_l} \tag{6.30}$$

Third-order approximation (AE3)

Considering the governing equation (6.14), the higher order approximation for the mode participation factor C_{ik} can be calculated from

$$C_{il}^{(3)} = C_{il}^{(2)} + \sum_{q=1}^{NEG}\sum_{r=1}^{NEG}\left(\sum_{k=1,k\neq i}^{NC} \frac{a_{lqk}^{u} a_{kri}^{a}}{(\lambda_i^{*} - \lambda_l)(\lambda_i^{*} - \lambda_k)}\right)\alpha_q \alpha_r \tag{6.31}$$

then the third-order approximation of equation (6.12) can be expressed by

$$\sum_{p=1}^{NEG} a_{pi}^{(1)}\alpha_p + \sum_{p=1}^{NEG}\sum_{q=1}^{NEG} a_{pqi}^{(2)}\alpha_p\alpha_q + \sum_{p=1}^{NEG}\sum_{q=1}^{NEG}\sum_{r=1}^{NEG} a_{pqri}^{(3)}\alpha_p\alpha_q\alpha_r - \phi_i^{a^{*}} = 0 \tag{6.32}$$

where vector $a_{pqri}^{(3)}$ is defined as

$$a_{pqri}^{(3)} = \sum_{l=1,l\neq i}^{NC}\sum_{k=1,k\neq i}^{NC} \frac{a_{pl}^{u} a_{lqk}^{u} a_{kri}^{a}}{(\lambda_i^{*} - \lambda_l)(\lambda_i^{*} - \lambda_k)} \tag{6.33}$$

The above basic approximate equations that directly use incomplete modal data, i.e., equations (6.26), (6.29), and (6.32), comprise a total of equations *NA*, i.e., the total number of the measured DOF's readings for the total *NL* damaged modes.

It should be noted that the coeffiecients, $a_{pi}^{(1)}$, $a_{pqi}^{(2)}$ and $a_{pqri}^{(3)}$, defined here, are vectors, which differ greatly from the quantities, $a_{ipi}^{(1)}$, $a_{ipqi}^{(2)}$ and $a_{ipqri}^{(3)}$, defined in Section 5.5.1, although the forms of both appear very similar.

6.5.2 Computational procedure

With reference to the **GNLS** technique developed in Section 6.3.2, these basic approximate equations for the **AE1, AE2** and **AE3** techniques, i.e. equations (6.26), (6.29) and (6.32), can be expressed in a similar form to equation (6.22), i.e.,

$$f_i(\alpha_j) = 0 \tag{6.34}$$

where i ranges from 1 to NL.

Similarly, for the first-order approximate equation (6.26), the first derivative of function $f_i(\alpha_j)$ with respect to α_j, which is required by the **GNLS** technique, is expressed as

$$\frac{\partial f_i}{\partial \alpha_j} = a_{ji}^{(1)} \tag{6.35}$$

for second-order approximate equation (6.29) as

$$\frac{\partial f_i}{\partial \alpha_j} = a_{ji}^{(1)} + \sum_{p=1}^{NEG}\left(a_{pji}^{(2)} + a_{jpi}^{(2)}\right)\alpha_p \tag{6.36}$$

and for the third-order approximate equation (6.32) as

$$\frac{\partial f_i}{\partial \alpha_j} = a_{ji}^{(1)} + \sum_{p=1}^{NEG}\left(a_{pji}^{(2)} + a_{jpi}^{(2)}\right)\alpha_p + \sum_{p=1}^{NEG}\sum_{q=1}^{NEG}\left(a_{pqji}^{(3)} + a_{pjqi}^{(3)} + a_{jpqi}^{(3)}\right)\alpha_p\alpha_q \tag{6.37}$$

Although the forms of the equations formulated above appear similar to those given in Section 5.5.2, all coefficients used in the above equations are in the forms of vectors, as indicated earlier.

The computational procedure for the **GNLS** technique has been developed in Section 5.3.2.

6.6 Non-Linear Optimisation (NLO) Technique

Following similar arguments as in Section 5.6, the optimisation techniques are employed to solve the problem of structural damage identification when using directly incomplete modal data.

6.6.1 Basic equations

The procedure developed in Section 5.6 utilises the information about natural frequencies only. Here, the objective function J is defined by using φ_i^a in stead of ϕ_i in equations (5.32) and (5.34). Using the basic approximate equations discussed in

Section 6.5, i.e., equations (6.26), (6.29), and (6.32), as equality constraints, the optimisation problem for damage identification using incomplete modal data will be outlined as follows.

Minimise the objective function

$$J = \sum_{p=1}^{NEG}\sum_{q=1}^{NEG} b_{pq}^{KK^a}\alpha_p\alpha_q + 2\sum_{p=1}^{NEG} b_p^{KM^a}\alpha_p \tag{6.38a}$$

Subject to the equality constraint

for the first-order approximation **(NLO1)**

$$\sum_{p=1}^{NEG} a_{pi}^{(1)}\alpha_p - \phi_i^{a^*} = 0 \tag{6.38b1}$$

or for the second-order approximation **(NLO2)**

$$\sum_{p=1}^{NEG} a_{pi}^{(1)}\alpha_p + \sum_{p=1}^{NEG}\sum_{q=1}^{NEG} a_{pqi}^{(2)}\alpha_p\alpha_q - \phi_i^{a^*} = 0 \tag{6.38b2}$$

or for the third-order approximation **(NLO3)**

$$\sum_{p=1}^{NEG} a_{pi}^{(1)}\alpha_p + \sum_{p=1}^{NEG}\sum_{q=1}^{NEG} a_{pqi}^{(2)}\alpha_p\alpha_q + \sum_{p=1}^{NEG}\sum_{q=1}^{NEG}\sum_{r=1}^{NEG} a_{pqri}^{(3)}\alpha_p\alpha_q\alpha_r - \phi_i^{a^*} = 0 \tag{6.38b3}$$

and the inequality constraint

$$\alpha_j \le 0 \tag{6.38c}$$

where the coefficients in equation (6.38a), $b_{pq}^{KK^a}$ and $b_p^{KM^a}$, are defined as

$$b_{pq}^{KK^a} = \sum_{i=1}^{NL} \varphi_i^{a^T} K_p W_i K_q \varphi_i^a \tag{6.39a}$$

$$b_p^{KM^a} = \sum_{i=1}^{NL} \varphi_i^{a^T} K_p W_i (K - \lambda_i^* M)\varphi_i^a \tag{6.39b}$$

Similar to earlier arguments, the problem discussed here is a constrained linear optimisation problem if first-order approximate equation is utilised for equality

constraint, or a constrained non-linear optimisation problem if second or third-order approximate equation is considered.

6.6.2 Computational procedure

The constrained non-linear optimisation methods, such as the Flexible Tolerance method as indicated before (Himmelblau, 1972), can be employed for solving the optimisation problem discussed above.

6.7 Optimisation and Iteration (OI) Technique

The Optimisation and Iteration (**OI**) technique discussed here, i.e. the combination of the optimisation technique discussed in Section 6.6 and the direct iteration technique discussed in Section 6.2, can directly adopt the information about incomplete modal data.

6.7.1 Basic equations

Optimisation technique

It is again assumed that the mode participation factor C_{ik} has been known, then the eigenvector for the damaged structure ϕ_i^* can be computed using equations (6.3) and (6.6).

Similar to the procedure discussed in Section 5.7 where information about only natural frequencies is considered, using the governing equation (6.12) as the equality constraint, the optimisation problem can now be outlined as follows

Minimise the objective function

$$J = \sum_{p=1}^{NEG}\sum_{q=1}^{NFG} b_{pq}^{KK^*}\alpha_p\alpha_q + 2\sum_{p=1}^{NEG} b_p^{KM^*}\alpha_p \qquad (6.40a)$$

Subject to the equality constraint

$$\sum_{j=1}^{NEG} a_{ji}^{*}\alpha_j - \phi_i^{a^*} = 0 \qquad (6.40b)$$

and the inequality constraint

$$\alpha_j \leq 0 \tag{6.40c}$$

where the coefficients in equation (6.40a), $b_{pq}^{KK^*}$ and $b_p^{KM^*}$, are the same as those defined in equation (5.42a, b), and the vector in equation (6.40b), a_{ji}^*, is defined as

$$a_{ji}^* = \sum_{k=1}^{NC} \frac{\phi_k^T K_j \phi_i^*}{\lambda_i^* - \lambda_k} \phi_k^a \tag{6.41}$$

The problem described above is a dual quadratic programming problem with linear equality and inequality constraints.

Direct Iteration technique

Using the optimisation technique presented previously, the estimate of damage parameter α_j is then obtained. Consequently, the mode participation factor C_{ik} can be computed using basic equation (6.19) and then the estimate of eigenvector for the damaged structure ϕ_i^* can be computed using equations (6.3) and (6.6).

6.7.2 Computational procedure

The computational procedure for the **OI** technique directly using incomplete modal data is similar to that discussed in Section 5.7.2, where information about natural frequencies only is considered.

6.8 Verification of Proposed Techniques

A one-bay six-bar truss shown in Figure 6.1 is adopted to demonstrate the effectiveness and the convergence performance of the proposed techniques, such as the **DI**, the **GNLS**, the **TSI**, the **AE**, the **NLO**, and the **OI** techniques. The truss model has 6 structural members, 4 nodes and 5 DOFs. All structural members have the identical material properties with Young's modulus E=2.1×10^{11}N/m^2 and density ρ =7800kg/m^3, and the same cross section area A=0.0004m^2. The geometry of the truss model and the element numbering are also shown in Figure 6.1.

A hypothetical damage scenario with the reduced Young's modulus in truss element 2 (-10%), element 3 (-20%) and element 5 (-30%) is considered as listed in Figure 6.1. A finite element analysis was performed for both the original and the damaged cases to calculate natural frequencies and the corresponding mode shapes. The first four natural frequencies for the original and the damaged structure as well as the corresponding mode shapes for the original structure are listed in Table 6.1. In addition, a set of selected sensor positions is considered, i.e., 2 sensors placed at nodes 2 and 3, and the set of incomplete damaged modal data is composed of DOF's readings at node 2 in y direction and at node 3 in x direction for the damaged mode 1, DOF's readings at node 2 in y direction for the damaged mode 3, and DOF's readings at node 2 in y direction and at node 3 in both x and y directions for the damaged mode 4, as summarised in Table 6.1.

Table 6.1 First 4 natural frequencies (Hz) and the corresponding mode shapes

Mode	1	2	3	4
Original Frequency	214.47	509.73	570.35	719.64
Damaged Frequency	205.94	491.00	557.52	680.18
Measured DOF	2-y, 3-x	/	2-y	2-y, 3-x,y
Original Mode Shape	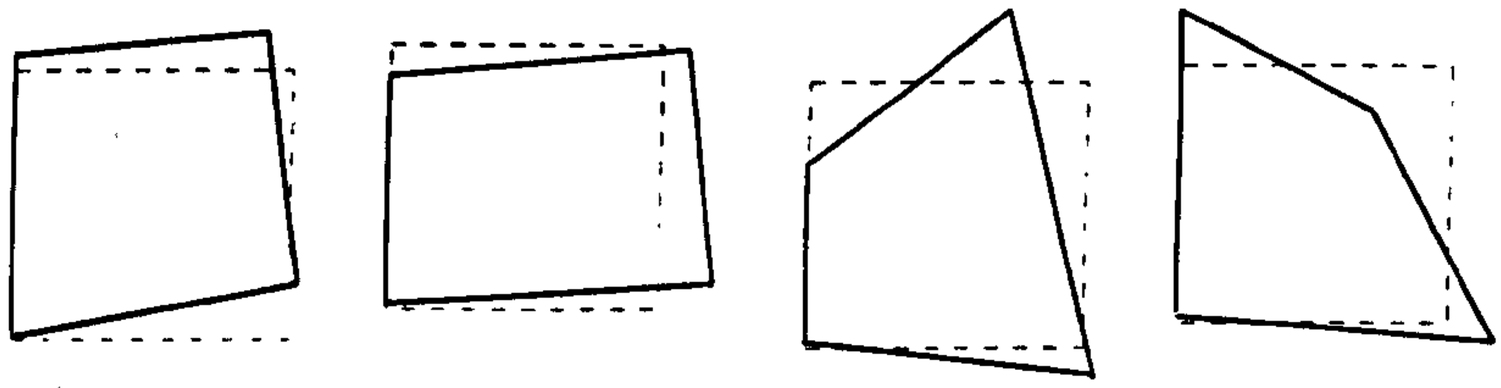			

6.8.1 Verification of DI technique

The information about the set of incomplete damaged modal data is now used to determine inversely the location and the amount of structural damage. The convergence performance of structural damage parameters for the **DI** technique is shown in Figure 6.2. It can be seen that the **DI** technique achieves convergence after only a few iterations.

The correlation between eigenvectors for the original structure and the damaged structure is checked using the *MAC* factors, as listed in Table 6.2. From the results, it is found that the modes for the damaged structure obtained from the **DI** technique directly using incomplete modal data match very well the corresponding modes for the original structure.

Table 6.2 *MAC* factors of the eigenvectors for original and damaged structure

	Original Eigenvector				
Damaged	1	2	3	4	5
1	0.9985	0.0140	0.0211	0.0040	0.0052
2	0.0087	0.9880	0.0037	0.0069	0.0044
3	0.0169	0.0276	0.9792	0.0126	0.0033
4	0.0004	0.0063	0.0146	0.9709	0.0186

6.8.2 Verification of GNLS technique

Again, the information about the set of incomplete damaged modal data as listed in Table 6.1 is utilised for inverse identification of the location and the extent of structural damage. The convergence performance of structural damage parameters for these two **GNLS** techniques with different procedures, Procedure **MRF** and Procedure **MRE**, are shown in Figure 6.3(a) and Figure 6.3(b), respectively. It can be seen that both procedures achieve convergence rapidly after only a few iterations, and no great difference exists between these two procedures since the mass at each node which affects the weighting matrix is very close. Furthermore, it is found that the modes for the damaged structure obtained from the **GNLS** techniques match very well the corresponding modes for the original structure, which is similar to the results listed in Table 6.2.

6.8.3 Verification of TSI technique

Here, a set of incomplete damaged modal data is composed of the set of modal data as listed in Table 6.1, but missing measuring the DOF's reading at node 3 in y direction for the damaged mode 4. The **DI** technique is employed for computing the values of structural damage parameters in this example.

The convergence performance of structural damage parameters for the **TSI** technique is shown in Figure 6.4. At first stage, the structural damage parameters are considered to be converged after three iterations. The estimate of structural damage parameters is checked. Since the values of the damage parameters for elements 1, 4, and 6 are less then the chosen threshold, elements 1, 4, and 6 are treated as intact elements. Consequently, the damage parameters for elements 1, 4 and 6 are removed from the system of equations, and the corresponding values are fixed to be zero. Finally, the

remaining three structural damage parameters can be exactly determined using the information on the given incomplete modal data, as shown in Figure 6.4.

6.8.4 Verification of AE technique

In order to identify inversely both the location and the extent of structural damage, the information about the set of incomplete damaged modal data as listed in Table 6.1 is now employed. Three **AE** techniques, i.e., the first-order approximate equation **(AE1)**, the second-order approximate equation **(AE2)**, and the third-order approximate equation **(AE3)** techniques, are utilised to compare their effectiveness as shown in Figure 6.5. The results indicate that structural damage can be predicted quite well using all three **AE** techniques. As expected, the predictions of structural damage improve with an increase of the order of approximate equation.

6.8.5 Verification of NLO technique

Here again, the information about the set of incomplete damaged modal data as listed in Table 6.1 is used to identify the given structural damage. Three **NLO** techniques, i.e., the first-order approximate equation for equality constraint **(NLO1)**, the second-order approximate equation for equality constraint **(NLO2)**, and the third-order approximate equation for equality constraint **(NLO3)** techniques, are utilised to compare their effectiveness as shown in Figure 6.6. From the results, it can be seen that structural damage can be predicted correctly using all three **NLO** techniques. As expected again, the predictions of structural damage improve with an increase of the order of approximate equation for equality constraint.

6.8.6 Verification of OI technique

The information about the set of incomplete damaged modal data as listed in Table 6.1 is again utilised for inverse predictions of the given structural damage. The **OI** technique is utilised to compare the effectiveness of structural damage identification with the **AE** technique and the **NLO** technique, as shown in Figure 6.7, where the first-order approximation is considered for both the **AE** and the **NLO** techniques. The results show that the predictions of structural damage from the **NLO** technique are better than those from the **AE** technique, while predictions from the **OI** technique produce the best results from all techniques considered.

Parameters of the Problem	
Total DOFs	5
Structural members	6
Damage parameters	6

Hypothetical Damage Scenario

Element No	1	2	3	4	5	6
Damage Amount	0%	-10%	-20%	0%	-30%	0%

Selected Sensor Scenario

Damaged Mode	1	3	4
Measured DOF	2-y, 3-x	2-y	2-y, 3-x,y

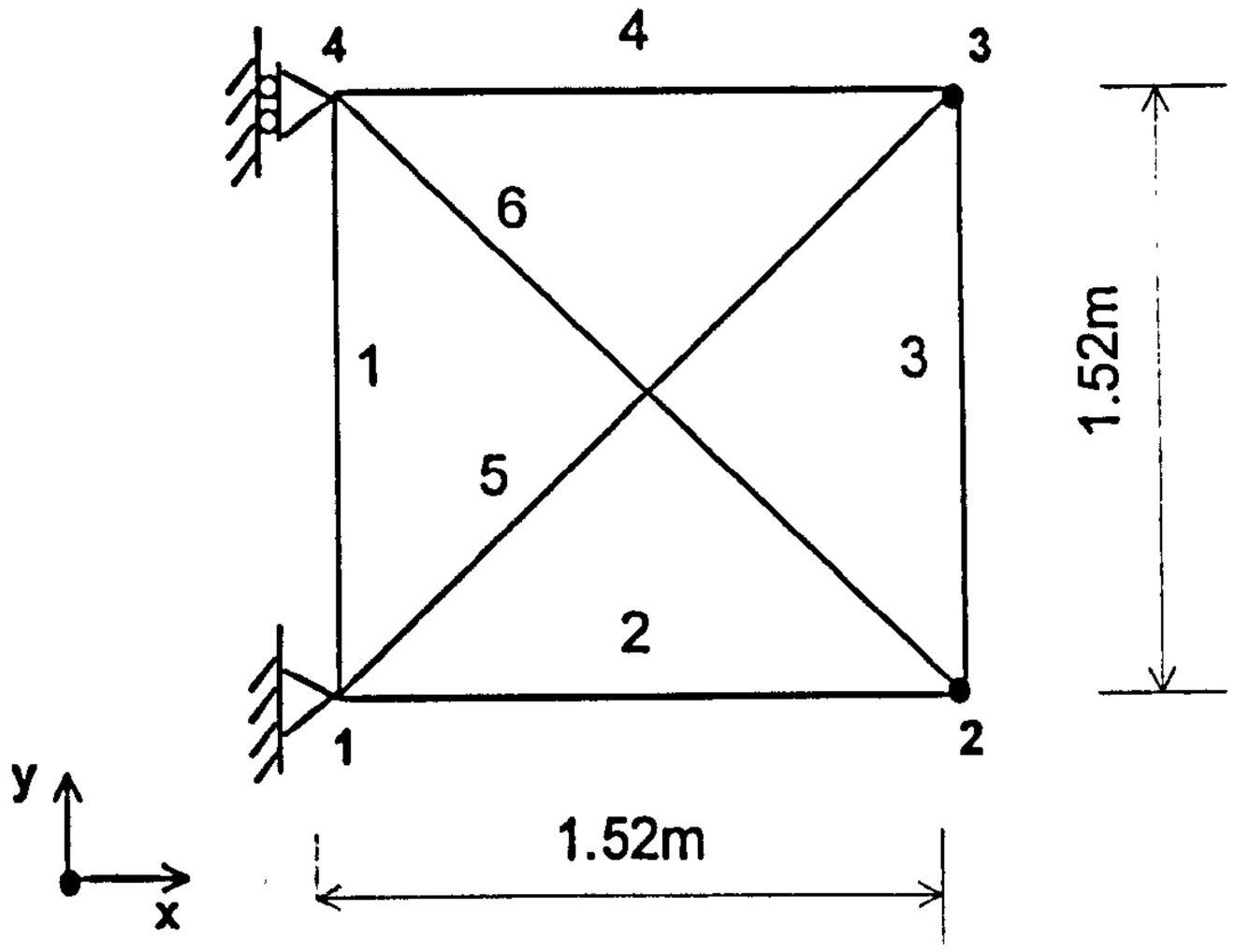

Figure 6.1 One-bay plane truss model problem

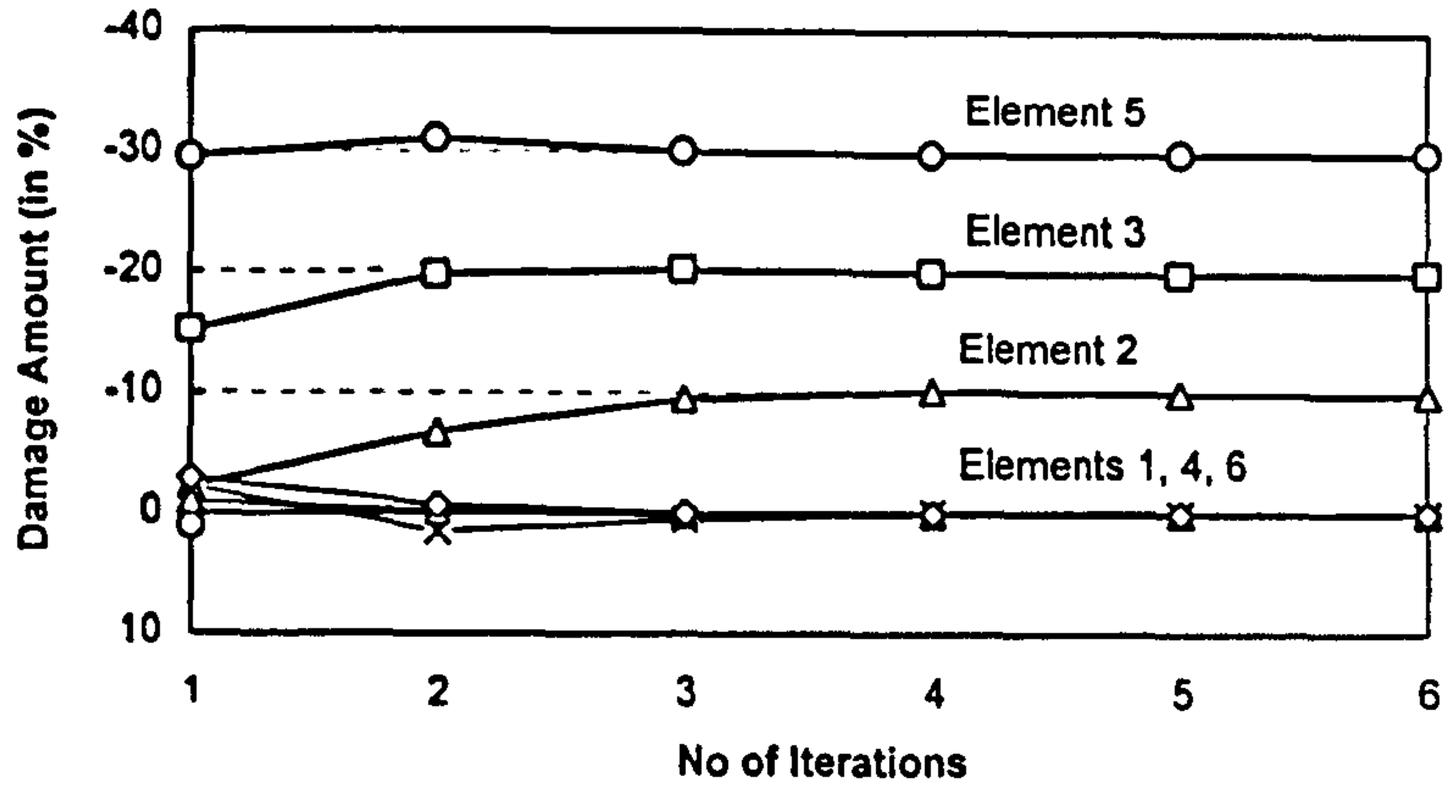

Figure 6.2 Convergence performance of the **DI** technique

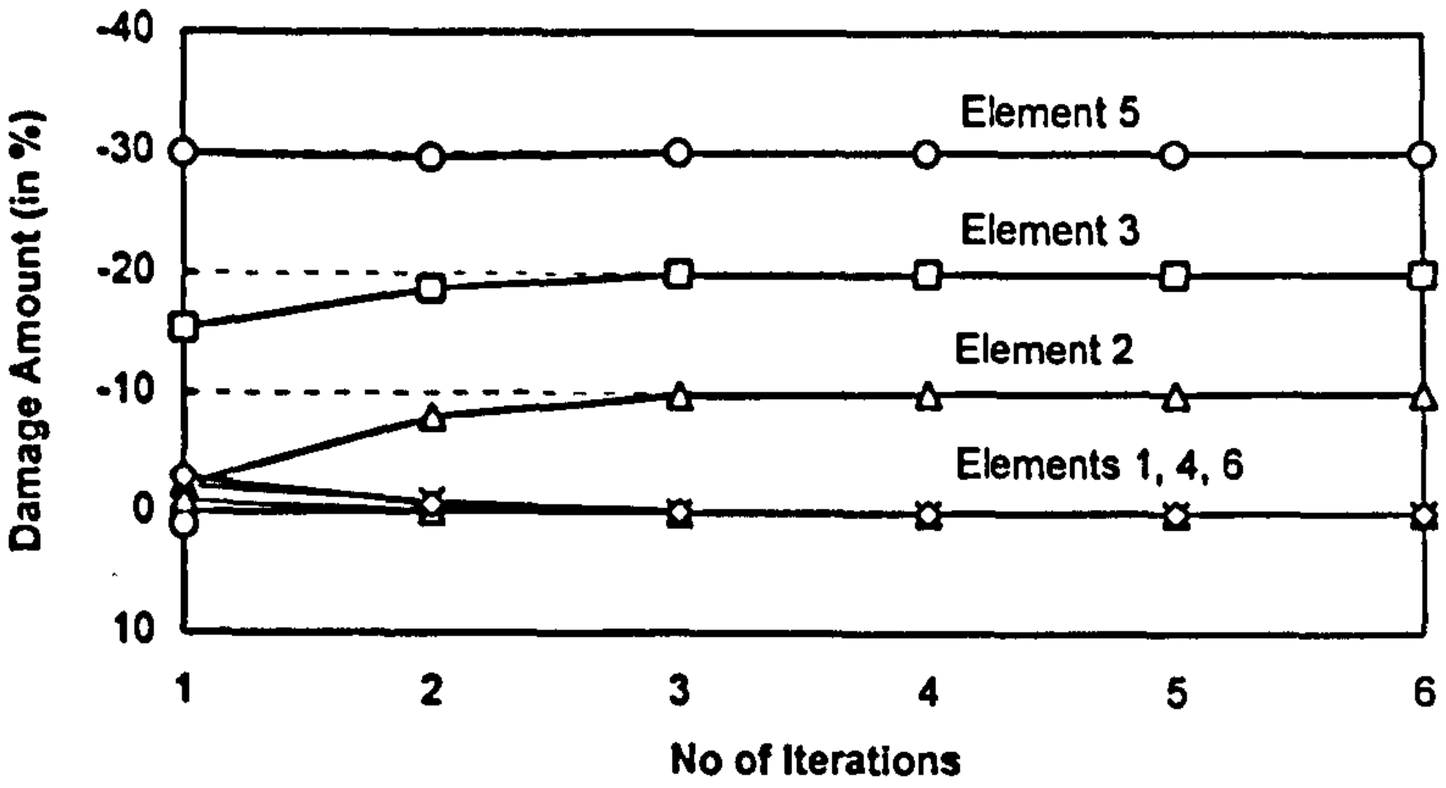

Figure 6.3(a) Convergence performance of the **GNLS** technique, Procedure **MRF**

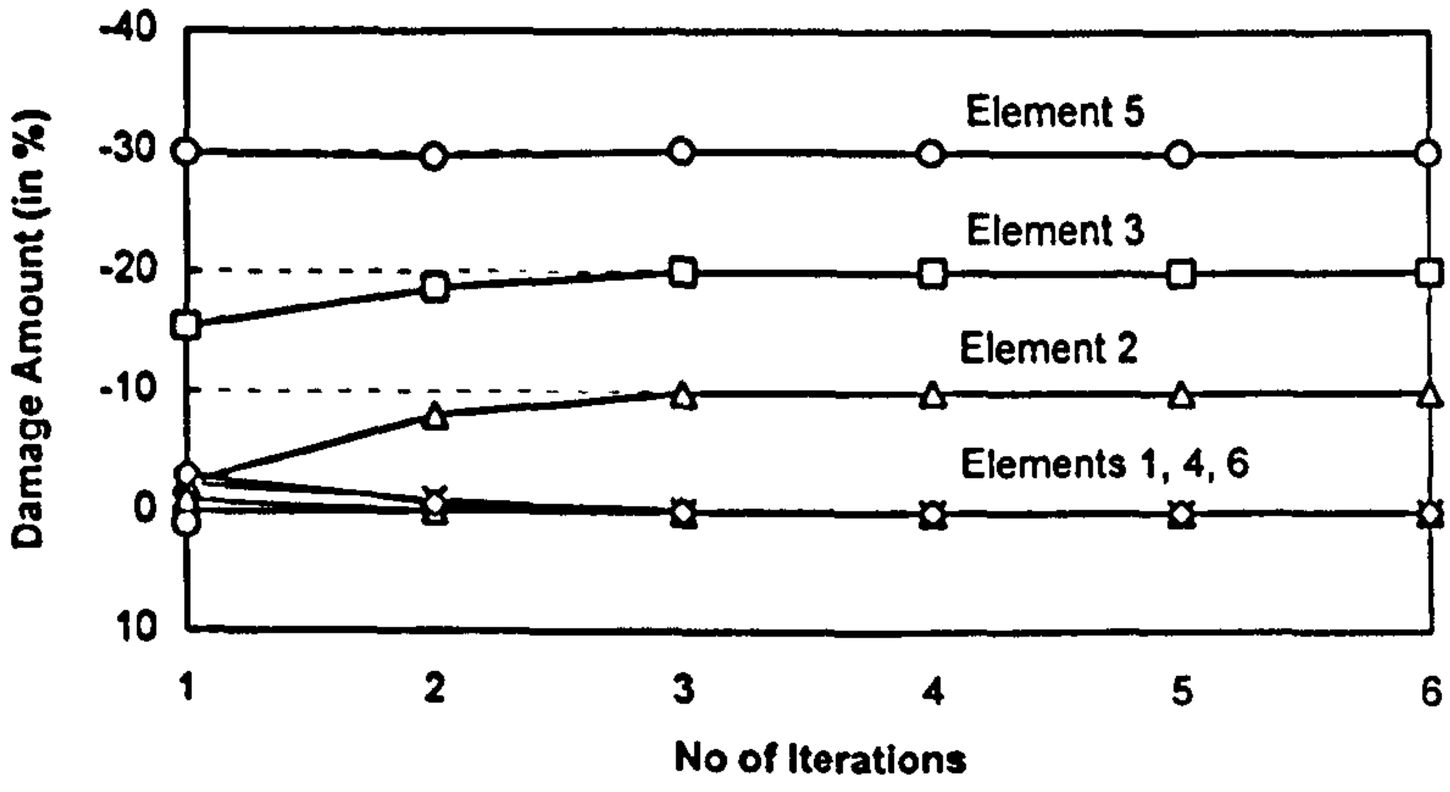

Figure 6.3(b) Convergence performance of the **GNLS** technique, Procedure **MRE**

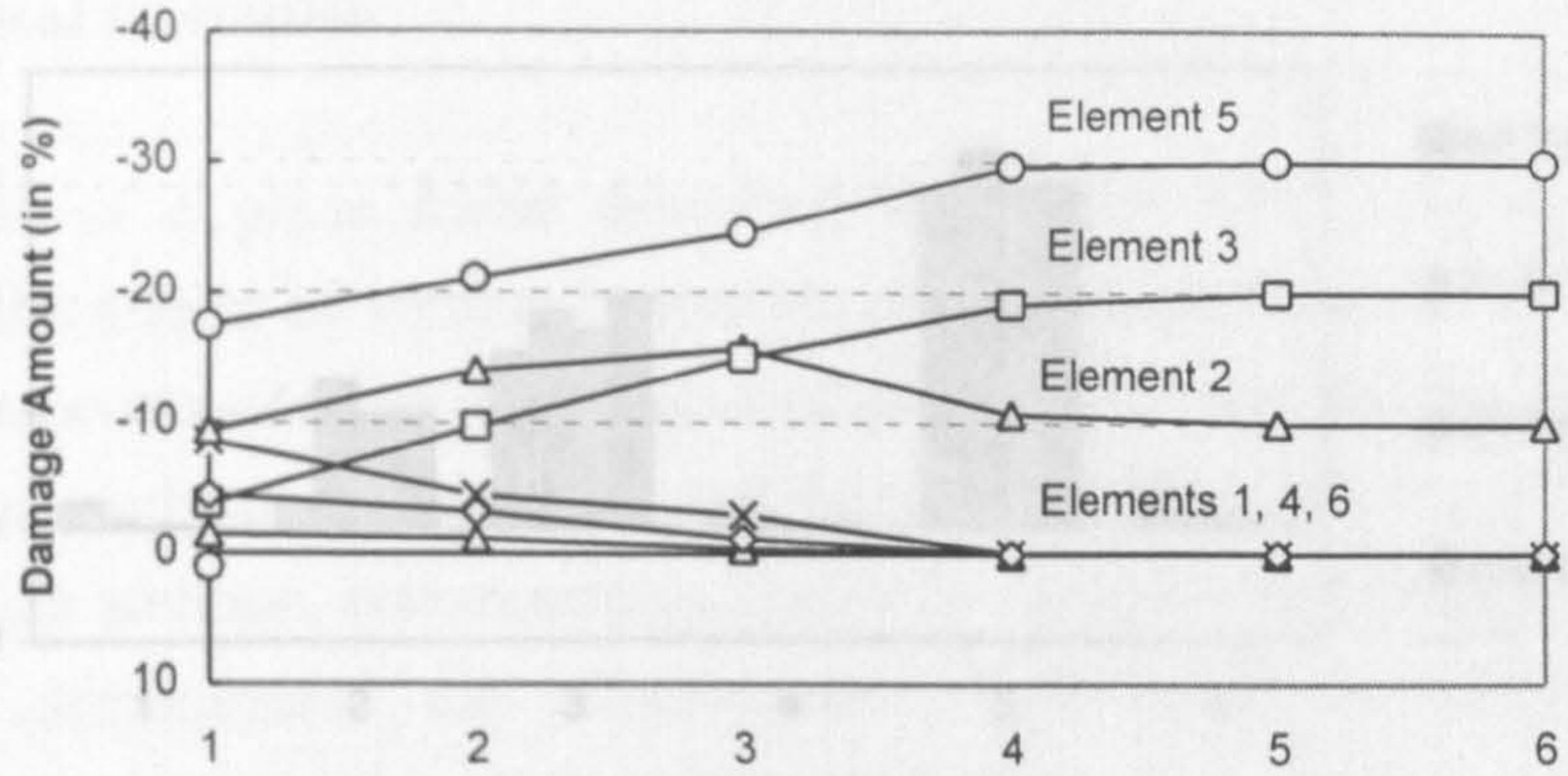

Figure 6.4 Convergence performance of the **TSI** technique

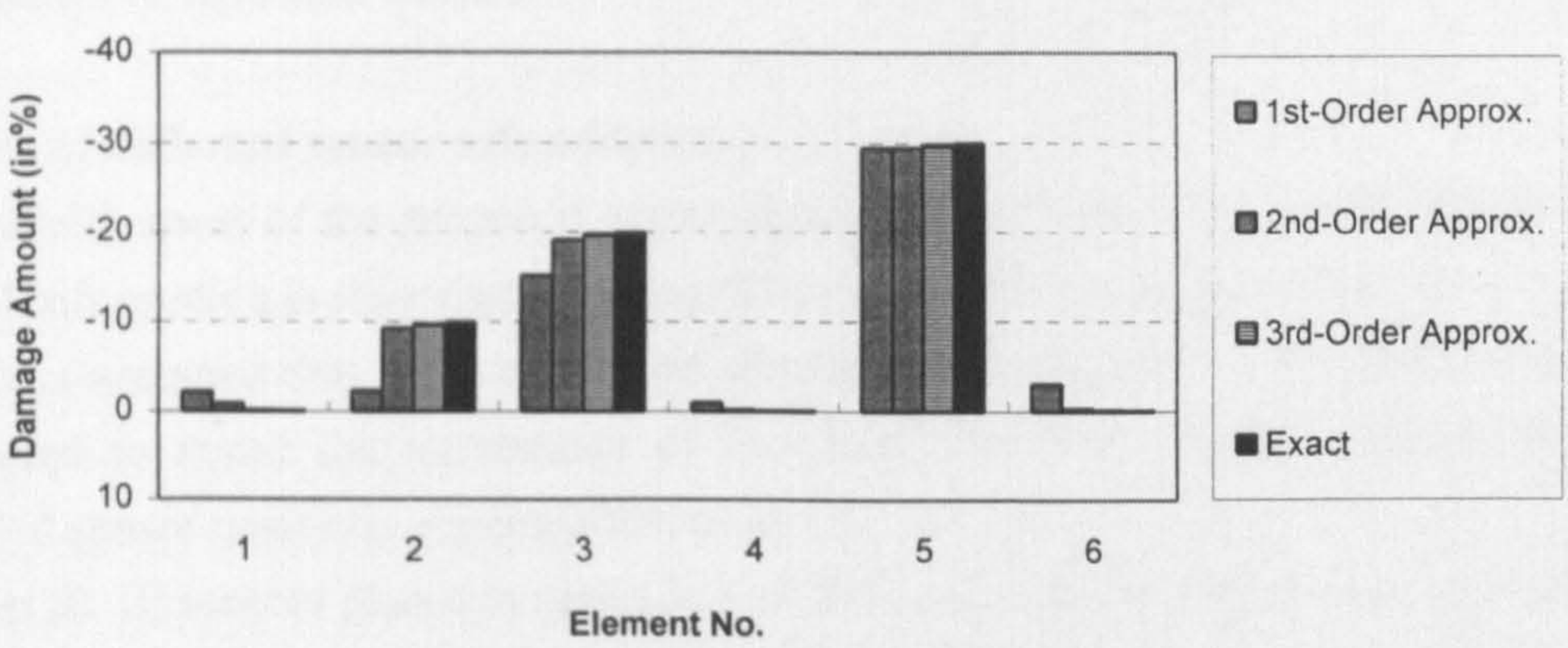

Figure 6.5 Comparison for various approximations for the **AE** technique

Figure 6.6 Comparison for various approximations for the **NLO** technique

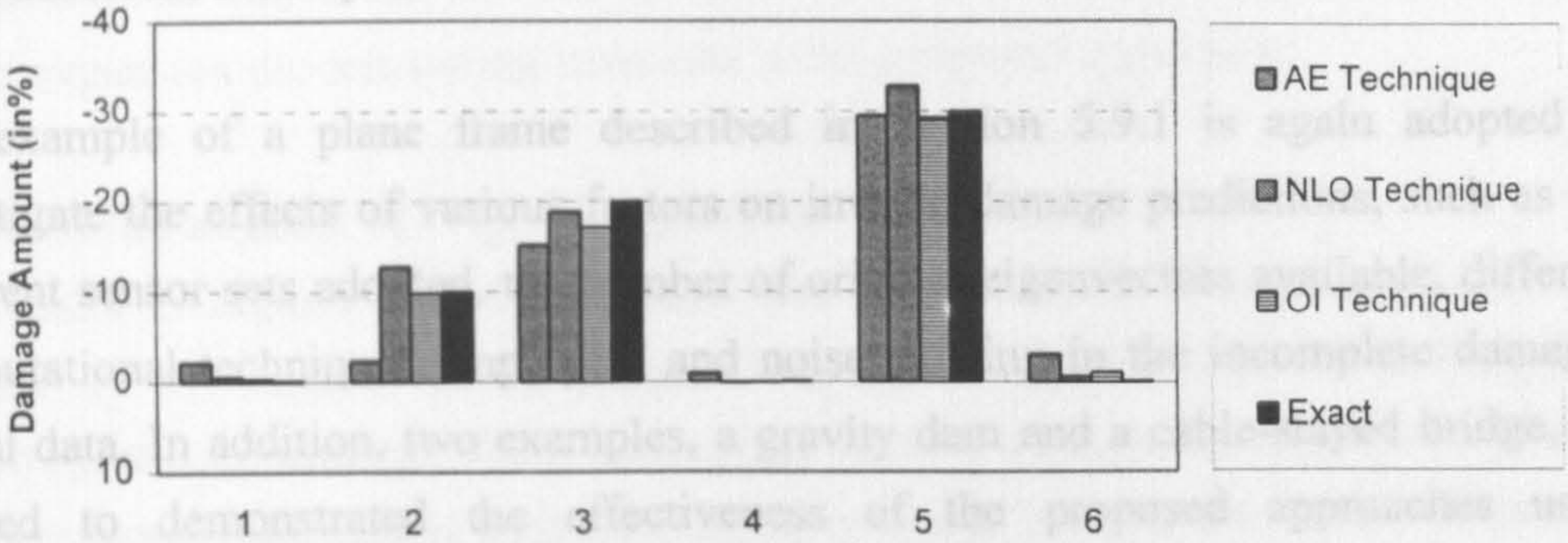

Figure 6.7 Comparison for the **OI** technique with other techniques

6.9 Numerical Examples

The example of a plane frame described in Section 5.9.1 is again adopted to investigate the effects of various factors on inverse damage predictions, such as the different sensor sets adopted, the number of original eigenvectors available, different computational techniques employed, and noise existing in the incomplete damaged modal data. In addition, two examples, a gravity dam and a cable-stayed bridge, are utilised to demonstrated the effectiveness of the proposed approaches using information about incomplete damaged modal data.

6.9.1 Plane frame

The plane frame model, which has been employed in Section 5.9.1 as shown again in Figure 6.8, is now utilised to investigate the effects of various factors on inverse predictions of structural damage.

Effects of different sensor sets adopted

The effectiveness of the proposed approaches with respect to the required amount of modal information is investigated using different sensor sets as summarised in Figure 6.8. It is assumed that only translation displacement readings at selected nodes are measured to avoid the uncertainty of measuring rotation readings. Three sets of selected sensor positions are considered, i.e.,

Set A: 10 sensors placed at nodes 3, 5, 7, 9, 11, 12, 13, 14, 16 and 18.

Set B: 6 sensors placed at nodes 5, 7, 9, 12, 13 and 14.

Set C: 4 sensors placed at nodes 3, 5, 7, and 9.

The results in Figures 6.9(a)–(d) show the inverse predictions for the given damage scenario using information about various sensor sets and incomplete damaged modes. Here, the **DI** technique is employed and all original eigenvectors are considered to identify the structural damage. From the results in Figures 6.9(a) and (b), it can be seen very similar results are obtained when information about incomplete modal data for either damaged mode 2 or damaged mode 3 is used. Furthermore, the results in Figures 6.9(c) and (d) show that the structural damage can properly be identified from a smaller number of sensors, if the number of damaged modes considered increases.

It should be noted that the proposed approaches are capable of not only predicting the damage in structure, but also can provide information on the expanded damaged mode shapes, even if a very limited DOF's readings are available. Therefore, the exact

expanded mode shapes can be obtained since the exact damaged stiffness is employed for the expansion process during iterations in the proposed approaches.

Effects of the number of original eigenvectors available

The results in Figures 6.10(a)–(d) show that the quality of damage predictions is affected by the number of the original eigenvectors used. The **DI** technique is employed, and information about incomplete data for a single damaged mode 2 with DOF's readings measured at the sensor Set A is used to identify the structural damage. Predictions of structural damage clearly improve with an increase of a number of the original eigenvectors used as shown in Figures 6.10(a)–(d), and become very close to the values of the exact solution when the number of the original eigenvectors used is close to the total number of DOFs.

Comparison of the results from different approaches

The results shown in Figures 6.11(a)–(d) are obtained from different computational techniques, such as the **AE1** technique, the **AE2** technique, the **AE3** technique, and the **GNLS** technique with Procedure **MRE**. Here, information about incomplete damaged mode 2 with DOF's readings measured at the sensor Set A is used, and all original eigenvectors are considered in structural damage identification for each computational technique. It is found that inverse predictions for the given damage scenario improve significantly with an increase of the order of approximate equation for the **AE** techniques, as shown in Figures 6.11(a)–(c). Excellent predictions of the structural damage can be obtained when the **GNLS** technique with Procedure **MRE** is used, as shown in Figure 6.11(d).

Effects of the noise existing in incomplete damaged modal data

To investigate the effects of noise existing in the measured incomplete modal data on structural damage identification, it is assumed that each measured DOF's reading (which are used in place of a experimentally measured data) is corrupted by a certain random noise level, i.e., the exact analytical DOF's readings are scaled by the factor $1+\varepsilon$ where ε indicates a level of random noise, while natural frequencies are assumed to be noise free. Here, information about the incomplete damaged mode 2 with DOF's readings measured at sensor the Set A is used, and all original eigenvectors are considered in inverse damage predictions from the **DI** technique. The results in Figures 6.12(a)–(d) show that the quality of predictions for structural damage is highly affected by the noise levels existing in damaged modal data, even when random noise is introduced at 0.05% level. These very high sensitive predictions of structural damage are caused by the ill-conditioned system of governing equations.

Parameters of the Problem

Total DOFs	48
Structural members	18
Damage parameters	18

Hypothetical Damage Scenario

Element No	5	10	15
Damage Amount	-10%	-20%	-30%

Selected Sensor Scenarios

Sensor Set	Measured Node
Set A	3, 5, 7, 9, 11, 12, 13, 14, 16, 18
Set B	5, 7, 9, 12, 13, 14
Set C	3, 5, 7, 9

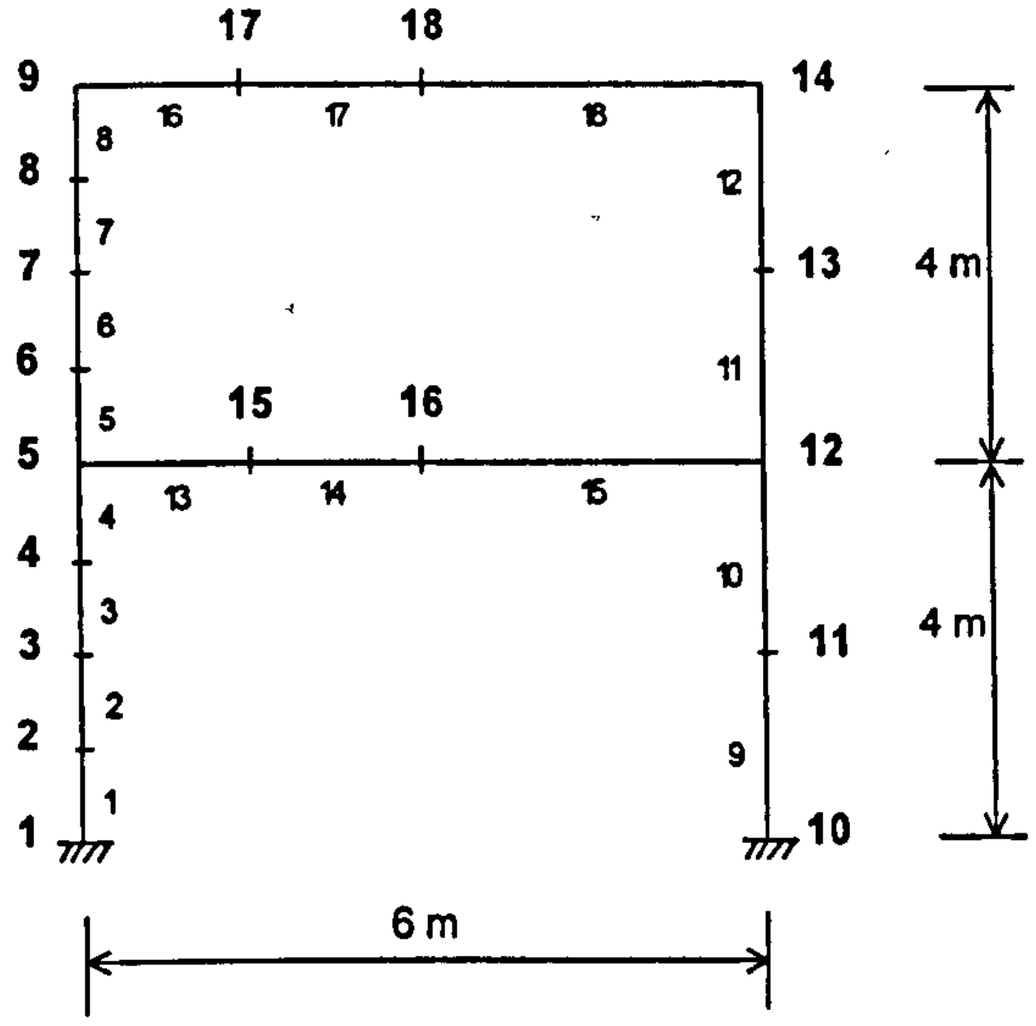

Figure 6.8 Symmetric model plane frame problem

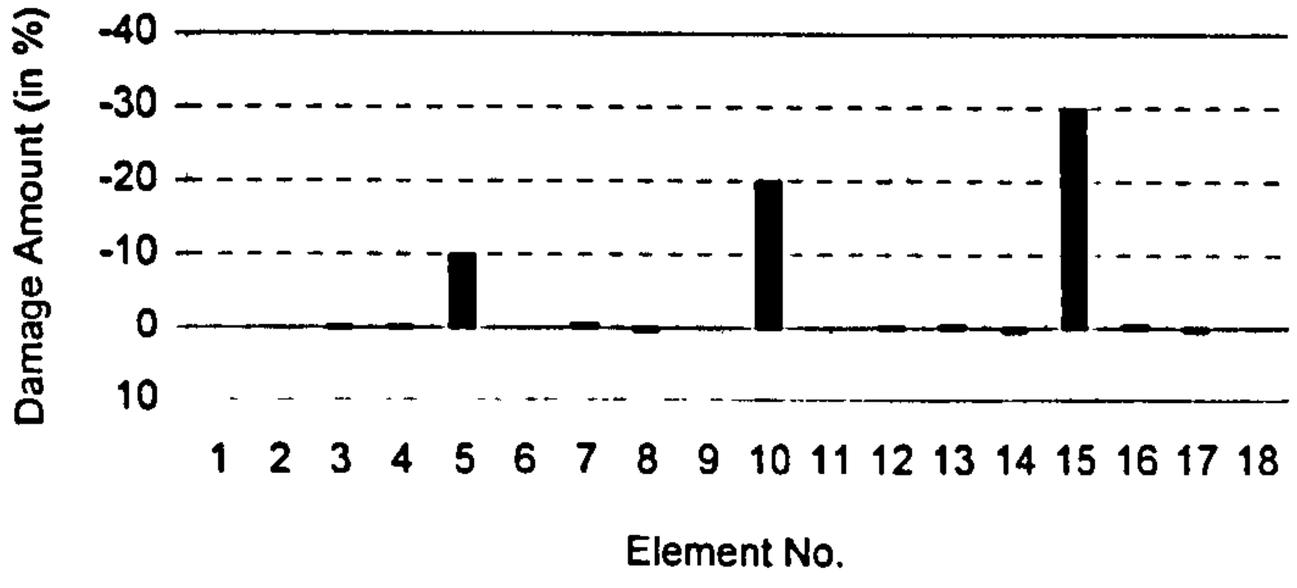

Figure 6.9(a) Incomplete damaged mode 2 used, sensor set A measured

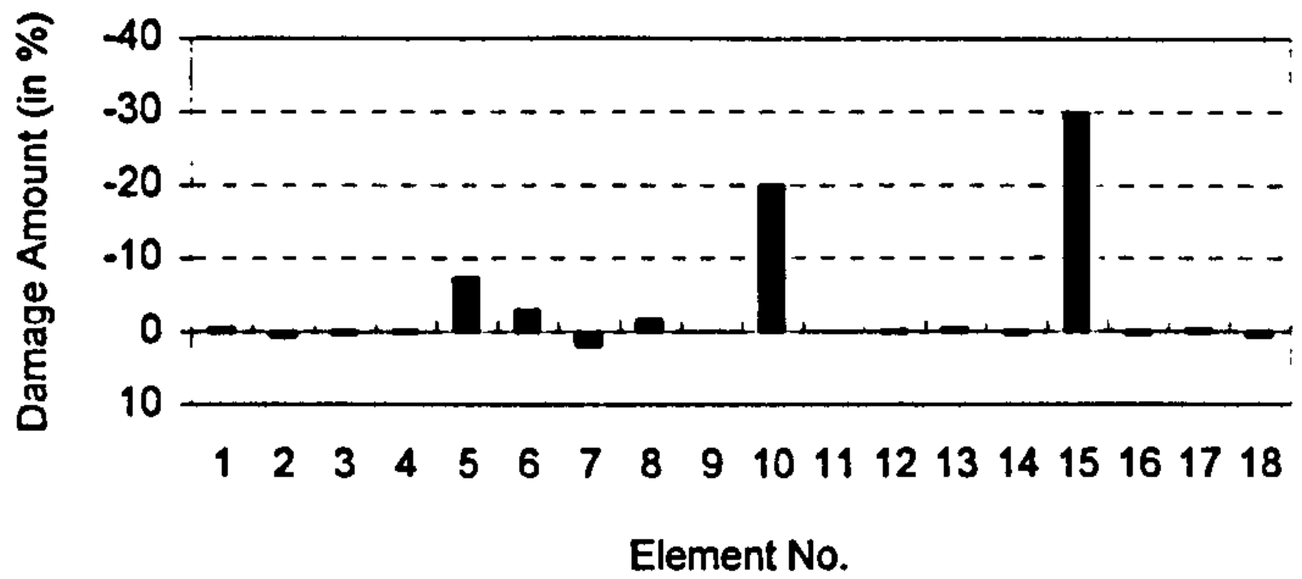

Figure 6.9(b) Incomplete damaged mode 3 used, sensor set A measured

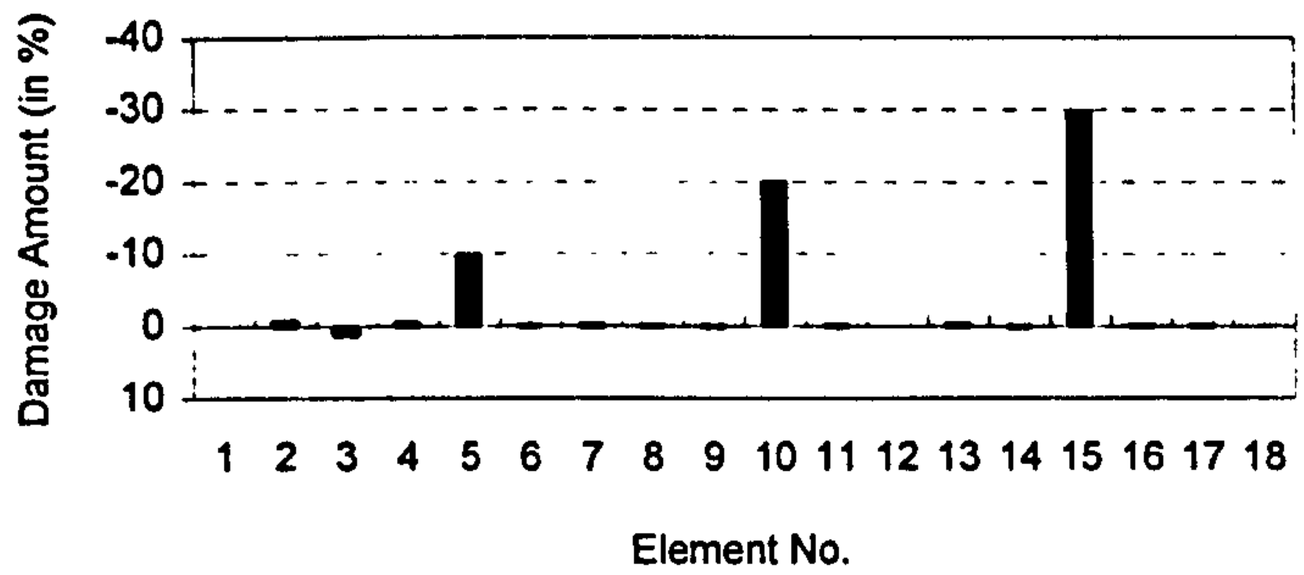

Figure 6.9(c) Incomplete damaged modes 2 and 3 used, sensor set B measured

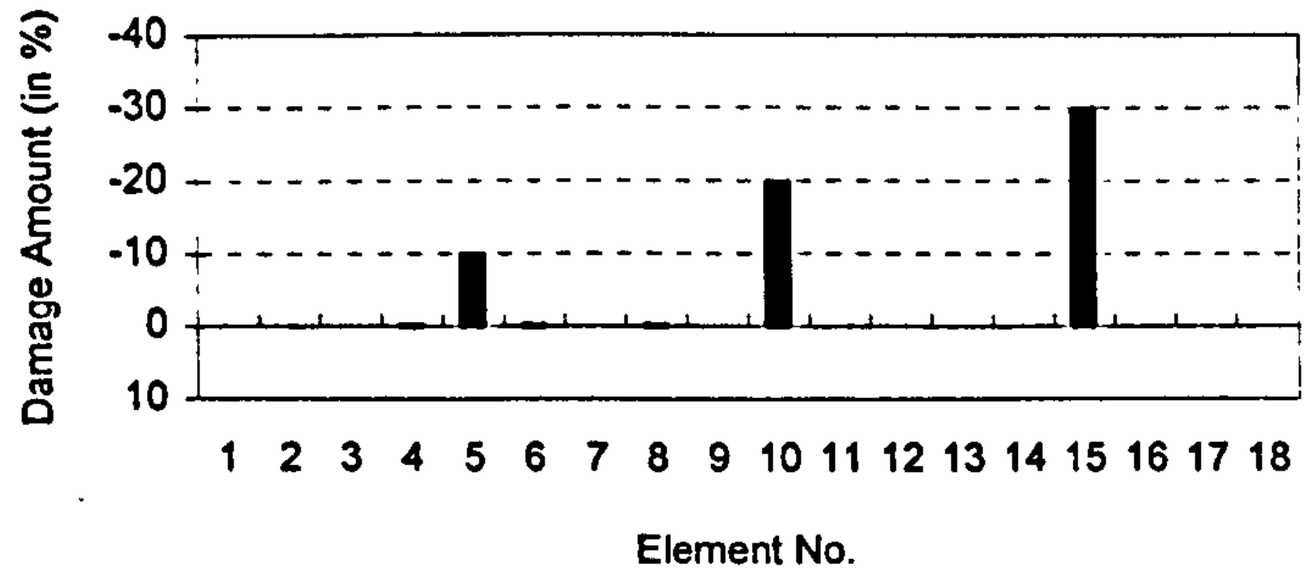

Figure 6.9(d) Incomplete damaged modes 1 to 6 used, sensor set C measured

Figure 6.9 Inverse damage predictions using information on various incomplete damaged modes and various sensor sets, all original eigenvectors used

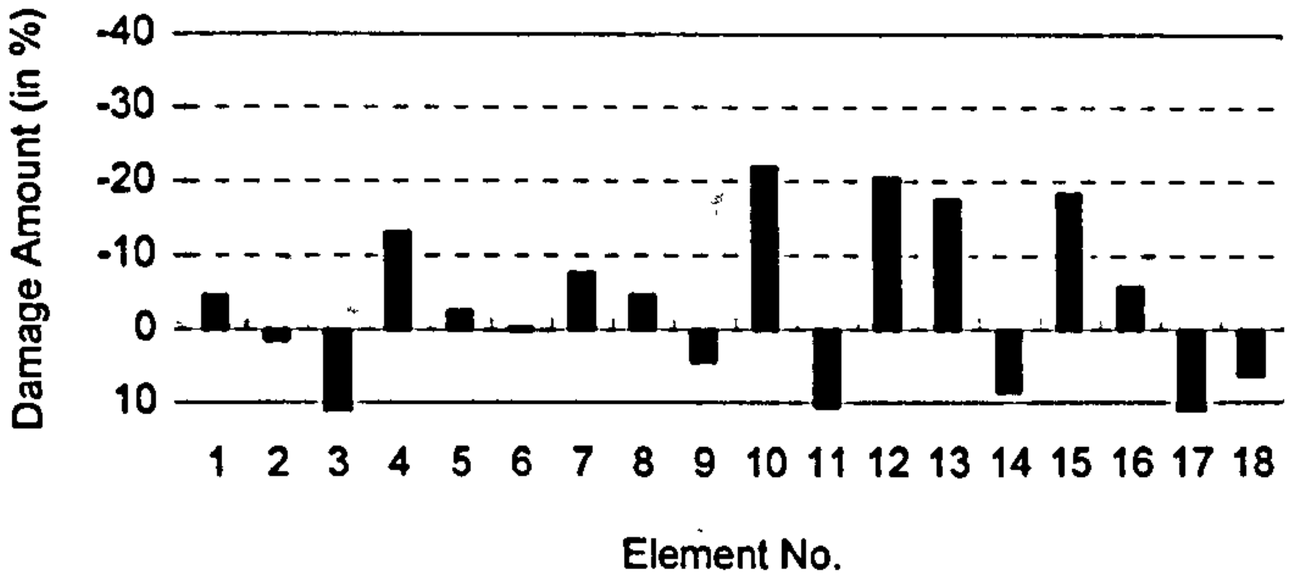

Figure 6.10(a) 40 original eigenvectors used

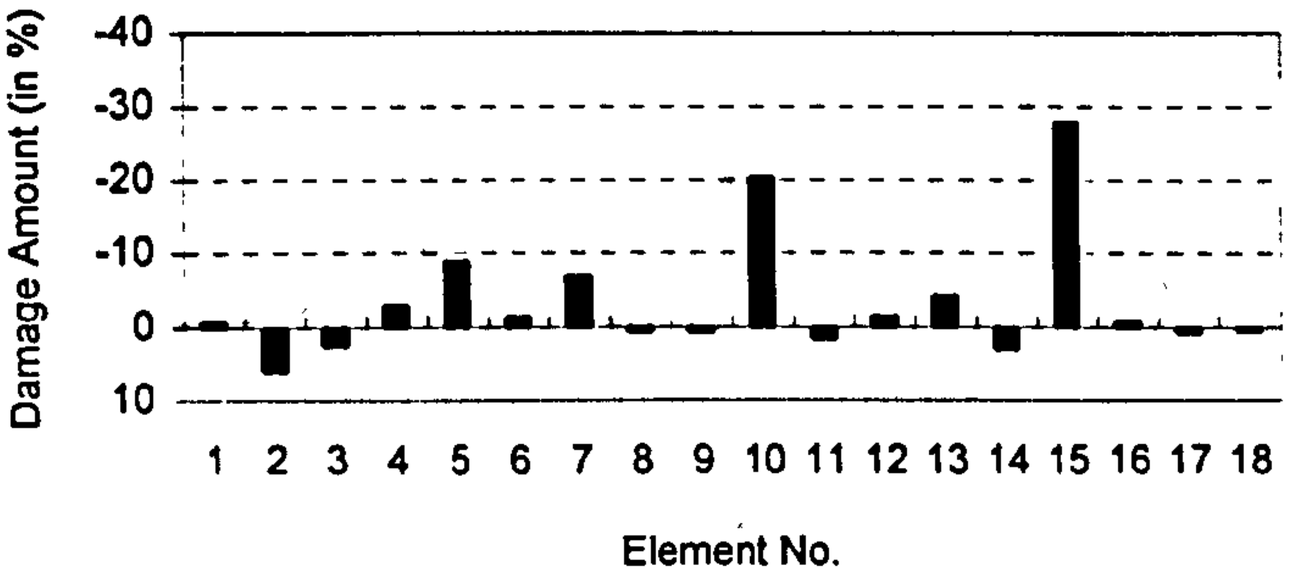

Figure 6.10(b) 42 original eigenvectors used

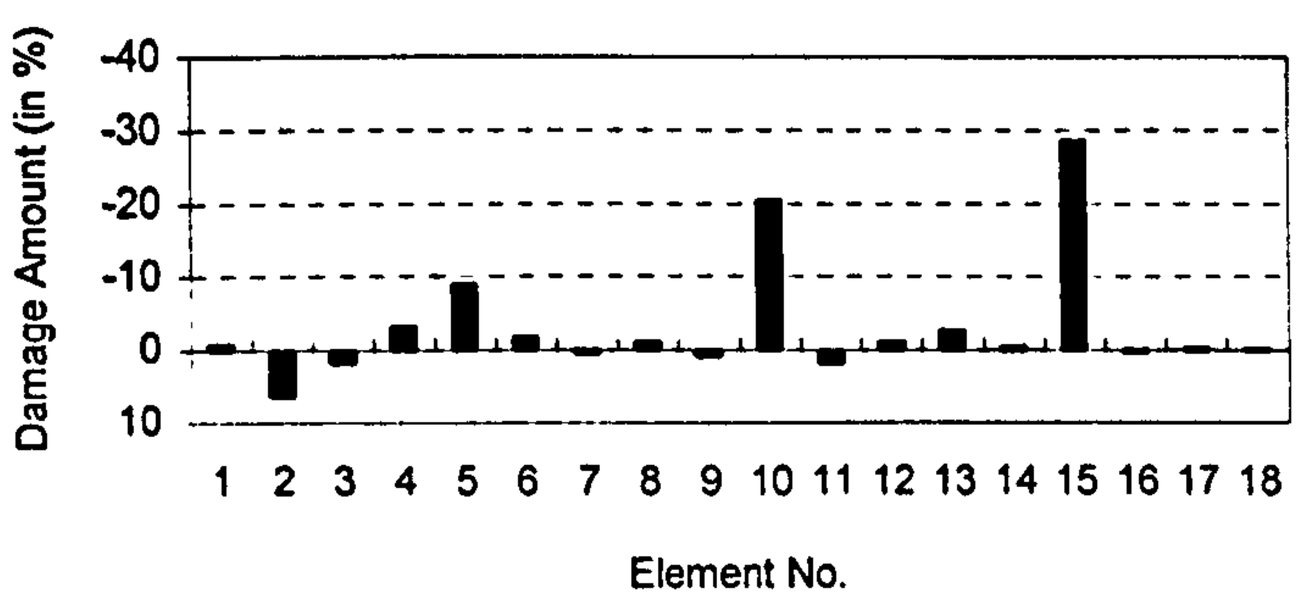

Figure 6.10(c) 44 original eigenvectors used

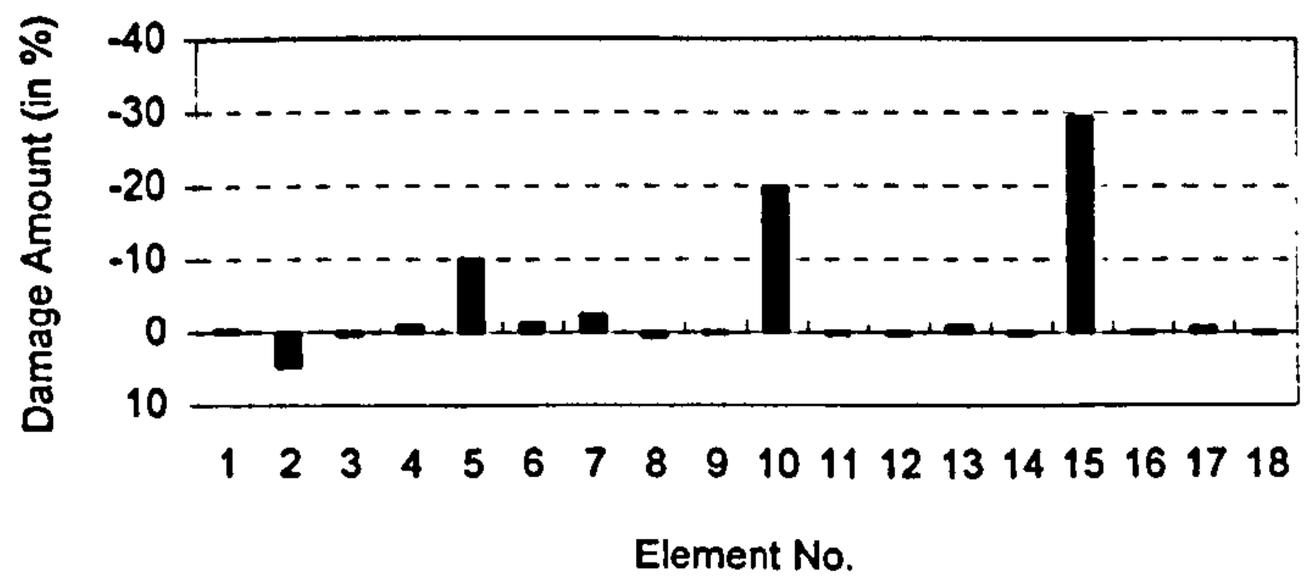

Figure 6.10(d) 46 original eigenvectors used

Figure 6.10 Inverse damage predictions affected by the number of original eigenvectors, information on incomplete damaged mode 2 with sensor set A used

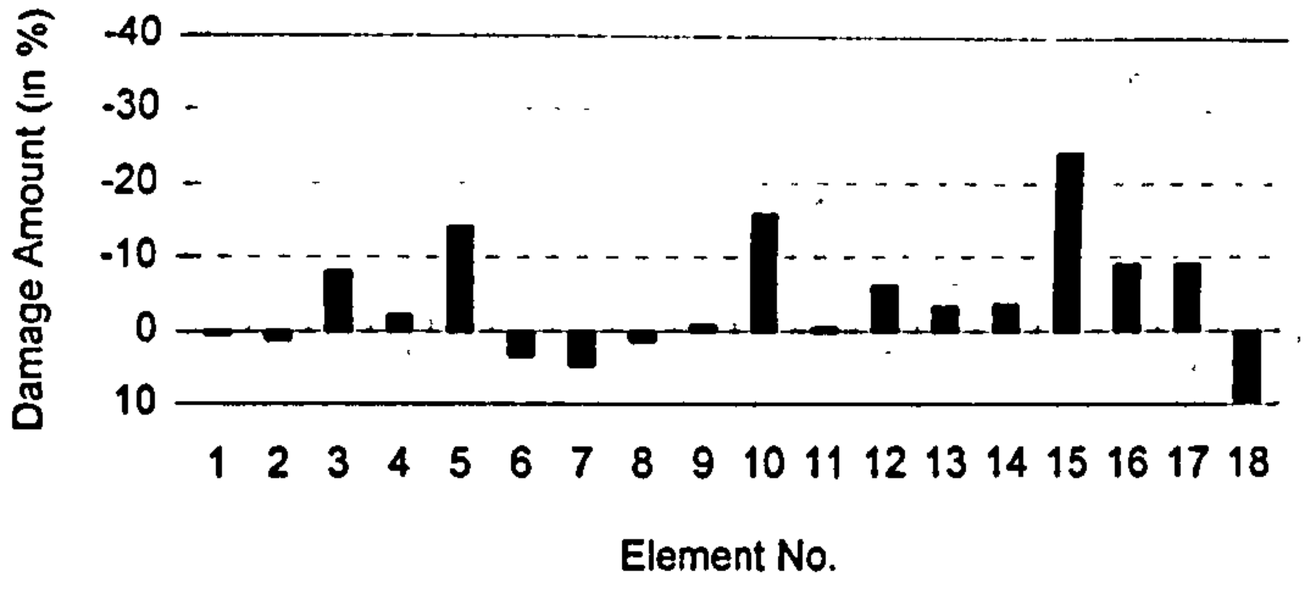

Figure 6.11(a) The **AE1** technique used

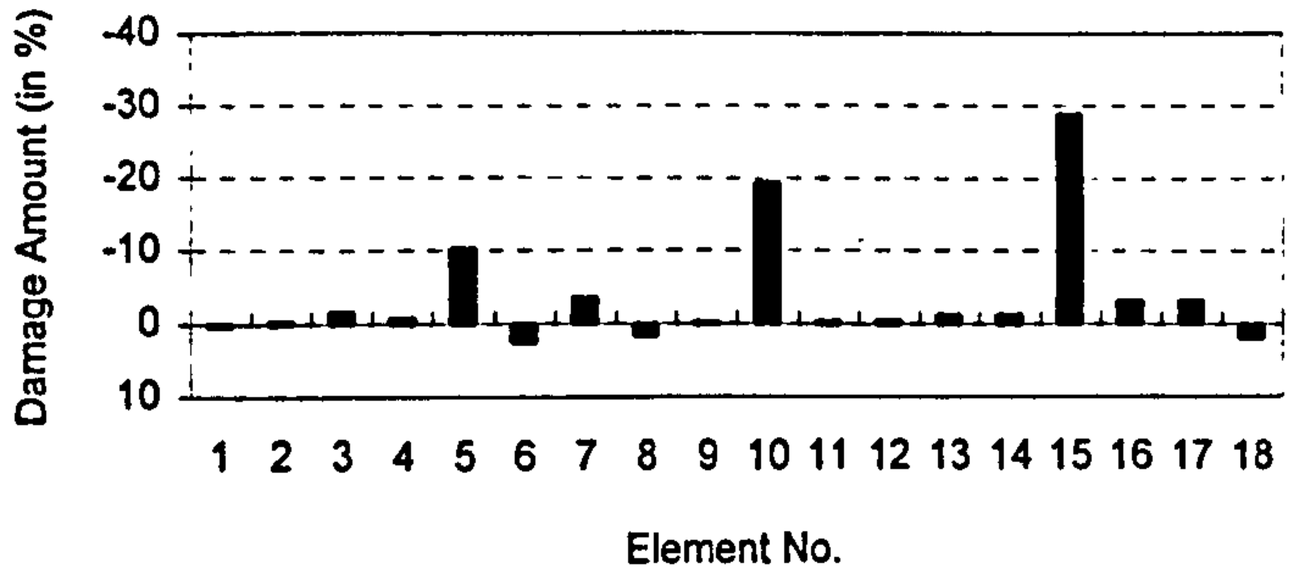

Figure 6.11(b) The **AE2** technique used

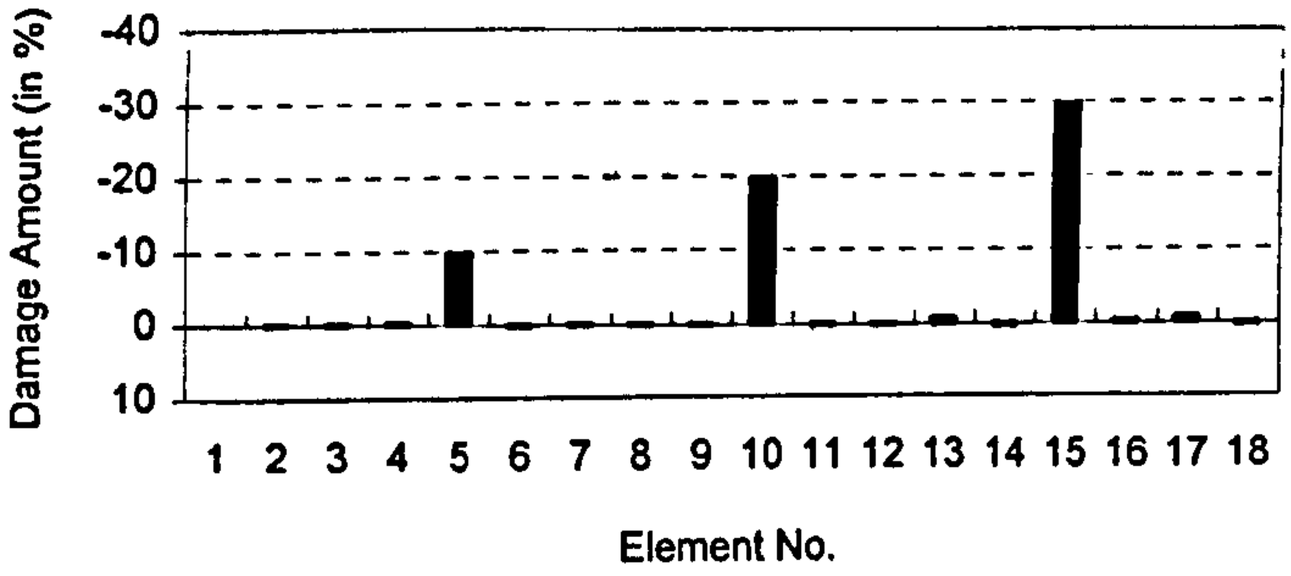

Figure 6.11(c) The **AE3** technique used

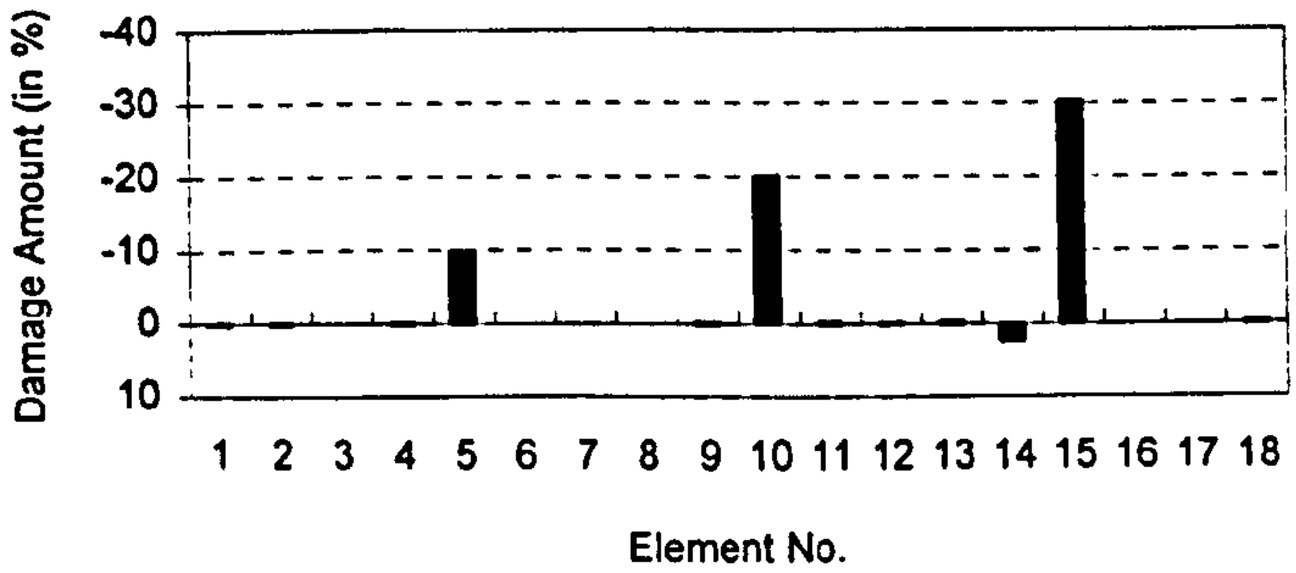

Figure 6.11(d) The **GNLS** technique with Procedure **MRE** used

Figure 6.11 Comparison of inverse damage predictions from different computational techniques, information on incomplete damaged mode 2 with sensor set A used

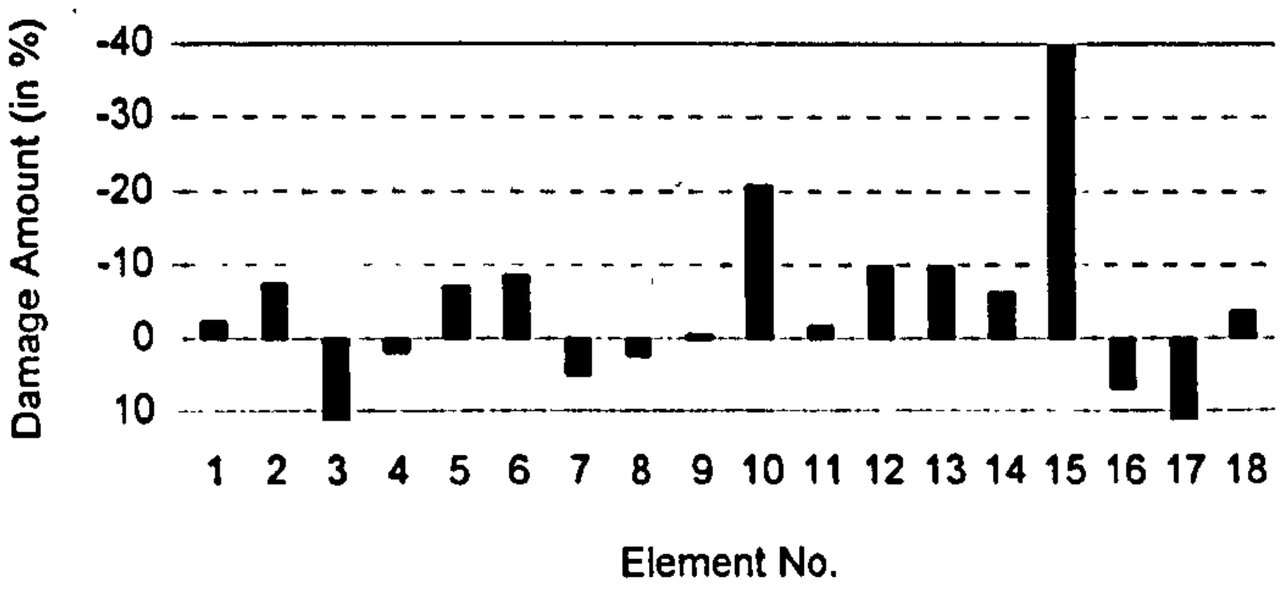

Figure 6.12(a) 0.01% random noise level introduced

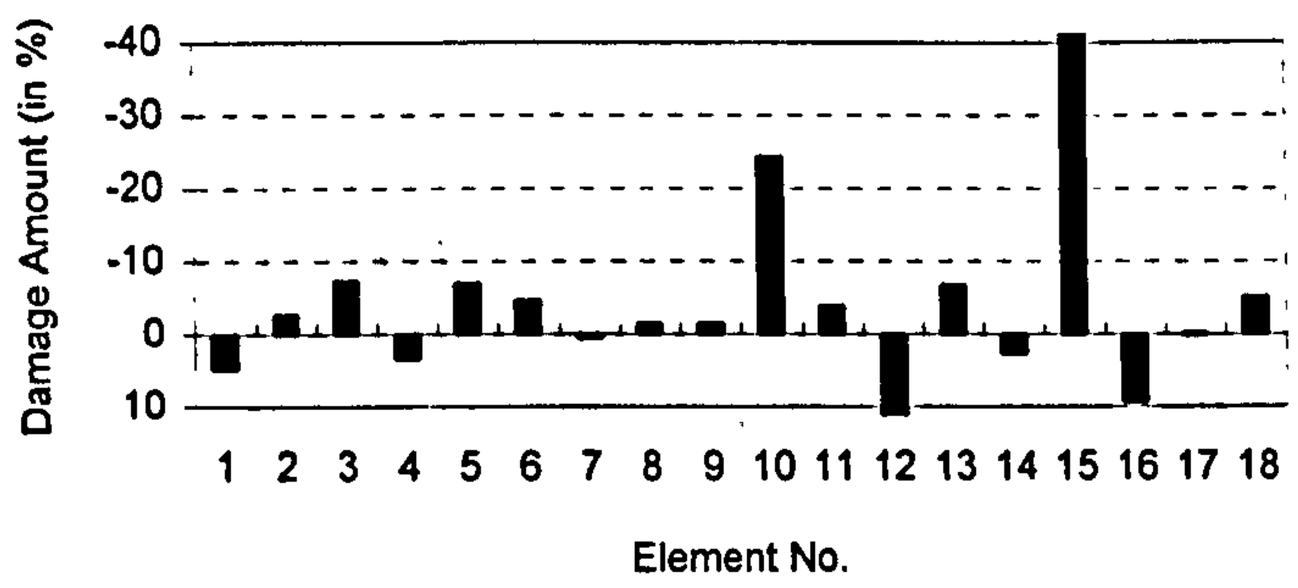

Figure 6.12(b) 0.02% random noise level introduced

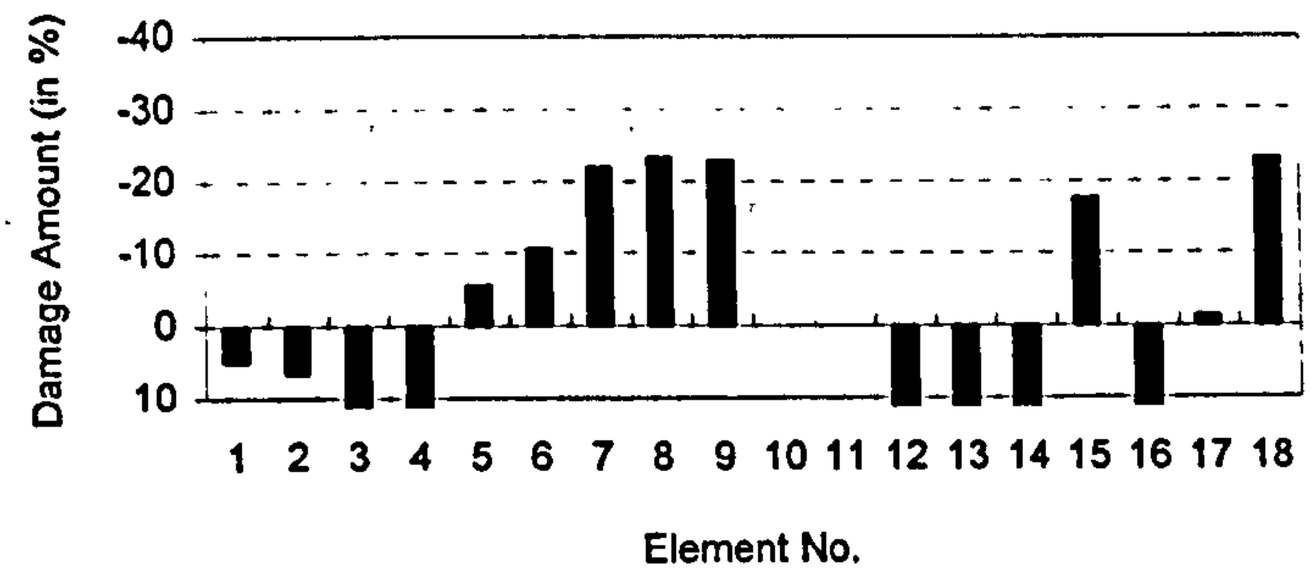

Figure 6.12(c) 0.05% random noise level introduced

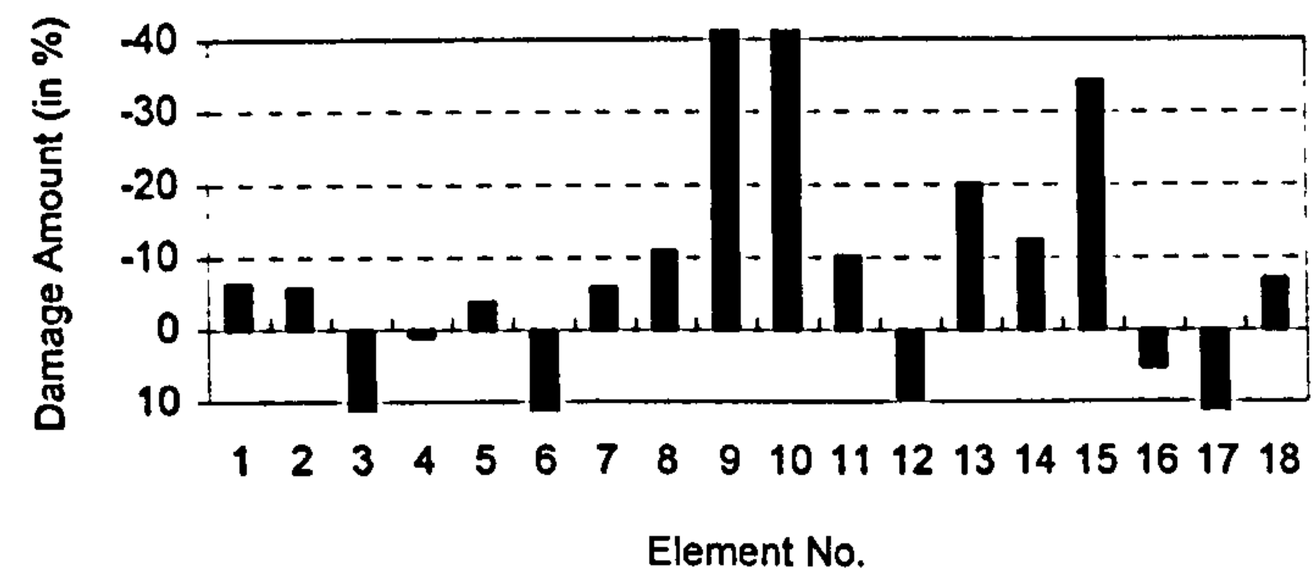

Figure 6.12(d) 0.10% random noise level introduced

Figure 6.12 Inverse damage predictions affected by various noise levels for incomplete modal data, information on incomplete damaged mode 2 with sensor set A used

6.9.2 Gravity dam

A gravity dam shown in Figure 6.13 is used to demonstrate the effectiveness of the proposed approaches directly using incomplete modal data in a continuum setting. A finite element mesh with 24 8-node isoparametric plane strain elements is generated. Four Gauss integration points are considered for each element. All Gauss points have the same material properties with elastic modulus E=2.8×10^{10}N/m^2, Poisson's ratio υ =0.15 and density ρ=2400kg/m^3. The geometry of the structure, element and Gauss point numbering, a hypothetical damage scenario, as well as two sets of selected sensor scenarios are shown in Figure 6.13.

The results in Figures 6.14(a)–(d) show inverse predictions of the given damage scenario using information about different combinations of the incomplete damaged mode shapes with DOF's readings measured at the sensor Set A. The **DI** technique is employed for structural damage identification. Very similar results are obtained when information on modal data for different combinations of incomplete damaged modes is used. The results obtained are not as good as expected, since only some of the original eigenvectors are utilised in the calculation due to the difficulties in computing the modes with high frequencies.

The results shown in Figures 6.15(a)–(d) are inverse damage predictions using information about two different incomplete damaged mode shapes with DOF's readings measured at the sensor Set B. Here, the **GNLS** technique with Procedure **MRF** is employed for structural damage identification. It is found that structural damage can be determined correctly by using a combination of any two incomplete damaged modes, and predictions of structural damage become excellent when information about incomplete damaged modes 2 and 4 is used, as shown in Figure 6.15(d).

Parameters of the Problem

Total DOFs	186
Structural elements	24
Gauss points	24×4=96
Damage parameters	96

Hypothetical Damage Scenarios

Element No	4	8	13	14	17	18	21
Gauss Point No	13, 15	30, 32	51	53	68	70	81, 83
Damage Amount	-10%	-10%	-20%	-20%	-20%	-20%	-30%

Selected Sensor Scenarios

Sensor Set	Measured Node
Set A	Only nodes marked with ■
Set B	Nodes marked with both ■ and •

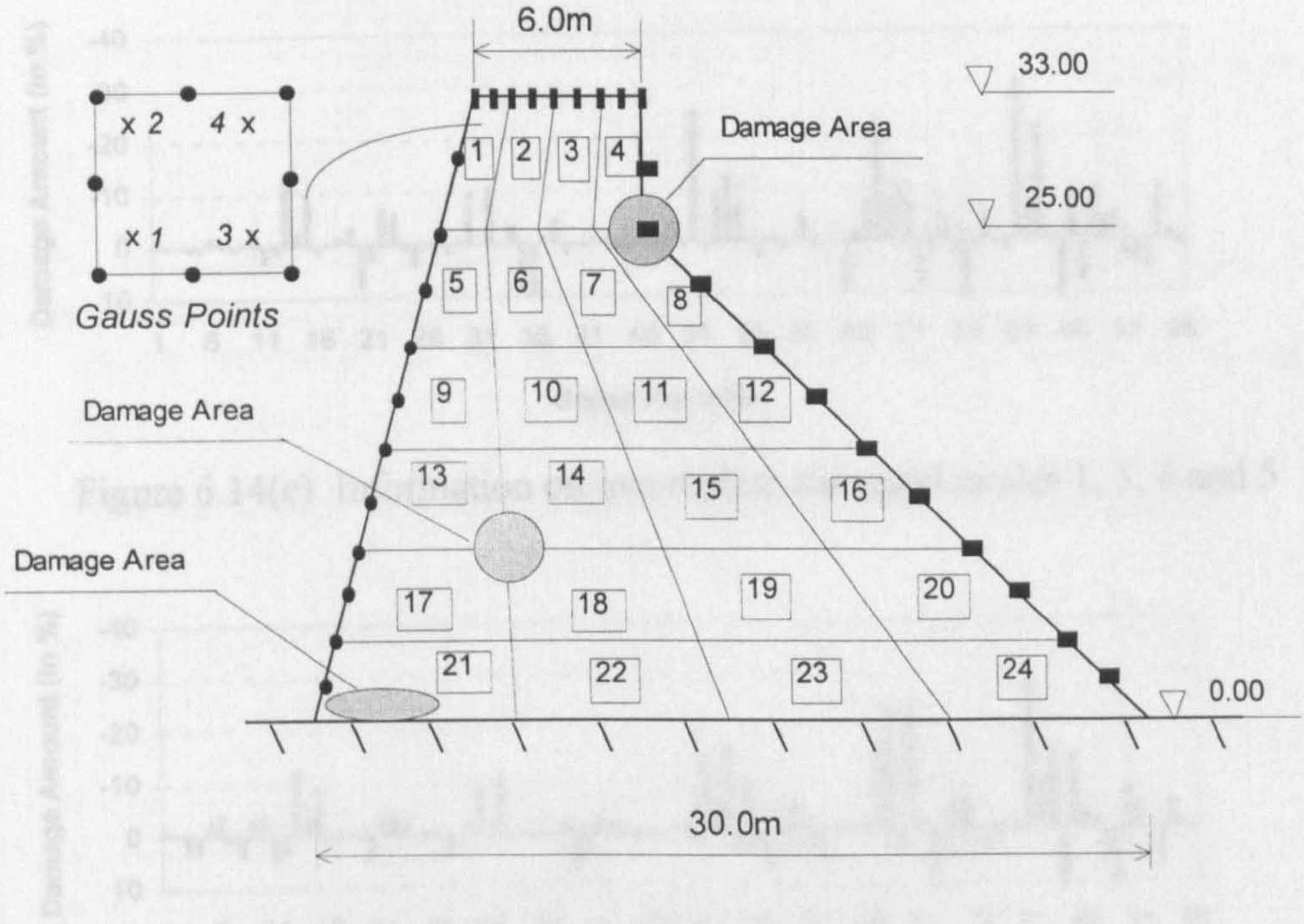

Figure 6.13 Gravity dam model problem

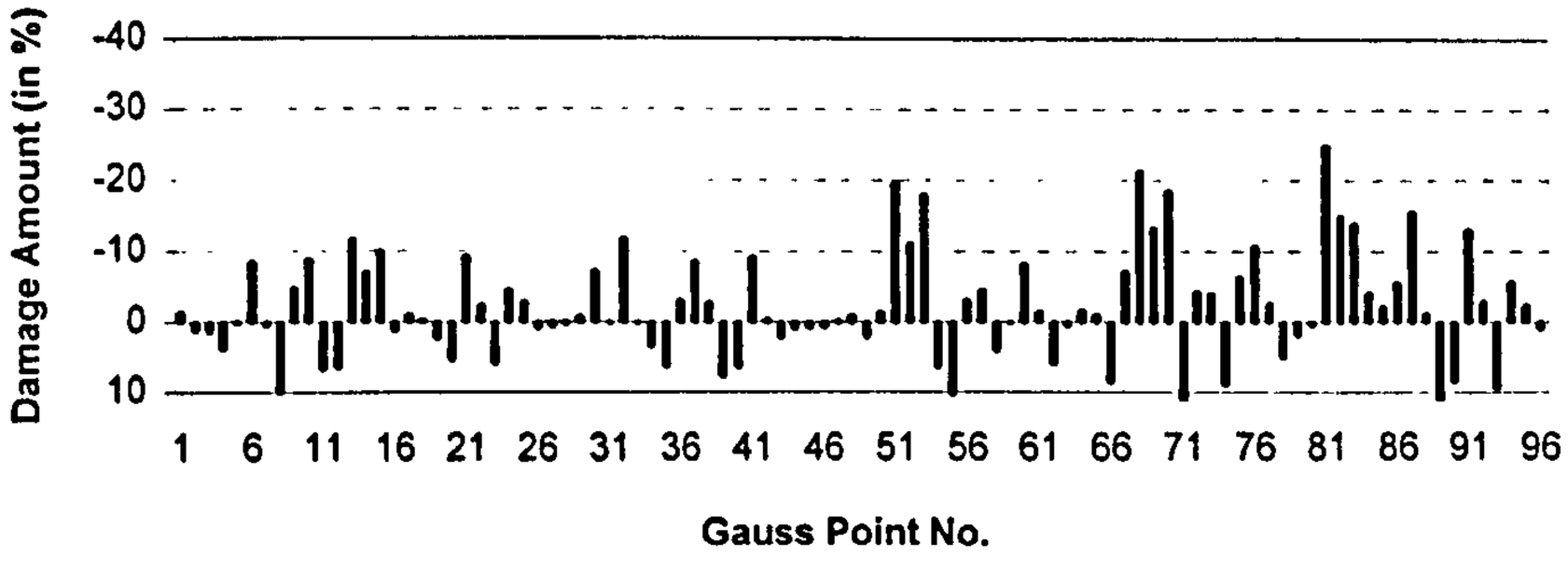

Figure 6.14(a) Information on incomplete damaged modes 1, 2, 3 and 5

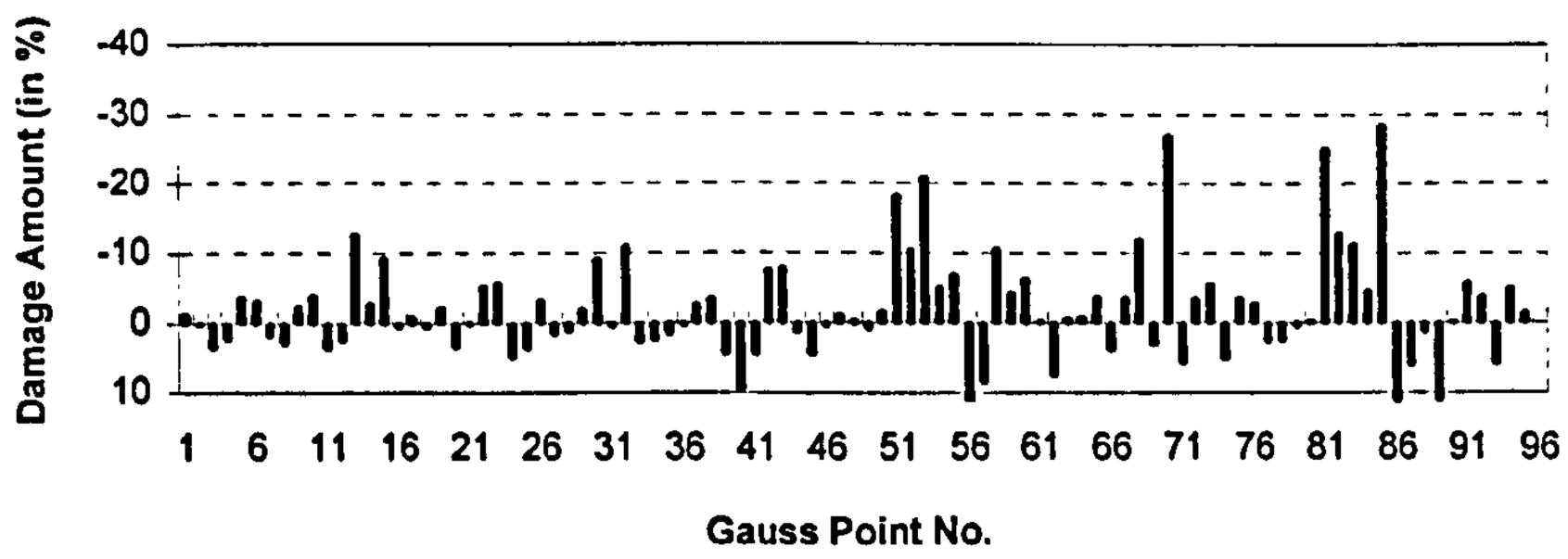

Figure 6.14(b) Information on incomplete damaged modes 1, 2, 4 and 5

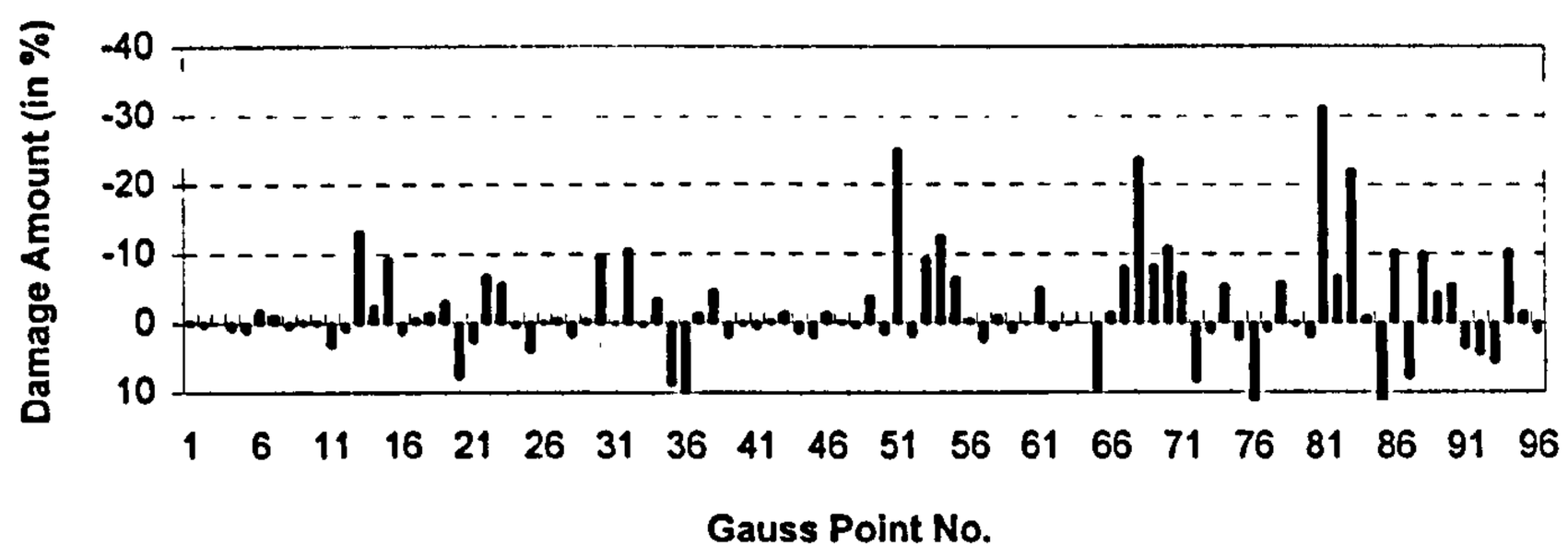

Figure 6.14(c) Information on incomplete damaged modes 1, 3, 4 and 5

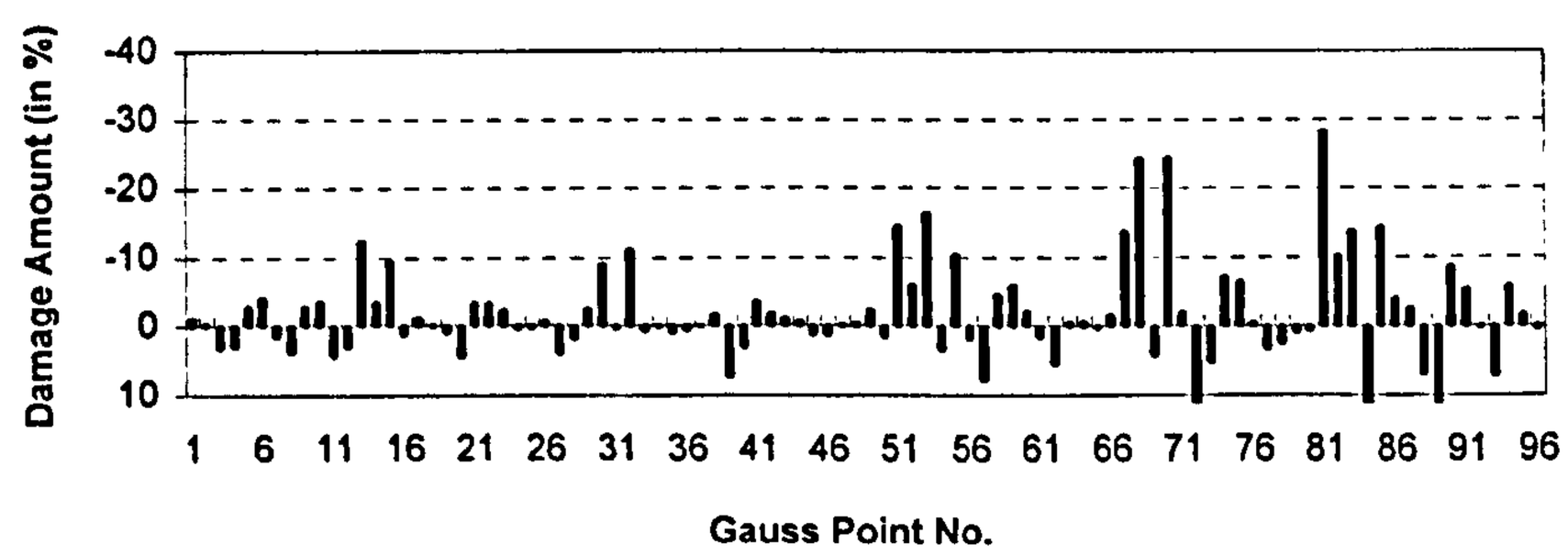

Figure 6.14(d) Information on incomplete damaged modes 2, 3, 4 and 5

Figure 6.14 Inverse damage predictions using information on various incomplete damaged modes with sensor set A, the **DI** technique used

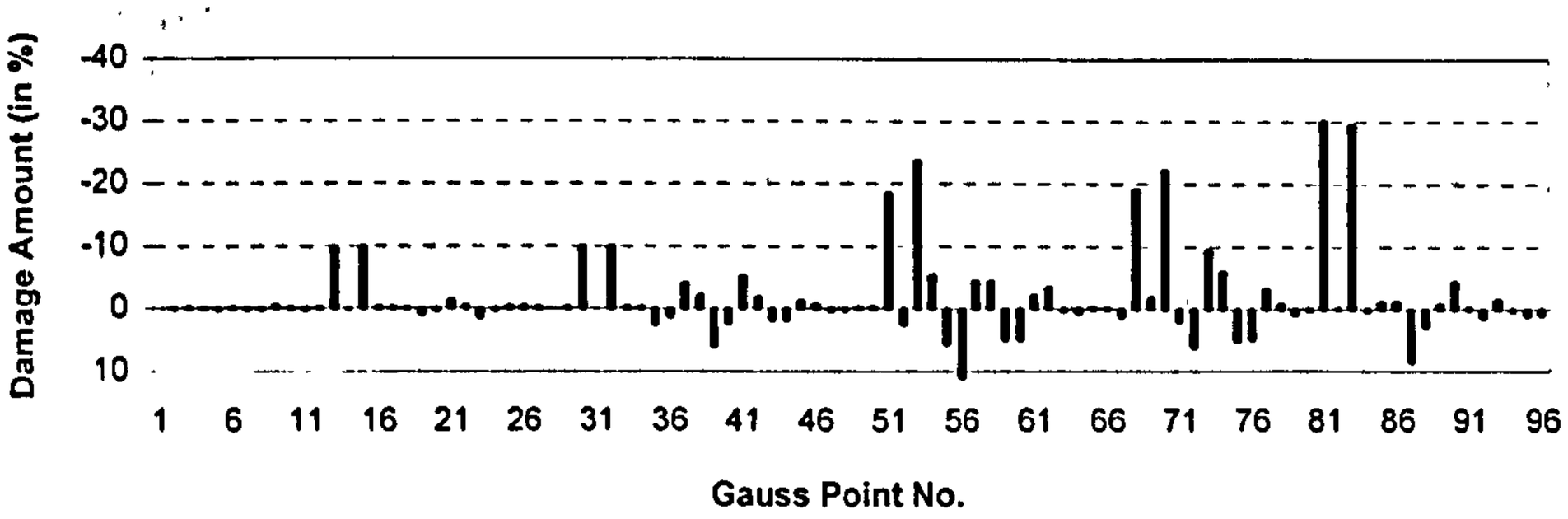

Figure 6.15(a) Information on incomplete damaged modes 1 and 2

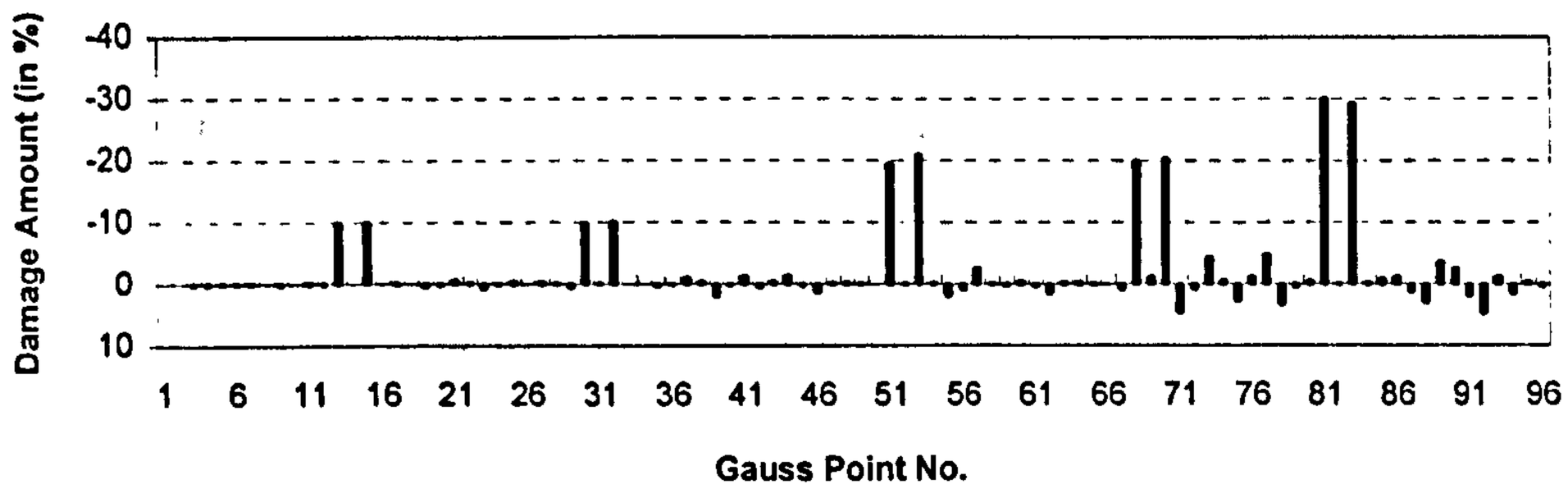

Figure 6.15(b) Information on incomplete damaged modes 1 and 3

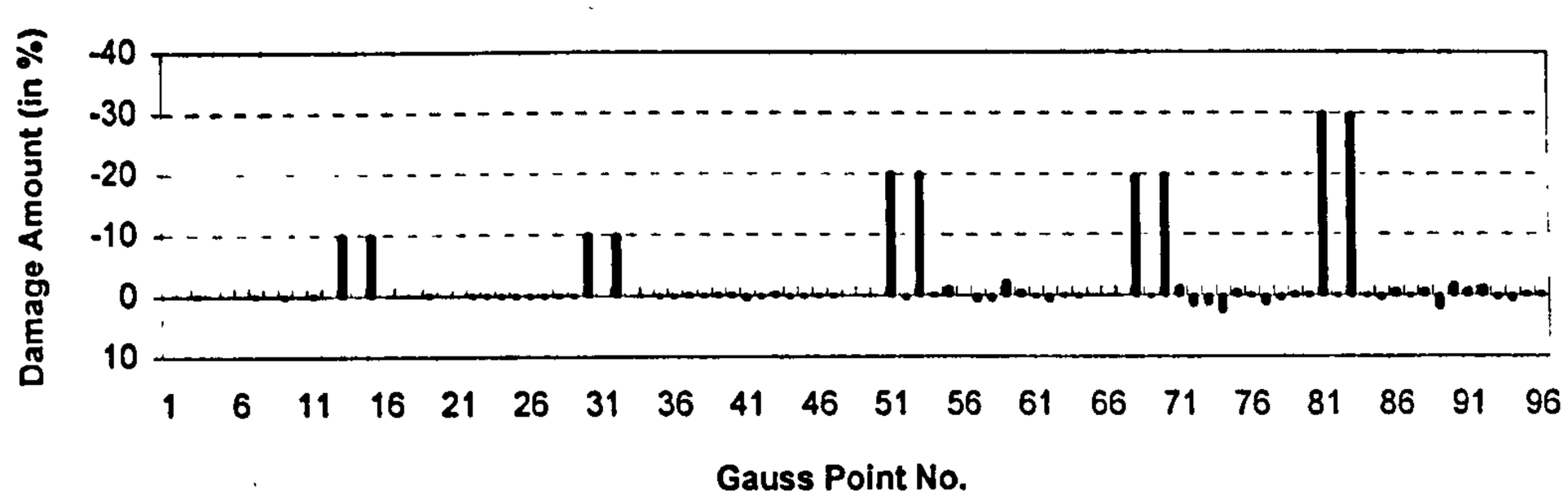

Figure 6.15(c) Information on incomplete damaged modes 2 and 3

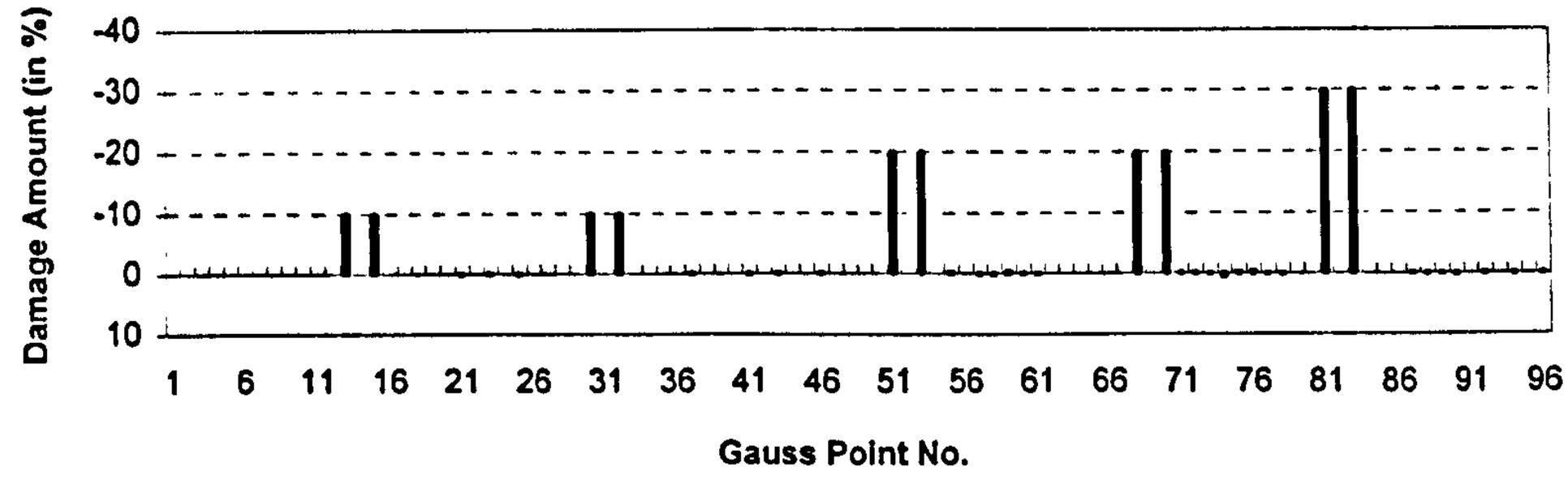

Figure 6.15(d) Information on incomplete damaged modes 2 and 4

Figure 6.15 Inverse damage predictions using information on various incomplete damaged modes with sensor set B, the **GNLS** technique with Procedure **MRF** used

6.9.3 Cable-stayed bridge

A model of the real fan-system cable-stayed bridge (Wang and Huang, 1992) is now adopted to demonstrate the effectiveness of the proposed approaches for different damage scenarios and different structural models. The elevation and dimension of cable-stayed bridge are shown in Figure 6.16(a). The cross-sectional properties of each component are listed in Table 6.3. The numbers of structural members shown in Table 6.3 correspond to those in Figure 6.16(a). The modulus of elasticity for steel is E=2.1×10^{11}N/m^2, and for concrete it is E=3.2×10^{10}N/m^2.

The girder is supported vertically at the towers but is independent of the towers. Therefore, the bending moments are not transferred between the girder and the tower. The cables have initial tensile forces due to the dead loads, so that they are capable of resisting compressive forces during vibration of the structure.

Table 6.3 Main data of cable-stayed bridge

Member	Number of Members	Area (m^2)	Moment of Inertia (10^{-4}m^4)	Mass (10^{3}kg/m)
Girder	1	4.976	2.730	16.213
Girder	2	4.976	2.730	17.194
Girder	3	5.420	3.462	18.415
Girder	4	6.012	4.662	18.522
Girder	5	4.560	2.814	16.971
Girder	6	3.444	2.125	11.094
Girder	7	0.007032	/	0.120
Cable	8, 12	0.009897	/	0.168
Cable	9, 13	0.012722	/	0.218
Tower	10	4.800	1.600	12.274
Pier	11	30.000	19.980	79.894

Four damage scenarios are generated with damage at different locations. Only translation displacement readings at the nodes marked with "•" on the girder are measured, as shown in Figure 6.16(b). Two different element types are used to model the cable-stayed bridge, which results in different numbers of structural damage parameters. The detail of element stiffness matrices used in cable-stayed bridge is given in Appendix A.2.

The results in Figures 6.17(a)–(d) show inverse predictions for different damage scenarios simulated at element level as shown in Figure 6.16(b). Direct element stiffness matrices for all structural members of the model are utilised. The **DI** technique is employed and information about only the incomplete damaged modes 3 and 5 is used to identify structural damage. It can be seen that structural damage can be identified correctly for each of the damage scenarios.

Figures 6.18(a)–(d) show the results for inverse predictions for different damage scenarios simulated at Gauss point level as shown in Figure 6.16(b). Here, numerically integrated element stiffness matrices obtained from Gauss integrations for all structural members of the model are utilised, and three Gauss integration points are considered for all structural elements. The **DI** technique is employed, and information about the incomplete damaged modes 1, 3, 5 and 6 is used for structural damage identification. It is found that structural damage can be located properly for each of the damage scenarios, while the extent of structural damage can also be estimated if the total amount of structural damage within a cable instead of its Gauss point locations is considered. The results presented here show that the inverse predictions for structural damage may not be unique, as the same damaged stiffness can result from different structural damage scenarios, e.g. the cases of element stiffness for cables.

Parameters of the Problem

Total DOFs	136
Structural elements	66
Gauss points	66×3=198
Damage parameters	66/198

Hypothetical Damage Scenarios

	Damage Scenario 1	Damage Scenario 2	
Element No	35, 36, 37	35, 36, 57	
Gauss Point No	105, 106, 108, 109	105, 106, 169	
Damage Amount	-30%	-30%	
	Damage Scenario 3	Damage Scenario 4	
Element No	18, 19, 25, 30	14, 15, 30	51, 57, 62
Gauss Point No	54, 55, 75, 90	42, 43, 88	151, 172, 186
Damage Amount	-30%	-20%	-30%

Selected Sensor Scenarios

Sensor Set: Measuring nodes marked with • on the girder

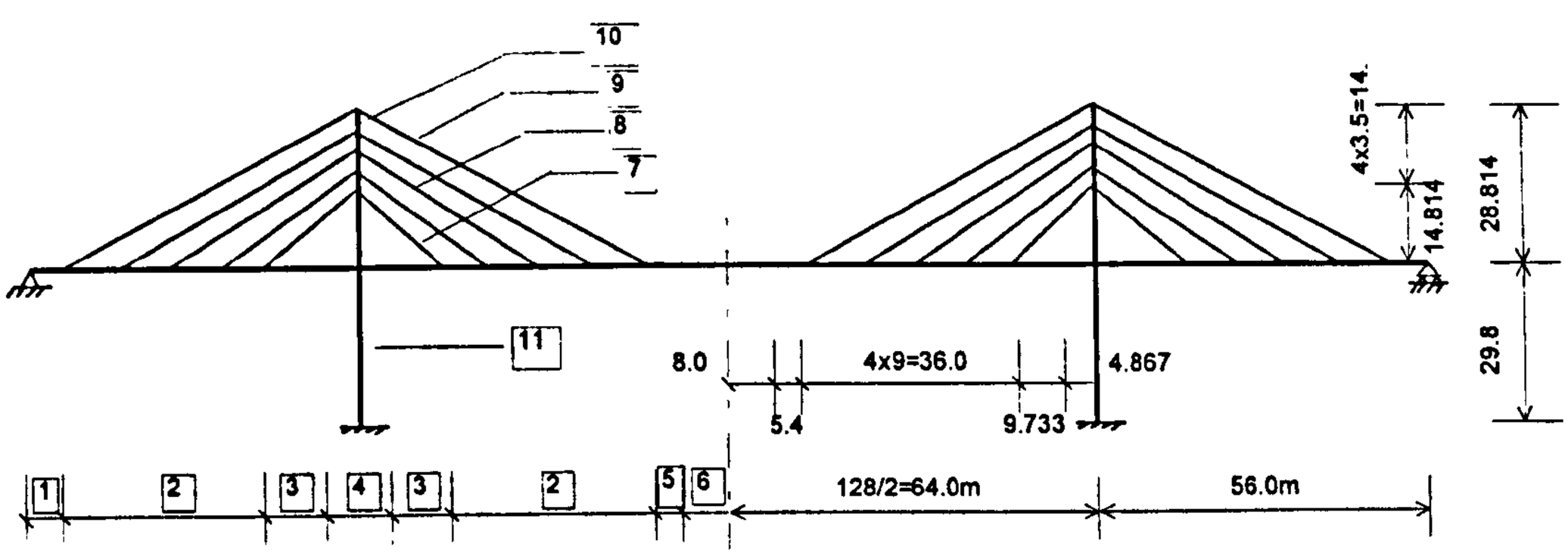

Figure 6.16(a) Elevation and dimension of cable-stayed bridge

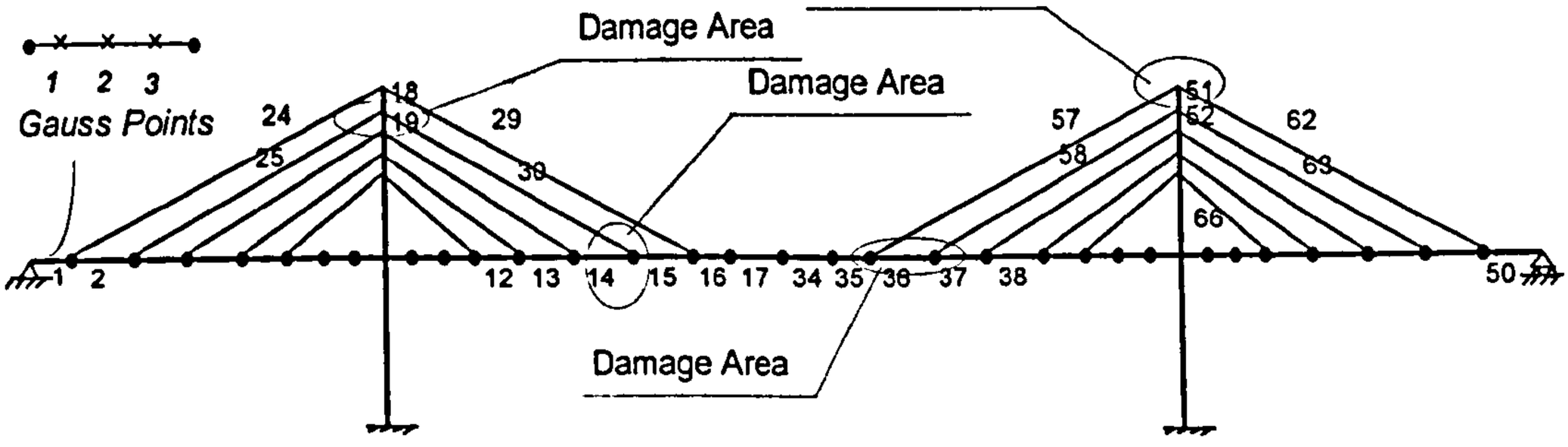

Figure 6.16(b) Cable-stayed bridge model problem

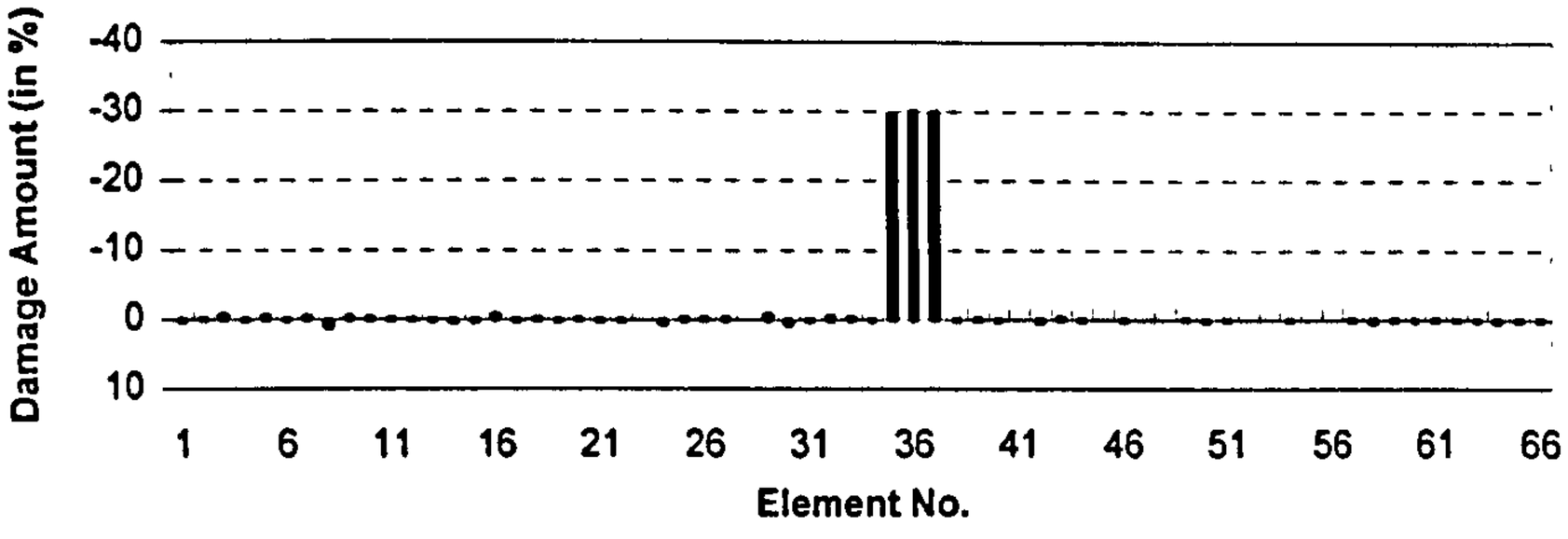

Figure 6.17(a) Predicted damage for scenario 1

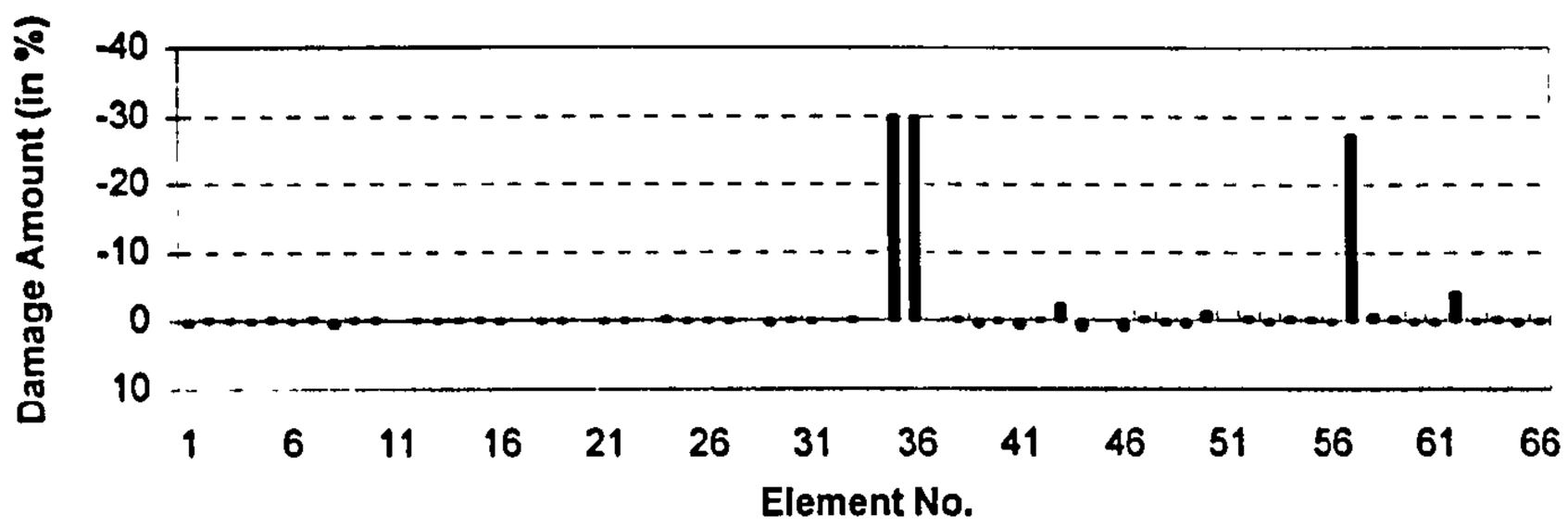

Figure 6.17(b) Predicted damage for scenario 2

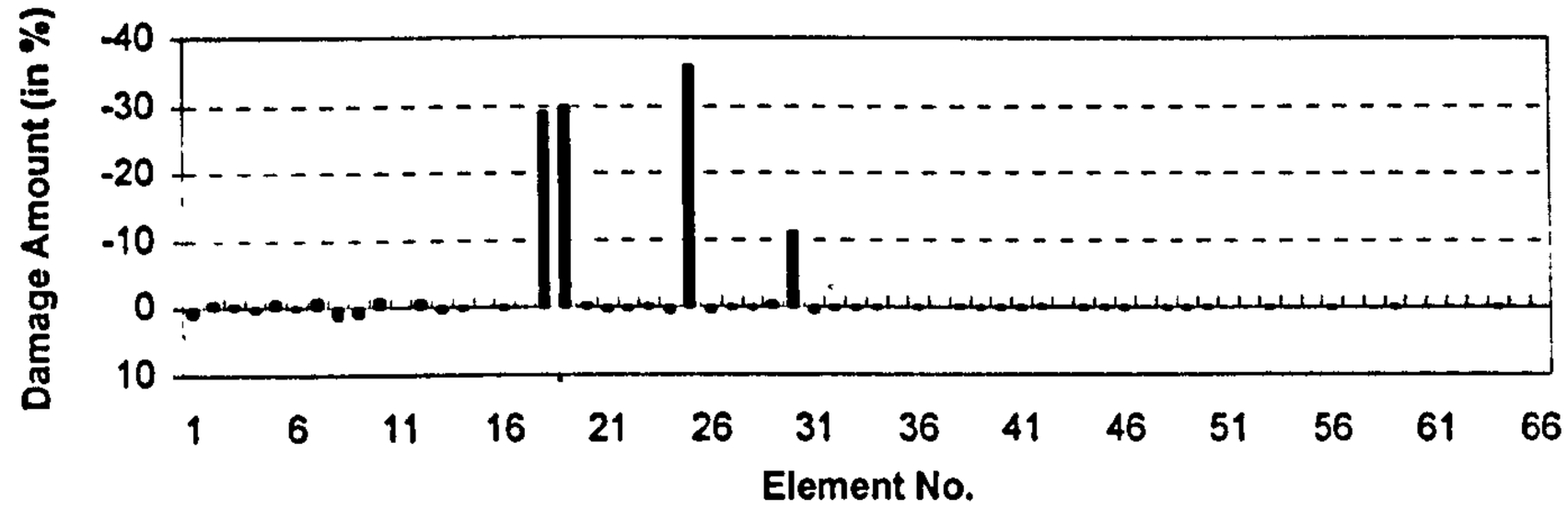

Figure 6.17(c) Predicted damage for scenario 3

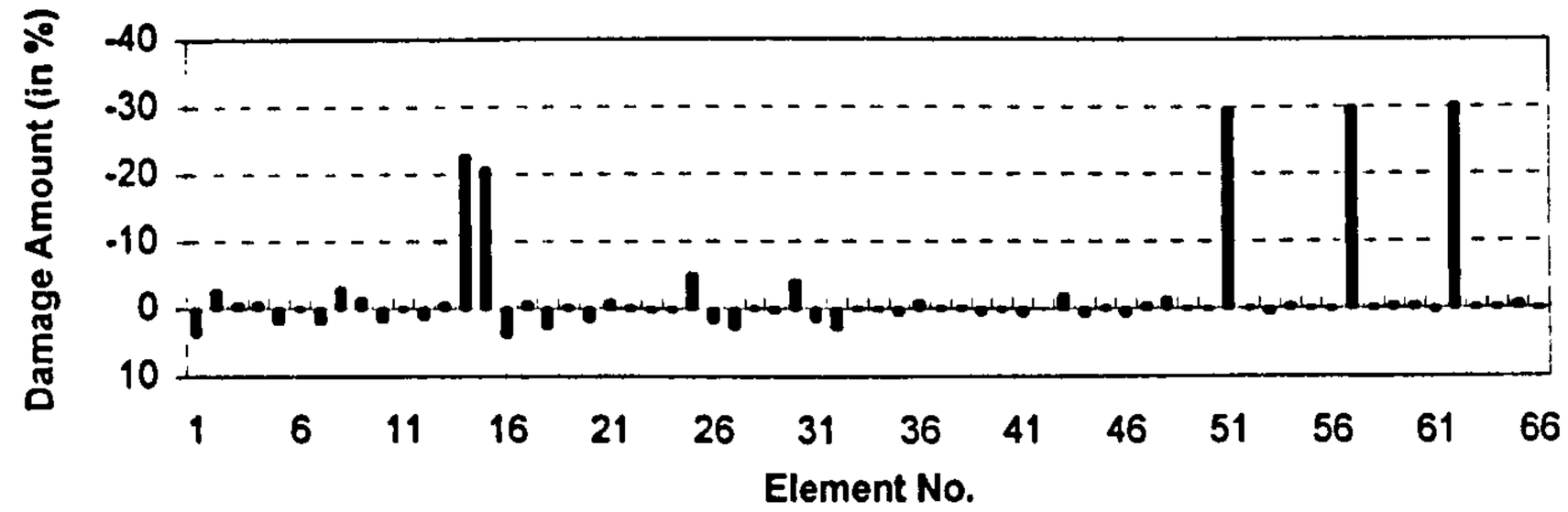

Figure 6.17(d) Predicted damage for scenario 4

Figure 6.17 Inverse damage predictions for different damage scenarios at element level, information on incomplete damaged modes 3 and 5 with the sensor set used

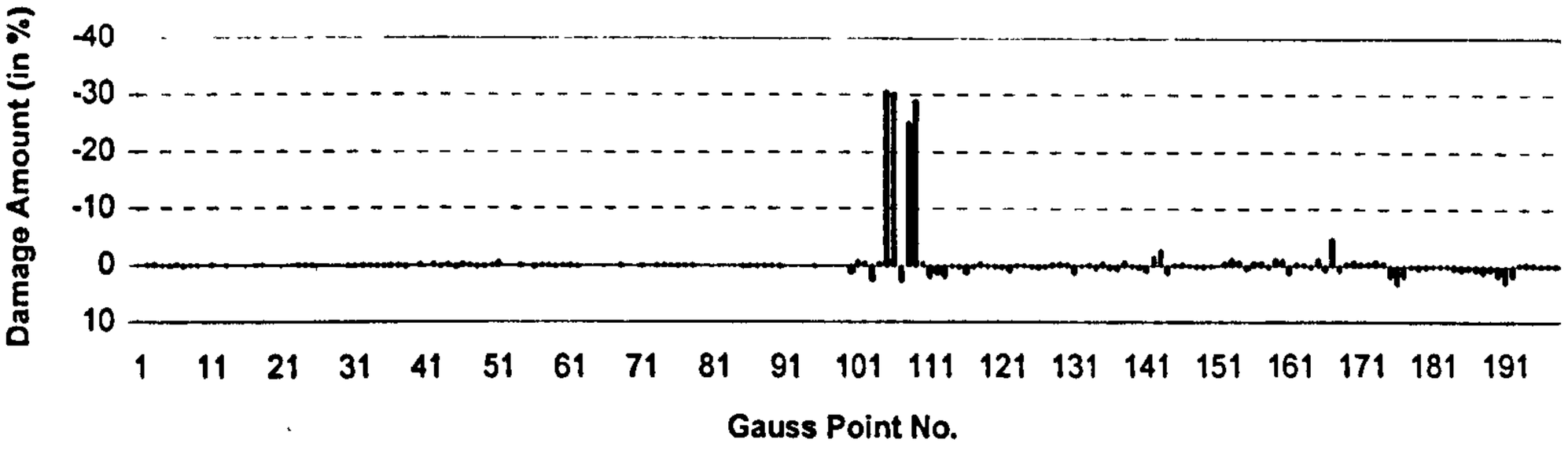

Figure 6.18(a) Predicted damage for scenario 1

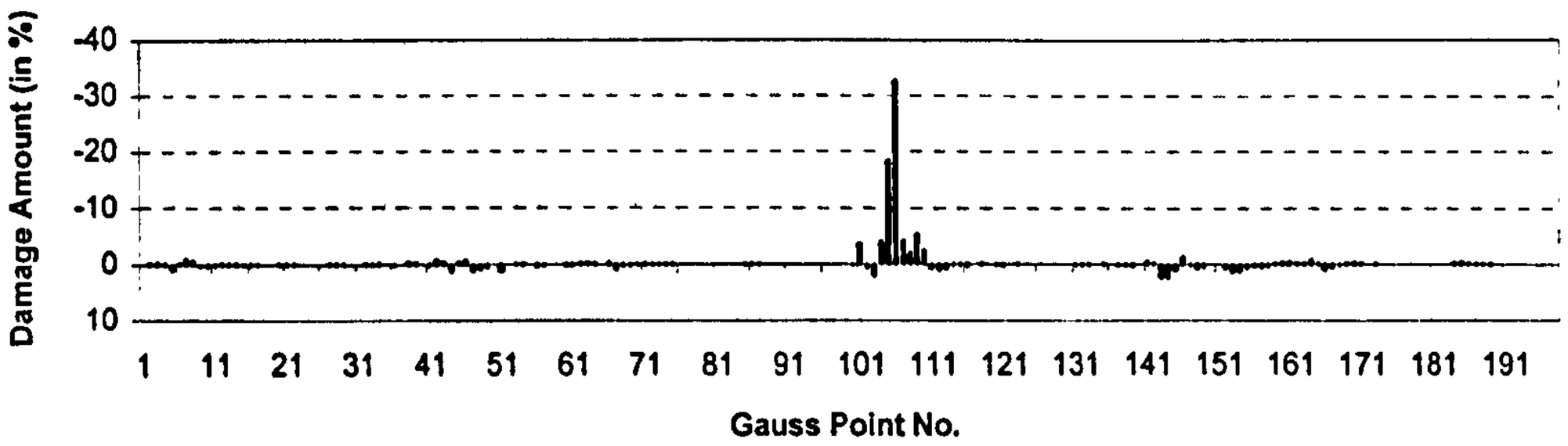

Figure 6.18(b) Predicted damage for scenario 2

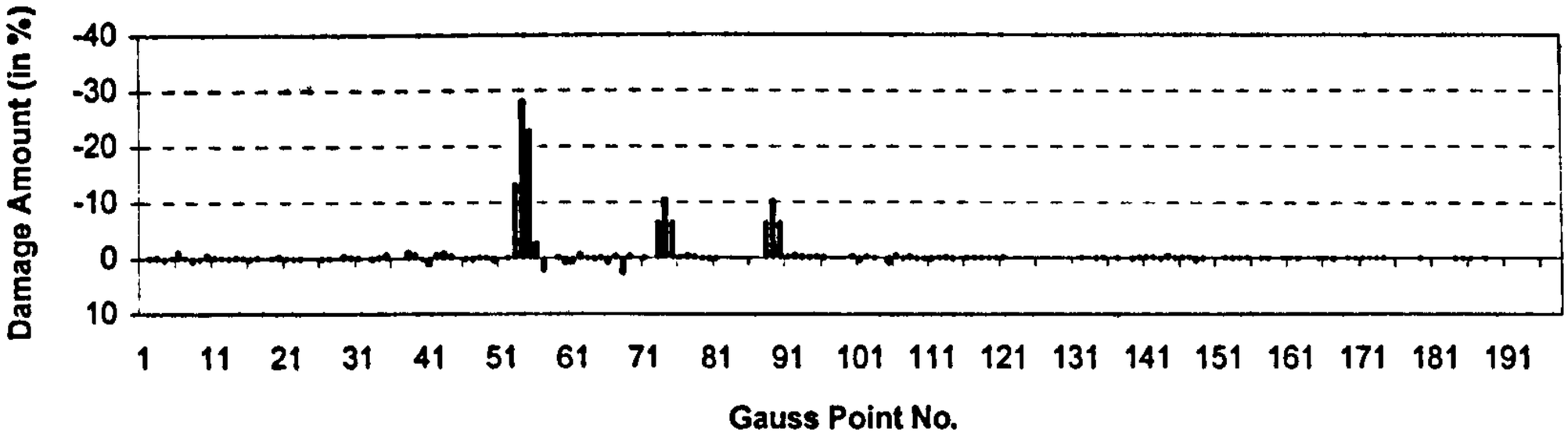

Figure 6.18(c) Predicted damage for scenario 3

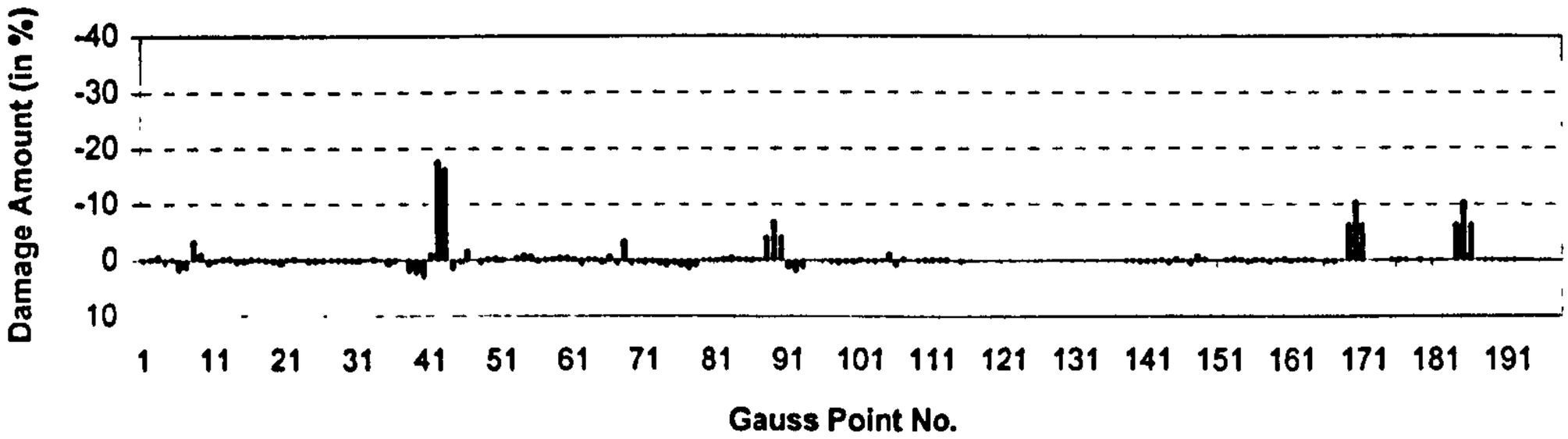

Figure 6.18(d) Predicted damage for scenario 4

Figure 6.18 Inverse damage predictions for different damage scenarios at Gauss point level, information on incomplete damaged modes 1, 3, 5 and 6 with the sensor set used

6.10 Conclusions

Several computational techniques based on the characteristic equation for the damaged structure and non-linear perturbation analysis have been developed, which can properly identify both the location and the extent of structural damage, either in framed structures or in continua. Many distinct advantages have been highlighted.

1) A set of non-linear equations is developed using non-linear sensitivity analysis, which offers a promising approach to identify exactly structural damage directly using incomplete modal data.

2) Several computational techniques are proposed, and their effectiveness and convergence performance have been demonstrated using various numerical examples.

3) Only information about incomplete modal data with a limited number of DOF's readings is sufficient to determine damage in structures, even for symmetric structures.

4) The proposed approaches are capable of not only predicting the damage in a structure, but also can provide information on the exact expanded damaged mode shapes, even if a very limited DOF's readings are available.

Furthermore, it is found that the proposed approaches are significantly sensitive to the quality of the measured incomplete modal data for structural damage assessment, which is caused by the ill-conditioned system of governing equations.

CHAPTER 7

COMPARISON OF PROPOSED APPROACHES ON MODELLING PROBLEMS

A given structure may be considered by different types of structural models, and in turn the different types of elements adopted for a given structural model can be employed to carry out structural analysis and damage identification. Here, the same model problem, a cantilever beam, is utilised to investigate the effectiveness of the proposed approaches for different types of structural models using different types of structural elements, such as beam elements with an explicit stiffness matrix or a stiffness matrix obtained by numerical integration for one-dimensional beam problems, plane stress or plate bending elements for two-dimensional continuum problems, and three-dimensional solid brick elements for three-dimensional solid problems. The results obtained from different structural models indicate that structural damage can properly be identified using the proposed approaches.

7.1 Cantilever Beam Problem

A cantilever beam 5.0m in length, 0.5m in width and height, respectively, shown in Figure 7.1, is adopted to investigate the effectiveness of the proposed approaches for different modelling problems. The material properties for the cantilever beam are elastic modulus E=3.2×10^{10}N/m^2, Poisson's ratio υ=0.15 and density ρ=2400kg/m^3. The geometry of the structure and the cross-section are also shown in Figure 7.1.

Since the cantilever beam shown in Figure 7.1 is a continuous solid structure, it can be considered in various ways, leading to a series of model problems, such as one-dimensional conventional or Timoshenko beam problem, two dimensional plate stress or plate bending problem, and three-dimensional solid problem. Consequently, structural analysis and damage identification for these model problems can be performed using the corresponding types of elements, such as conventional beam elements with explicit or numerically integrated stiffness, or Timoshenko beam elements for one-dimensional beam model problem, plane stress elements or plate

bending elements for two-dimensional continuum model problem, and solid brick elements for three-dimensional model problem.

A finite element analysis was performed for both the original and the damaged cases to calculate natural frequencies and mode shapes. The first 5 natural frequencies for the original structure for different model problems of the cantilever beam are listed in Table 7.1.

Table 7.1 First 5 original natural frequencies (Hz) for different model problems

Problem Idealisation	Element Type	Original Mode 1	2	3	4	5
1-D Beam	Explicit	11.7968	73.9319	207.0575	406.0334	672.2537
	Integrated	11.7968	73.9319	207.0578	406.0374	672.2820
	Timoshenko	11.7139	70.5350	186.7041	341.3871	524.4700
2-D Continuum	Plane Stress	11.7401	71.0200	182.6583	189.1143	348.1219
	Plate Bending	11.7263	70.5867	114.8138	186.7733	341.3830
3-D Solid	Solid Brick	11.7565[R]	71.1085[R]	120.3859	182.7632	189.3234[R]

R: Repeated frequency

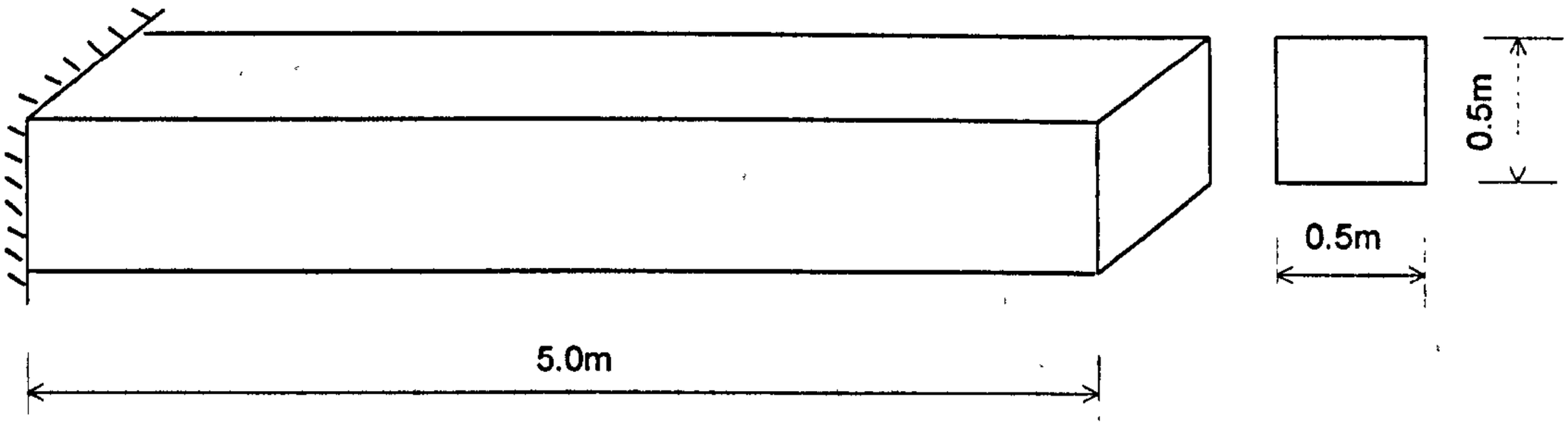

Figure 7.1 Cantilever beam used for different modelling problems

7.2 Modelling with Direct Conventional Beam Elements

The cantilever beam presented in Section 7.1 and shown in Figure 7.1 is now considered as an one-dimensional cantilever conventional beam problem as shown in Figure 7.2, where conventional beam elements with explicit stiffness are utilised. A finite element mesh with 10 conventional beam elements is generated. A hypothetical damage scenario with the reduced Young's modulus at some elements, and a set of selected sensors measuring only the vertical displacements at nodes marked with "•" are also shown in Figure 7.2.

The results in Figures 7.3(a) and (b) illustrate inverse predictions for the given damage scenario using 6 and 10 damaged frequencies, respectively. The **DI** technique using only damaged frequencies is employed for structural damage identification. It is found that a good estimate can be obtained using only 6 damaged frequencies, reaching an excellent result when 10 damaged frequencies are used.

In Figures 7.3(c) and (d), the results show inverse damage predictions from different sets of incomplete damaged modal data. Here, the **GNLS** technique with Procedure **MRF** using incomplete damaged modal data is employed to identify structural damage. It can be seen that structural damage can be determined correctly even if only three incomplete damaged modes are used.

Parameters of the Problem	
Total DOFs	20
Structural elements	10
Damage parameters	10

Hypothetical Damage Scenario

Element No	3	8
Damage Amount	-20%	-30%

Selected Sensor Scenario

Sensor Set: Measuring nodes marked with "•"

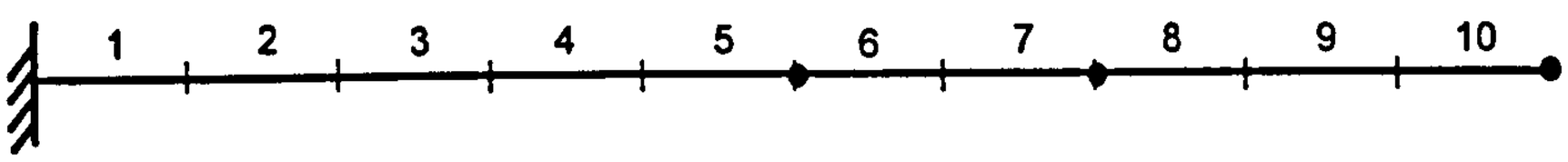

Figure 7.2 Cantilever beam modelled as conventional beam problem, conventional beam elements with explicit stiffness used

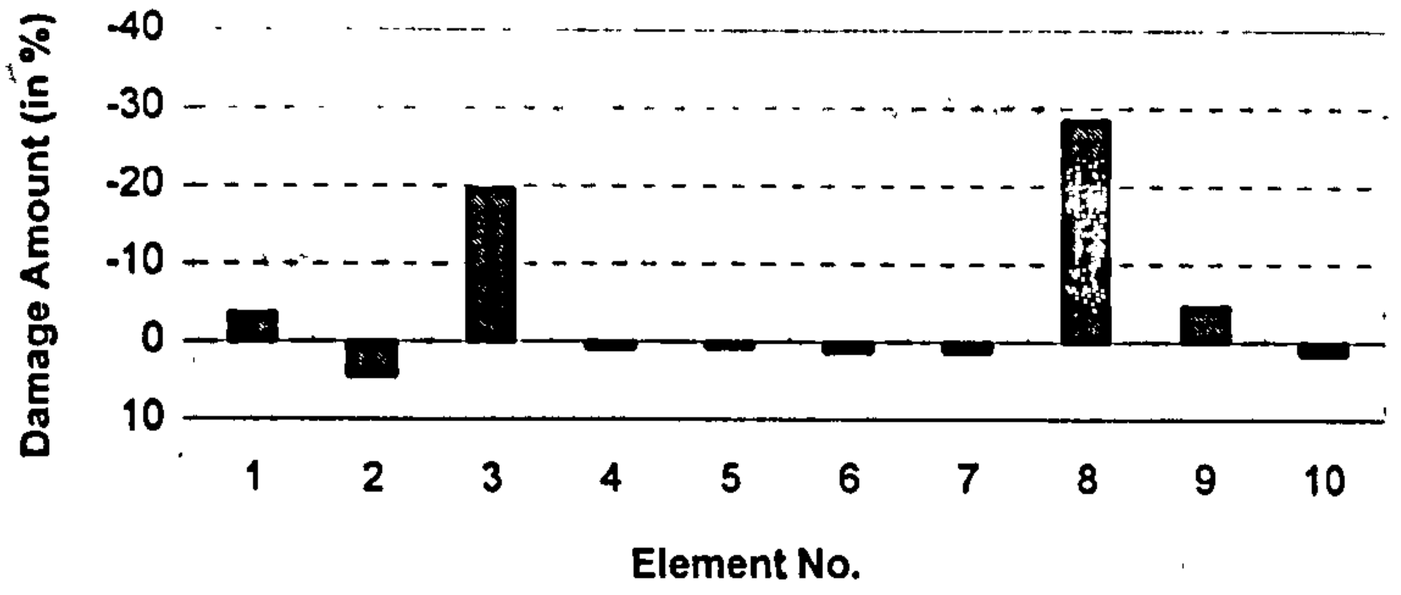

Figure 7.3(a) 6 damaged frequencies used, the **DI** technique employed

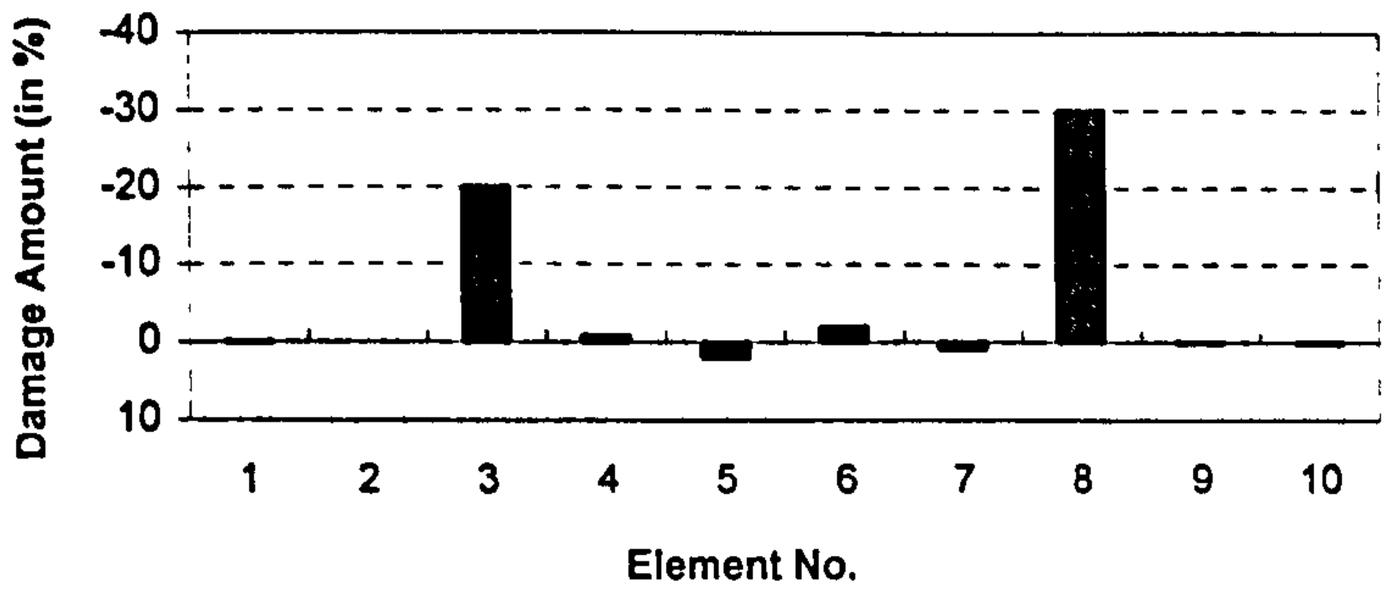

Figure 7.3(b) 10 damaged frequencies used, the **DI** technique employed

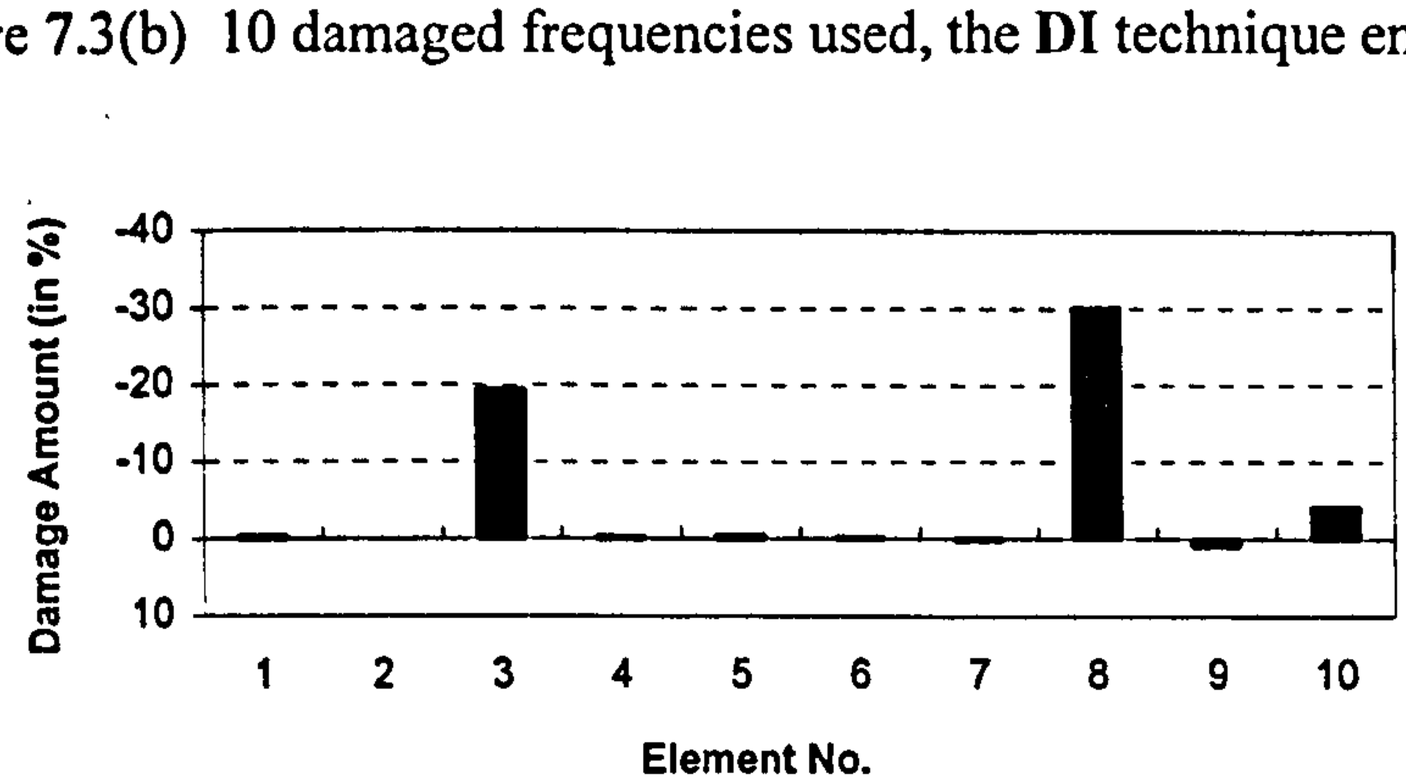

Figure 7.3(c) Incomplete damaged modes 1, 3, and 4 used, the **GNLS** technique employed

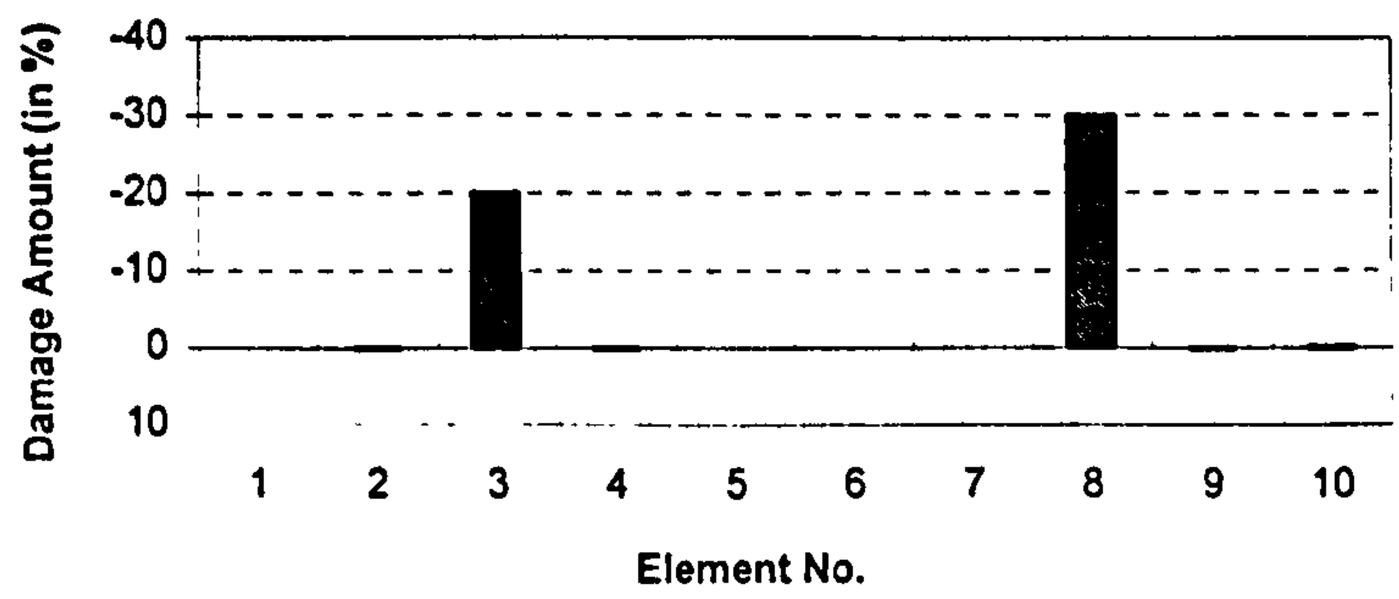

Figure 7.3(d) Incomplete damaged modes 1, 2, 3 and 4 used, the **GNLS** technique employed

Figure 7.3 Inverse damage predictions at element level using different types of modal data, conventional beam elements with explicit stiffness used

7.3 Modelling with Numerically Integrated Conventional Beam Elements

The cantilever beam shown in Figure 7.1 is considered as an one-dimensional cantilever conventional beam problem as shown in Figure 7.4, where conventional beam elements with numerically integrated stiffness adopting three Gauss integration points are employed. A finite element mesh with 10 conventional beam elements is generated. A hypothetical damage scenario with the reduced Young's modulus at some Gauss points, and a set of selected sensors measuring only the vertical displacements at nodes marked with "•" are also shown in Figure 7.4.

Figures 7.5(a) and (b) show the results for inverse predictions for the given damage scenario using 6 and 10 damaged frequencies, respectively. The **DI** technique using only damaged frequencies is employed for structural damage identification. It is found that structural damage can be located well, and the amount of structural damage is obviously distributed around the damaged points.

In Figures 7.5(c) and (d), the results show inverse damage predictions from different sets of incomplete damaged modal data. Here, the **GNLS** technique with Procedure **MRF** directly using incomplete damaged modal data is employed to identify structural damage. It can be seen that structural damage simulated at Gauss points can be determined properly using information about only a limited amount of incomplete modal data.

Parameters of the Problem	
Total DOFs	20
Structural elements	10
Gauss points	10×3=30
Damage parameters	30

Hypothetical Damage Scenarios

Element No	3	4	8
Gauss Point No	9	10	23
Damage Amount	-20%	-20%	-30%

Selected Sensor Scenario

Sensor Set: Measuring nodes marked with "•"

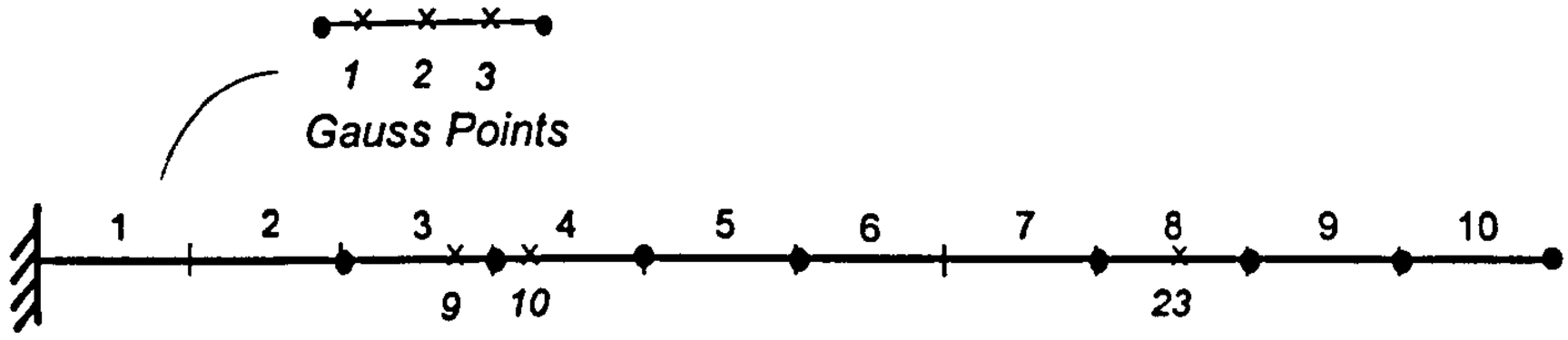

Figure 7.4 Cantilever beam modelled as conventional beam problem, conventional beam elements with numerically integrated stiffness used

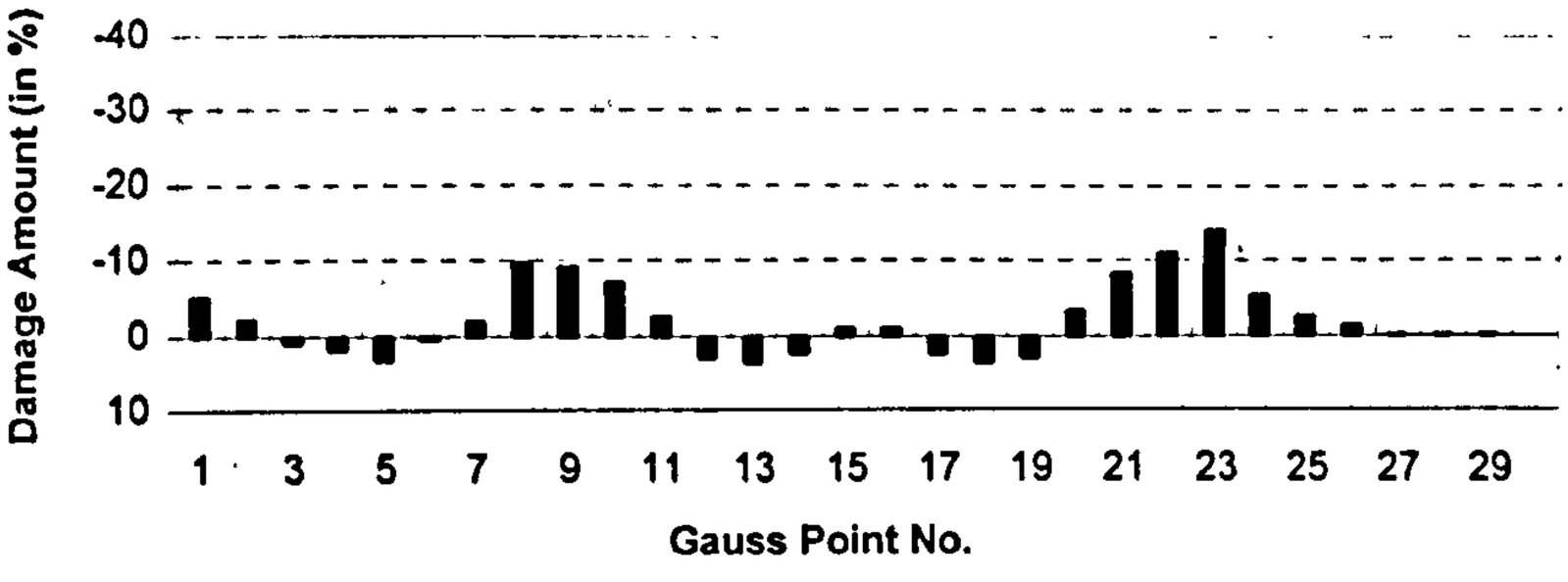

Figure 7.5(a) 6 damaged frequencies used, the **DI** technique employed

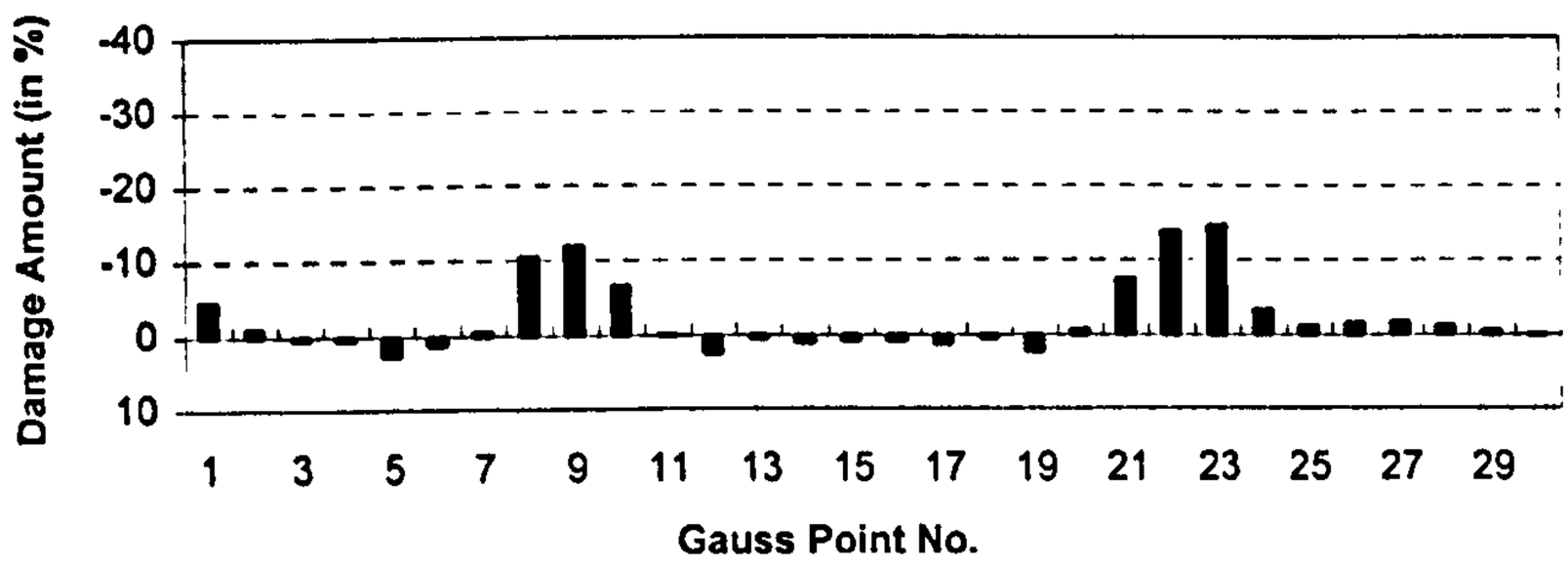

Figure 7.5(b) 10 damaged frequencies used, the **DI** technique employed

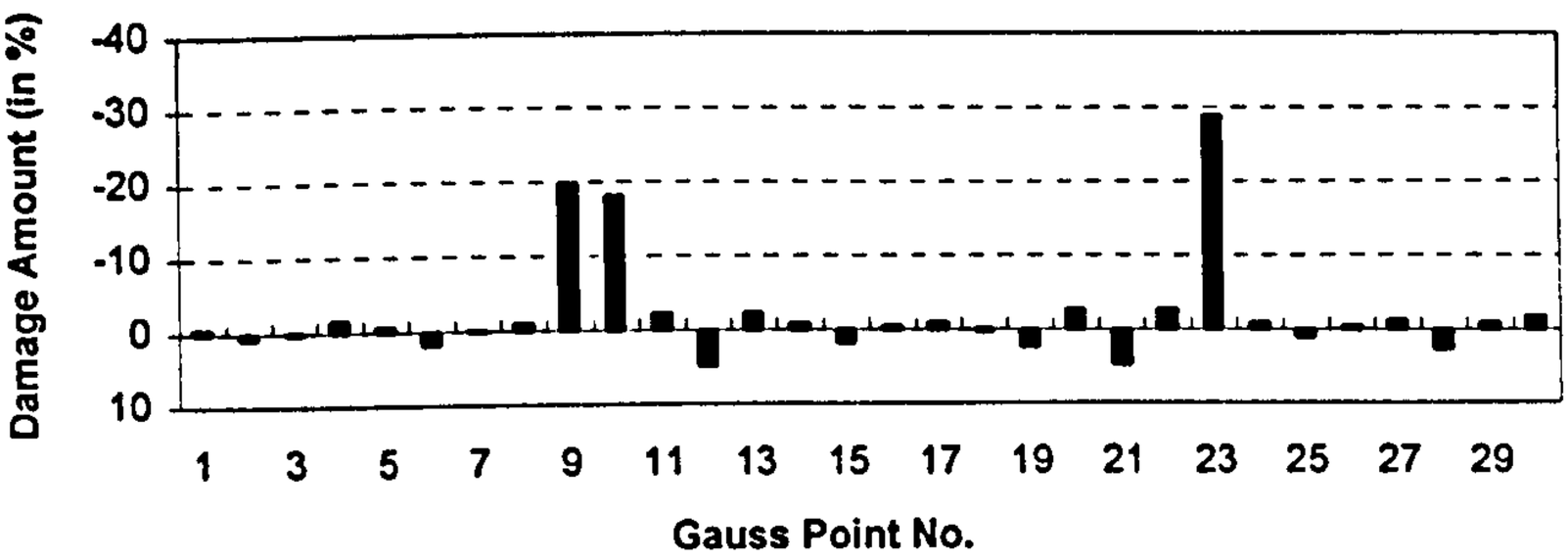

Figure 7.5(c) Incomplete damaged modes 1, 3 and 4 used, the **GNLS** technique employed

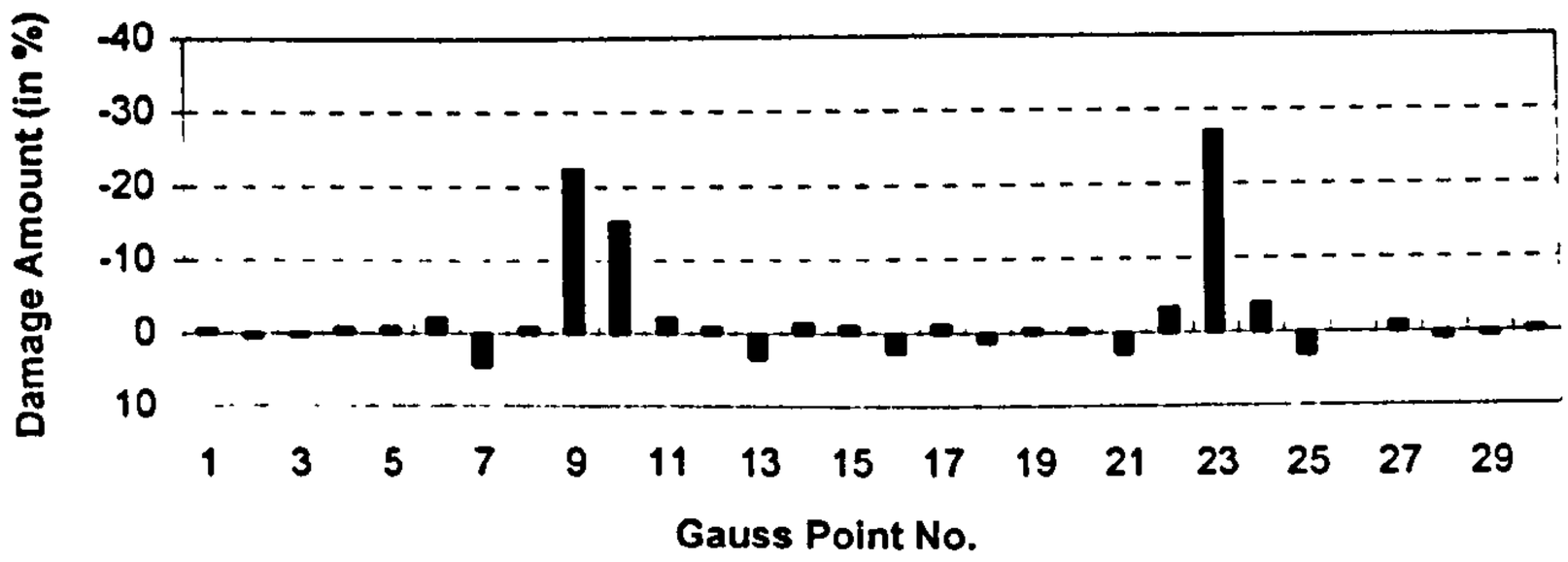

Figure 7.5(d) Incomplete damaged modes 1, 2, 3 and 4 used, the **GNLS** technique employed

Figure 7.5 Inverse damage predictions at Gauss point level using different types of modal data, conventional beam elements with numerically integrated stiffness used

7.4 Modelling with 3-Node Timoshenko Beam Elements

Here, the cantilever beam shown in Figure 7.1 is considered as an one-dimensional Timoshenko beam problem, as shown in Figure 7.6. A finite element mesh with 10 quadratic Timoshenko beam elements is generated, and three Gauss integration points for each element are adopted. A hypothetical damage scenario simulated by reducing the Young's modulus at some Gauss points, and a set of selected sensors measuring only the vertical displacements at nodes marked with "•" are also shown in Figure 7.6.

The results in Figures 7.7(a) and (b) show inverse predictions for the given damage scenario using 6 and 10 damaged frequencies, respectively. The **DI** technique using only damaged frequencies is employed for structural damage identification. It can be seen that the location of structural damage can be identified properly, and the extent of structural damage can also be found obviously around the damaged points.

Figures 7.7(c) and (d) show the results for inverse damage predictions from different sets of incomplete damaged modal data. Here, the **DI** technique directly using incomplete damaged modal data is employed to identify structural damage. It can be seen that excellent results are obtained using information about either three incomplete damaged modes or four incomplete damaged modes.

Parameters of the Problem

Total DOFs	20
Structural elements	10
Gauss points	10×3=30
Damage parameters	30

Hypothetical Damage Scenarios

Element No	3	4	8
Gauss Point No	9	10	23
Damage Amount	-20%	-20%	-30%

Selected Sensor Scenario

Sensor Set: Measuring nodes marked with "•"

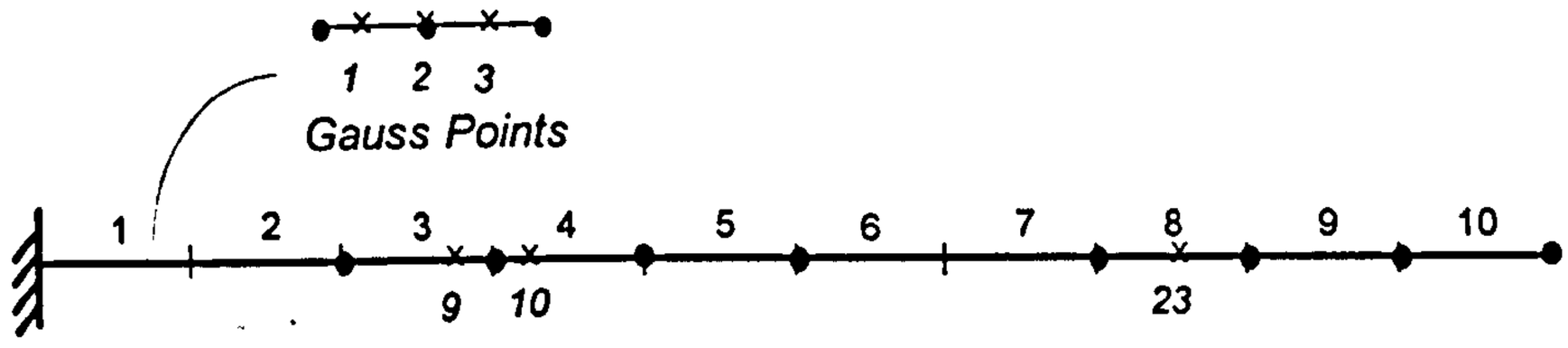

Figure 7.6 Cantilever beam modelled as Timoshenko beam problem, quadratic Timoshenko beam elements used

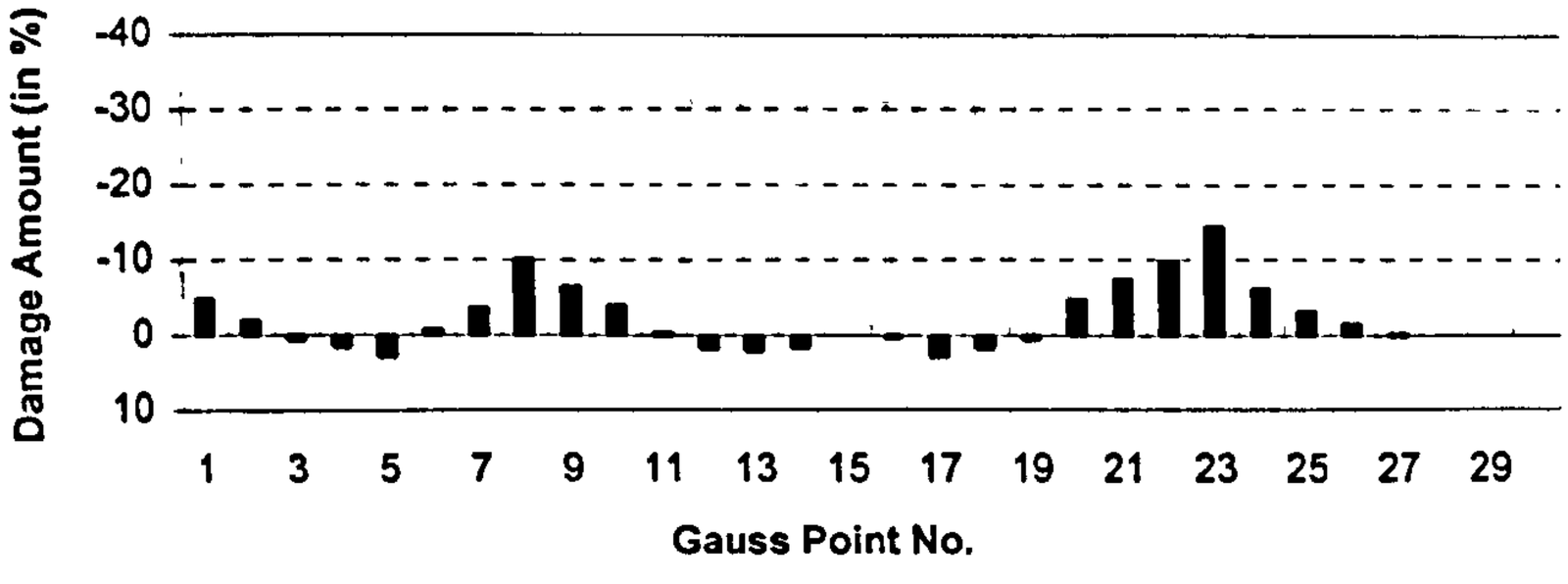

Figure 7.7(a) 6 damaged frequencies used, the **DI** technique employed

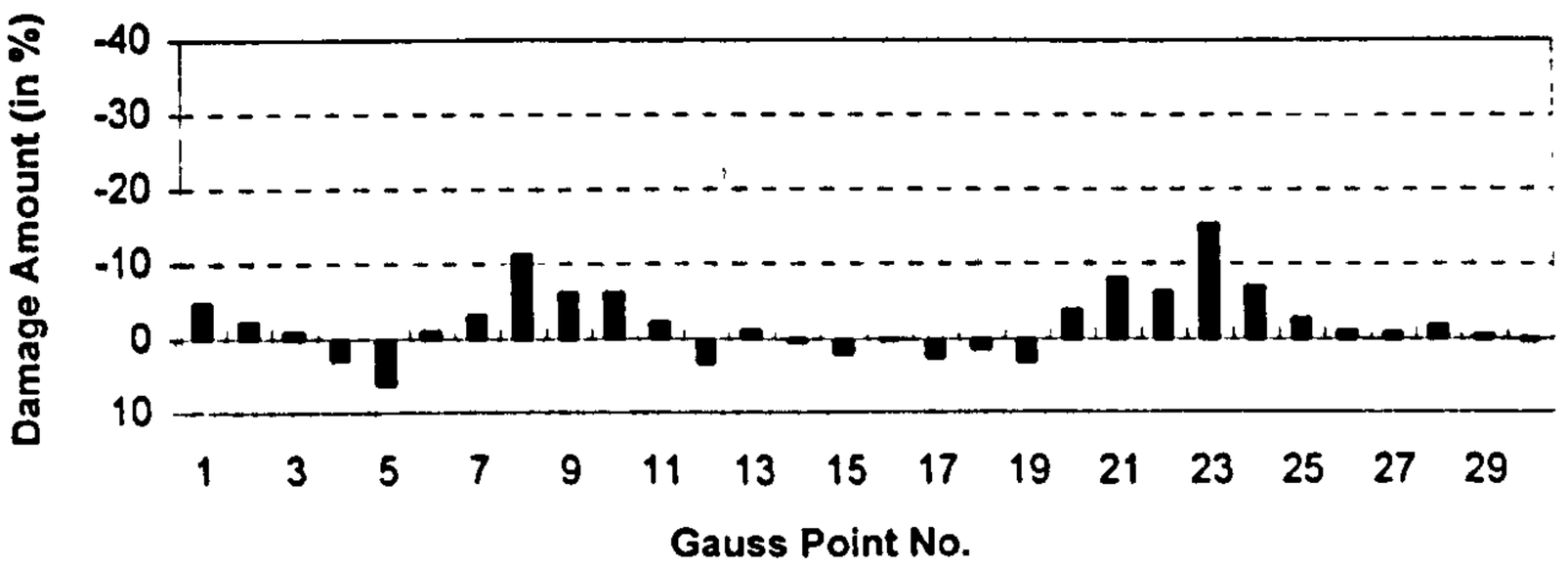

Figure 7.7(b) 10 damaged frequencies used, the **DI** technique employed

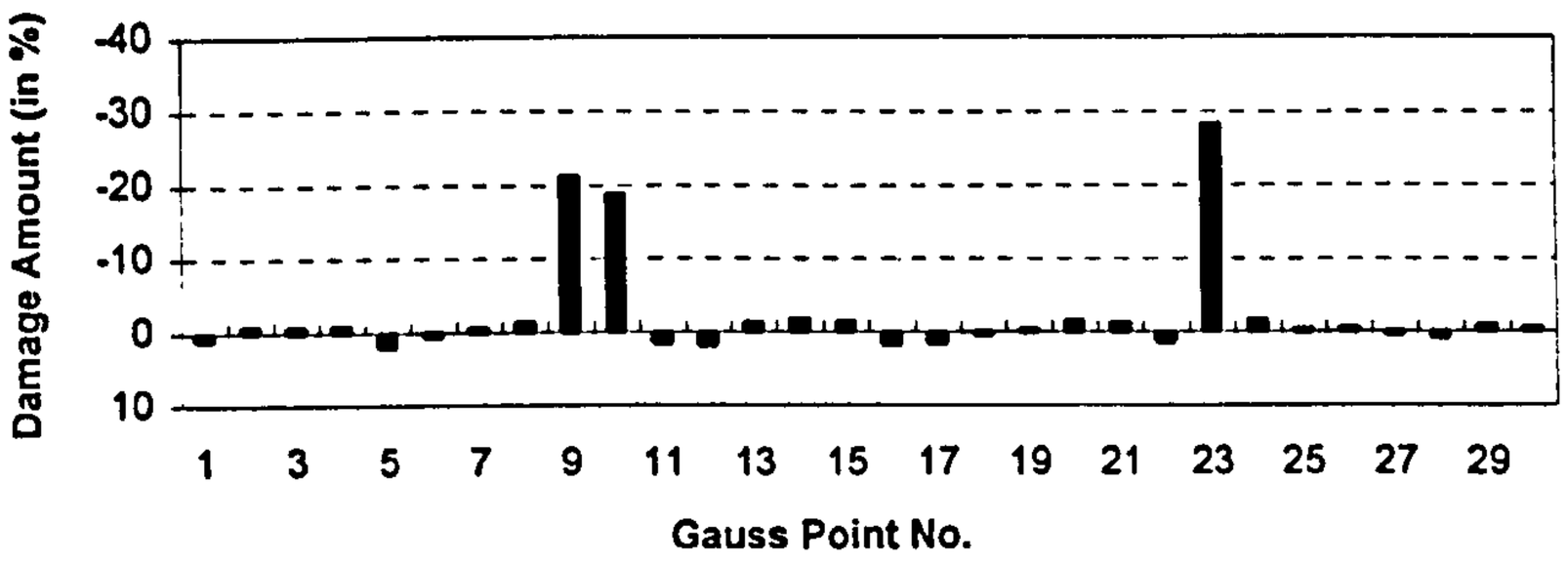

Figure 7.7(c) Incomplete damaged modes 1, 3 and 4 used, the **DI** technique employed

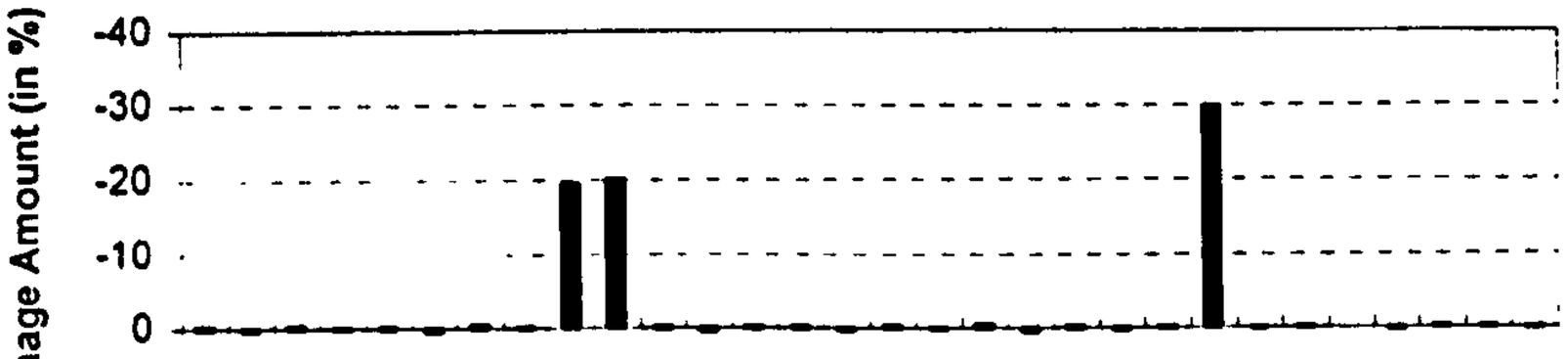

Figure 7.7(d) Incomplete damaged modes 1, 2, 3 and 4 used, the **DI** technique employed

Figure 7.7 Inverse damage predictions at Gauss point level using different types of modal data, quadratic Timoshenko beam elements used

7.5 Modelling with 8-Node Plane Stress Elements

The cantilever beam presented in Section 7.1 and shown in Figure 7.1 is now considered as a two-dimensional continuum problem, plane stress problem, as shown in Figure 7.8. A finite element mesh with ten 8-node isoparametric plane stress elements is generated, and 3×3 Gauss integration points for each element are adopted. A hypothetical damage scenario with the reduced Young's modulus at some Gauss points, and a set of selected sensors measuring the displacements at nodes marked with "•" are also shown in Figure 7.8.

The **DI** technique directly using incomplete damaged modal data is employed, and different combinations of three incomplete damaged modes are utilised to identify structural damage. From the results shown in Figures 7.9(a)–(d), it can be seen that very close predictions for the given damage scenario are obtained, and structural damage at Gauss points can be determined correctly, regardless of information about different combinations of incomplete damaged modes used.

Parameters of the Problem	
Total DOFs	100
Structural elements	10
Gauss points	10×9=90
Damage parameters	90

Hypothetical Damage Scenarios

Element No	3	4	8
Gauss Point No	27	30	68, 69
Damage Amount	-20%	-20%	-30%

Selected Sensor Scenario

Sensor Set: Measuring nodes marked with "•"

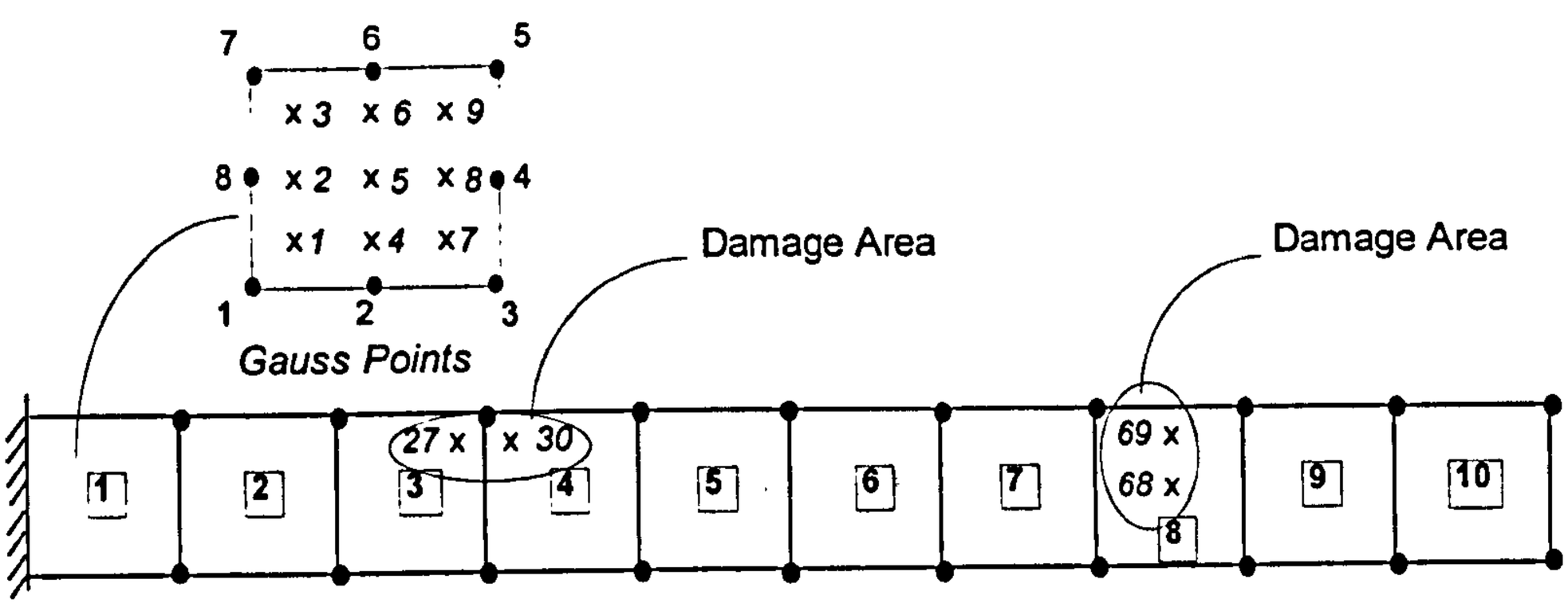

Figure 7.8 Cantilever beam modelled as plane stress problem, 8-node isoparametric plane stress elements used

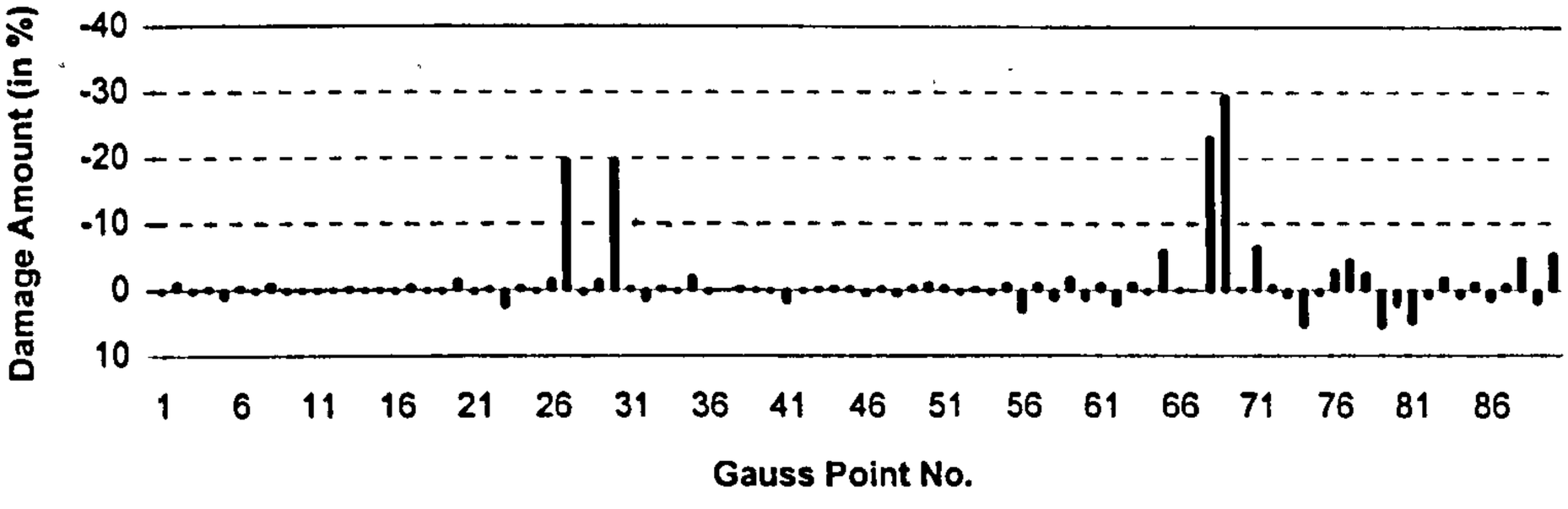

Figure 7.9(a) Incomplete damaged modes 1, 3, and 4 used

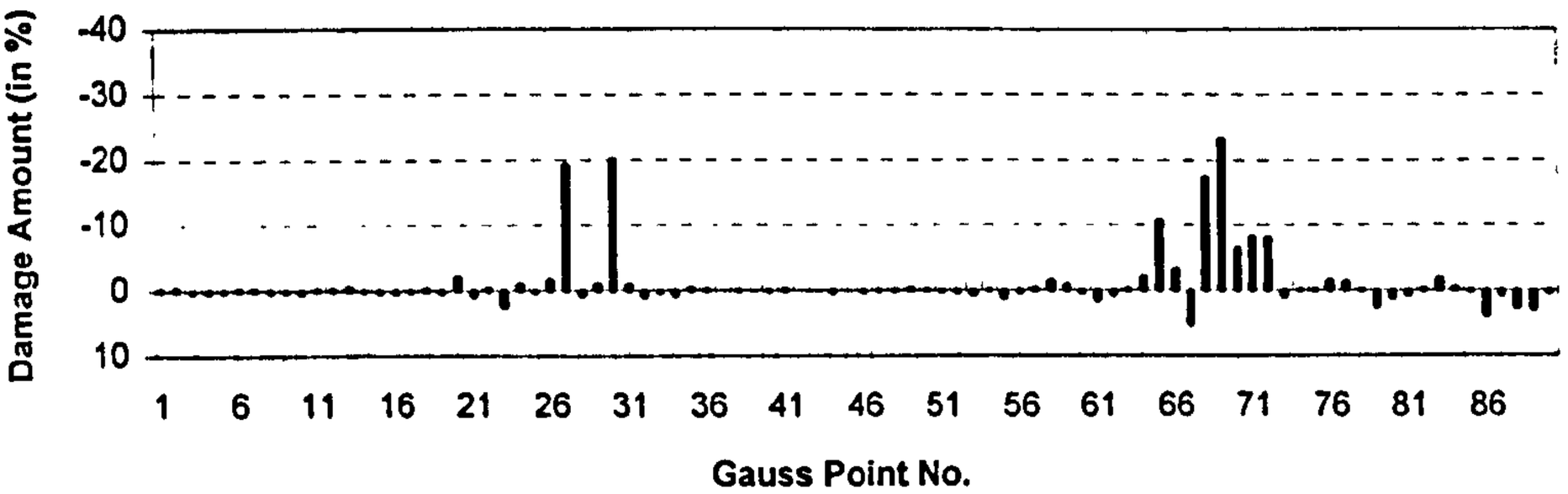

Figure 7.9(b) Incomplete damaged modes 1, 2, and 3 used

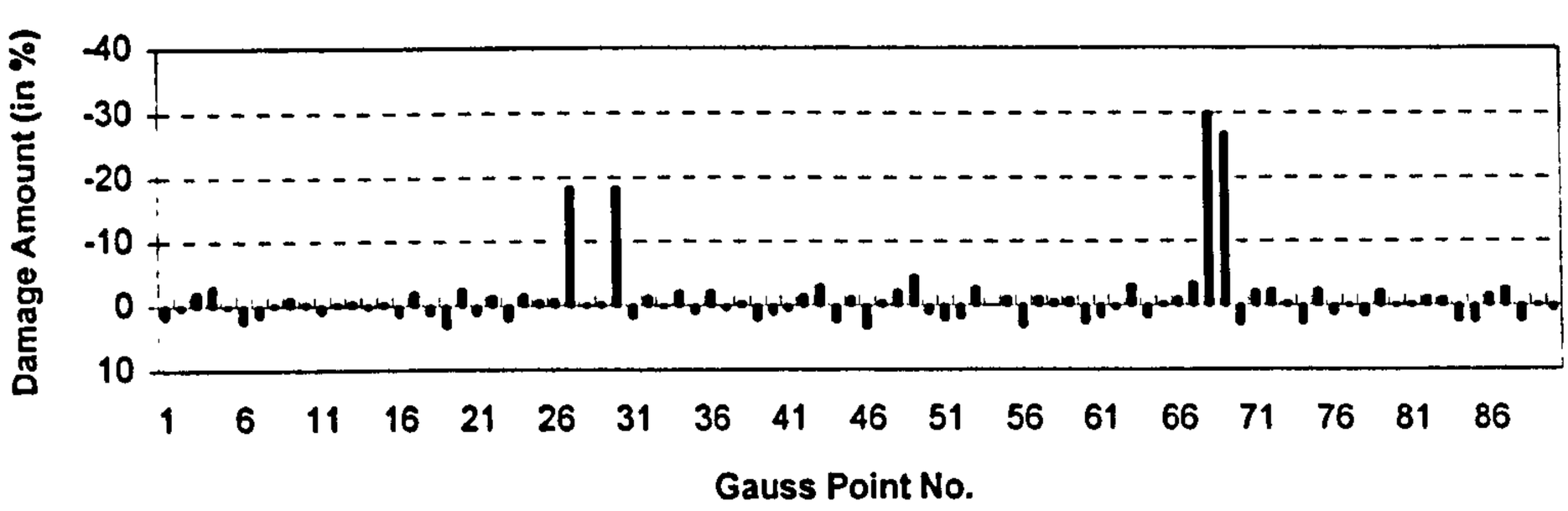

Figure 7.9(c) Incomplete damaged modes 2, 3, and 4 used

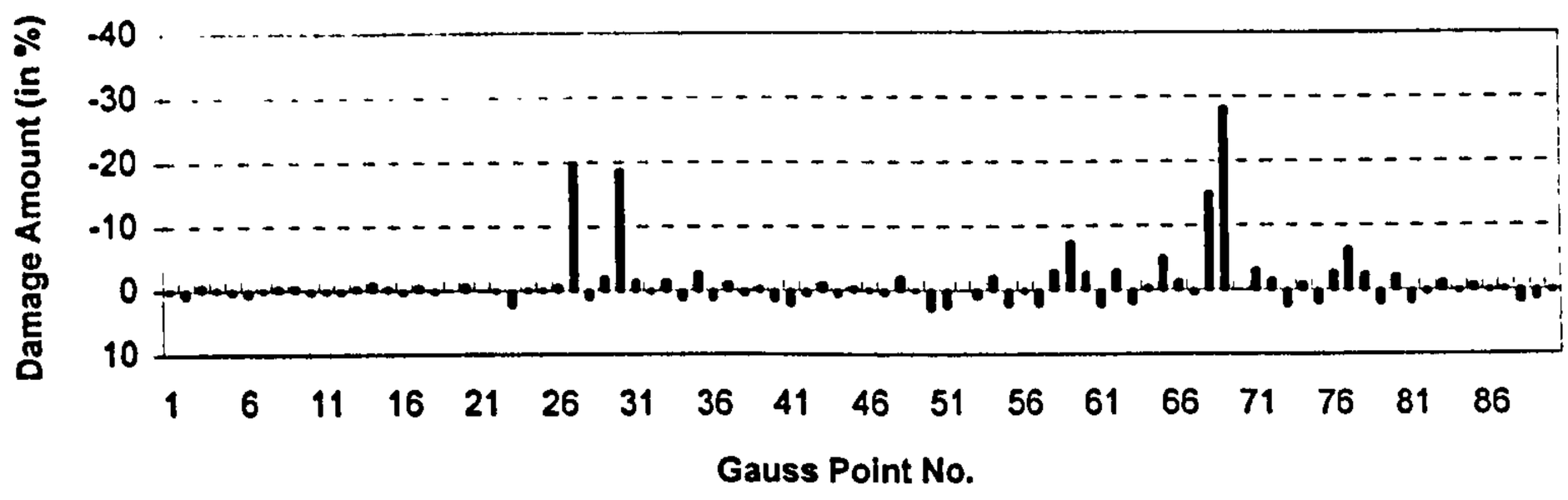

Figure 7.9(d) Incomplete damaged modes 1, 2, and 4 used

Figure 7.9 Inverse damage predictions using information on various incomplete damaged modes with the sensor set, 8-node isoparametric plane stress elements used

7.6 Modelling with 8-Node Plate Bending Elements

Now, the cantilever beam is considered as a plate bending problem as shown in Figure 7.10. A finite element mesh with ten 8-node isoparametric plate bending elements is generated, and 3×3 Gauss integration points for each element are adopted. A hypothetical damage scenario simulated by reducing the Young's modulus at some Gauss points, and a set of selected sensors measuring only the vertical displacements at nodes marked with "•" are also shown in Figure 7.10.

The **DI** technique directly using incomplete damaged modal data is employed, and different combinations of four incomplete damaged modes are utilised to identify structural damage. From the results shown in Figures 7.11(a)–(d), it can be seen that similar results for the given damage scenario are obtained, and structural damage at Gauss points can be predicted when information about different combinations of incomplete damaged modes is used. Some discrepancies existing in these results may be caused by insufficient original eigenvectors used, since the modes with high frequencies are in general difficult to be computed.

Parameters of the Problem	
Total DOFs	150
Structural elements	10
Gauss points	10×9=90
Damage parameters	90

Hypothetical Damage Scenarios

Element No	3	4	8
Gauss Point No	27	30	68, 69
Damage Amount	-20%	-20%	-30%

Selected Sensor Scenario

Sensor Set: Measuring nodes marked with "•"

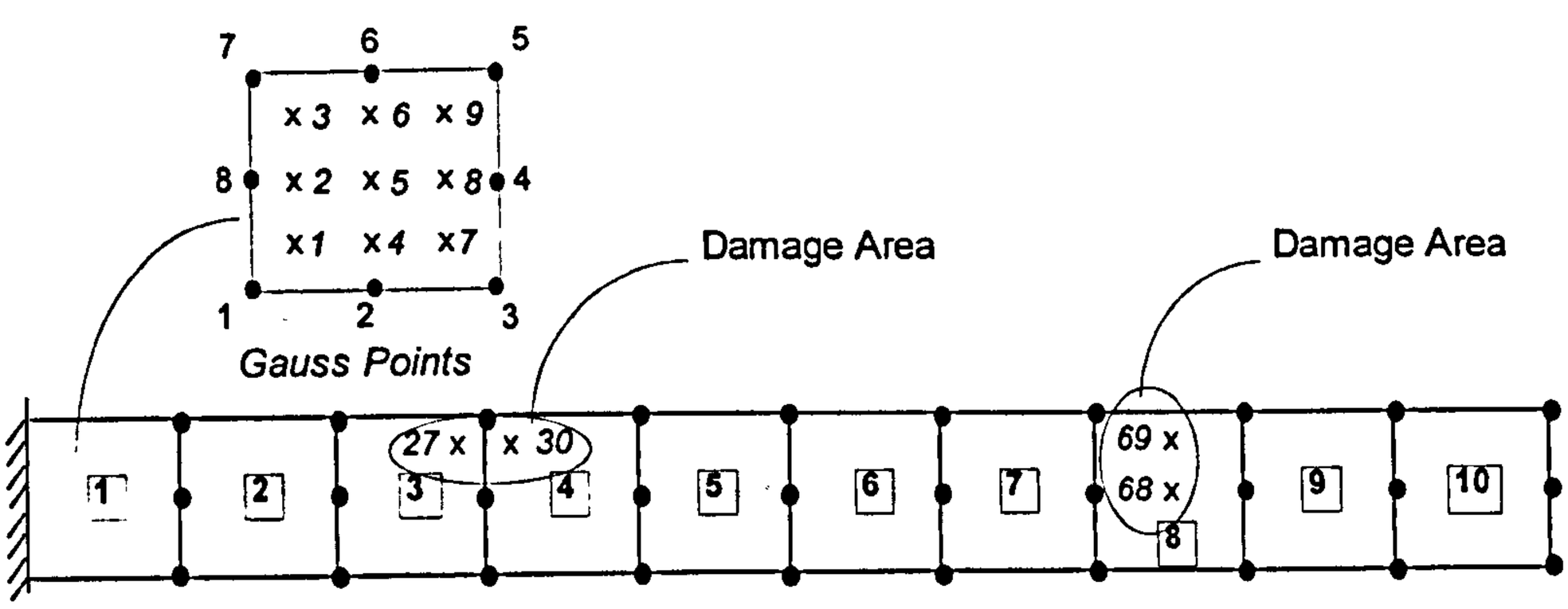

Figure 7.10 Cantilever beam modelled as plate bending problem, 8-node isoparametric plate bending elements used

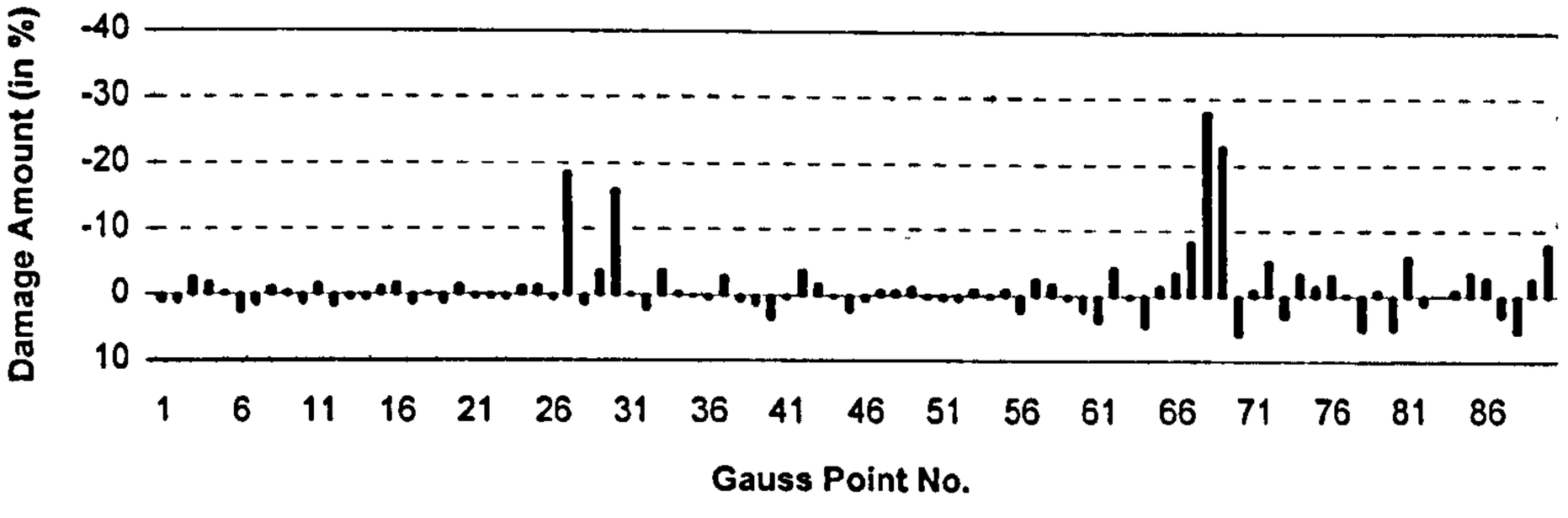

Figure 7.11(a) Incomplete damaged modes 1, 2, 3 and 4 used

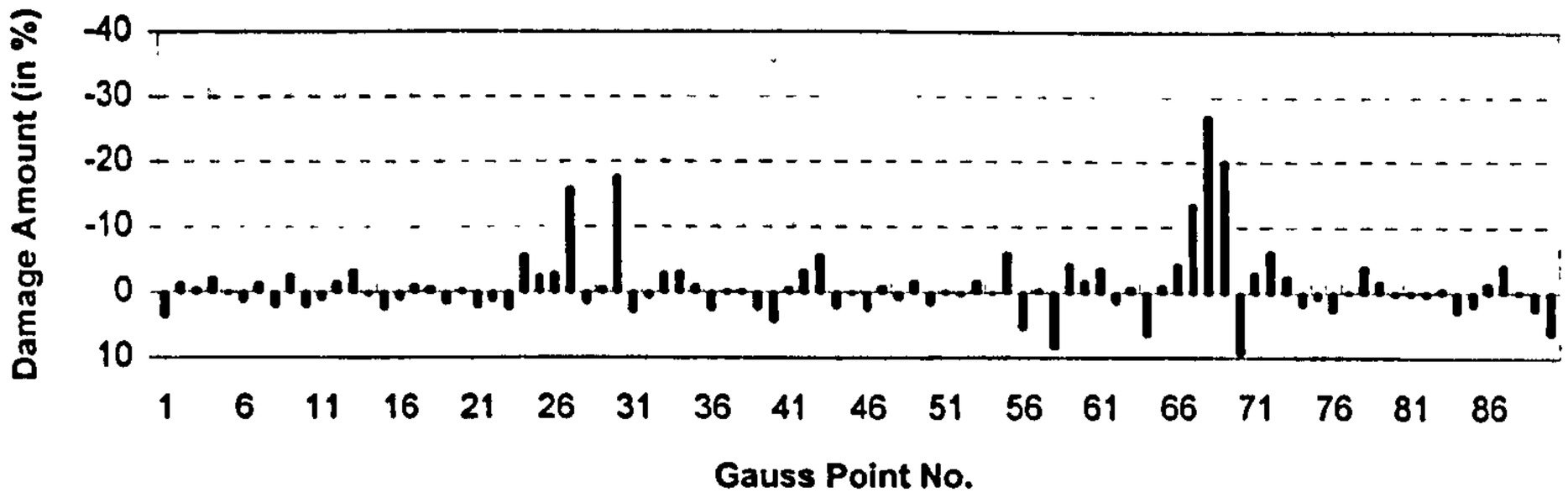

Figure 7.11(b) Incomplete damaged modes 1, 2, 4 and 5 used

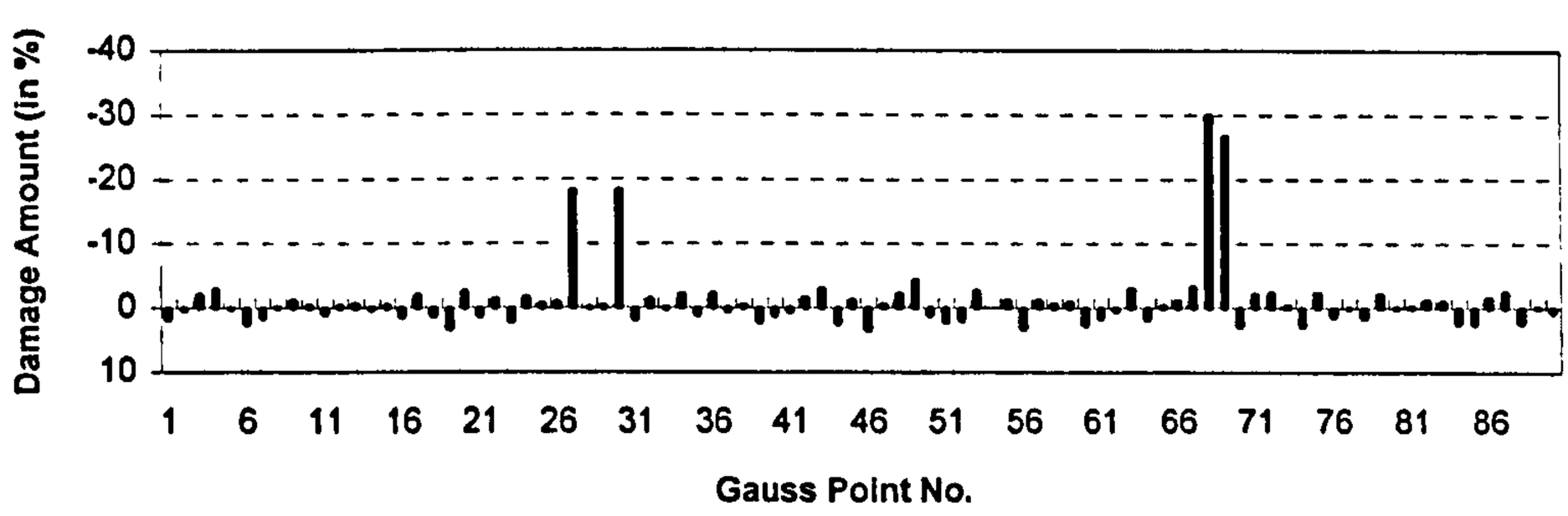

Figure 7.11(c) Incomplete damaged modes 1, 3, 4 and 5 used

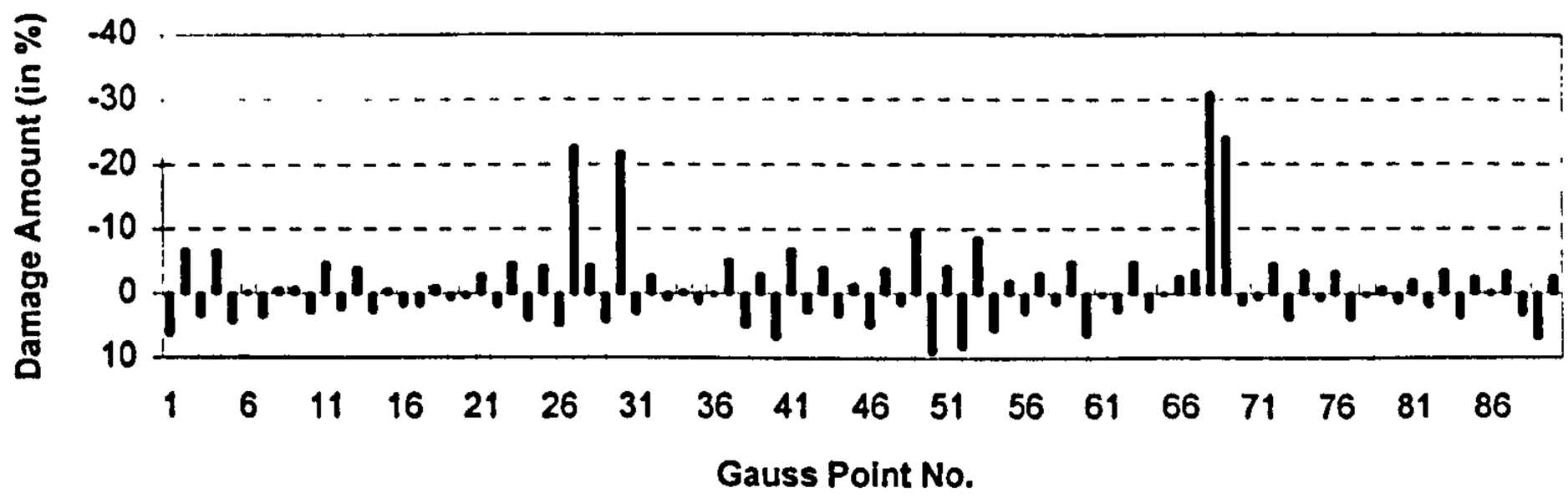

Figure 7.11(d) Incomplete damaged modes 2, 3, 4 and 5 used

Figure 7.11 Inverse damage predictions using information on various incomplete damaged modes with the sensor set, 8-node isoparametric plate bending elements used

7.7 Modelling with 20-Node Solid Brick Elements

Finally, the cantilever beam shown in Figure 7.1 is considered as a three-dimensional continuum problem, as shown in Figure 7.12. A finite element mesh with ten 20-node isoparametric solid brick elements is generated, and 3×3×3 Gauss integration points for each element are adopted. A hypothetical damage scenario with the reduced Young's modulus at some Gauss points, and a set of selected sensors measuring the displacements at nodes for elements 2–10 are also shown in Figure 7.12.

The **GNLS** technique with Procedure **MRE** directly using incomplete damaged modal data is employed, and information on various incomplete damaged modes is utilised to identify structural damage. From the results shown in Figures 7.13(a)–(d), it can be seen that similar results for the given damage scenario are obtained using information about different incomplete damaged modes. Furthermore, it is found that when DOF's readings for nodes near the damaged Gauss points are measured completely, inverse predictions for structural damage at these Gauss points are quite good, otherwise inverse predictions of structural damage may become poor, as shown in Figures 7.13(b). 7.13(c), and 7.13(d).

Parameters of the Problem

Total DOFs	360
Structural elements	10
Gauss points	10×27=270
Damage parameters	270

Hypothetical Damage Scenarios

Element No	2	3	8
Gauss Point No	51	60	201, 207
Damage Amount	-20%	-20%	-30%

Selected Sensor Scenario

Sensor Set: Measuring nodes for elements 2-10

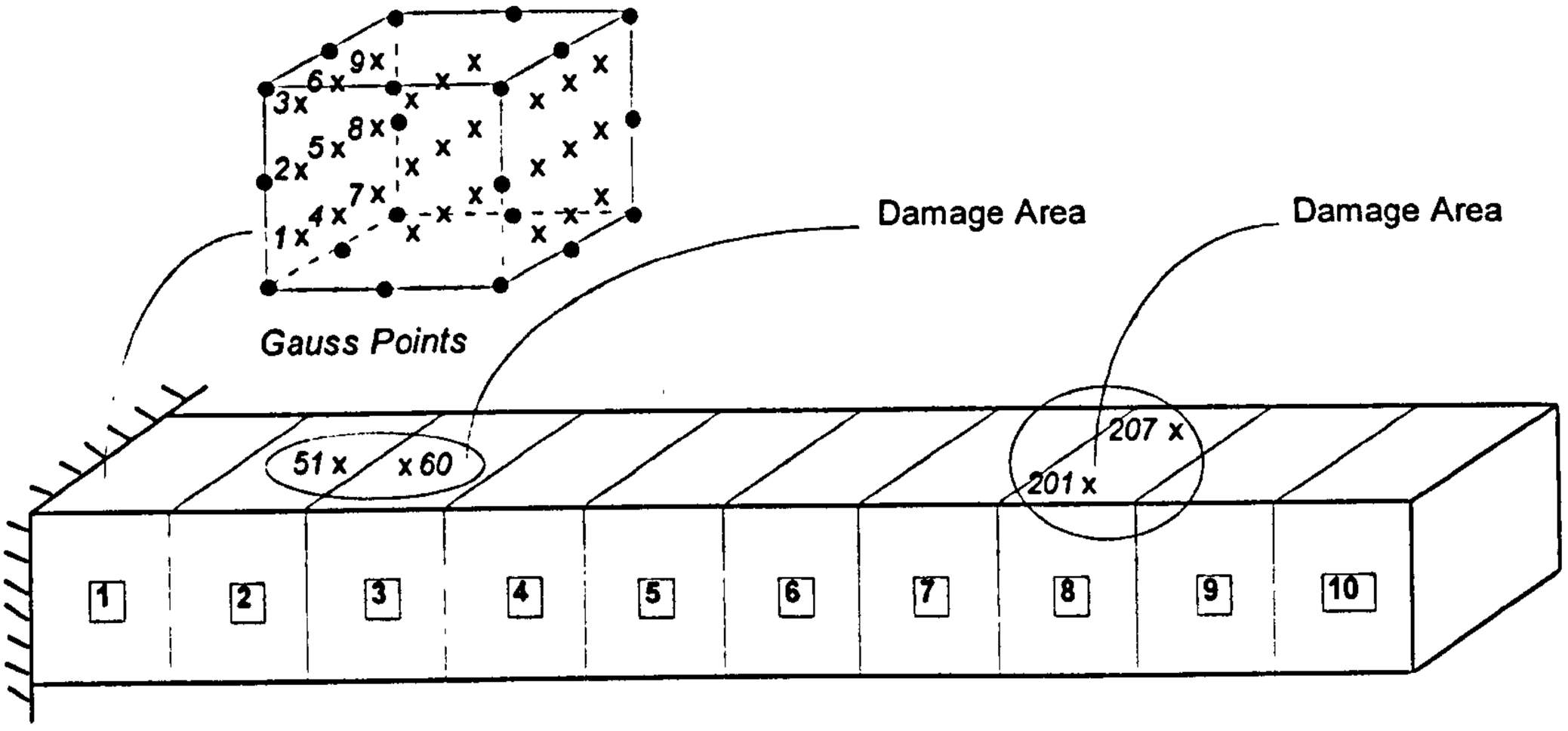

Figure 7.12 Cantilever beam modelled as 3-D solid problem, 20-node isoparametric solid brick elements used

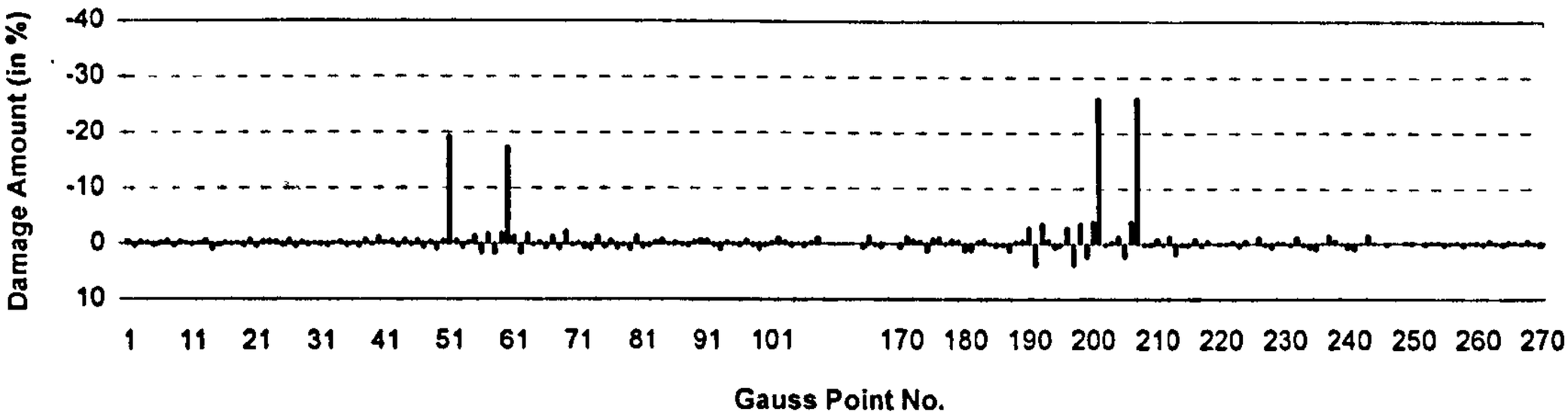

Figure 7.13(a) Incomplete damaged mode 1 used

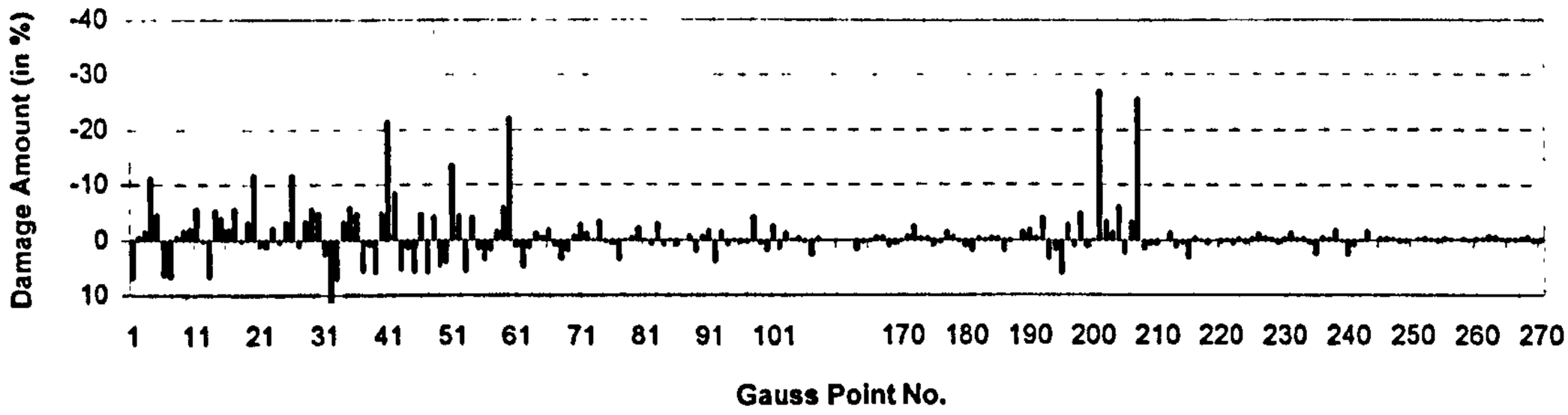

Figure 7.13(b) Incomplete damaged mode 2 used

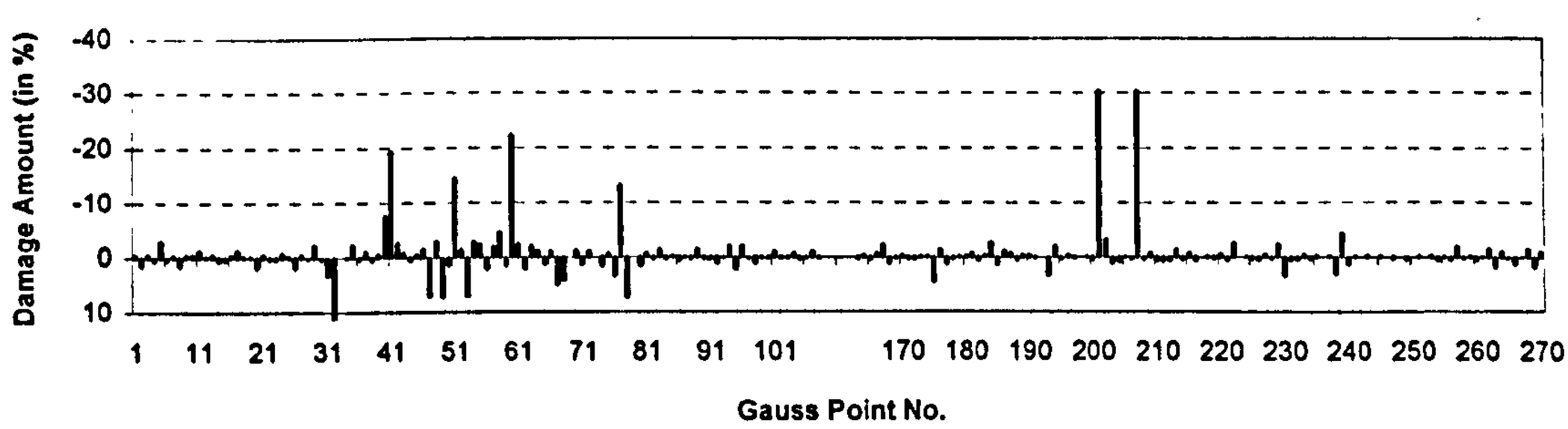

Figure 7.13(c) Incomplete damaged mode 3 used

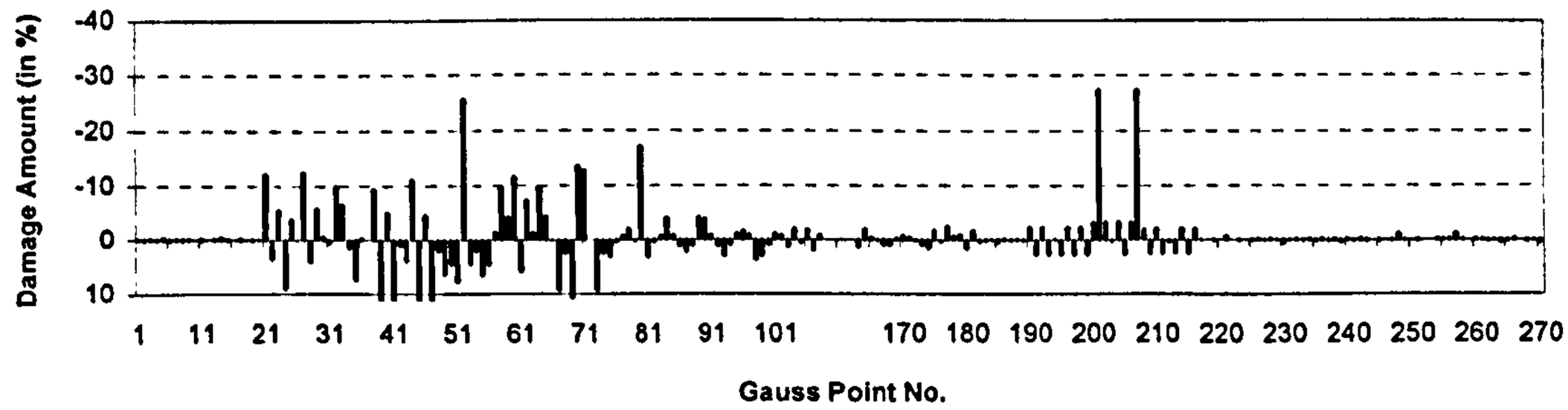

Figure 7.13(d) Incomplete damaged mode 5 used

Figure 7.13 Inverse damage predictions using information on various incomplete damaged modes with the sensor set, 20-node isoparametric solid brick elements used

7.8 Conclusions

The presented results show that the proposed approaches can be successful in not only using information about different types of damaged modal data, e.g., damaged natural frequencies and incomplete damaged mode shapes, but also in application to different levels of discretisation leading to different model problems for structural damage identification. Various structural models for a cantilever beam, such as one-dimensional beam models, two-dimensional continuum models, and three-dimensional solid model, were considered in turn. Different types of elements for the corresponding structural models, e.g., conventional beam element with explicit or numerically integrated stiffness, Timoshenko beam element, plane stress element, plate bending element, and solid brick element, are employed for structural analysis and damage identification for the cantilever beam. It is shown that both the location and the extent of structural damage simulated either at element level or at Gauss point level can be identified properly using information about the measured vibration modal data irrespective of which of the levels of idealisation is adopted, i.e. irrespective of the different models considered.

CHAPTER 8

CONCLUSIONS AND RECOMMENDATIONS

8.1 Remarks in Conclusion

The thesis was aimed at studying the detection, location, and quantification of structural damage using the measured vibration modal data. The particular aim has been to contribute to the knowledge in cases where structural damage can be identified correctly using various proposed approaches and information about only a limited amount of the measured modal data is required. The more significant conclusions are now summarised.

* The novel general governing equations based on the developed non-linear perturbation theory are capable of providing an exact relationship between the changes of structural parameters and modal parameters, which can be utilised for different types of structures (such as framed structures and continua) and for different purposes (such as eigendata modification, model updating and damage identification).

* When information about only one or two complete modes for the damaged structure is available, both the location and the extent of structural damage can be determined exactly using the proposed procedures. Furthermore, structural damage at a local area can be estimated correctly when information on only damaged DOF's readings completely measured at the local area is available.

* The proposed approaches, where information about only natural frequencies for the damaged structure is required, can be successful in not only predicting the location of damage but also in determining the extent of structural damage, even when only a limited number of damaged natural frequencies are adopted. Moreover, the proposed approaches are suitable for symmetric structures, if some methods are employed to desymmetrise these structures.

* Information about incomplete damaged modal data with only a limited number of DOF's readings is sufficient to determine damage in structure, when the proposed approaches directly using incomplete modal data are employed. In addition, the proposed approaches can provide information on the exact expanded damaged mode shapes, even if a very limited DOF's readings are available.

* Structural damage can be identified correctly from the proposed approaches using information about different types of the measured modal data, regardless of different discretisation levels or structural models considered and different types of elements used. Therefore, depending on information about the measured modal data, a suitable structural model could be selected in order to identify properly damage in structure.

Furthermore, the results also show that the proposed approaches are quite sensitive to the quality of the measured modal data for structural damage identification. The reason for this is due to the fact the developed governing equations for inverse damage predictions represent in general ill-conditioned systems.

8.2 Suggestions for Further Research

The presented theories and computational techniques for structural damage identification using the measured vibration modal data also offer some suggestions for future research. The suggestions that are considered most relevant are as follows.

* The effectiveness of the proposed approaches should be demonstrated by laboratory tests, large-scale tests, and finally full scale tests, which will make these approaches applicable to real engineering structures and provide an effective and reliable technique for structural damage identification.

* The high sensitivity to the quality of the measured modal data for identification of structural damage should be reduced at an acceptable level. Some methods for estimation of structural parameters might be introduced, such as maximum-likelihood estimation method, Bayesian estimation method, and the extended weighted least squares method (Natke and Cempel, 1997).

* An assessment of the current state of structural systems may be made objectively by the estimation of structural damage parameters and the modification of the structural systems, which can be obtained by the proposed approaches using measured vibration modal data.

* The integrity, reliability, safety, and future conditions of structural systems may be provided by model-based diagnosis using the knowledge of the current state and the resulting predictions, where structural model can be adjusted by structural damage parameter estimation obtained from routine monitoring and vibration measurements.

APPENDICES

A.1 Computer Program -- *SuDDen*

A FORTRAN computer program for **S**tructural **D**amage **D**etection – ***SuDDen*** has been developed based on the knowledge of computational procedures presented above. The details for the program, e.g., program structure, element types included, computational techniques adopted, and an example of input data, are introduced.

A.1.1 Program structure

The structure of the computer program ***SuDDen*** used for dynamic analysis and damage identification is summarised as shown in Figure A.1.

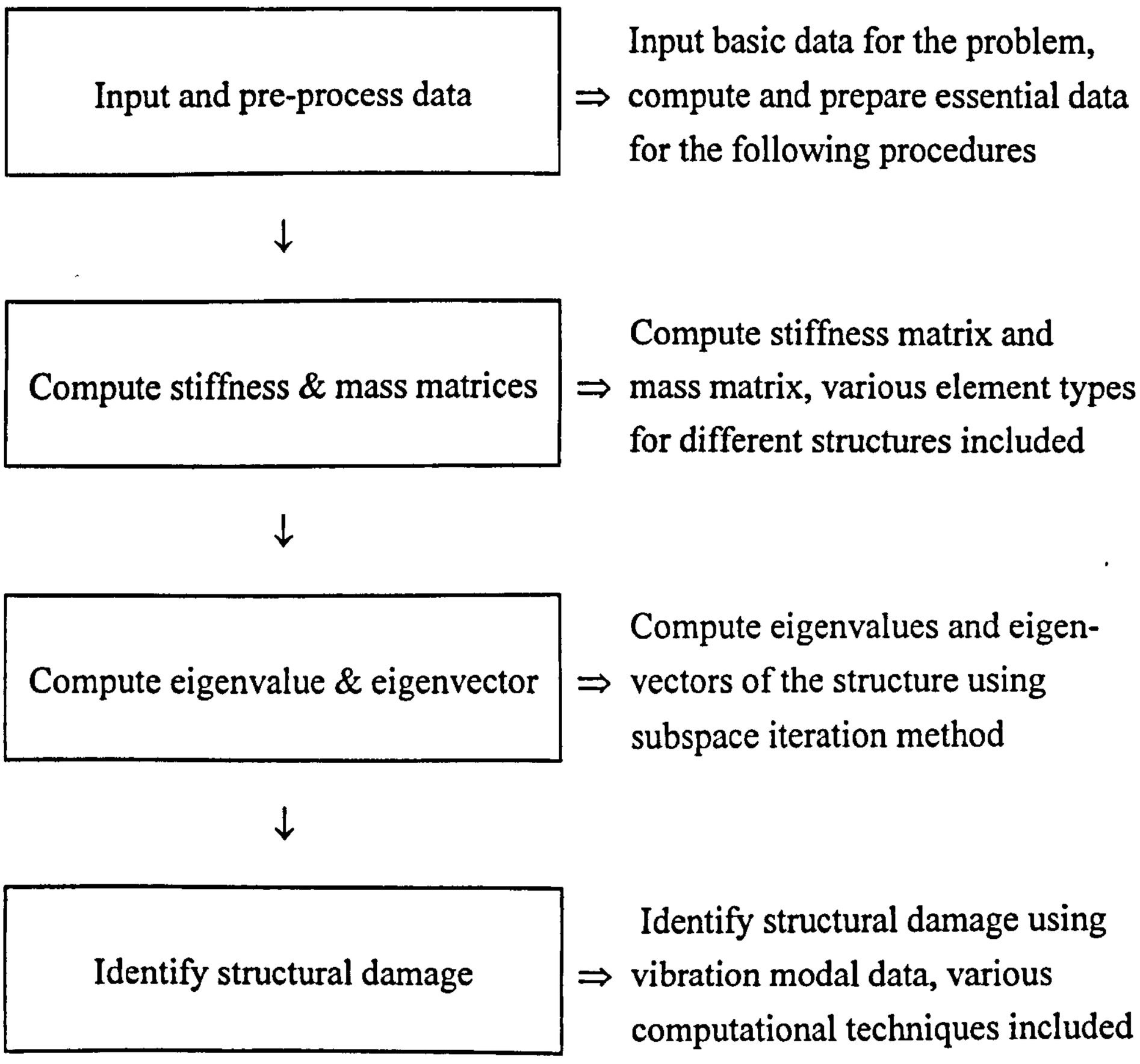

Figure A.1 Program organisation

A.1.2 Element types

A number of element types used for modelling different types of structures are included in the computer program, as listed in Table A.1.

Table A.1 Element types and their indices used in the program

SYMBOL	INDEX	ELEMENT TYPE
	DS1ND	01	1-NODE MASS SYSTEM
	PT2ND	11	2-NODE PLANE TRUSS
	ST2ND	12	2-NODE SPACE TRUSS
EXPLICIT	CB2ND	21	2-NODE CONVENTIONAL BEAM
STIFFNESS	PF2ND	22	2-NODE PLANE FRAME
	GD2ND	23	2-NODE GRID
	SF2ND	24	2-NODE SPACE FRAME
	SB2ND	25	2-NODE SHEAR BUILDING
	BG2ND	26	2-NODE BRIDGE GIRDER
	PT2NG	31	2-NODE CABLE (PLANE TRUSS)
	PT3NG	32	3-NODE CABLE (PLANE TRUSS)
	CB2NG	41	2-NODE CONVENTIONAL BEAM
	TB3NG	42	3-NODE TIMOSHENKO BEAM
INTEGRATED	PF2NG	43	2-NODE CONVENTIONAL FRAME
STIFFNESS	PF3NG	44	3-NODE TIMOSHENKO FRAME
	BG2NG	45	2-NODE BRIDGE GIRDER
	PS8NG	51	8-NODE PLANE STRESS
	PN8NG	52	8-NODE PLANE STRAIN
	PB8NG	61	8-NODE PLATE BENDING
	SB8NG	71	8-NODE 3-D SOLID BRICK
	SB20G	72	20-NODE 3-D SOLID BRICK

A.1.3 Computational techniques

Depending on information about the measured vibration modal data available, various computational techniques for structural damage identification are included in the program, as listed in Table A.2. The theories and computational procedures for these techniques have been presented in Chapters 4, 5, and 6.

Table A.2 Computational techniques and their indices used in the program

SYMBOL	INDEX	MODAL DATA NEEDED	COMPUTATIONAL TECHNIQUE
MSFMD	11	COMPLETE MODE	NO ITERATION, SVD
MSLMD	12	LOCAL COMPLETE	NO ITERATION, SVD
NFDIT	21	NATURAL FREQUENCY	DIRECT ITERATION
NFTSI	22	NATURAL FREQUENCY	TWO-STAGE ITERATION
NFGNT	31	NATURAL FREQUENCY	GAUSS-NEWTON LEAST SQ.
NFAEQ	32	NATURAL FREQUENCY	APPROXIMATE EQS, GNLS
NFNLO	61	NATURAL FREQUENCY	NONLINEAR OPTIMISATION
NFOIT	62	NATURAL FREQUENCY	OPTIM AND ITERATION
IMDIT	41	INCOMPLETE MODE	DIRECT ITERATION
IMDEG	42	INCOMPLETE MODE	DIRECT EIGEN-EQUATION
IMMRF	51	INCOMPLETE MODE	GNLS, PROCEDURE MRF
IMMRE	52	INCOMPLETE MODE	GNLS, PROCEDURE MRE
IMAEQ	53	INCOMPLETE MODE	APPROXIMATE EQS, GNLS
IMNLO	71	INCOMPLETE MODE	NONLINEAR OPTIMISATION
IMOIT	72	INCOMPLETE MODE	OPTIM AND ITERATION

A.1.4 Input data format

An example of the format for inputing data used for the computer program is given, which corresponds to the one-bay plane truss model problem, as shown in Figure 6.1, using the **GNLS** technique with Procedure **MRE** when information on incomplete modal data is available, as discussed in Section 6.3.3.

```
* ONE-BAY PLANE TRUSS, ELEMENT TYPE: 11, EXAMPLE S633; FILE: S633-b.DAT *

***NN,  NE, NDF, NNE, NBN, NCR, NPK, NPM  - Basic Data
    4,   6,   2,   2,   2,   0,   0,   0
*NPAU,NPAD, NPR, NGT, NGS  - Material, Geometry & Integration
    1,   5,   1,   0,   0
*NEVU,NEVD  - NO Of UnDamaged/Damaged Eigenvalues/Vectors
    5,   5

*IND,       X,       Y,       Z,  INC  - Node Coordinates
   1,      0.,      0.,      0.,    0
   2,    1.52,      0.,      0.,    0
   3,    1.52,    1.52,      0.,    0
   4,      0.,    1.52,      0.,    0

*IEL, NELTI, NON(IEL,NNE), INE, IND  - Element Types & Connections
   1,    11,      1,      4,   0,   0
   2,    11,      1,      2,   0,   0
   3,    11,      2,      3,   0,   0
   4,    11,      3,      4,   0,   0
   5,    11,      2,      4,   0,   0
   6,    11,      1,      3,   0,   0

*IPU,         E,      G/v,       RHO  - Undamaged Material Parameters
   1,  2.10E11,      0.3,    7800.0

*IPD,         E,      G/v,       RHO  - Damaged Material Parameters
   1,  2.10E11,      0.3,    7800.0
   2,  1.89E11,      0.3,    7800.0
   3,  1.68E11,      0.3,    7800.0
   4,  1.47E11,      0.3,    7800.0
   5,  0.21E11,      0.3,    7800.0

*IPR, NELTI,      A/t,   Iz,   Iy,   J,   Xp,   Yp,   Zp  - Geometry
   1,    11,  4.0E-4,

*IUO, IUN, INC, IPAU, IPRU  - Undamaged Material Types
   1,   6,   1,    1,    1

*IDO, IDN, INC, IPAD, IPRD  - Damaged Material Types
   1,   6,   1,    1,    1
   2,   2,   0,    2,    1
   3,   3,   0,    3,    1
   5,   5,   0,    4,    1
```

```
*IND, DOF1, DOF2, DOF3, DOF4, DOF5, DOF6  - Boundary (0: fixed, 1: free)
   1,     0,     0,     0
   4,     0,     1,     0

*MSDD,   NC,    NL, NOISE  - Basic Data for Structural Damage Detection
  52,    5,     5,     1

*NMODE, NNODE, NWEIT  - Control Data for MSDD 52
     3,     3,     1

*VNOIS  - Noise Level for Measured Modal Data if NOISE .NE. 0
0.00

*IP(NMODE,NNODE,NDF1)  - Data for Selected Modes (NMODE Sets)
*IMODE                 - Selected Mode No
     3,
*IND, DOF1, DOF2, DOF3  - Selected DOFs Reading (1-Known, 0-UNknown)
   2,     0,     1,
   3,     0,     0,
   4,     0,     0,
*IMODE                 - Selected Mode No
     1,
*IND, DOF1, DOF2, DOF3  - Selected DOFs Reading (1-Known, 0-UNknown)
   2,     0,     1,
   3,     1,     0,
   4,     0,     0,
*IMODE                 - Selected Mode No
     4,
*IND, DOF1, DOF2, DOF3  - Selected DOFs Reading (1-Known, 0-UNknown)
   2,     0,     1,
   3,     1,     1,
   4,     0,     0,
```

A.2 Element Stiffness and Mass Matrices

There are a total 21 element types as listed in Table A.1 adopted in the computer program, such as mass system element, plane and space truss elements, beam elements, cable-stayed bridge elements, plane stress/strain and plate bending elements, and solid brick elements. Some elements for framed structures may utilise Gauss integrations to compute their element stiffness matrices.

Elements with explicit stiffness for framed structures. The properties of elements and their explicit stiffness matrices and mass matrices for framed structures, such as element types DS1ND, PT2ND, ST2ND, CB2ND, PF2ND, GD2ND, SF2ND, and SB2ND, as listed in Table A.1, can be found in general textbooks for structural analysis or in Bathe's book (Bathe, 1996) in which the theory and computer program for subspace iteration method used for solving eigenproblems are also presented.

Elements with numerically integrated stiffness for framed structures. The element stiffness matrices and mass matrices for framed structures obtained from Gauss integrations, such as element types PT2NG, PT3NG, CB2NG, and PF2NG, as listed in Table A.1, are given in the book of Hinton and Owen (1985). The formulations for element stiffness matrices and mass matrices for 2-node linear axially-loaded rod element and 2-node conventional beam element are summarised as follows.

The shape functions for 2-node linear axially-loaded rod element are

$$N_{1u} = \tfrac{1}{2}(1-\xi) \tag{A.1a}$$

$$N_{2u} = \tfrac{1}{2}(1+\xi) \tag{A.1b}$$

and the shape functions for 2-node conventional beam element are

$$N_{1v} = \tfrac{1}{4}(2+\xi)(1-\xi)^2 \tag{A.2a}$$

$$N_{2v} = \tfrac{1}{4}(2-\xi)(1+\xi)^2 \tag{A.2b}$$

$$N_{1\theta} = \tfrac{1}{4}(1+\xi)(1-\xi)^2 \tag{A.2c}$$

$$N_{2\theta} = -\tfrac{1}{4}(1-\xi)(1+\xi)^2 \tag{A.2d}$$

Elements for cable-stayed bridge. Two different sets of element types, e.g., elements with explicit stiffness PT2ND and BG2ND, and elements with numerically integrated

stiffness PT2NG and BG2NG, can be utilised for a cable-stayed bridge. The details of elements used for a cable-stayed bridge are given in the work of Wang and Huang (1992). Here, the formulations employed in the computer program are outlined as follows.

For cables, an appropriate method for considering the nonlinearity in the inclined cable stays is to consider an equivalent straight member with an equivalent modulus of elasticity, i.e.,

$$E_{eq} = \frac{E_c}{1 + \dfrac{(wl_c)^2 E_c A}{12P^3}} \tag{A.3}$$

Where E_{eq} is the equivalent modulus of elasticity; E_c is the cable material modulus of elasticity; l_c is the horizontal projected length of the cable; w is the weight per unit length of the cable; A is the cross-sectional area; and P is the cable tensile force due to dead loads. Then, the element stiffness matrix for the cable can be computed using a standard 2-node linear axially-loaded rod element.

For girders, the element stiffness matrix can be computed from the sum of the standard linear stiffness matrix and the geometric stiffness matrix which represents the effect of axial force on the bending rigidity of the element and is expressed as follows,

$$k_{bg} = -\frac{P}{30l}\begin{bmatrix} 0 & 0 & 0 & 0 & 0 & 0 \\ 0 & 36 & 3l & 0 & -36 & 3l \\ 0 & 3l & 4l^2 & 0 & -3l & -l^2 \\ 0 & 0 & 0 & 0 & 0 & 0 \\ 0 & -36 & -3l & 0 & 36 & 3l \\ 0 & 3l & -l^2 & 0 & 3l & 4l^2 \end{bmatrix} \tag{A.4}$$

Where P is the axial force due to dead loads.

Elements for Timoshenko beam and continua. The properties of elements and their stiffness matrices and mass matrices for Timoshenko beam, plane stress/strain problems, plate bending problems, and solid structures, such as element types TB3NG, PF3NG, PS8NG, PN8NG, PB8NG, SB8NG, and SB20G, as listed in Table A.1, can be found in books, such as Hinton and Owen (1977), and Zienkiewicz and Taylor (1994).

A.3 Sensitivity of Element Stiffness and Mass Matrices

Here, the case of a general one-dimensional beam element with explicit stiffness and mass matrices is considered. The system parameters related to structural element stiffness and/or mass matrix in this case, such as Young's modulus E, mass density ρ, element length l, cross-sectional area A, and moment of inertia I, are characterised at element level. The sensitivity of the element level stiffness matrix and mass matrix to a variation in system parameter described above is given as follows.

The element stiffness matrix for a general one-dimensional beam can be rewritten as

$$K = \begin{bmatrix} k_{uu} & & & & & \\ 0 & 12k_{vv} & & & & \\ 0 & 6k_{v\theta} & 4k_{\theta\theta} & & & \\ -k_{uu} & 0 & 0 & k_{uu} & & \\ 0 & -12k_{vv} & -6k_{v\theta} & 0 & 12k_{vv} & \\ 0 & 6k_{v\theta} & 2k_{\theta\theta} & 0 & -6k_{v\theta} & 4k_{\theta\theta} \end{bmatrix} \tag{A.5}$$

where stiffness coefficients

$$\begin{aligned} k_{uu} &= EA/l \quad , & k_{vv} &= EI/l^3 \\ k_{v\theta} &= EI/l^2 \quad , & k_{\theta\theta} &= EI/l \end{aligned} \tag{A.6}$$

and the element mass matrix is rewritten as

$$M = \begin{bmatrix} \frac{1}{3}m_{uu} & & & & & \\ 0 & \frac{13}{35}m_{vv} & & & & \\ 0 & \frac{11}{210}m_{v\theta} & \frac{1}{105}m_{\theta\theta} & & & \\ \frac{1}{6}m_{uu} & 0 & 0 & \frac{1}{3}m_{uu} & & \\ 0 & \frac{9}{70}m_{vv} & \frac{13}{420}m_{v\theta} & 0 & \frac{13}{35}m_{vv} & \\ 0 & -\frac{13}{420}m_{v\theta} & -\frac{1}{140}m_{\theta\theta} & 0 & -\frac{11}{210}m_{v\theta} & \frac{1}{105}m_{\theta\theta} \end{bmatrix} \tag{A.7}$$

where mass coefficients

$$\begin{aligned} m_{uu} &= \rho Al \quad , & m_{vv} &= \rho Al \\ m_{v\theta} &= \rho Al^2, & m_{\theta\theta} &= \rho Al^3 \end{aligned} \tag{A.8}$$

Consequently, the coefficients of the sensitivity of element stiffness matrix $K_{,p}^{(e)}$ with respect to system parameters E, A, I, and l are listed in Table A.3.

Table A.3 Sensitivity coefficients of stiffness with respect to system parameters

	System Parameter			
Stiffness Coefficient	E	A	I	l
k_{uu}	A/l	E/l	0	$-EA/l^2$
k_{vv}	I/l^3	0	E/l^3	$-3EI/l^4$
$k_{v\theta}$	I/l^2	0	E/l^2	$-2EI/l^3$
$k_{\theta\theta}$	I/l	0	E/l	$-EI/l^2$

and the coefficients of the sensitivity of element mass matrix $M_{,p}^{(e)}$ with respect to system parameters ρ, A, and l are listed in Table A.4.

Table A.4 Sensitivity coefficients of mass with respect to system parameters

	System Parameter		
Mass Coefficient	ρ	A	l
m_{uu}	Al	ρl	ρA
m_{vv}	Al	ρl	ρA
$m_{v\theta}$	Al^2	ρl^2	$2\rho Al$
$m_{\theta\theta}$	Al^3	ρl^3	$3\rho Al^2$

REFERENCES

Abraham, M. A., Park, S., and Stubbs, N., (1995), "Loss of Prestress Prediction Based on Nondestructive Damage Location Algorithms", *Proceedings of SPIE - The International Society for Optical Engineering*, **2446**, 60-67.

Adelmam, H. M. and Haftka, R. T., (1986), "Sensitivity Analysis of Discrete Structural Systems", *AIAA Journal*, **24**(5), 823-832.

Afolabi, D., (1987), "An Anti-Resonance Technique for Detecting Structural Damage", *Proceedings of the 5th International Modal Analysis Conference*, London, 491-495.

Agbabian, M. S., Masri, S. F., Miller, R. K., and Caughey, T. K., (1988), "A System Identification Approach to the Detection of Changes in Structural Parameters", *Proceedings of Workshop Structural Safety Evaluation Based on System Identification Approaches*, Natke and Yao (Eds), Vieweg, 341-355.

Akgun, M. A., Ju, F. D., and Paez, T. L., (1985), "Transmissibility as a Means to Diagnose Damage in Structures", *Proceedings of the 3rd International Modal Analysis Conference*, Orlando, FL., 701-707.

Akgun, M. A. and Ju, F. D., (1990), "Damage Diagnosis in Frame Structures with a Dynamic Response", *Mechanics of Structures and Machines*, **18**(2).

Alampalli, S., Fu, G., and Aziz, I. A., (1992), "Modal Analysis as a Bridge Inspection Tool", *Proceedings of the 10th International Modal Analysis Conference*, San Diego, California, 1359-1366.

Arkadan, A. A., Sareen, T., and Subramaniam, S., (1994), "Genetic Algorithms for Nondestructive Testing in Crack Identification", *IEEE Transactions on Magnetic*, **30**(6), 4320-4322.

Baruch, M. and Bar Itzhack, Y., (1978), "Optimal Weighted Orthogonalisation of Measured Modes", *AIAA Journal*, **16**(4), 346-351.

Baruh, H. and Ratan, S., (1993), "Damage Detection in Flexible Structures", *Journal of Sound and Vibration*, **166**(1), 21-30.

Bathe, K. J., (1996), *Finite Element Procedures*, Prentice Hall, Englewood Cliffs, New Jersey.

Beliveau, J. G., Cogan, S., Lallement, G., and Ayer, F., (1996), "Iterative Least-Squares Calculation for Modal Eigenvector Sensitivity", *AIAA Journal*, **34**(2), 385-391.

Berman, A. and Nagy, E. J., (1983), "Improvement of a Large Analytical Model Using Test Data", *AIAA Journal*, **21**(8), 1168-1173.

Bernasconi, O. and Ewins, D. J., (1989), "Application of Strain Modal Testing to Real Structures", *Proceedings of the 7th International Modal Analysis Conference*, Las Vegas, NV, 1453-1464.

Bicanic, N. and Chen, H. P., (1997), "Damage Identification in Framed Structures Using Natural Frequencies", *International Journal for Numerical Methods in Engineering*, (in press).

Biswas, M., Pandey, A. K., and Bluni, S. A., (1994), "Modified Chain-Code Computer Vision Techniques for Interrogation of Vibration Signatures for Structural Fault Detection", *Journal of Sound and Vibration*, **175**(1), 89-104.

Biswas, M., Pandey, A. K., and Samman, M. M., (1990), "Diagnostic Experimental Spectral/Modal Analysis of a Highway Bridge", *Modal Analysis IJAEMA*, **5**(1), 33-42.

Brincker, R., Krenk, S., and Jensen, J. L., (1991), "Estimation of Correlation Functions by the Random Detection Technique", *Proceedings of the 9th International Modal Analysis Conference*, Florence, Italy.

Bucher, I. and Braun, S., (1993), "The Structural Modification Inverse Problem: An Exact Solution", *Mechanical Systems and Signal Processing*, **7**, 217-238.

Caesar, B. and Peter, J., (1987), "Direct Update of Dynamic Mathematical Models from Modal Test Data", *AIAA Journal*, **25**(11), 1494-1499.

Cawley, P. and Adams, R. D., (1979a), "The Location of Defects in Structures from Measurements of Natural Frequencies", *Journal of Strain Analysis*, **14** (2), 49-57.

Cawley, P. and Adams, R. D., (1979b), "A Vibration Technique for Non-Destructive Testing of Fibre Composite Structures", *Journal of Composite Materials*, **13**, 161-175.

Chen, H. P., (1997a), "Stress Singularities in Anisotropic Multi-Material Wedges and Junctions", *International Journal of Solids and Structures*, (in press).

Chen, H. P., (1997b), "*SuDDen* -- A Programme for Structural Damage Detection from Modal Data", *Internal report*, Department of Civil Engineering, Glasgow University.

Chen, H. P. and Bicanic, N., (1996a), "Identification of the Location and the Extent of Structural Damage from Modified Eigenvalues -- A Two-Stage Iterative Method", *Proceedings of the 4th ACME-UK* , Glasgow, 164-167.

Chen, H. P. and Bicanic N., (1996b), "Damage Identification in Statically Determinate Space Trusses Using Single Arbitrary Mode", *Proceedings of the 2nd International Structural Dynamics Modelling Conference*, *NAFEMS*, Cumbria, 357-363.

Chen, H. P. and Bicanic, N., (1997a), "Structural Damage Detection from Natural Frequencies", *Proceedings of the 5th ACME-UK* , London, 64-67.

Chen, H. P. and Bicanic, N., (1997b), "Structural Damage Assessment Using a Minimum of Measured Modal Data", *Mechanical Systems and Signal Processing*, (submitted for publication).

Chen, H. P. and Bicanic, N., (1997c), "Damage Identification of Continua from Vibration Modal Data", *Proceedings of the MRS 1997 Fall Meeting*, Boston, USA, 1997.

Chen, J. C. and Garba, J. A., (1980), "Analytical Model Improvement Using Modal Test Results", *AIAA Journal*, **18**(6), 648-690.

Chen, J. C. and Garba, J. A., (1988), "On-Orbit Damage Assessment for Large Space Structures", *AIAA Journal*, **26**(9), 1119-1126.

Chondros, T. G. and Dimarogonas, A. D., (1989), "Dynamic Sensitivity of Structures to Cracks", *Journal of Vibration, Acoustics, Stress, and Reliability in Design*, **111**, 251-256.

Cobb, R. G., Canfield, R. A., and Liebst, B. S., (1996), "Finite Element Model Tuning Using Automated Structural Optimisation System Software", *AIAA Journal*, **34**(2), 392-399.

Coppolino, R. N. and Rubin, S., (1980), "Detectability of Structural Failures in Offshore Platforms by Ambient Vibration Monitoring", *Proceedings of the 12th Offshore Technology Conference*, Huston, TX, Paper OTC 3865, 101-106.

DiPasquede, E., and Ju, J. W., (1990), "Relation Between Global Damage Indices and Local Stiffness Degradation", *Journal of Structural Engineering, ASCE*, **116**(5), 1440-1456.

Doebling, S. W., Hemez, F. M., Barlow, M. S., Peterson, L. D., and Farhat, C., (1993), "Selection of Experimental Modal Data Sets for Damage Detection via Model Update", *Collection of Technical Papers - AIAA/ASME Structures, Structural Dynamics and Materials Conference*, 1506-1517.

Ewins, D. J., (1984), *Modal Testing: Theory and Practice*, Research Studies, Lechworth, Hertfordshire, England.

Farhat, C. and Hemez, F. M., (1993), "Updating Finite Element Dynamic Models Using an Element-by-Element Sensitivity Methodology", *AIAA Journal*, **31**(9), 1702-1711.

Farrar, C. R., Baker, W. E., Bell, T. M., Cone, K. M., Darling, T. W., Duffey, T. A., and Migliori, A., (1994), "Dynamic Characterisation and Damage Detection in the I-40 Bridge Over the Rio Grande", *Technical report No. LA-12767-MS, UC-906*, Las Alamos National Laboratory, New Mexico, USA.

Farrar, C. R. and Cone, K. M., (1995), "Vibration Testing of the I-40 Bridge Before and After the Introduction of Damage", *Proceedings of the 13th International Modal Analysis Conference*, Nashville, TN, 203-209.

Foster, C. D. and Mottershead, J. E., (1990), "A Method for Improving Finite Element Models by Using Experimental Data: Application and Implications for Vibration Monitoring", *International Journal of Mechanical Sciences*, **32**(3), 191-203.

Fox, C. H. J., (1992), "The Location of Defects in Structures: A Comparison of the Use of Natural Frequency and Mode Shape Data", *Proceedings of the 10th International Modal Analysis Conference*, San Diego, California, 522-528.

Freed, A. M. and Flanigan, C. C., (1991), "A Comparison of Test-Analysis Model Reduction Methods", *Sound and Vibration*, 30-35.

Friswell, M. I. and Penny, J. E. T., (1992), "A Simple Nonlinear Model of a Cracked Beam", *Proceedings of the 10th International Modal Analysis Conference*, San Diego, California, 516-521.

Friswell, M. I. and Penny, J. E. T., (1994), "Using Vibration Data and Statistical Measures to Locate Damage in Structures", *Modal Analysis IJAEMA*, 9(4), 239-254.

Fritzen, C. P. and Zhu, S., (1991), "Updating of Finite Element Models by Means of Measured Information", *Computers and Structures*, **40**(2), 457-486.

Fritzen, C. P., Zhu, S., and Kiefer, T., (1990), "System Identification as Tool for the Systematic Correction of Finite-Element Models", *Structural Dynamics*, Kratzig *et al.* (eds), Balkema, Rotterdam, 331-337.

Garcia, G. and Stubbs, N., (1995), "The Effect of Damage Size and Location on the Stiffness of a Rectangular Beam", *Proceedings of SPIE - The International Society for Optical Engineering*, **2446**, 151-160.

Gladwell, G. M. L., (1986), *Inverse Problems in Vibration*, The Hague, Martinus Nijhoff.

Gounaris, G. D., Papadopoulos, C. A., and Dimarogonas, A. D., (1996), "Crack Identification in Beams by Coupled Response Measurements", *Computers & Structures*, **58**(2), 299-305.

Gudmundson, P., (1982), "Eigenfrequency Changes of Structures due to Crack, Notches and Other Geometrical Changes", *Journal of the Mechanics and Physics of Solids*, **30**(5), 339-353.

Guyan, R. J., (1965), "Reduction of Mass and Stiffness Matrices", *AIAA Journal*, **3**(2), 380.

Gysin, H., (1990), "Comparison of Expansion Methods for FE Modelling Error Localisation", *Proceedings of the 8th International Modal Analysis Conference*, Kissimmee, FL, 195-204.

Haisty, B. S. and Springer, W. T., (1988), "A General Beam Element for Use in Damage Assessment of Complex Structures", *Journal of Vibration, Acoustics, Stress, and Reliability in Design*, **110**, 389-394.

Hajela, P. and Soeiro, F. J., (1990a), "Recent Developments in Damage Detection Based on System Identification Methods", *Structural Optimisation*, Springer-Verlag, **2**, 1-10.

Hajela, P. and Soeiro, F. J., (1990b), "Structural Damage Detection Based on Static and Modal Analysis", *AIAA Journal*, **28**(6), 1110-1115.

Hassiotis, S. and Jeong, G. D., (1993), "Assessment of Structural Damage from Natural Frequency Measurements", *Computes & Structures*, **49**(4), 679-691.

He, J., (1993), "On Model Correlation Using Measured Frequency Response Function Data", *Proceedings of the 1st International Structural Dynamics Modelling Conference, NAFEMS*, Milton Keynes, 401-410.

He, J. and Ewins, D. J., (1986), "Analytical Stiffness Matrix Correction Using Measured Vibration Modes", *Modal Analysis IJAEMA*, **1**(3), 1-9.

He, J. and Ewins, D. J., (1991), "Compatibility of Measured and Predicted Vibration Modes in Model Improvement Studies", *AIAA Journal*, **29**(5), 798-803.

Hearn, G and Testa, R. B., (1991), "Modal Analysis for Damage Detection in Structures", *Journal of Structural Engineering*, **117**(10), 3042-3063.

Hemez, F. M. and Farhat, C., (1993), "Locating and Identifying Structural Damage Using a Sensitivity-Based Model Updating Methodology", *Collection of Technical Papers - AIAA/ASME Structures, Structural Dynamics and Materials Conference*, 2641-2653.

Hemez, F. M. and Farhat, C., (1994), "Comparing Mode Shape Expansion Methods for Test-Analysis Correlation", *Proceedings of the 12th International Modal Analysis Conference*, Honolulu, Hawaii, 1560-1567.

Hemez, F. M. and Farhat, C., (1995a), "On the Efficiency of Model Updating via Genetic Algorithm for Structural Damage Detection", *36th AIAA/ASME/ASCE/AHS/ASC Structures, Structural Dynamics and Materials Conference*, New Orleans, Louisiana, 2792-2801.

Hemez, F. M. and Farhat, C., (1995b), "Structural Damage Detection via a Finite Element Model Updating Methodology", *Modal Analysis IJAEMA*, **10**(3), 152-166.

Hemez, F. M. and Farhat, C., (1995c), "Bypassing Numerical Difficulties Associated with Updating Simultaneously Mass and Stiffness Matrices", *AIAA Journal*, **33**(3), 539-546.

Himmelblau, D. M., (1972), *Applied Nonlinear Programming*, McGraw-Hill, Inc. New York.

Hinton, E. and Owen, D. R. J., (1977), *Finite Element Programming*, Academic Press, London, New York, San Francisco.

Hinton, E. and Owen, D. R. J., (1985), *An Introduction to Finite Element Computations*, Pineridge Press, Swansea, U. K..

Huang, C. H. and Yan, J. Y., (1996), "An Inverse Problem in Predicting Temperature Dependent Heat Capacity Per Unit Volume Without Internal Measurements", *International Journal for Numerical Methods in Engineering*, **39**, 605-618.

Jerry, S. E. and Yao, J. T. P., (1987), "Damage Assessment Using Response Measurements", *Journal of Structural Engineering, ASCE*, **113**(4), 787-801.

Kabe, A. M., (1985), "Stiffness Matrix Adjustment Using Modal Data", *AIAA Journal*, **23**(9), 1431-1436.

Kam, T. Y. and Lee, T. Y., (1994a), "Crack Size Identification Using an Expanded Mode Method", *International Journal of Solids and Structures*, **31**(7), 925-940.

Kam, T. Y. and Lee, T. Y., (1994b), "Identification of Crack Size via an Energy Approach", *Journal of Nondestructive Evaluation*, **13**(1), 1-11.

Kammer, D. C., (1987), "Test-Analysis Model Development Using an Exact Model Reduction", *Modal Analysis IJAEMA*, **3**, 174-179.

Kammer, D. C., (1988), "Optimum Approximation for Residual Stiffness in Linear System Identification", *AIAA Journal*, **26**(1), 104-112.

Kammer, D. C., (1991), "A Hybrid Approach to Test-Analysis Model Development for Large Space Structures", *Journal of Vibration and Acoustics*, **113**, 325-332.

Kammer, D. C., Jensen, B. M., and Mason, D. R., (1989), "Test-Analysis Correlation of the Space Shuttle Solid Rocket Motor Centre Segment", *Journal of Spacecraft and Rocket*, **26**(4), 266-273.

Kaouk, M. and Zimmermam, D. C., (1994), "Structural Damage Assessment Using a Generalised Minimum Rank Perturbation Theory", *AIAA Journal*, **32**(4), 836-842.

Kaouk, M. and Zimmermam, D. C., (1995), "Reducing the Required Number of Modes for Structural Damage Assessment", *36th AIAA/ASME/ASCE/AHS/ASC Structures, Structural Dynamics and Materials Conference*, New Orleans, Louisiana, 2802-2812.

Kashangaki, T. A. L., Smith, S. W., and Lim, T. W., (1992), "Underlying Modal Data Issues for Detecting Damage in Truss Structures", *33rd AIAA/ASME/ASCE/ AHS/ASC Structures, Structural Dynamics and Materials Conference*, Dallas, TX, 1437-1446.

Kidder, R. L., (1973), "Reduction of Structural Frequency Equations", *AIAA Journal*, **11**(6), 892.

Kim, J. T., (1995), "Robust Damage Localisation Algorithm for Highway Plate-Girder Bridge", *Proceedings of SPIE - The International Society for Optical Engineering*, **2446**, 116-126.

Kim, K. O., Aderson, W. J., and Sandstrom, R. E., (1983), "Nonlinear Inverse Perturbation Method in Dynamic Analysis", *AIAA Journal*, **21**(9), 1310-1316.

Kim, H. M. and Bartkowicz, T. J., (1993), "Damage Detection and Health Monitoring of Large Space Structures", *Collection of Technical Papers - 34th AIAA/ASME Structures, Structural Dynamics and Materials Conference*, 3527-3533.

Kim, J. T. and Stubbs, N., (1995a), "Damage Localisation Accuracy as a Function of Model Uncertainty in the I-14 Bridge over the Rio Grande", *Proceedings of SPIE - The International Society for Optical Engineering*, **2446**, 193-203.

Kim, J. T. and Stubbs, N., (1995b), "Damage Detection in Offshore Jacket Structures from Limited Modal Information", *International Journal of Offshore and Polar Engineering*, **5**(1), 58-66.

Kim, J. T. and Stubbs, N., (1995c), "Model-Uncertainty Impact and Damage-Detection Accuracy in Plate Girder", *Journal of Structural Engineering, ASCE*, **121**(10), 1409-1417.

Kudva, J., Munir, N, and Tan, P. W., (1992), "Damage Detection in Smart Structures Using Neural Networks and Finite-Element Analysis", *Smart Material Structures*, **1**, 108-112.

Kuo, C. P. and Wada, B. K., (1987), "Nonlinear Sensitivity Coefficients and Corrections in System Identification", *AIAA Journal*, **25**(11), 1463-1468.

Ladevcze, P., Nedjar, D., and Reynier, M., (1994), "Updating of Finite Element Models Using Vibration Tests", *AIAA Journal*, **32**(7), 1485-1491.

Lallement, G., (1988), "Localisation Techniques", *Structural Safety Evaluation Based on System Identification Approaches*, Vieweg, Braunschweig, FRG, 212-233.

Lancaster, P. and Maroulas, J., (1987), "Inverse Eigenvalue Problem for Damped Vibrating Systems", *Journal of Mathematical Analysis and Applications*, **123**(1), 238-261.

Larson, C. B., and Zimmerman, D. C., (1993), "Structural Modal Refinement Using a Genetic Algorithm Approach", *Proceedings of the 11th International Modal Analysis Conference*, Kissimmee, FL, 1095-1101.

Levine-West, M., Milman, M., and Kissil, A., (1996), "Mode Shape Expansion Techniques for Prediction: Experimental Evaluation", *AIAA Journal*, **34**(4), 821-829.

Lew, J. S., (1995a), "Using Transfer Function Parameter Changes for Damage Detection of Structures", *AIAA Journal*, **33**(11), 2189-2193.

Lew, J. S., (1995b), "Using Transfer Function Parameter Changes for Damage Detection of Structures", *Collection of Technical Papers - AIAA/ASME Structures, Structural Dynamics and Materials Conference*, 2893-2900.

Li, C. and Smith, S. W., (1995), "Hybrid Approach for Damage Detection in Flexible Structures", *Journal of Guidance, Control, and Dynamics*, **18**(3), 419-425.

Liang, R. Y., Hu, J., and Choy, F., (1992), "Quantitative NDE Techniques for Assessing Damage in Beam Structures", *Journal of Structural Engineering, ASCE*, **118**(7), 1468-1487.

Lim, T. W., (1991), "Structural Damage Detection Using Model Test Data", *AIAA Journal*, **29**(12), 2271-2274.

Lim, T. W., (1995), "Structural Damage Detection Using Constrained Eigenstructure Assignment", *Journal of Guidance, Control, and Dynamics*, **18**(3), 411-418.

Lim, T. W., Bosse, A., and Fisher, S., (1996), "Structural Damage Detection Using Real-Time Modal Parameter Identification Algorithm", *AIAA Journal*, **34**(11), 2370-2376.

Lim, T. W. and Kashangaki, T. A. L., (1994), "Structural Damage Detection of Space Truss Structures Using Best Achievable Eigenvectors", *AIAA Journal*, **32**(5), 1049-1057.

Lin, C. S., (1990), "Location of Modelling Errors Using Modal Test Data", *AIAA Journal*, **28**(9), 1650-1654.

Lin, R. M. and Lim, M. K., (1996), "Analytical Model Updating and Model Reduction", *AIAA Journal*, **34**(9), 1966-1969.

Link, M., (1990a), "Localisation of Errors in Computational Models Using Dynamic Test Data", *Structural Dynamics*, Kratzig *et al.* (eds), Balkema, Rotterdam, 305-313.

Link, M., (1990b), "Identification and Correction of Errors in Analytical Models Using Test Data -- Theoretical and Practical Bounds', *Proceedings of the 8th International Modal Analysis Conference*, Kissimmee, FL, 570-578.

Link, M., Weiland, M., and Barragan, J. M., (1987), "Direct Physical Matrix Identification as Compared to Phase Resonance Testing: An Assessment Based on Practical Application", *Proceedings of the 5th International Modal Analysis Conference*, London, 804-811.

Liu, P. L., (1995), "Identification and Damage Detection of Trusses Using Modal Data", *Journal of Structural Engineering, ASCE*, **121**(4), 599-608.

Liu, X. and Onoda, J., (1996), "Partitioned Model Reduction for Large Space Structural Control Problem", *AIAA Journal*, **34**(10), 2149-2153.

Maia, N. M. M., (1989), "An Introduction to the Singular Value Decomposition Technique (SVD)", *Proceedings of the 7th International Modal Analysis Conference*, Las Vegas, NV, 335-338.

Maia, N. M. M., Reynier, M., and Ladeveze, P., (1994), "Error Localisation for Updating Finite Element Models Using Frequency Response Functions", *Proceedings of the 12th International Modal Analysis Conference*, Honolulu, Hawaii, 1299-1308.

Mayes, R. L., (1995), "An Experimental Algorithm for Detecting Damage Applied to the I-40 Bridge Over the Rio Grande", *Proceedings of SPIE - The International Society for Optical Engineering*, **2446**, 204-214.

Mazurek, D. F. and DeWolf, J. T., (1990), "Experimental Study of Bridge Monitoring Technique", *Journal of Structural Engineering, ASCE*, **116**(9), 2532-2549.

Minas, C. and Inman, D. J., (1990), "Matching Finite Element Models to Modal data", *Journal of Vibration and Acoustics, Transactions of ASME*, **112**(1), 84-92.

Mix, P. E., (1985), *Introduction to Nondestruction Testing -- A Training Guide*, John Wiley & Sons, Newyork.

Mottershead, J. E. and Friswell, M. I., (1993), "Model Updating in Structural Dynamics: A Survey", *Journal of Sound and Vibration*, **167**(2), 347-375.

Mottershead, J. E. and Stanway, R., (1986), "Identification of Structural Vibration Parameters by Using a Frequency Domain Filter", *Journal of Sound and Vibration*, **109**, 495-506.

Natke, H. G. and Cempel, C., (1991), "Fault Detection and Localisation in Structures: A Discussion", *Mechanical Systems and Signal Processing*, **5**(5), 345-356.

Natke, H. G. and Cempel, C., (1997), *Model-Aided Diagnosis of Mechanical Systems*, Springer-Verlag, Berlin, Heidelberg, New York.

O'Callaham, J., (1989), "A Procedure for an Improved Reduced System (IRS) Model", *Proceedings of the 7th International Modal Analysis Conference*, Las Vegas, NV, 17-21.

O'Callaham, J., Avitabile, P., and Riemer, R., (1989), "System Equivalent Reduction Expansion Process (SEREP)", *Proceedings of the 7th International Modal Analysis Conference*, Las Vegas, NV, 29-37.

Ojalvo, I. U. and Pilon, D., (1988), "Diagnostic for Geometrically Locating Structural Math Model Error from Modal Test Data", *Proceedings of the 29th AIAA Structures, Structural Dynamics and Materials Conference*, Williamsburg, VA, 1174-1186.

Ojalvo, I. U. and Zhang, L. M., (1993), "Tutorial: Fundamentals of Ill-Conditioning", *Modal Analysis IJAEMA*, **8**(2), 165-176.

Osegueda, R. A. and DSouza, P. D., (1992), "Damage Evaluation of an Offshore Structure Model Using Vibration Measurements", *Proceedings of the 2nd International Offshore and Polar Engineering Conference*, San Francisco, USA, 550-557.

Pandey, A. K. and Biswas, M., (1995a), "Damage Diagnosis of Truss Structures by Estimation of Flexibility Change", *Modal Analysis IJAEMA*, **10**(2), 104-117.

Pandey, A. K. and Biswas, M., (1995b), "Experimental Verification of Flexibility Difference Method for Locating Damage in Structures", *Journal of Sound and Vibration*, **184**(2), 311-328.

Pandey, A. K., Biswas, M., and Samman, M. M., (1991), "Damage Detection from Changes in Curvature Mode Shapes", *Journal of Sound and Vibration*, **145**(2), 321-332.

Park, Y. S., Park, H. S., and Lee, S. S., (1988), "Weighted-Error-Matrix (WEM) Application to Detect Stiffness Damage by Dynamic Characteristic Measurement", *Modal Analysis IJAEMA*, **3**(3), 101-107

Park, S. and Stubbs, N., (1995), "Reconstruction of Mode Shapes Using Shannon's Sampling Theorem and Its Application to the Nondestructive Damage Localisation Algorithm", *Proceedings of SPIE - The International Society for Optical Engineering*, **2446**, 280-292.

Peterson, L. D., Alvin, K. F., Doebling, S. W., and Park, K. C., (1993), "Damage Detection Using Experimentally Measured Mass and Stiffness Matrices", *Collection of Technical Papers - AIAA/ASME Structures, Structural Dynamics and Materials Conference*, 1518-1528.

Raghavendrachar, M. and Aktan, A. E., (1992), "Flexibility by Multireference Impact Testing for Bridge Diagnostics", *Journal of Structural Engineering, ASCE*, **118**(8), 2186-2203.

Ricles, J. M. and Kosmatka, J. B., (1992), "Damage Detection in Elastic Structures Using Vibratory Residual Forces and Weighted Sensitivity", *AIAA Journal*, **30**(9), 2310-2316.

Roitman, N., Viero, P. F., Magluta, C., Batista, R. C., and Rosa, L. F. L., (1992), "Identification of Offshore Platform Structural Damage Using Modal Analysis Techniques", *Mechanical Systems and Signal Processing*, **6**(3), 287-295.

Rubin, S. and Coppolino, R. N., (1983), "Flexibility Monitoring of Offshore Jacket Platforms", *15th Annual offshore Technology Conference*, Houston, Texas.

Rytter, A., (1993), "Vibrational Based Inspection of Civil Engineering Structures", *Fracture and Dynamics*, University of Aalborg.

Rytter, A., Brincker, R., and Kirkegaard, P. K., (1992), "An Experimental Study of the Modal Parameters of a Damaged Cantilever", *Fracture and Dynamics*, University of Aalborg.

Samman, M. M. and Biswas, M., (1994a), "Vibration Testing for Nondestructive Evaluation of Bridges. I: Theory", *Journal of Structural Engineering*, **120**(1), 269-289.

Samman, M. M. and Biswas, M., (1994b), "Vibration Testing for Nondestructive Evaluation of Bridges. II: Results", *Journal of Structural Engineering*, **120**(1), 290-306.

Samman, M. M., Biswas, M., and Pandey, A. K., (1991), "Employing Pattern Recognition for Detecting Cracks in a Bridge Model", *Modal Analysis IJAEMA*, **6**(1), 35-44.

Sanayei, M. and Onipede, O., (1991), "Damage Assessment of Structures Using Static Test Data", *AIAA Journal*, **29**(7), 1174-1179.

Sanayei, M. and Scampoli, S. F., (1991), "Structural Element Stiffness Identification from Static Test Data", *Journal of Engineering Mechanics, ASCE*, **117**(5), 1021-1036.

Shahrivar, F. and Bouwkamp, J. G., (1986), "Damage Detection in Offshore Platforms Using Vibration Information", *Journal of Energy Resources Technology*, **108**(6), 97-106.

Sheinman, I., (1994), "Damage Detection in Framed Structures", *AIAA Journal*, **32**(5), 1103-1105.

Sheinman, I., (1996), "Damage Detection and Updating of Stiffness and Mass Matrices Using Mode Data", *Computers & Structures*, **59**(1), 149-156.

Shen, M. H. and Taylor, J. E., (1991), "An Identification Problem for Vibrating Cracked Beams", *Journal of Sound and Vibration*, **150**(3), 457-484.

Simonian, S. S., (1981a), "Inverse Problems in Structural Dynamics--I: Theory", *International Journal of Numerical Methods in Engineering*, **17**(3), 357-365.

Simonian, S. S., (1981b), "Inverse Problems in Structural Dynamics--II: Applications", *International Journal of Numerical Methods in Engineering*, **17**(3), 367-386.

Smith, S. W. and Beattie, C. A., (1990), "Simultaneous Expansion and Orthogonalisation of Measured Modes for Structure Identification", *Proceedings of the AIAA Dynamics Specialist Conference, AIAA*, Washington, DC, 261-270.

Smith, S. W. and Beattie, C. A., (1991), "Secant-Method Adjustment for Structural Models", *AIAA Journal*, **29**(1), 119-126.

Smith, S. W. and Hendricks, S. L., (1987), "Evaluation of Two Identification Methods for Damage Detection in Large Space Trusses", *Dynamics and Control of Large Structures, Proceedings of the 6th VPI & SU/AIAA Symposium*, Blackburg, Virgina, 127-141.

Soeiro, F. J. and Hajela, P., (1993), "Damage Detection in Composite Materials Using Identification Techniques", *Journal of Aerospace Engineering*, **6**(4), 363-380.

Stubbs, N., Broome, T. H. and Osegueda, R., (1990), "Nondestructive Construction Error Detection in Large Space Structures", *AIAA Journal*, **28**(1), 146-152.

Stubbs, N. and Osegueda, R., (1990a), "Global Non-Destructive Damage Evaluation in Solids", *Modal Analysis IJAEMA*, **5**(2), 67-79.

Stubbs, N. and Osegueda, R., (1990b), "Global Damage Detection in Solids - Experimental Verification", *Modal Analysis IJAEMA*, **5**(2), 81-97.

Sunder, S. S. and Ting, S. K., (1985), "Flexibility Monitoring of Offshore Platforms", *Applied Ocean Research*, **7**(1).

Sundermeyer, J. N. and Weaver, R. L., (1995), "On Crack Identification and Characterisation in a Beam by Non-Linear Vibration Analysis", *Journal of Sound and Vibration*, **183**(5), 857-871.

Szewczyk, Z. P. and Hajela, P., (1994), "Damage Detection in Structures Based on Feature-Sensitive Neural Networks", *Journal of Computing in Civil Engineering, ASCE*, **8**(2), 163-178.

To, W. M. and Ewins, D. J., (1991), "Non-Linear Sensitivity Analysis of Mechanical Structures Using Modal Data", *Journal of Mechanical Engineering Science, Proceedings of Institute of Mechanical Engineer*, **205**, 67-75.

To, W. M., Lin, R. M., and Ewins, D. J., (1990), "A Criterion for the Localisation of Structural Modification Sites Using Modal Data", *Proceedings of the 8th International Modal Analysis Conference*, Kissimmee, FL, 961-967.

Topole, K. G. and Stubbs, N., (1995a), "Nondestructive Damage Evaluation in Complex Structures from a Minimum of Modal Parameters", *Modal Analysis IJAEMA*, **10**(2), 95-103.

Topole, K. G. and Stubbs, N., (1995b), "Non-Destructive Damage Evaluation of a Structure from Limited Modal Parameters", *Earthquake Engineering and Structural Dynamics*, **24**, 1427-1436.

Tsai, T. and Yang, J. C. S., (1985), "Damage Detection and Location in Complex Structure", *Proceedings of the Failure Prevention and Reliability Conference, ASME*, Cincinatti, Ohio, 15-22.

Tsai, T., Yang, J. C. S., and Chen, R. Z., (1985), "Detection of Damage in Structures by the Cross Random Decrement Method", *Proceedings of the 3rd International Modal Analysis Conference*, Orlando, FL, 691-700.

Tseng, S. S. M., (1993), "Studies on Global Methods for Localised-Damage Detection in Large-Scale Structures", *PhD Dissertation*, University of Akron.

Tsyfanskii, S. L., Magone, M. A., and Ozhiganov, V. M., (1985), "Using Nonlinear Effects to Detect Cracks in the Rod Element of Structures", *The Soviet Journal of Nondestructive Testing*, **21**(3), 224-229.

Wang, T. L. and Huang, D. Z., (1992), "Cable-Stayed Bridge Vibration due to Road Surface Roughness", *Journal of Structural Engineering, ASCE*, **118**(5), 1354-1374.

Worden, K., Ball, A. D., and Tomlinson, G. R., (1993), "Fault Location in a Framework Structure Using Neural Networks", *Smart Material Structures*, **2**, 189-200.

Wu, X., Ghaboussi, J., and Garrett, J. H., (1992), "Use of Neural Networks in Detection of Structural Damage", *Computers & Structures*, **42**(4), 649-659.

Yang, J. C. S., Chen, J., and Dagalakis, N. G., (1984), "Damage Detection in Offshore Structures by the Random Decrement Technique", *Journal of Energy Resources Technology*, **106**, 38-42.

Yao, G. C., Chang, K. C., and Lee, G. C., (1992), "Damage Diagnosis of Steel Frames Using Vibrational Signature Analysis", *Journal of Engineering Mechanics*, **118**(9), 1949-1961.

Yao, J. T. P. and Natke, H. G., (1994), "Damage Detection and Reliability Evaluation of Existing Structures", *Structural Safety*, **15**, 3-16.

Yin, Z. K., Jun, G. A., and Wen, L. J., (1992), "Diagnosis of a Slot Fault on a Frame Structure", *Proceedings of the 10th International Modal Analysis Conference*, San Diego, California, 549-553.

Yuen, M. M. F., (1985), "A Numerical Study of the Eigenparameters of a Damage Cantilever", *Journal of Sound and Vibration*, **103**(3), 301-310.

Zienkiewicz, O. C. and Taylor, R. L., (1994), *The Finite Element Method*, 4th Edition, McGraw-Hill, London.

Zimmerman, D. C. and Kaouk, M., (1992), "Eigenstructure Assignment Approach for Structural Damage Detection", *AIAA Journal*, **30**(7), 1848-1855.

Zimmerman, D. C. and Kaouk, M., (1994), "Structural Damage Detection Using a Minimum Rank Updating Theory", *Journal of Vibration and Acoustics, Transaction of ASME*, **116**(1), 222-231.

Zimmerman, D. C., Smith, S. W., Kim, H. M., and Bartkowicz, T. J., (1994), "An Experimental Study of Structural Damage Detection Using Incomplete Measurements", *Proceedings of the AIAA Dynamics Specialist Conference, AIAA*, Hilton Head, SC, 307-317.

Zimmerman, D. C. and Widengren, M., (1990), " Correcting Finite Element Models Using a Symmetric Eigenstructure Assignment Technique", *AIAA Journal*, **28**(9), 1670-1679.